AGARD-AR-248

AGARD-AR-248

AD-A218 764

ADVISORY GROUP FOR AEROSPACE RESEARCH & DEVELOPMENT

AGARD ADVISORY REPORT No.248

Propulsion and Energetics Panel Working Group 15 on The Uniform Engine Test Programme

DTIC
S ELECTE
MAR 0 8 1990
D

NORTH ATLANTIC TREATY ORGANIZATION

90 03 07 000

NORTH ATLANTIC TREATY ORGANIZATION

ADVISORY GROUP FOR AEROSPACE RESEARCH AND DEVELOPMENT

(ORGANISATION DU TRAITE DE L'ATLANTIQUE NORD)

AGARD Advisory Report No.248

THE UNIFORM ENGINE TEST PROGRAMME

Report of the Propulsion and Energetics Panel Working Group 15

Principal Author
Peter F.Ashwood

Editor
James J. Mitchell

A-1

This Advisory Report was prepared at the request of the Propulsion and Energetics Panel of AGARD.

THE MISSION OF AGARD

According to its Charter, the mission of AGARD is to bring together the leading personalities of the NATO nations in the fields of science and technology relating to aerospace for the following purposes:

— Recommending effective ways for the member nations to use their research and development capabilities for the common benefit of the NATO community;

— Providing scientific and technical advice and assistance to the Military Committee in the field of aerospace research and development (with particular regard to its military application);

— Continuously stimulating advances in the aerospace sciences relevant to strengthening the common defence posture;

— Improving the co-operation among member nations in aerospace research and development;

— Exchange of scientific and technical information;

— Providing assistance to member nations for the purpose of increasing their scientific and technical potential;

— Rendering scientific and technical assistance, as requested, to other NATO bodies and to member nations in connection with research and development problems in the aerospace field.

The highest authority within AGARD is the National Delegates Board consisting of officially appointed senior representatives from each member nation. The mission of AGARD is carried out through the Panels which are composed of experts appointed by the National Delegates, the Consultant and Exchange Programme and the Aerospace Applications Studies Programme. The results of AGARD work are reported to the member nations and the NATO Authorities through the AGARD series of publications of which this is one.

Participation in AGARD activities is by invitation only and is normally limited to citizens of the NATO nations.

RECENT PUBLICATIONS OF THE PROPULSION AND ENERGETICS PANEL

Conference Proceedings

Turbine Engine Testing
AGARD Conference Proceedings No.293, 56th Meeting, Sep/October 1980

Helicopter Propulsion Systems
AGARD Conference Proceedings No.302, 57th Meeting, May 1981

Ramjets and Ramrockets for Military Applications
AGARD Conference Proceedings No.307, 58th Meeting, October 1981

Problems in Bearings and Lubrication
AGARD Conference Proceedings No.323, 59th Meeting, May/June 1982

Engine Handling
AGARD Conference Proceedings No.324, 60th Meeting, October 1982

Viscous Effects in Turbomachines
AGARD Conference Proceedings No.351, 61st A Meeting, June 1983

Auxiliary Power Systems
AGARD Conference Proceedings 352, 61st B Meeting, May 1983

Combustion Problems in Turbine Engines
AGARD Conference Proceedings 353, 62nd Meeting, October 1983

Hazard Studies for Solid Propellant Rocket Motors
AGARD Conference Proceedings 367, 63rd A Meeting, May/June 1984

Engine Cyclic Durability by Analysis and Testing
AGARD Conference Proceedings No.368, 63rd B Meeting, May/June 1984

Gears and Power Transmission Systems for Helicopters and Turboprops
AGARD Conference Proceedings No.369, 64th Meeting October 1984

Heat Transfer and Cooling in Gas Turbines
AGARD Conference Proceedings No.390, 65th Meeting, May 1985

Smokeless Propellants
AGARD Conference Proceedings No.391, 66th A Meeting, September 1985

Interior Ballistics of Guns
AGARD Conference Proceedings No.392, 66th B Meeting, September 1985

Advanced Instrumentation for Aero Engine Components
AGARD Conference Proceedings No.399, 67th Meeting, May 1986

Engine Response to Distorted Inflow Conditions
AGARD Conference Proceedings No.400, 68th A Meeting, September 1986

Transonic and Supersonic Phenomena in Turbomachines
AGARD Conference Proceedings No.401, 68th B Meeting, September 1986

Advanced Technology for Aero Engine Components
AGARD Conference Proceedings No.421, 69th Meeting, September 1987

Combustion and Fuels in Gas Turbine Engine
AGARD Conference Proceedings No.422, 70th Meeting, October 1987

Engine Condition Monitoring — Technology and Experience
AGARD Conference Proceedings No.448, 71st Meeting, May/June 1988

Application of Advanced Material for Turbomachinery and Rocket Propulsion
AGARD Conference Proceedings No.449, 72nd A Meeting, October 1988

Combustion Instabilities in Liquid-Fuelled Propulsion Systems
AGARD Conference Proceedings No.450, 72nd B Meeting, October 1988

Working Group Reports

Through Flow Calculations in Axial Turbomachines
AGARD Advisory Report 175. Results of WG 12 (October 1981)

Alternative Jet Engine Fuels
AGARD Advisory Report 181. Vol.1 and Vol.2. Results of WG 13 (July 1982)

Suitable Averaging Techniques in Non-Uniform Internal Flows
AGARD Advisory Report 182 (in English and French). Results of WG 14 (June/August 1983)

Producibility and Cost Studies of Aviation Kerosines
AGARD Advisory Report 227. Results of WG 16 (June 1985)

Performance of Rocket Motors with Metallized Propellants
AGARD Advisory Report 230. Results of WG 17 (September 1986)

Recommended Practices for Measurement of Gas Path Pressures and Temperatures for Performance Assessment of
Aircraft Engines and Components
AGARD Advisory Report 245. Results of WG 19 (In production, 1990)

The Uniform Engine Test Programme
AGARD Advisory Report 248. Results of WG 15 (In production, 1990)

Test Cases for Computation of Internal Flows in Aero Engine Components
AGARD Advisory Report 275. Results of WG 18 (In production, 1990)

Lecture Series

Aircraft Fire Safety
AGARD LS 123 (June 1982)

Operation and Performance Measurement of Engines in Sea Level Test Facilities
AGARD LS 132 (April 1984)

Ramjet and Ramrocket Propulsion Systems for Missiles
AGARD LS 136 (September 1984)

3-D Computation Techniques Applied to Internal Flows in Propulsion Systems
AGARD LS 140 (June 1985)

Engine Airframe Integration for Rotorcraft
AGARD LS 148 (June 1986)

Design Methods Used in Solid Rocket Motors
AGARD LS 150 (April 1987)
AGARD LS 150 (Revised) (April 1988)

Blading Design for Axial Turbomachines
AGARD LS 167 (June 1989)

Other Publications

Airbreathing Engine Test Facility Register
AGARD AG 269 (July 1981)

Rocket Altitude Test Facility Register
AGARD AG 297 (March 1987)

Manual for Aeroelasticity in Turbomachines
AGARD AG 298 1 (March 1987)
AGARD AG 298 2 (June 1988)

Application of Modified Loss and Deviation Correlations to Transonic Axial Compressors
AGARD Report 745 (November 1987)

Measurement Uncertainty within the Uniform Engine Test Programme
AGARD AG 307 (May 1989)

FOREWORD

Performance of the propulsion system must be known to a high degree of accuracy throughout the entire flight envelope to achieve the level of operational capability demanded from today's high-performance aircraft. The starting point for a synthesis of propulsion system behaviour is the performance of the basic engine and this is normally obtained from measurements made during full scale tests on the ground in test beds and altitude simulation facilities. In the latter, the environmental conditions of pressure and temperature met in flight can be accurately reproduced.

During the late 1970s joint engine development and licensed production programmes among companies from different countries were becoming common. Further, engines which were developed in one country often were used in airframes developed in another. Both situations require engine performance information which can be interpreted internationally and provide a valid basis for performance comparisons. However, experience showed that there was incomplete understanding of the meaning of engine performance characteristics as derived from test facility measurements in the different countries.

Because of the critical nature of engine test measurements and their influence on aircraft performance predictions, as well as the need for a sound understanding of test-related factors which may influence such measurements, an inter-facility comparison was proposed by the Propulsion and Energetics Panel (PEP) of AGARD. The basic idea was that a nominated engine would be tested in several facilities, both ground-level and altitude, the results then compared, and explanations sought for any observed differences.

AGARD offered a unique structure to execute such a programme and precedent for AGARD sponsorship existed in the earlier test of uniform aerodynamic models in wind tunnels under the auspices of the Fluid Dynamics Panel. A formal proposal was presented to the Propulsion and Energetics Panel (PEP) of AGARD in April 1979 by the US Delegation. Although the scope of the effort was of a magnitude and timespan uncharacteristic for an AGARD undertaking, the PEP agreed to sponsorship and Working Group 15 was chartered to conduct the project which became known as the Uniform Engine Test Program (UETP). Dr James G.Mitchell, Chief Scientist at the US Arnold Engineering Development Center, was appointed as Chairman of this major new effort and members of the engine test community throughout AGARD were selected to serve on Working Group 15 along with PEP representatives.

The Working Group set up a small steering group (Overview Committee) to observe the test data as it became available for the purpose of monitoring engine health and detection of any large departures from expected values. This Committee was initially made up of those members of the Working Group not directly involved with the test, but as each facility completed its test programme and presented its data, its representative began to participate. The first formal meeting of the Working Group took place in Turin, Italy, during the PEP-sponsored Symposium on Engine Testing in September 1980. Following meetings of the Working Group/Overview Committee were held in Toulouse, France, May 1981; London, England, October 1981; Ottawa, Canada, June 1982; Nea Makri, Greece, October 1982; Copenhagen, Denmark, May 1983; Çeşme, Turkey, October 1983; Lisse, Netherlands, May 1984; Lisbon, Portugal, October 1984; Bergen, Norway, May 1985; Florence, Italy, September 1985; Philadelphia, USA, May 1986; Munich, Germany, September 1986; Paris, France, May 1987; and Chania, Greece, October 1987.

Specially prepared and instrumented turbine engines were tested in ground test beds and altitude facilities in five countries (eight test facilities) in a closely controlled test programme. The participating agencies bore the entire cost of testing and the costs of all subsequent data analyses. These testing agencies in order of testing were: National Aeronautical and Space Administration Lewis Research Center (NASA, US), Arnold Engineering Development Center (AEDC, US), National Research Council of Canada (NRCC, Canada), Centre d'Essais des Propulseurs (CEPr, France), Turkish Air Force Supply and Maintenance Centre (TUAF, Turkey), Royal Aircraft Establishment at Pyestock (RAE(P), UK) and the Naval Air Propulsion Center (NAPC, US).

The AGARD Propulsion and Energetics Panel is appreciative of support provided by the US Air Force in the loan of two J57 engines and assistance in the transportation of the engines between testing sites. Appreciation is also extended to the US NASA Lewis Research Center for their efforts in preparing the engines and instrumentation for initial testing. Both NASA and NRCC gave extra support to the programme by repeating the testing of one engine near the end of the test cycle to provide additional data to validate engine performance retention. Finally, recognition is given to Mr Peter F.Ashwood (UK) for his leadership in organising and reporting the results of the UETP. Mr Ashwood is the retired Head of the Engine Test Department at RAE(P) and served as an AGARD consultant to Working Group 15.

The reader who is interested in data accuracy and error analysis is referred to AGARDograph 307 "Measurement Uncertainty Within The Uniform Engine Test Programme", edited by J.P.K.Vleghert (The Netherlands). This analysis became so involved and attracted such interest that it has been reported under its own cover. The AGARD PEP appreciates the contributions of Dr R.B.Abernethy of Pratt & Whitney Aircraft (US) and Mr J.C.Ascough, RAE(P) UK to this programme.

WORKING GROUP 15 MEMBERSHIP

Dr J.G.Mitchell (*Chairman*)
Micro Craft. Inc.
Corporate Headquarters
207 Big Springs Avenue
PO Box 370
Tullahoma, Tennessee 37388-0370
United States

BELGIUM

Professeur R.Jacques
Ecole Royale Militaire
30 Avenue de la Renaissance
1040 Bruxelles

CANADA

Dr W.L.Macmillan
Project Manager
EHF Communication Satellite
Defence Research Establishment
Ottawa, Ontario K1A 0Z4

Mr D.M.Rudnitski
Head, Engine Laboratory
Division of Mechanical Engineering
National Research Council of Canada
Ottawa, Ontario K1A 0R6

FRANCE

Mr F.Fagegaltier
Service Technique des Programmes Aéronautiques —
    STPA/MO 4
4 Avenue de la Porte d'Issy
75015 Paris

GERMANY

Professor Dr-Ing. W.Braig
Stuttgart Universität
Pfaffenwaldring 6
7000 Stuttgart 80

Professor Dr D.K. Hennecke
Fachgebiet Flugantriebe
Technische Hochschule Darmstadt
Petersenstrasse 30
6100 Darmstadt

ITALY

Dr-Ing. G.Maoli
Fiat s.p.a. Direzione
Via L.Bissolati 57
00187 Roma

NETHERLANDS

Ir. J.P.K.Vleghert
National Aerospace Laboratory
PO Box 90502
Anthony Fokkerweg 2
1006 BM Amsterdam

TURKEY

Major F.Algun
Hava Kuvvetleri Komutanlığı
Lojistik Teknik Bakım Dairesi
Ankara

Professor Dr A.Üçer
Middle East Technical University
O D T Ü
Makina Muh. Bölümü
Ankara

UNITED KINGDOM

Mr P.F.Ashwood
36 Lynch Road
Farnham, Surrey GU9 8BY

Mr M.Holmes
Head of Engine Test Department
Royal Aerospace Establishment
Pyestock
Farnborough, Hants GU14 0LS

Mr N.A.Mitchell
Rolls Royce plc
PO Box 3
Filton, Bristol BS12 7QE

UNITED STATES

Mr J.R.Bednarski
PE-63
Naval Air Propulsion Center
PO Box 7176
Trenton, New Jersey 08628

Mr W.M.Braithwaite
Head, Experimental Section B
Engine System Division
Aeronautics Directorate
21000 Brookpark Road
Cleveland, Ohio 44235

Professor E.E.Covert
Center for Aerodynamic Studies
Room 37-401
Masschusetts Institute of Technology
Cambridge, Massachusetts 02139

Mr A.A.Martino
Manager, Systems Development and Evaluation Group —
    Code PE2
Naval Air Propulsion Center
PO Box 7176
Trenton, New Jersey 08628

Mr J.Tate
Manager, C1/C2 Test Projects
AEDC Group
Sverdrup Technology Inc.
Mail Stop 900
Arnold Air Force Station
Tennessee 37389-9998

ABSTRACT

The Advisory Report summarises the results of the Propulsion and Energetics Panel Working Group 15. The Group was in operation 1980–1987 and performed test runs of two J 57 turbojet engines at eight different facilities for ground-level and altitude tests, in five different nations. At two facilities the tests were repeated in order to review a possible deterioration of the engines. The test rig accompanied the engines to the test facilities. The tests were performed observing a carefully composed General Test Plan, being the same for all facilities. Each facility used its own data acquisition and processing system.

The activity was not only an enormous effort of man power and facility time during the tests but also included many man years for evaluating and discussing the test results. At the end of the Advisory Report, thirteen conclusions were drawn from the results.

The assessment of the measurement uncertainties was performed by a special sub-Group which reported separately (AGARDograph 307 on Measurement Uncertainty within the Uniform Engine Testing Programme).

This Advisory Report was prepared on the request of the Propulsion and Energetics Panel of AGARD.

*   *   *

Le rapport consultatif résume les résultats des travaux du Groupe de travail No.15 du Panel AGARD de Propulsion et d'Energétique. Le groupe a été actif de 1980 à 1987 et pendant cette période huit installations d'essai dans cinq pays différents ont servi au Groupe pour les essais au sol et en vol de deux turboreacteurs J 57. Dans deux cas, les essais furent repris afin de vérifier l'éventuelle dégradation des moteurs. Le montage d'essai a accompagné les moteurs d'installation en installation. Les essais ont été conduits selon un Plan d'Essai Global, pour toutes les installations. Chaque installation s'est servie de son propre système de saisie et de traitement de données.

L'opération représente non seulement un énorme effort en personnel et en moyens pour ce qui est de la période des essais, mais aussi un nombre considérable d'années homme consacrées à l'évaluation et à la discussion des résultats. Le rapport consultatif fait état de treize conclusions tirées des résultats.

L'évaluation de l'incertitude sur les mesures fut réalisée par un sous-groupe spécifique (AGARDOGRAPHIE 307 sur l'incertitude sur les mesures dans le programme uniforme des essais moteur).

Ce rapport consultatif a été réalisé à la demande du Panel AGARD de Propulsion et d'Energétique.

EXECUTIVE SUMMARY

The UETP is one of the most extensive experimental and analytical programmes ever sponsored by AGARD. The programme was proposed by the Propulsion and Energetics Panel and approved by AGARD in 1980. The objectives of the programme were:

"To provide a basis for upgrading the standards of turbine engine testing within AGARD countries by comparing test procedures, instrumentation techniques and data reduction methods, thereby increasing confidence in performance data obtained from engine test facilities.

To compare the performance of an engine measured in ground-level test facilities and in altitude facilities at the same non-dimensional conditions and establish the reasons for any observed differences."

The UETP involved testing two turbojet engines in five countries (US, Canada, France, Turkey and UK) using four altitude test facilities and four ground-level test beds. The testing programme began in 1981 and extended over a period of approximately seven years, with the supporting data analysis programme progressing concurrently on a cooperative multi-national basis. The programme has an historic importance in that for the first time it has made possible direct comparisons of engine performance as measured in a closely controlled test programme over a range of altitudes and flight speeds, in different facilities, and using different methods of data acquisition and processing.

The test facilities which participated in the test programme are noted in the order of testing and with comments on the type of test programme.

National Aeronautics and Space Administration (NASA)	2 engines at altitude
Arnold Engineering Development Center (AEDC)	2 engines at altitude
National Research Council of Canada (NRCC)	2 engines at ground-level
Centre d'Essais des Propulseurs (CEPr)	1 engine at altitude
	2 engines at ground-level
Turkish Air Force Overhaul Base (TUAF)	1 engine at ground-level
Royal Aircraft Establishment Pyestock (RAE(P))	1 engine at altitude
Naval Air Propulsion Center (NAPC)	1 engine at ground-level (open air facility)

NOTE: NASA and NRCC performed repeat testing prior to testing at NAPC.

The test vehicle selected for the programme was the Pratt & Whitney J57-P-19W twin-spool turbojet. This engine was chosen because of its rugged, mature configuration with minimum mechanical variable geometry features which could introduce small performance variations from test to test. It was also of a size which made it acceptable for test in the facilities under consideration. The fact that, by modern standards, it is of modest aero-thermodynamic design was of no consequence. Two engines were loaned to the programme by the US Air Force. Due to higher priority test workload at some of the participating facilities, it was not possible to test both engines in all facilities as was the original intention.

At the commencement of the programme a General Test Plan was prepared which defined the location and extent of the engine instrumentation, the test conditions, the test procedure and the equations to be used for calculating the engine performance parameters. Test results were only interchanged between facilities after each completed their test programme so that each facility went into its testing 'blind' and with no basis for comparison. As the programme progressed, inter-facility comparisons became possible and extensive investigations were undertaken to discover the cause of the observed differences.

Before realistic inter-facility comparisons could be made it was necessary to establish whether the performance of the engine changed with running hours. Since the differences in most parameters were in the region of one to three per cent, it was not easy to reach a definite conclusion. Engine health was monitored carefully at each test facility and useful results were obtained from two 'loop-closing' tests made at the conclusion of the main programme (one in the altitude facility at NASA and one on the ground-level test bed at NRCC). The results from these repeat tests are not entirely conclusive, although they did give a valuable opportunity to investigate other issues which had not been foreseen at the commencement of the programme. Finally, by careful scrutiny of all the available results and the rejection of those data known to be of high risk to error, it was concluded that engine performance remained essentially constant from beginning to end of the UETP. Thus the engines were not significant contributors to the differences in engine performance as measured in the eight facilities.

The General Test Plan called for a pre-test evaluation and declaration of measurement uncertainty and this eventually developed into a subsidiary investigation which has been reported in a separate AGARDograph. The subject of error analysis is highly specialised and requires rigorous treatment; this is exemplified by the error audit procedure developed by the North American facilities and applied by each of the participating facilities. This was a valuable outcome of the UETP and resulted in better identification of error sources with consequent improvement in overall standards. In particular, the error analysis programme demonstrated the importance of setting up procedures for checking all measurement systems and applying them continuously at all stages of the test programme.

The measure of agreement between the four altitude facilities was assessed using engine performance curves based on six sets of fundamentally related parameters. The agreement was generally good with four of the six parameter sets having virtually 90 percent of all their data points within one percent (plus or minus) of the mean curves over the entire engine thrust range tested. The exceptions were fuel flow (63 percent) and net thrust (69 percent) where the data from one facility (CEPr) were significantly different at some test conditions than those from the other three facilities. Omitting the CEPr data for these two

parameters increased the proportion of data points within the one percent band to 85 percent for fuel flow and 92 percent for net thrust. Generally, the experimental results validated the facility uncertainty estimates. This is considered a good result and gives confidence in the engine performance measurements obtained in different altitude facilities.

An alternative measure of the altitude inter-facility differences is given by the spread in the engine performance parameters. The magnitudes of these spreads depend on the choice of indpendent variable held fixed as the basis of comparison as well as on the engine power setting. The figures below, which show the spread in results taken over all the ten conditions tested, were evaluated at approximately the mid-thrust level of the engine power range for the fixed parameters indicated.

Engine Parameter	Independent Variable	Inter-facility Spread (max-min) median (percent)
Net Thrust	Engine Pres. Ratio	3.4−5.4 (0.3−3.3)
Specific Fuel Cons.	Net Thrust	0.9−2.4 (0.9−2.4)
Airflow	Low Rotor Speed	1.3−3.6 (1.3−2.9)

The figures in brackets ( ) show the spreads excluding the CEPr results which contained confirmed anomalies.

Three of the ground-level test beds were compared along with the only altitude facility capable of reproducing the sea-level static test conditions (AEDC). The fourth ground-level test was at NAPC and was completed in May 1987; this test was delayed due to higher priority workload until after the other UETP tests were completed and the majority of this report written. The NAPC test results were not included in the basic comparisons for this reason. These tests are discussed separately in Appendix VIII. One might expect the spreads in data from the ground-level test beds to be less than those from the altitude facilities since only one test condition is possible in the ground-level beds and it is at relatively high pressure conditions. However, the variation in ambient temperature (16°C) at the various test sites adds considerable variability. Even with this additional variability, the experimental results generally validated the facility uncertainty estimates. Maximum spreads for ground-level conditions are noted.

Engine Parameter	Independent Variable	Inter-facility spread (percent)
Thrust	Engine press ratio	0.7 (2.5)
Specific Fuel Cons.	Net Thrust	1.8 (3.5)
Airflow	Low Rotor Speed	1.9 (4.8)

Values in brackets ( ) include TUAF data inappropriate for direct comparison in some cases

Altitude and ground test facility data were compared by adjusting the data to a common environment through use of specified UETP referred equations. The adjustment technique was shown to be adequate for small inlet temperature differences. Engine performance results derived from ground-level beds and from altitude test cells generally agree when test environmental factors are properly introduced through the use of the engine mathematical model.

Key contributions of the UETP to the participating countries are:

— A standard methodology for objective assessment of the quality of measured engine performance in the various test facilities was derived and implemented.

— A data base of standard engine performance parameters was created for each test facility. This information permits future evaluation of current capabilities of engine test facilities and provides the basis and impetus for facility improvements.

— Each participant in the UETP found anomalies in his facility test and evaluation techniques which have caused an internal re-evaluation. Problems varied in degree, but in some cases the problem would not have been discovered without the ability to compare with the other facilities. This has emphasised the importance of providing redundant instrumentation and analyses in solo testing programmes so that performance cross-checks can be applied.

— Experienced turbine engine testing experts from each country participated in the UETP. Their analysis of the UETP test data and facility differences have explained the sensitivities of many test parameters which have not previously been explored for lack of a unique set of comparative test data.

— Well-established national test centres have been provided with an incentive to improve their turbine engine test data by adopting better methodology, procedures or equipment.

— Test facilities which were previously used primarily for logistic overhaul evaluations have been placed well up the learning curve as they seek research and development test status.

— Those AGARD countries which did not test the engine but provided active experts for the analysis have gained unique experience. Such experience can prove invaluable as those countries build or modify their own test facilities or as turbine engine test data are interpreted across international borders.

Finally, the extent to which the UETP has been of value and will lead to improvements in future test techniques will depend upon actions taken by each participating facility. However, there is no doubt that the growth in knowledge of better ways of testing engines has been and will continue to be reflected in an improved and more standardised test operation in all the participating countries.

CONTENTS

LIST OF FIGURES

For ease of reference the Figures are interleaved with the text in the Sections to which they refer. The numbering system reflects this arrangement — for example, Figure 13-3 is the third Figure of those relating to Section 13. Since not all the Sections have figures, there are gaps in the numerical sequence.

xv

LIST OF TABLES

1. INTRODUCTION

The general performance objectives of the UETP, as stated in the General Test Plan (Reference 1), are:

"To provide a basis for upgrading the standards of turbine engine testing within AGARD countries by comparing test-procedures, instrumentation techniques and data reduction methods, thereby increasing confidence in performance data obtained from engine test facilities.

To compare the performance of an engine measured in ground level test facilities and in altitude facilities at the same non-dimensional conditions and establish the reasons for any observed differences."

Each participating facility was required to provide a pretest Facility Test Plan defining the following:

– Test Installation

– Instrumentation Schematic

– Test Hardware

– Data Reduction Procedures and Equations

– Estimated Operational Procedures

– Engine Operational Procedures

– Engine Service Systems (Fuel, Oil, Electrical)

– Basic Engine Performance Systems (Thrust, Airflow, and Fuel Flow)

The Facility Test Plans are listed as References 2–7.

2. TEST PROGRAMME

Five countries participated in the programme and tests were undertaken in eight facilities. The facilities were located at the following Centres:

National Aeronautics and Space Administration	(NASA)
Arnold Engineering Development Center	(AEDC)
National Research Council of Canada	(NRCC)
Centre d'Essais des Propulseurs	(CEPr)
Royal Aircraft Establishment (Pyestock)	(RAE(P))
Turkish Air Force Supply and Maintenance Centre	(TUAF)*
Naval Air Propulsion Center	(NAPC)

The programme was planned on the basis that tests on ground level beds would alternate with those in altitude cells. With the exception of the first two tests (at NASA and AEDC) the original aim was maintained.

Two engines were made available for the programme and it was intended that both would be tested in each of the participating facilities thus providing a back-up in the event of failure of one engine. However, restrictions on facility availability resulted in only one engine being tested in the altitude facilities at CEPr and RAE(P) and one on the ground-level bed in Turkey and at NAPC.

Due to a higher priority workload it did not prove possible to undertake testing at NAPC until after the other UETP tests had been completed and the major part of this Report compiled. For this reason the NAPC tests are reported separately in Appendix VIII and are not included in the data comparisons within the body of the Report.

*A Turkish abbreviation of the name of this Establishment is 1. HIBM. but for simplicity it will be referred to in this Report as TUAF.

The chronological order of testing and the types of test are shown in Table 2-1:

Table 2-1
UETP test chronology

FACILITY		ALTITUDE		Ground-level	
ENGINE		607594	615037	607594	615037
NASA (FE)	US	T	T	NT	NT
AEDC	US	T	T	NT	NT
NRCC (FE)	Can	NT	NT	T	T
CEPr	Fr	T	NT	T	T
RAE(P)	UK	T*	NT	NT	NT
TUAF	TU	NT	NT	NT	T
RAE(P)	UK	T	NT	NT	NT
NASA (SE)	US	T	T	NT	NT
NRCC (SE)	Can	NT	NT	T	T
NAPC	US	NT	NT	NT	T

T = Tested   NT = Not Tested   T* = Test Aborted
FE = First Entry (first test series)
SE = Second Entry (second test series)

3. CHOICE OF TEST ENGINE

Several factors had to be taken into account when selecting the test engine, including size, availability, freedom from commercial or military restriction, consistency of performance with running hours and simplicity of the thermodynamic cycle. These requirements demanded a rugged, simple, fixed physical geometry engine with no reheat capability.

Initially nine candidate engines were considered, ranging in size from the 15.6 kN thrust GE J85 turbojet to the 97.8 kN thrust GE/SNECMA CFM56, but the choice was quickly narrowed to two, the J85 and the P&W J57. The J85 was attractive as a test vehicle because its small size would keep down testing costs, particularly in altitude facilities. However, small size was a disadvantage in that some participating facilities wished to dedicate their larger test cells to the programme and this meant that the J85 was too small to be satisfactorily tested. A more serious objection to the J85 was that the compressor incorporated some variable geometry and it was felt that this could cause small performance differences which would mask any real inter-facility effects. The choice therefore fell on the J57, a two-shaft turbojet with a take-off thrust of 50.7 kN.

4. TEST HARDWARE

This Section describes briefly the major items of the test installation which were common to all test locations, namely the engines, modified tailpipe nozzle assembly, compressor bleed, oil cooler, engine inlet bullet nose, fuel and instrumentation.

4.1 Test Article

4.1.1 Engine

Two J57-19W non-afterburning turbojet engines, were furnished by the US Air Force for the UETP. The serial numbers of the engines were P607594 and F615037. Throughout this Report they will be referred to as Engine

607594 and Engine 615037. The basic J57 engine is a two spool axial flow machine with a nine-stage low pressure compressor, seven stage high pressure compressor, cannular combustor, single stage high pressure turbine, two stage low pressure turbine and fixed convergent nozzle with a tail cone extending through the nozzle exit plane. The only variable features are the intercompressor bleed which discharges air overboard during starting and low power operation and the aerodynamically coupled spools.

4.1.2 Modified Tailpipe and Reference Nozzle

The tailcone on the standard J57 engine extends through the nozzle exit plane and it was felt that this arrangement would make it difficult to determine with sufficient accuracy the nozzle flow and thrust coefficients, parameters considered to be of prime importance in establishing engine performance. Accordingly the standard nozzle was replaced by a cylindrical tailpipe and a convergent nozzle, fabricated by rolling sheet metal, to provide a more uniform nozzle inlet profile as well as providing a more suitable platform for the pressure and temperature instrumentation needed to establish the nozzle inlet conditions.

4.1.3 Compressor Bleeds

The production engine configuration (J57-19W) is a "bomber configuration" and utilizes two compressor bleed valves (left and right sides). Operation of the engine with two bleed valves limits the high-power, bleeds-closed speed range. To expand the bleed-closed speed range, the engine manufacturer recommended modifying the compressor bleeds to the "fighter configuration" as noted below:

	"Bomber Configuration"
Left Bleed	0.08 meter Diam Orifice
Right Bleed	0.06 meter Diam Orifice
	"Fighter Configuration"
Left Bleed	0.11 meter Diam Orifice
Right Bleed	CAPPED

For this test programme the engine bleeds were modified to a "fighter configuration". In addition, anti-icing and customer bleed ports were capped at suitable locations.

4.1.4 Oil Cooler

Since the engine operation required the use of an external oil cooler (an aircraft part), a test stand mounted oil cooler was used and shipped with the engine. This oil cooler, which used water as the coolant, was set to maintain the oil temperature at 367 ± 6K at the outlet of the oil cooler.

4.1.5 Engine Inlet Bullet Nose

The engine inlet bullet nose, which is an aircraft rather than an engine part, was fabricated from existing designs (see Reference 1). This part was then modified to permit pinning of the engine inlet instrument rakes.

4.1.6 Fuel

Jet A fuel rather than JP4, the most commonly used fuel for this engine, was used for the UETP necessitating a one-time engine re-trim of both engines at NASA. Jet A was chosen as it was the most widely available.

4.2 Test Facilities

The test installations were of two kinds – those used for ground level testing, and those used for altitude testing. The main differences lay in the arrangements at the engine inlet, the ground-level beds using a simple bellmouth through which ambient air was drawn into the engine

compressor while in the altitude cells conditioned air was supplied by the test plant through a duct coupled to the engine and the exhaust removed by the plant exhausters.

4.2.1 Ground-level Test Beds

The ground-level tests beds differed from one another in two major respects: the size of the cell cross section and the layout of the flow path. The outdoor test stand at NAPC represented one extreme, the engine being in a free field environment with no inlet silencing splitters or exhaust detuner. The other beds were enclosed cells with the inlet arranged either horizontally (NRCC and CEPr) or vertically (TUAF) and with the exhaust discharging vertically upwards.

Detailed descriptions of the individual beds are given in Appendix II A.

4.2.2 Altitude Test Cells

The altitude cells were all of the same basic, direct connect type; the main differences were the size of the cell, the design of the joint between the fixed inlet ducting and the moveable portion attached to the thrust frame, the method of measuring the inlet air flow and the geometry of the exhaust collector and its positioning in relation to the engine nozzle.

Detailed descriptions of the individual cells are given in Appendix II B.

4.2.3 Comparison of Installation Geometries

In view of the possible influence of the test installation on the performance of the engine – at the inlet by virtue of the effect on inlet total pressure profile, particularly in the boundary layer, and at the exhaust through the influence of static pressure gradients resulting from the entrained air – it was thought desirable to record the major features of each installation geometry.

NRCC CELL No. 5

CEPr TO

TUAF

0 2 4 M
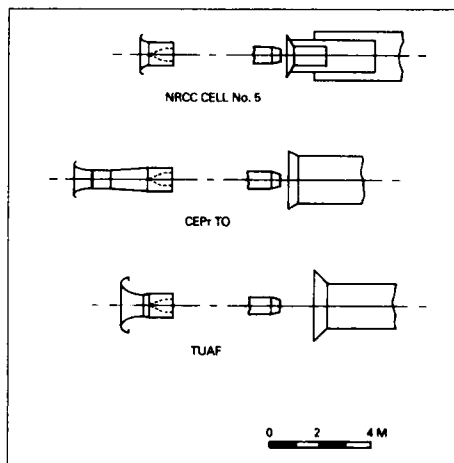
Fig.4-1 Comparison of inlet and exhaust geometries — ground level beds

The inlet and exhaust geometries of the ground-level beds are compared in Figure 4-1 and the geometries of the altitude cells in Figure 4-2. The main dimensions of the

exhaust collectors are summarised in Table 4-1. They resulted from the use of existing hardware but were considered adequate to accomplish the required tests.
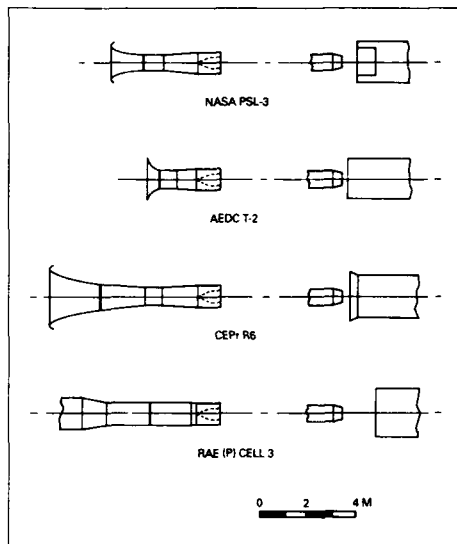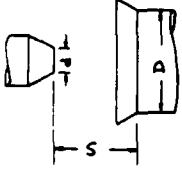
Fig.4-2 Comparison of inlet and exhaust geometries — altitude cells

Table 4-1
Comparison of exhaust geometries

d = 550 mm (nominal)

	D mm	S mm	$\frac{D}{d}$	$\frac{S}{d}$
NASA PSL3	1016	660	1.85	1.20
AEDC T2	1700	250	3.09	0.45
CEPr R6	1800	580	3.27	1.05
RAE(P) Cell 3	2134	1412	3.88	2.57
NRCC Cell 5	838	457	1.52	0.83
CEPr TO	1930	650	3.51	1.18
TUAF	1830	1500	3.33	2.73

4.3 Test Instrumentation

The instrumentation package was divided into two categories: facility peculiar, or primary instrumentation, and engine peculiar or referee instrumentation. The primary instrumentation was that used to measure those parameters required to calculate inlet total airflow, net thrust, specific fuel consumption (SFC) and pressures and temperatures to monitor the test cell environment and

engine oil condition. The referee instrumentation, which was used to set test conditions, monitor engine health and record engine performance retention, consisted of pressure and temperature probes at the engine inlet, high compressor discharge, turbine discharge, exhaust nozzle inlet and exhaust nozzle trailing edge. The referee instrumentation also included speed sensors, turbine-type fuel flow meters and associated thermocouples and vibration pickups.

Special attention was directed to the measurement of the total pressure and temperature at the compressor inlet (Station 2) and the static pressure at the nozzle outlet (Station 0.5) as these parameters have a critical influence on engine performance.

A special engine inlet bullet-nose was manufactured and used in conjunction with an instrumentation spool piece which contained an array of total pressure rakes, temperature rakes and boundary layer probes. These provided 20 mainstream total pressure measurements, 10 mainstream total temperature measurements with 16 and 10 probes measuring respectively the total pressures in the boundary layers adjacent to the outer and inner walls of the inlet annulus. Details of the location of the rakes and probes are given in Figure 4 on Page 92 of Reference 1.

PAMB was measured using probes attached to the outside of the nozzle at Station 0.5. Details of the probes and their location are given in Figures 4-3 and 4-4.

Instrumentation was provided at the high pressure compressor discharge (combustor inlet). This instrumentation provided data for some of the component performance calculations.

The locations for the majority of the instruments are shown schematically in Figure 4-3. The numbering system used to identify engine stations (not the one traditionally assigned to this engine) is in agreement with SAE ARP 755A recommendations.

Steady state instrumentation for pressure measurement was used except for the high response static pressure (several hundred Hz) needed to evaluate the turbulence characteristics of the engine inlet airflow during altitude cell testing and some transient instrumentation (several Hz) used to measure selected parameters to verify stable engine test cell conditions. All temperatures were measured with Chromel-Alumel thermocouples. Thermocouple probe designs were selected to provide negligible radiation, convection and conduction errors.

4.4 Measurement Technique and Data Recording

Detailed descriptions of the methods used to measure pressures, temperatures, shaft speeds, etc are given in Appendix II for each Facility. With the exception of TUAF, the methods used were broadly similar – analogue signals from transducers being converted to digital form and recorded for processing by computer, either in real time or off-line.

In the TUAF tests all recording was done by hand. Pressures were measured either by manometer or with Bourdon-type gauges and temperatures with a digital voltmeter. To reduce the total number of readings, the outputs from probes in similar positions were connected together. This applied particularly to the pressures and temperatures measured at the engine inlet (Station 2.0) and

ENGINE INSTRUMENTATION STATION LOCATIONS

STATION NUMBER	DESCRIPTION	NUMBER OF MEASUREMENTS				
		PRESSURES			TEMPERATURES	
		TOTAL	STATIC	DYNAMIC	TOTAL	SKIN
2.0	ENGINE OR LPC INLET	46	8	2	10	2
1.3	LPC BLEED ANNULUS	0	1	0	0	0
1.4	LPC BLEED PORT	2	0	0	4	0
3.0	COMBUSTOR INLET	6	0	0	6	0
3.1	HPC DISCHARGE	0	2	0	0	0
5.0	LPT EXIT	1	0	0	5	0
7.0	EXHAUST NOZZLE INLET	36	4	0	36	4
8.0	EXHAUST NOZZLE EXIT (INTERNAL)	0	0	0	0	0
0.4	EXHAUST NOZZLE (EXTERNAL)	0	4	0	0	0
0.5	EXHAUST NOZZLE EXIT (EXTERNAL)	0	4	0	0	2

Fig.4-3 UETP engine referee instrumentation

STAINLESS STEEL TUBE
1.6 MM DIAMETER x 0.3 MM WALL

0.8 MM R
TUBE END
PLUGGED

9.5 MM

AIR FLOW

NOZZLE EXIT PLANE

DRILL THROUGH .4 MM DIAMETER
(EACH SIDE OF TUBE)

SECTION A-A
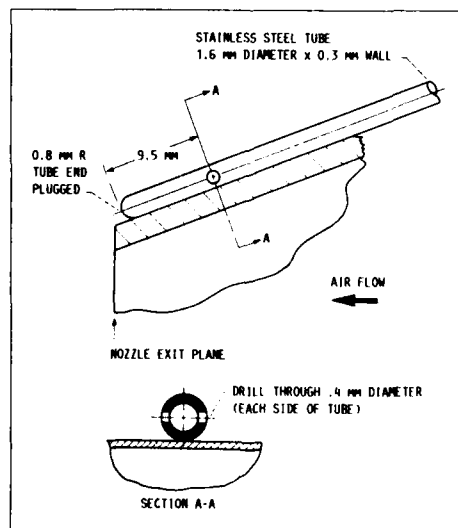
Fig.4-4 Nozzle exit lip static pressure probes

in the jet pipe (Station 7.0). At Station 2.0 the 20 mainstream total pressure probes were connected in such a way as to give eight separate outputs and the 10 thermocouples connected to give two outputs. At Station 7.0 the 36 total pressure probes were connected to give five outputs as were the 36 thermocouples. The choice of which probes to connect together was made in consultation with members of the Working Group.

5. TEST CONDITIONS

Two sets of test conditions were used for the UETP, one applicable to altitude test facilities and one to ground-level test facilities.

5.1 Altitude Testing

In an altitude facility it is possible to vary independently the three major parameters affecting engine performance – inlet total pressure, inlet total temperature and ram ratio.

When designing the matrix of test conditions for the UETP, it was decided to vary each of these major parameters in turn while keeping the other two constant. In this way the effects of each on the engine performance could be examined.

The range of conditions selected was to a large extent determined by the capabilities of the participating facilities, but it was agreed that it was desirable to cover as wide a range as possible. Accordingly the following conditions were chosen:

Table 5-1
UETP test conditions (extract from Table III of Reference 1)

TEST CONDITION	INLET TOTAL PRESSURE kPa	RAM RATIO	INLET TOTAL TEMPERATURE K
1	82.7	1.00	253
2	82.8	1.00	268
3	82.7	1.00	288
4	82.7	1.00	308
5	82.7	1.06	288
6	82.7	1.30	288
7	51.7	1.30	288
8	34.5	1.30	288
9	20.7	1.30	288
10	82.7	1.70	288
11*	101.3	1.00	288

*Optional sea level static test condition for altitude facilities.

For ease of reference, a shorthand convention was adopted in which the three test parameters, inlet pressure, ram ratio and inlet temperature, were quoted in a fixed sequence. Thus Test Condition 6 becomes 82.7/1.3/288. The magnitudes of the quantities involved are such that confusion is unlikely.

It will be seen that Conditions 1, 2, 3 and 4 examine the effect of inlet temperature; Conditions 6, 7, 8 and 9 the effect of inlet pressure and Conditions 3, 5, 6 and 10 the effect of ram ratio.

At each test condition data scans were taken at nine engine power settings approximately equally spaced from 'bleeds just closed' speed to mil power. The speeds used are given

in Reference 1. The test sequence for the nine speed settings followed the procedure set out in Reference 8 to minimise hysteresis and thermal effects. The sequence was:

1. Mil power
2. Approximately mid way between 1 and 3
3. Bleeds just closed speed
4. Between 3 and 2
5. Between 2 and 1
6. Between 2 and 4
7. Between 4 and 3
8. Between 2 and 5
9. Between 5 and 1

Graphically, the test sequence appears as follows:
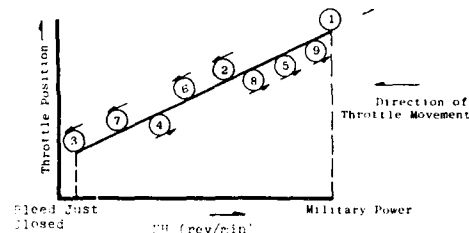
When approaching each setting the throttle lever was moved slowly towards the throttle position where the required speed was expected to be achieved and the engine allowed to stabilise. The set speed had to be within ± 25 rev/min of the desired. In going between two set speeds, the throttle direction was not allowed to change. In the event of a speed overshoot outside the tolerance band, the throttle setting was backed off approximately 100 rev/min and the speed reset.

At each power setting two data scans were obtained. The intent was to obtain stabilised engine performance (ie stabilised gas path). It was experimentally established that stabilised performance could be assessed after five minutes at set conditions for the initial data scan and after two minutes for the repeat data scan. Tests to confirm these values are described in Section 12.4.

5.2 Ground-level Testing

For ground-level testing, two regions of engine operation were specified:

1. Engine power setting from the 'bleeds just closed' speed to mil power (ie same as for the altitude facilities) and

2. Engine power settings from the 'bleeds just open' speed to idle power.

As ground-level test beds do not have environmental control, the engine power settings had to be established at the test temperature. For the high power region, values of NH were established for bleed valve closed and mil power. By dividing up the test range into eight equal increments, nine values of NH were obtained. The sequence of power settings was the same as in Section 4.1 and detailed in Table III of Reference 1. Two data scans after engine stabilisation were taken at each test condition. For the low power region, the speed range between idle and bleed valve closure was also divided up into nine equally spaced values of NH and the power settings sequenced in the same manner as for the high speed range.

6. THE TEST PROGRAMME

6.1 Configuration Changes during Testing

6.1.1 Station 7 rake alignment

During the initial UETP tests at NASA it was observed that the Station 7 total pressure, P7, appeared too low when compared with other engine data. The initial positions of the Station 7 instrument rakes (22½° clockwise from top dead centre (TDC)) were such that none of the rakes adequately defined the flow non-uniformities caused by the turbine exit struts. The tailpipe and rakes were therefore rotated 12.5° counter-clockwise to bring them to the "final" position (10° clockwise from TDC); this was the position for the remainder of the UETP at NASA and at other participating facilities. This rotation resulted in an increase in the P7 values and a minor change in the Station 7 temperatures. This investigation is reported in Section 17.2.

All the NASA data obtained with Engine 615037 and all but that for Test Conditions 5, 6 and 10 with Engine 607594 were obtained with the rakes in the final (10° clockwise) position.

6.1.2 Station 7 rake replacement

As the test programme progressed an increasing number of the Station 7 thermocouples developed faults. To retrieve the situation, two rakes (those at the 10° and 100° positions – see Figure 46 on p98 of Reference 1) were replaced during the tests at CEPr. Checks confirmed that the change did not influence the values recorded by the remaining "good" thermocouples.

6.1.3 Station 8 area checks

As explained in Section 4.1.2 the standard J57 nozzle was replaced for the UETP tests by a cylindrical tailpipe and convergent nozzle. The engine and replacement nozzle were adjusted until the appropriate performance match parameters (eg P5Q2, NL, T5 and NH) indicated equivalence with the standard nozzle.

Checks were made to determine the nozzle area by four of the participating facilities, NASA, AEDC, NRCC, RAE(P). The nozzle diameter was measured at several angular positions, either six or eight, the mean obtained and the area of the equivalent circle calculated. The measured values of A8 are shown below.

Table 6-1
Measurements of exhaust nozzle area

	A8 sq m	Diff from Average (%)
NASA	0.2376	0.04
AEDC	0.2378	0.13
NRCC	0.2372	−0.13
RAE(P)	0.2374	−0.04
Average	0.2375	

It will be seen that for all practical purposes the area remained constant. However, there was some concern that while the geometric area appeared constant the effective

area might have changed during the course of the tests. The effects of a change in A8 were therefore investigated during the second series of tests at NASA. The results are discussed in Section 17.1.

6.1.4 Fuel control replacement

After both engines had been tested at NRCC, a fuel control gasket failed during preservation of the Engine 615037. The fuel control was replaced and the engine retested. No difference in performance was observed. Performance data before and after the fuel control change are presented in Section 4.3.1 and Table 6 of Reference 9.

6.1.5 Fuel Meter Replacement

During initial engine running for the second entry at NRCC, the engine fuel meter (WFE1 – SN 261NA171) on Engine 607594 showed erroneous measurements. The problem was traced to the turbine meter itself and on inspection several ball bearings were found to be missing. Such damage could have caused faulty readings in previous tests at other facilities.

The meter was subsequently replaced by an NRCC flowmeter of the same type to ensure that the installation effects for the replacement meter were similar.

6.2 Data Scan Changes During Testing

At each Test Condition it was planned that a total of 18 data points would be obtained (ie two data scans at each of the nine power settings). The actual number of data points used at each test facility when analysing the test results is presented in Table 6-2. Variations from the plan were the result of differing facility practices, facility limitations or identified data faults.

Table 6-2
Number of data points used for analysis

a) Engine 607594

Test Condition	Planned Data Points	Actual Data Points					
		NASA(PE)	AEDC	NRCC	CEPr	RAE(P)	TUAF
1	18	18	17	-	18	-	-
2	"	18	18	-	18	-	-
3	"	-	16	-	16	-	-
4	"	18	16	-	18	18	-
5	"	18	18	-	15	9	-
6	"	18	18	-	-	9	-
7	"	18	19	-	18	9	-
8	"	20	18	-	18	9	-
9	"	18	18	-	18	-	-
10	"	19	16	-	18	9	-
11	"	-	18	18	-	-	-

b) Engine 615037

Test Condition	Planned Data Points	Actual Data Points					
		NASA(PE)	AEDC	NRCC	CEPr	RAE(P)	TUAF
1	18	18	17	-	-	-	-
2	"	18	18	-	-	-	-
3	"	20	17	-	-	-	-
4	"	17	17	-	-	-	-
5	"	17	18	-	-	-	-
6	"	18	16	-	-	-	-
7	"	21	17	-	-	-	-
8	"	18	18	-	-	-	-
9	"	18	18	-	-	-	-
10	"	14	18	-	-	-	-
11	"	-	18	16	16	-	16

7. ACHIEVED RUNNING TIMES

The order in which the tests were run is shown in Table 2-1. The corresponding build up of running times is given in Table 7-1 below:

Table 7-1
Engine running times (hours: minutes)

FACILITY	TOTAL HOT TIME		CUMULATIVE HOT TIME		WINDMILL		MILITARY	
	Eng 594	Eng 537	Eng 594	Eng 537	Eng 594	Eng 537	Eng 594	Eng 537
NASA (PE)	45:04	29:45	45:04	29:45	2:53	1:11		
AEDC	28:00	34:30	73:04	64:15	1:35	1:30	3:30	3:48
NRCC (PE)	39:04	28:29	112:08	92:44	N/A	N/A	1:54	3:56
GL TO CEPr	4:25	11:50	116:33	104:34	N/A	N/A	1:26	0:45
Alt R6	2:00	5:30	137:33	104:34	1:32	3:00	1:11	3:30
RAE(P)*	11:17	0:00	148:50	104:34	2:20	0:00	3:50	3:00
WPAFB	3:00	0:00	151:50	104:34	N/A	3:00	1:23	7:30
TUAF	0:00	7:17	151:50	111:51	3:30	N/A	1:00	2:11
RAE(P)	23:32	0:00	175:22	111:51	2:34	3:00	1:54	1:30
NASA (SE)	32:01	20:53	207:23	132:44	3:43	1:39	4:13	1:44
NRCC (SE)	50:57	35:48	258:20	168:32	N/A	N/A	5:14	1:36
NAPC	0:00	12:58	258:20	181:30	N/A	N/A	3:30	1:23

N.A: Not applicable - engine not windmilled or ground-level test bed.

*Shortly after the initial shakedown tests had been completed by RAE(P), it was observed that the engine oil pressure was considerably higher than had been expected. The oil consumption was very high and the engine vibration levels rose above recommended limits at the higher power conditions. It was decided to remove the engine from the cell and return it to the US for examination. The engine was run on a ground-level bed at Wright Patterson Air Force Base, but no unusual characteristics were observed. The problem was assumed to have been caused by a restricted breather vent. It was therefore returned to RAE(P) where it was subsequently tested satisfactorily.

8. DATA ANALYSIS PROCEDURE

Reduction of the UETP test data utilised a set of standard equations. These were provided by NASA and are set out in Section 9 of Reference 1. For the sake of completeness the UETP nomenclature and the main equations used to derive the engine performance are given in Appendices III and IV.

It is recognized that the standard UETP equations for FGR are not appropriate for ground-level test beds. For uniformity, the results presented are based on the agreed equations although all FGR and SFCR ground-level bed values are not appropriate. A comparison using the rigorous values is presented in Appendix VIII.

At the conclusion of each facility's test programme the data were screened and parameters containing obvious errors rejected. The methods of allowing for individual failed instrumentation points, particularly in the rakes at Stations 2 and 7, are described in Appendix VI.

After the data had been validated, copies were made available in tabular form and on magnetic tape as specified in the General Test Plan (Reference 1). A specimen Test Summary Sheet is reproduced as Appendix V.

The test results were released only to those participating facilities that had completed their UETP testing and to members of the Working Group nominated by the Chairman. References 9-15 present each facility's analysis of its own data.

9. INTERFACILITY COMPARISONS

9.1 Introduction

Sets of parameters were selected to enable an assessment to be made of differences in engine performance measured at the participating facilities. The selected parameter sets are:

NLQNH vs NHRD	WFRD vs NHRD
T7Q2 vs P7Q2	FNRD vs P7Q2
WA1RD vs NLRD	SFCRD vs FNRD

Comparisons of the altitude test facilities are based on data from Engine 607594 acquired at NASA, AEDC, CEPr and RAE(P). Comparisons of the ground-level test beds are based on data from Engine 615037 acquired at NRCC, CEPr and TUAF, with comparable data from Engine 615037 obtained at the AEDC altitude facility at sea-level-static conditions included for reference. Comparisons of ground-level test beds with altitude facilities are based on data from Engine 607594 acquired at the four altitude facilities and two of the ground-level test beds (NRCC and CEPr). Comparisons with NAPC data are included in Appendix VIII.

The altitude environmental conditions tested included four inlet temperature conditions (253, 268, 288, and 308K) at constant inlet pressure (82.7 KPa) and ram ratio (1.00); four inlet pressure conditions (82.7, 51.7, 34.7, and 20.7 KPa) at constant inlet temperature (288K) and ram ratio (1.3) and four ram ratio conditions (1.00, 1.06, 1.30, and 1.70) at constant inlet temperature (288K) and inlet pressure (82.7 KPa). The selected parameters are presented for each environmental test condition investigated and grouped to illustrate inlet temperature, ram ratio, and inlet pressure effects. NASA values of T7Q2 and P7Q2 obtained at Test Conditions 5 (82.7/1.06/288) and 10 (82.7/1.7/288) have been disregarded as the tests at these conditions were run with the jet pipe instrumentation in the 'original' position when wakes from the turbine bullet support struts influenced measurements of T7 and P7. (See Section 17.2 of this Report and Section 3.2.1 of Reference 8.) The altitude facility comparison data are normalized to the desired environmental test conditions to adjust the data for differences between the as-tested inlet pressure, inlet temperature and ram ratio, and the desired environmental test conditions.

The ground-level facility comparison data are normalized to standard sea-level-static conditions (101.3/1.0/288). The ground-level facility comparison parameters include data from ground-level facilities (NRCC, CEPr, and TUAF) together with comparable data taken at sea-level-static conditions in the AEDC altitude facility.

The engine performance parameters are presented in Figures 9-1, 9-2, 9-3, 9-4 and 9-5. The scales of the graphs were deliberately chosen to reveal differences as constant increments throughout the range of conditions tested. Although this results in some compression of the curves, this is outweighed by the advantage in visual presentation. The curves have been drawn from second order polynomial curve fits of the data points from each facility. The number of data points used in calculating the curve fits is presented in Table 6-2. To quantify inter-facility differences for the purpose of comparison, the maximum spread of each parameter (expressed as a percentage of the median value) was calculated at approximately the mid-thrust point. The

magnitudes of the spreads shown on the performance curves were derived from tabulated data.

9.2 Altitude Facility Comparisons

Table 9-1 will assist the reader in following the order of data presentation in this Section.

Table 9-1
Presentation order of engine performance graphs

	82.7/1.0 Var T2	88/1.30 Var P2	82.7/288 Var ram
NLQNH vs NHRD	9-1A	9-2A	9-3A
T7Q2 vs P7Q2	9-1B	9-2B	9-3B
WA1RD vs NLRD	9-1C	9-2C	9-3C
WFRD vs NHRD	9-1D	9-2D	9-3D
FNRD vs P7Q2	9-1E	9-2E	9-3E
SFCRD vs FNRD	9-1F	9-2F	9-3F

9.2.1 NLQNH vs NHRD

Rotor speed ratio (NLQNH), as a function of high-pressure-compressor rotor speed (NHRD), is presented in Figures 9-1A, 9-2A and 9-3A. The performance trends from all facilities were consistent (curve slopes similar) and the spreads at approximately the mid-thrust point varied between 0.4 and 0.8 per cent. The highest NLQNH values were obtained from NASA; the lowest values from CEPr. No consistent differences can be attributed to inlet temperature, inlet pressure, or ram ratio effects.

9.2.2 T7Q2 vs P7Q2

Engine temperature ratio (T7Q2), as a function of engine pressure ratio (P7Q2), is presented in Figures 9-1B, 9-2B and 9-3B. The performance trends from all facilities were consistent (curve slopes similar) and the spreads at approximately the mid-thrust point varied between 0.6 and 2.0 per cent. The highest T7Q2 values were generally obtained from CEPr, except at the two low inlet pressue conditions (34.5 and 20.7 KPa) where the highest T7Q2 values were obtained from RAE(P). The lowest levels were obtained from NASA and AEDC. AFDC values were within 0.5 per cent of the NASA levels. RAE(P) values were 0.5 to 1.0 per cent lower than those of CEPr (except at the noted low inlet pressure conditions). No consistent differences can be attributed to inlet temperature, inlet pressure, or ram ratio effects although the spread in T7Q2 at constant P7Q2 appears to decrease as inlet pressure decreases (differences at 34.5 and 20.7 KPa inlet pressure were less than one per cent).

9.2.3 WA1RD vs NLRD

Engine airflow (WA1RD), as a function of low-pressure-compressor rotor speed (NLRD), is presented in Figures 9-1C, 9-2C and 9-3C. The trends from all facilities were consistent (curve slopes similar); the spreads at approximately the mid-thrust point varied between 1.3 and 3.6 per cent. The highest WA1RD values were obtained from NASA, the lowest from RAE(P). The airflows from CEPr at 34.5 KPa, 1.3 ram, 288K appear to be high (two to three per cent) relative to the data at other conditions. Apart from the noted exceptions, AEDC and CEPr

airflows were in general agreement and were one to two per cent lower than NASA airflows. RAE(P) airflows were 0.5 to 1.5 per cent lower than the AEDC and CEPr values. No consistent differences can be attributed to inlet temperature or ram ratio effects.

9.2.4 WFRD vs NHRD

Engine fuel flow (WFRD), as a function of high-pressure-compressor-rotor speed (NHRD), is presented in Figures 9-1D, 9-2D and 9-3D. The performance trends from all facilities were consistent (curve slopes similar) but with significant differences in level; the spreads at approximately the mid-thrust point varied between 3.8 and 5.5 per cent. The highest values of WFRD were obtained from NASA, the lowest from CEPr. AEDC and RAE(P) WFRD values were in general agreement except at the low inlet temperature test conditions and were one to three per cent lower than NASA values. CEPr levels were less consistent relative to the other facility values; they varied from one to four per cent lower than the AEDC and RAE(P) levels. No consistent differences can be attributed to inlet temperature inlet pressure or ram ratio effects.

9.2.5 FNRD vs P7Q2

Net thrust (FNRD), as a function of engine pressure ratio (P7Q2), is presented in Figures 9-1E, 9-2E and 9-3E. The performance trends were consistent (curve slopes similar); the spreads at approximately the mid-thrust point varied between 3.4 and 5.4 per cent. The highest values of FNRD were obtained from CEPr, the lowest from AEDC. AEDC, RAE(P) and NASA values were in general agreement (about one per cent) except at the low inlet pressure test condition (20.7/1.3/288) where the AEDC values were approximately three per cent lower than the others. No consistent differences can be attributed to inlet temperature, inlet pressure or ram ratio effects.

9.2.6 SFCRD vs FNRD

Fuel consumption (SFCRD), as a function of net thrust (FNRD), is presented in Figures 9-1F, 9-2F and 9-3F. The performance trends from all facilities were generally consistent at the higher thrust levels (curve slopes similar); the spreads at approximately the mid-thrust point varied between 0.9 and 2.4 per cent. The highest values of SFCRD were obtained from NASA, the lowest from AEDC, except at the lowest inlet pressure test condition (20.7/1.3/288) where AEDC measured the highest SFCRD values. The curves from NASA, RAE(P), CEPr, and AEDC, lie in descending order. At 20.7/1.3/288, the AEDC data appear to be two per cent high relative to the data at other conditions.

9.3 Ground-level Facility Comparisons

Results from the ground-level facilities at NRCC, CEPr and TUAF are shown in Figure 9-4. For comparison, results from the AEDC altitude facility run at standard sea-level conditions are also included. This was the only altitude facility able to run at this condition.

The data show the same general trends (curve slopes similar) and, with the exception of the TUAF data, are in moderately good agreement. The reasons why the TUAF data depart rather more from the mean than do the data from the other facilities are most probably due to the lack of empirical corrections for this particular engine type. The TUAF test stand is designed for pre- and post-overhaul testing of only those engines in the TUAF inventory; since

the J57-19 is not one of these, cell correction factors were not available. In addition, manual recording of data increased the measurement uncertainty (see Section 4.4). The UETP results are not therefore considered representative of TUAF facility capability. In view of this the TUAF data have not been included when calculating the percentage spreads between facilities, but are included in the discussions which follow.

Reference should be made to Appendix VIII for a discussion of the influence of environmental factors on the measurement of thrust in a ground-level test bed. The UETP calculation procedures given in Appendix IV are known to lead to results which differ slightly from those obtained using standard methods and hence the values quoted in Sections 18.3.5 and 18.3.6 should be viewed with caution.

9.3.1 NLQNH vs NHR

Rotor Speed Ratio, NLQNH, as a function of high-pressure-rotor speed (NHR), is presented in Figure 9-4A. The performance trends from all facilities were consistent (curve slopes similar). The maximum spread at the mid-thrust point was 0.5 per cent. The NRCC and AEDC values were in close agreement, with the CEPr results slightly lower. TUAF recorded the highest values.

9.3.2 T7Q2 vs P7Q2

Engine temperature ratio (T7Q2), as a function of engine pressure ratio (P7Q2), is presented in Figure 9-4B. The performance trends were consistent (curve slopes similar). The maximum spread at the mid-thrust point was 1.1 per cent. The highest value of T7Q2 was obtained from CEPr, the lowest from TUAF.

9.3.3 WA1R vs NLR

Engine airflow (WA1R), as a function of low-pressure-compressor rotor speed (NLR), is presented in Figure 9-4C. The performance trends were consistent (curve slopes similar). The spread at the mid-thrust point was 1.9 per cent. The highest value of WA1R was obtained from TUAF, the lowest from NRCC. AEDC values were in close agreement with CEPr and lie about mid-way between the two extremes.

9.3.4 WFR vs NHR

Engine fuel flow (WFR), as a function of high-pressure-compressor rotor speed, is presented in Figure 9-4D. The performance trends were consistent (curve slopes similar). The spread in WFR at the mid-thrust point was 3.5 per cent. The highest value of WFR was obtained from TUAF the

lowest from CEPr.

9.3.5 FNR vs P7Q2

Net thrust (FNR), as a function of engine pressure ratio (P7Q2), is presented in Figure 9-4E. The performance trends were consistent (slopes of all facility curves similar). The spread in FNR at the mid-thrust point was 0.7 per cent. The TUAF values were lower than those of the other facilities.

9.3.6 SFCR vs FNR

Fuel consumption (SFCR), as a function of net thrust (FNR), is presented in Figure 9-4F. The performance trends from all facilities were consistent (curve slopes similar) except for data from TUAF which indicate a decreasing SFCR level with increasing FNR, crossing the other facility curves at the higher thrust level. The spread in SFCR at FNR = 33 kN was 1.8 per cent. At FNR values less than 43 kN the highest values of SFCR were obtained from TUAF, with values from NRCC, CEPr and AEDC in descending order.

9.4 Ground-Level Facility/Altitude Facility Comparisons

Results from tests on Engine 607594 in ground-level facilities at NRCC and CEPr and in altitude facilities at NASA, AEDC, RAE(P) and CEPr are shown in Figures 9-5A to F.

With the exception of NASA, all the altitude facility data related to an inlet temperature of 288K. Because Test Condition 3 for Engine 607594 was omitted by NASA due to a restricted test window, Test Condition 4 (308K) was substituted. In view of this difference and the uncertain magnitude of its effect on the levels of the parameters considered, the NASA data were disregarded when evaluating percentage spreads. However, to prevent misre, esentation of facility test capability, the NASA data were included in the facility comparisons.

The data show the same general trends (curve slopes similar) and are in good agreement. Except in the case of SFCR, the individual curves lie close together and no unexpected results are evident. The highest SFCR values were obtained in the NASA altitude facility, the lowest in the AEDC altitude facility.

9.5 Summary of Ground-level and Altitude Facility Comparisons

The percentage spreads in the selected performance parameters at approximately the mid-thrust point, were within the limits shown below:

Engine Parameter	NLQNH	T7Q2	WA1RD	WFRD	FNRD	SFCRD
Independent Variable	NHRD	P7Q2	NLRD	NHRD	P7Q2	FNRD
Altitude Facilities	0.4 to 0.8	0.6 to 2.0	1.3 to 3.6	3.8 to 5.5	3.4 to 5.4	0.9 to 2.4
Engine Parameter	NLQNH	T7Q2	WA1R	WFR	FNR	SFCR
Independent Variable	NHR	P7Q2	NLR	NHR	P7Q2	FNR
Ground-Level Facilities*	0.5	1.1	1.9	3.5	0.7	1.8
Ground-Level Facilities†	1.5	2.5	4.8	8.0	2.5	3.5

*Excluding TUAF (see Section 9.3)
†Including TUAF

Possible reasons for these peformance differences are discussed in subsequent Sections.
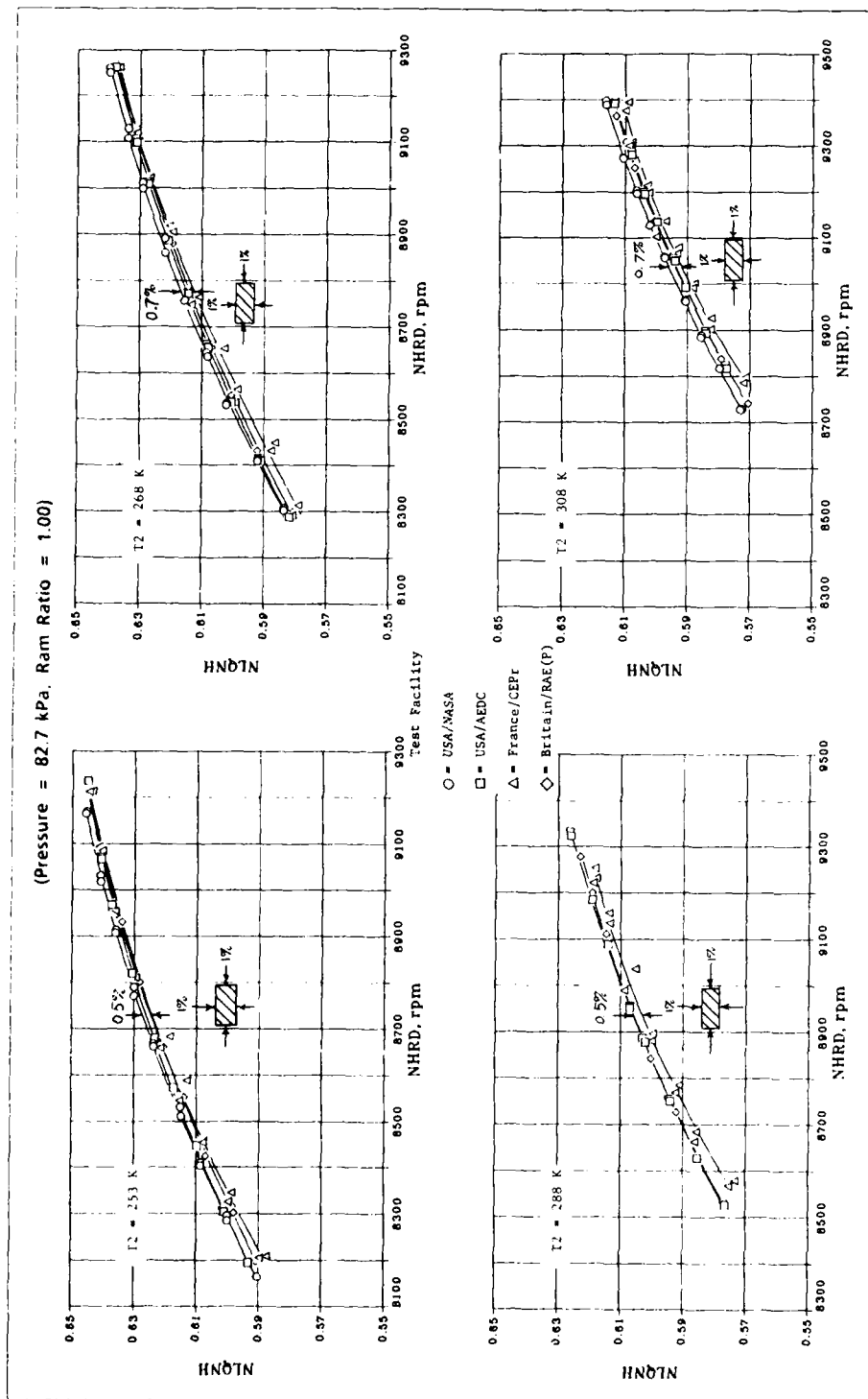
Fig 9-1a Altitude facility speed match comparison with variable inlet temperature (engine 607954)
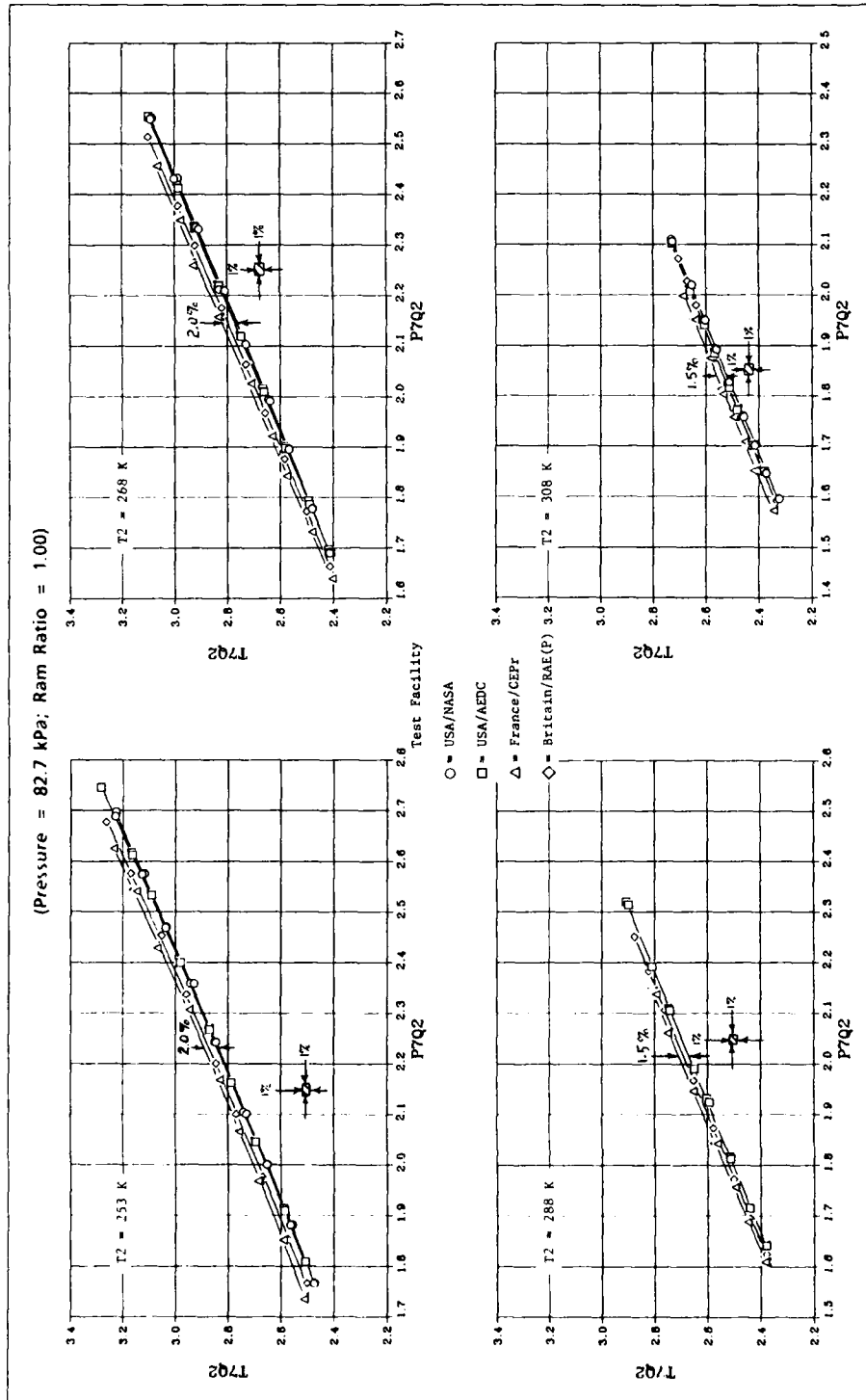
Fig.9-1b Altitude facility temperature rise comparison with variable inlet temperature (engine 607954)

12

Fig.9-1c Altitude facility airflow comparison with variable inlet temperature (engine 607954)
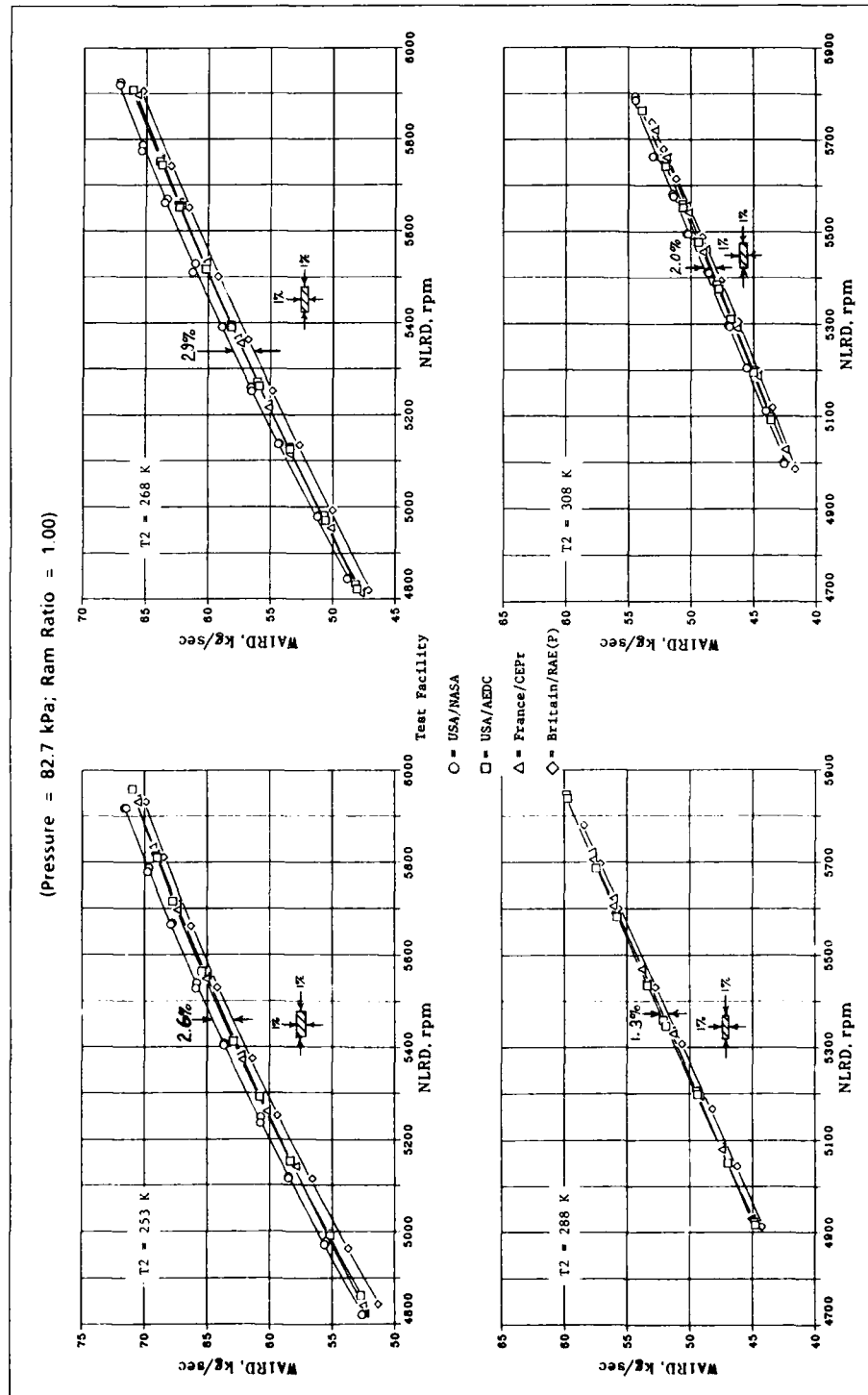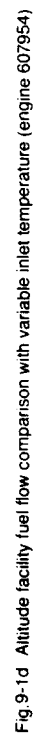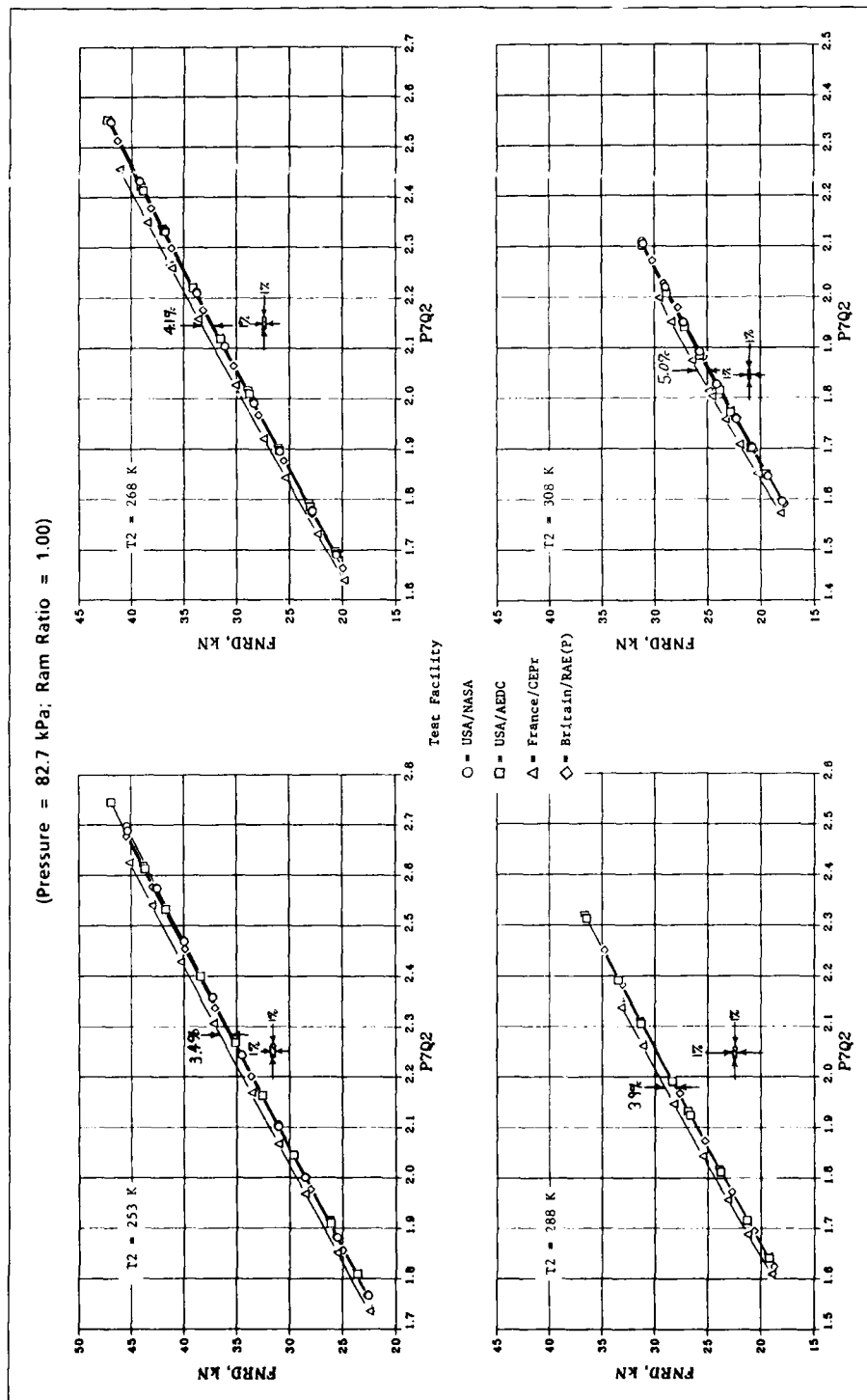
Fig. 9-1d Altitude facility fuel flow comparison with variable inlet temperature (engine 607954)

14

Fig. 9-1e Altitude facility net thrust comparison with variable inlet temperature (engine 607954)

15

(Pressure = 82.7 kPa; Ram Ratio = 1.00)

Test Facility

O = USA/NASA
□ = USA/AEDC
△ = France/CEPr
◇ = Britain/RAE(P)
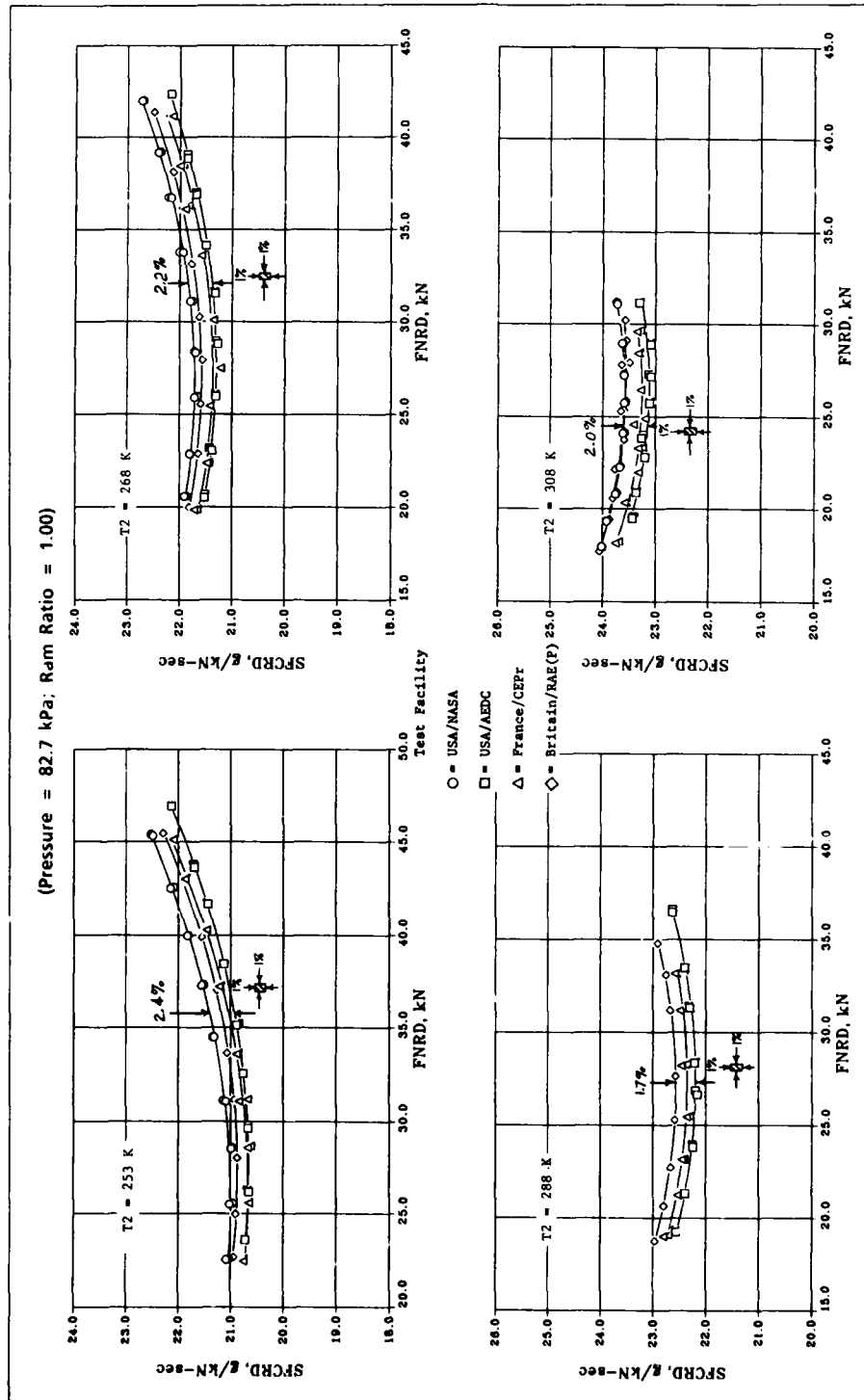
Fig.9-1f Altitude facility specific fuel consumption with variable inlet temperature (engine 607954)
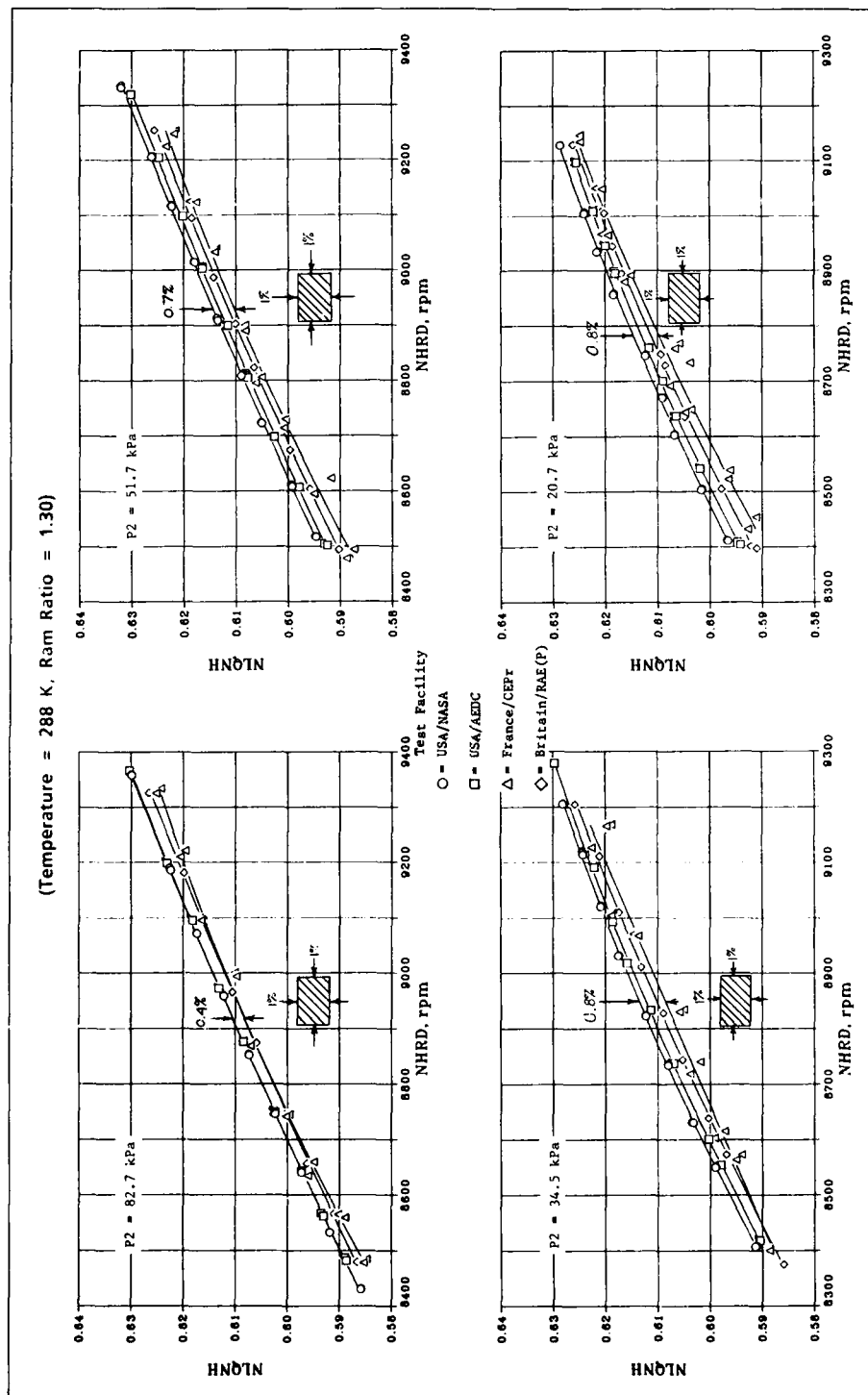
Fig. 9-2a Altitude facility speed match comparison with variable inlet pressure (engine 607954)

(Temperature = 288 K, Ram Ratio = 1.30)
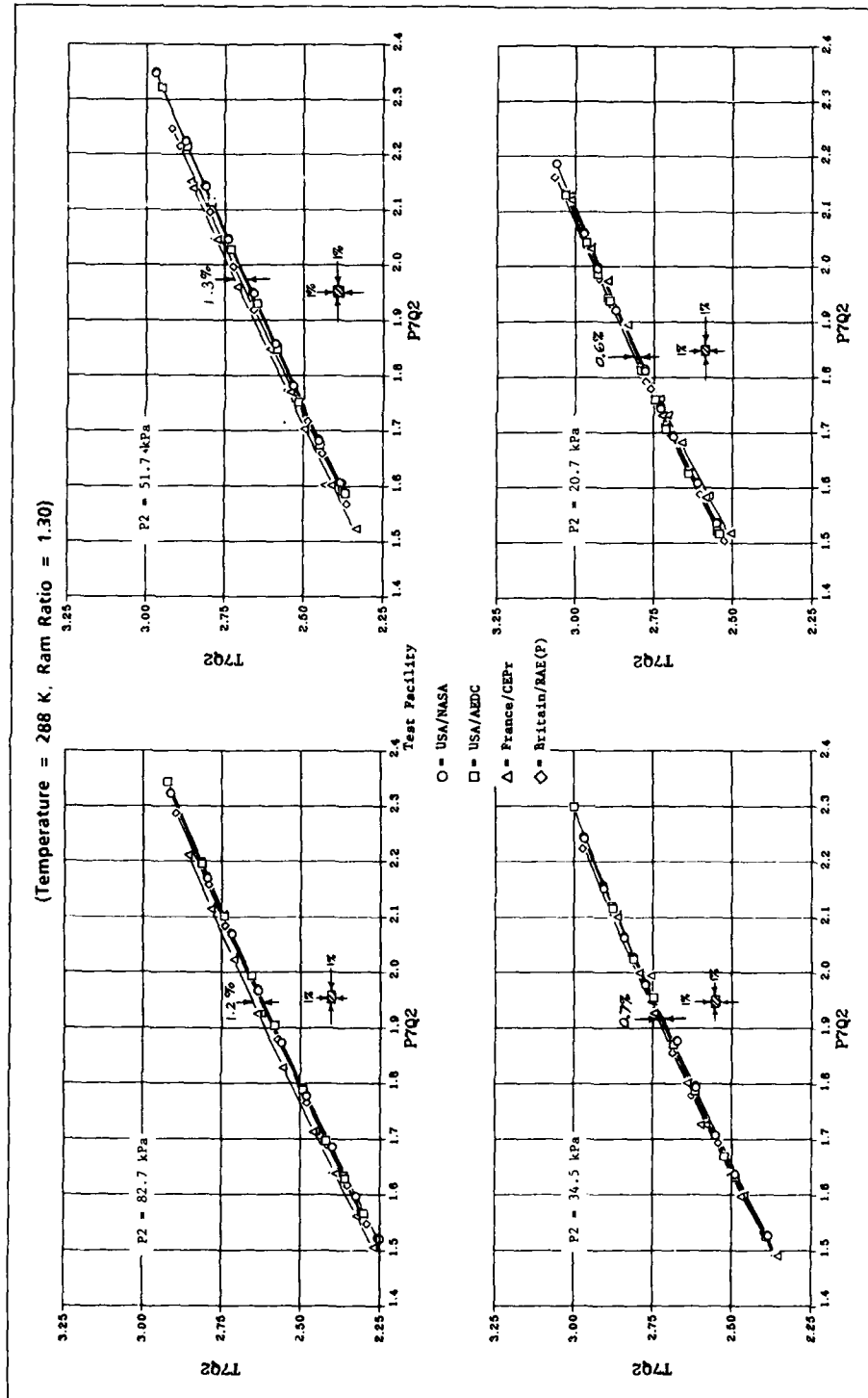
Fig. 9-2b Altitude facility temperature rise comparison with variable inlet pressure (engine 607954)

18
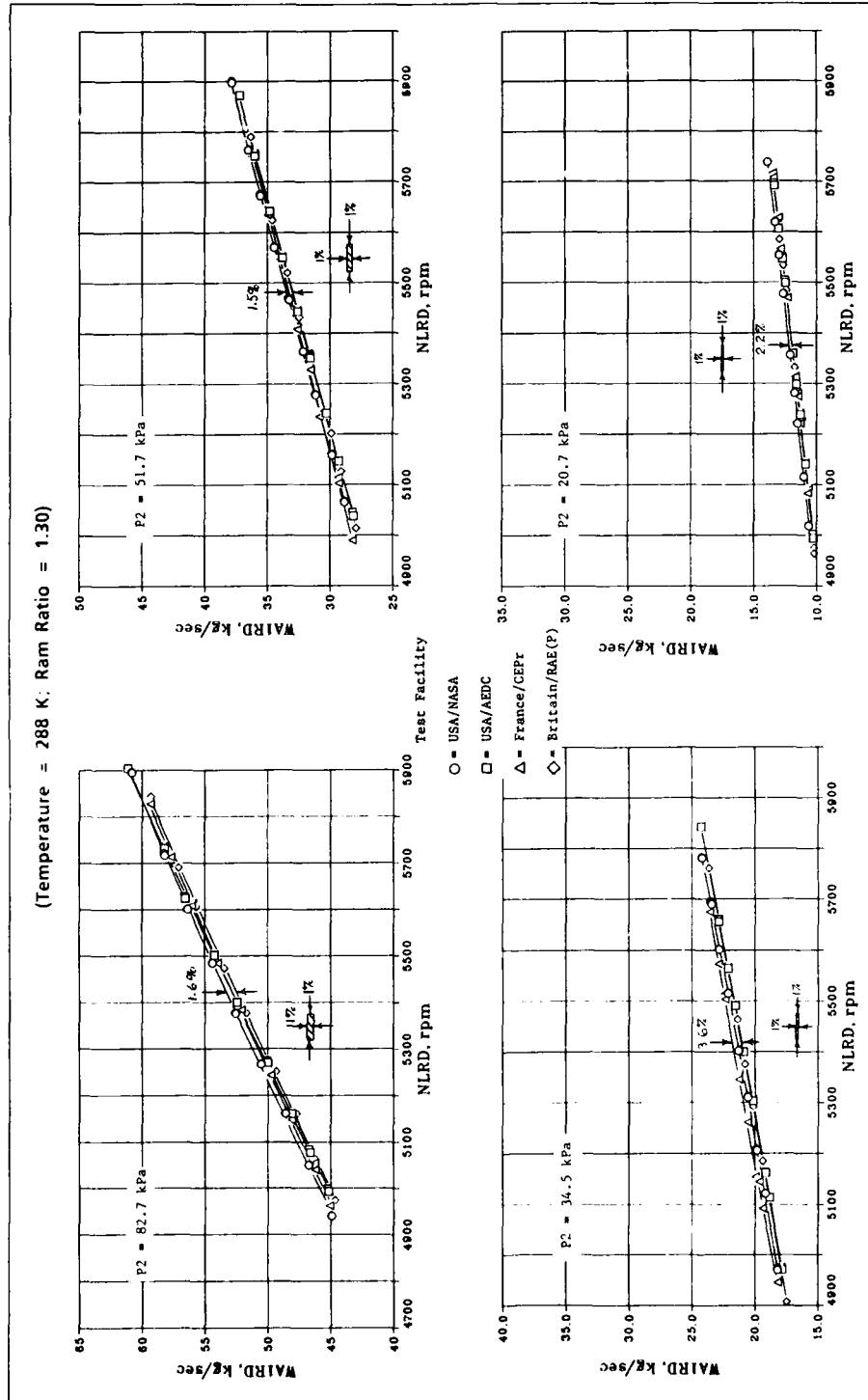
Fig 9-2c Altitude facility airflow comparison with variable inlet pressure (engine 607954)

19
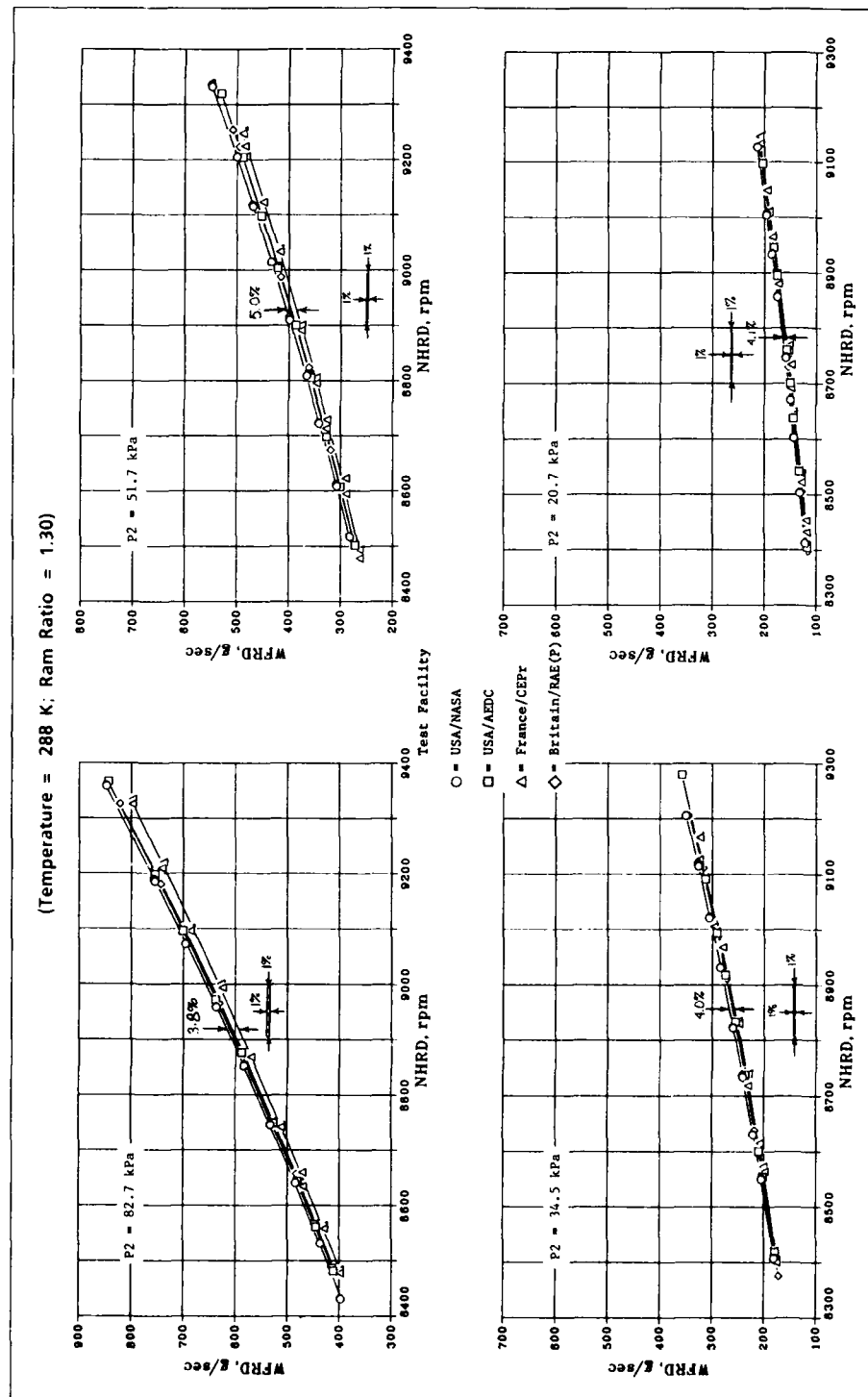
Fig.9-2d Altitude facility fuel flow comparison with variable inlet pressure (engine 607954)
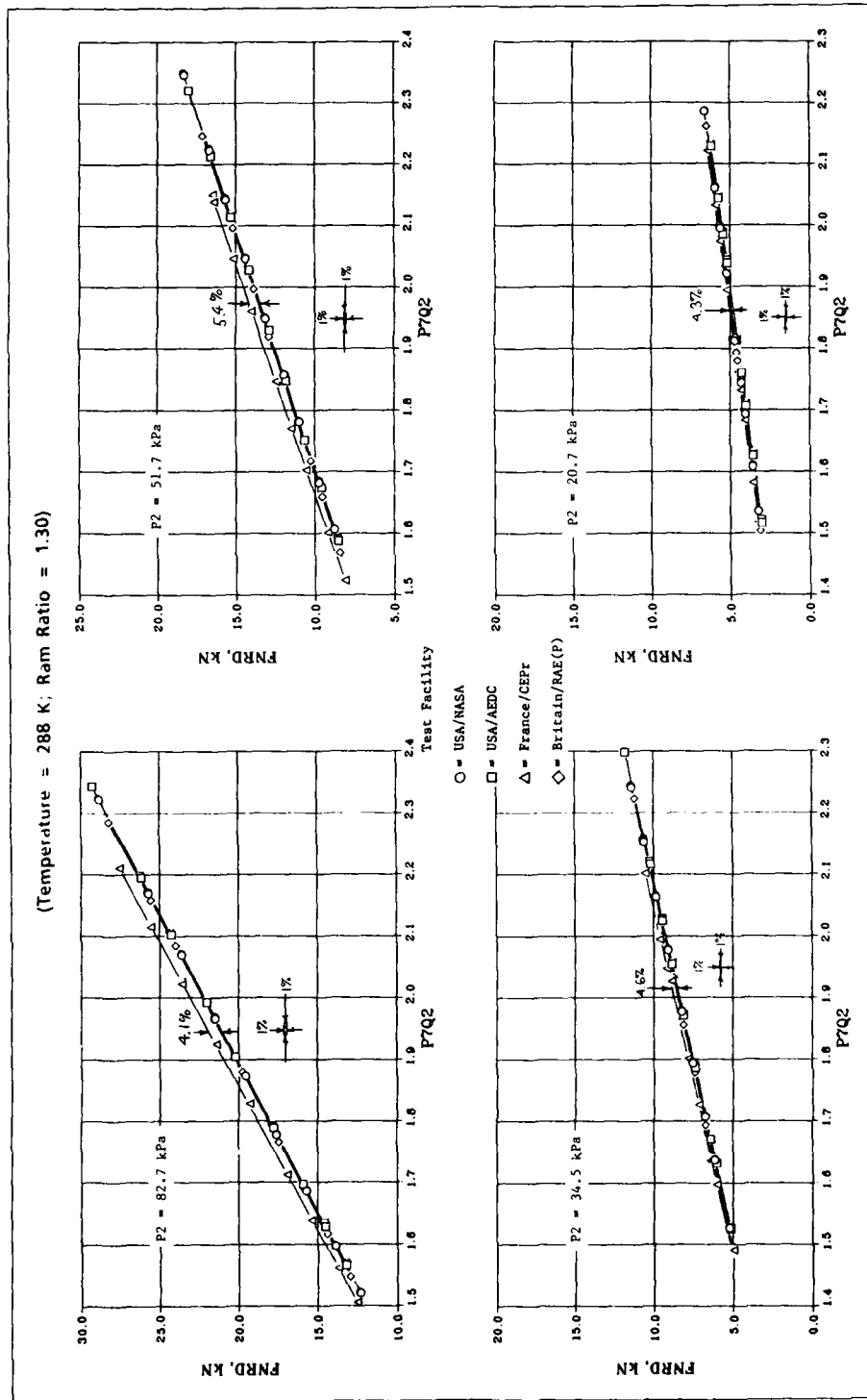
Fig.9-2e Altitude facility net thrust comparison with variable inlet pressure (engine 607954)
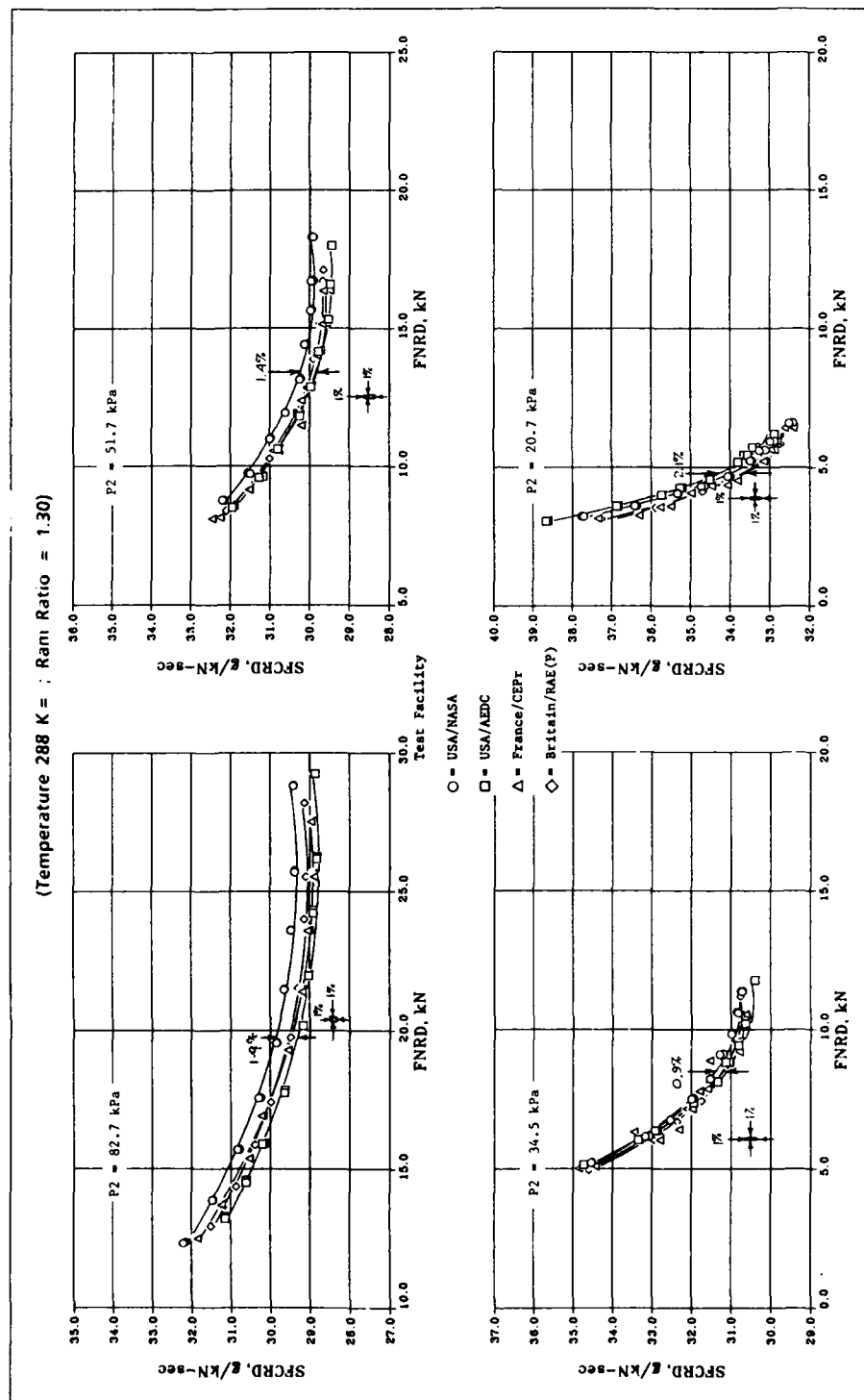
Fig 9-21 Altitude facility specific fuel consumption comparison with variable inlet pressure (engine 607954)
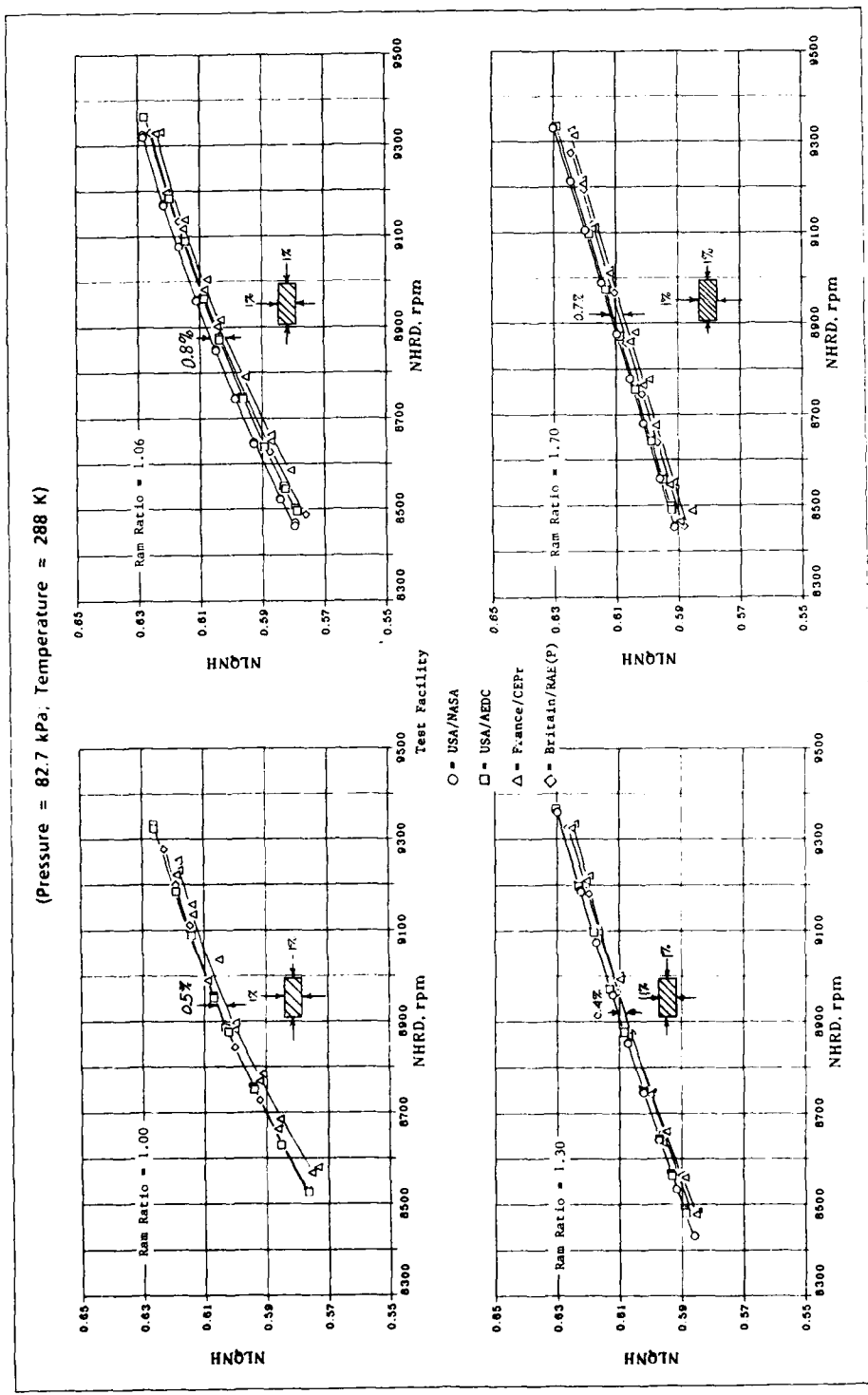
Fig 9-3a Altitude facility speed match comparison with variable RAM ratio (engine 6079954)
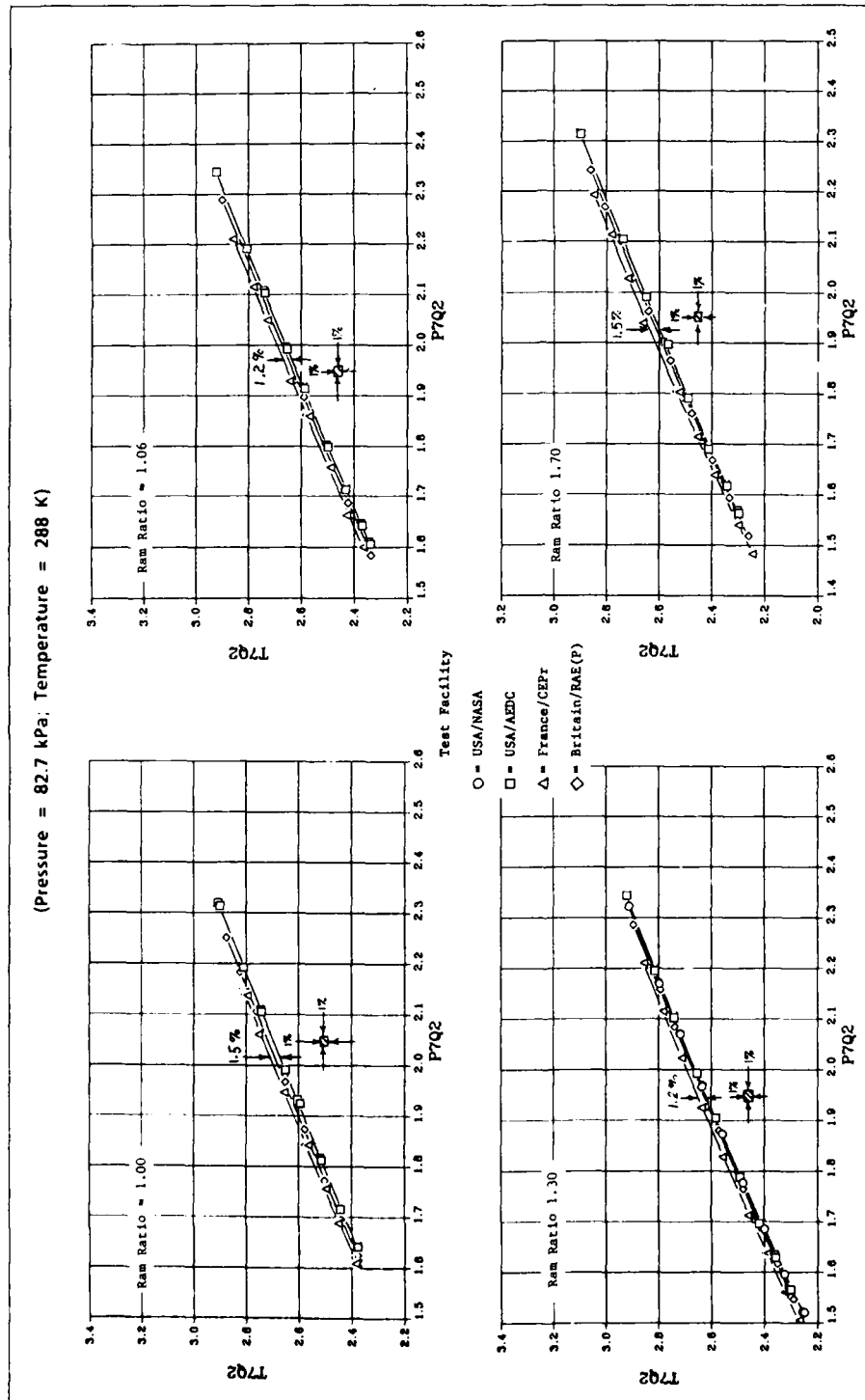
Fig 9-3b Altitude facility temperature rise comparison with variable RAM ratio (engine 607954)
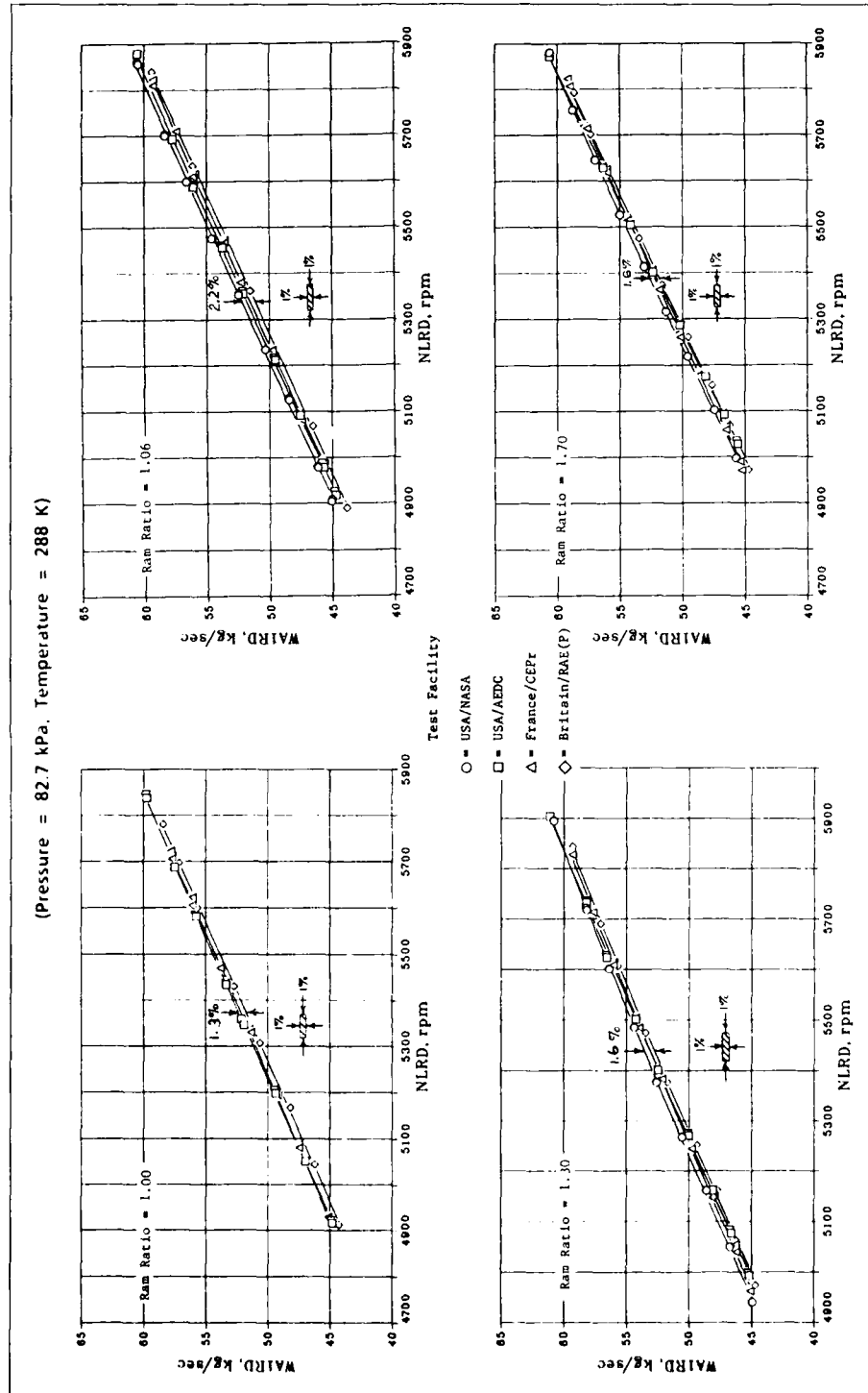
Fig 9-3c Altitude facility airflow comparison with variable RAM ratio (engine 607954)
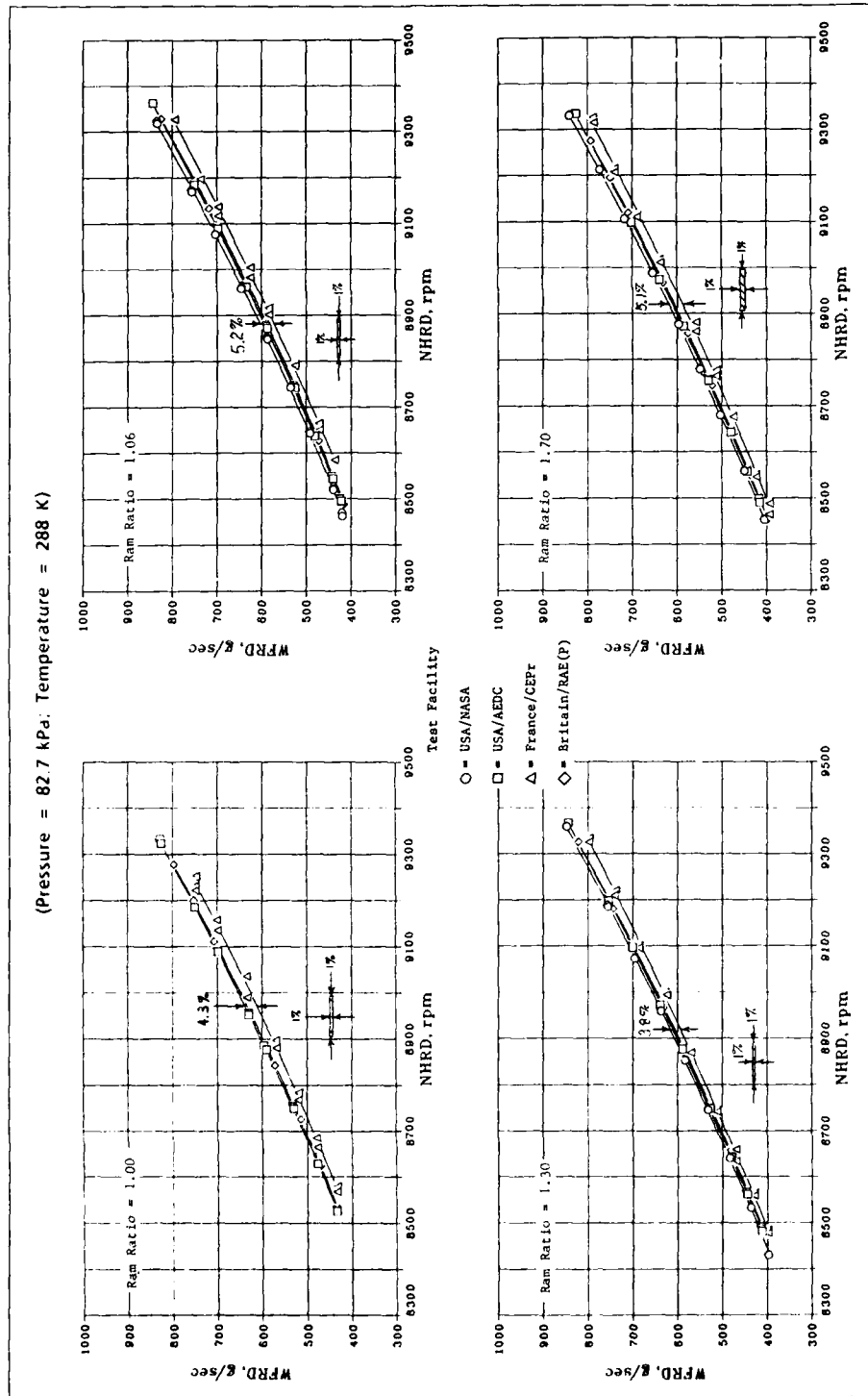
Fig 9-3d Altitude facility fuel flow comparison with variable RAM ratio (engine 607954)

26
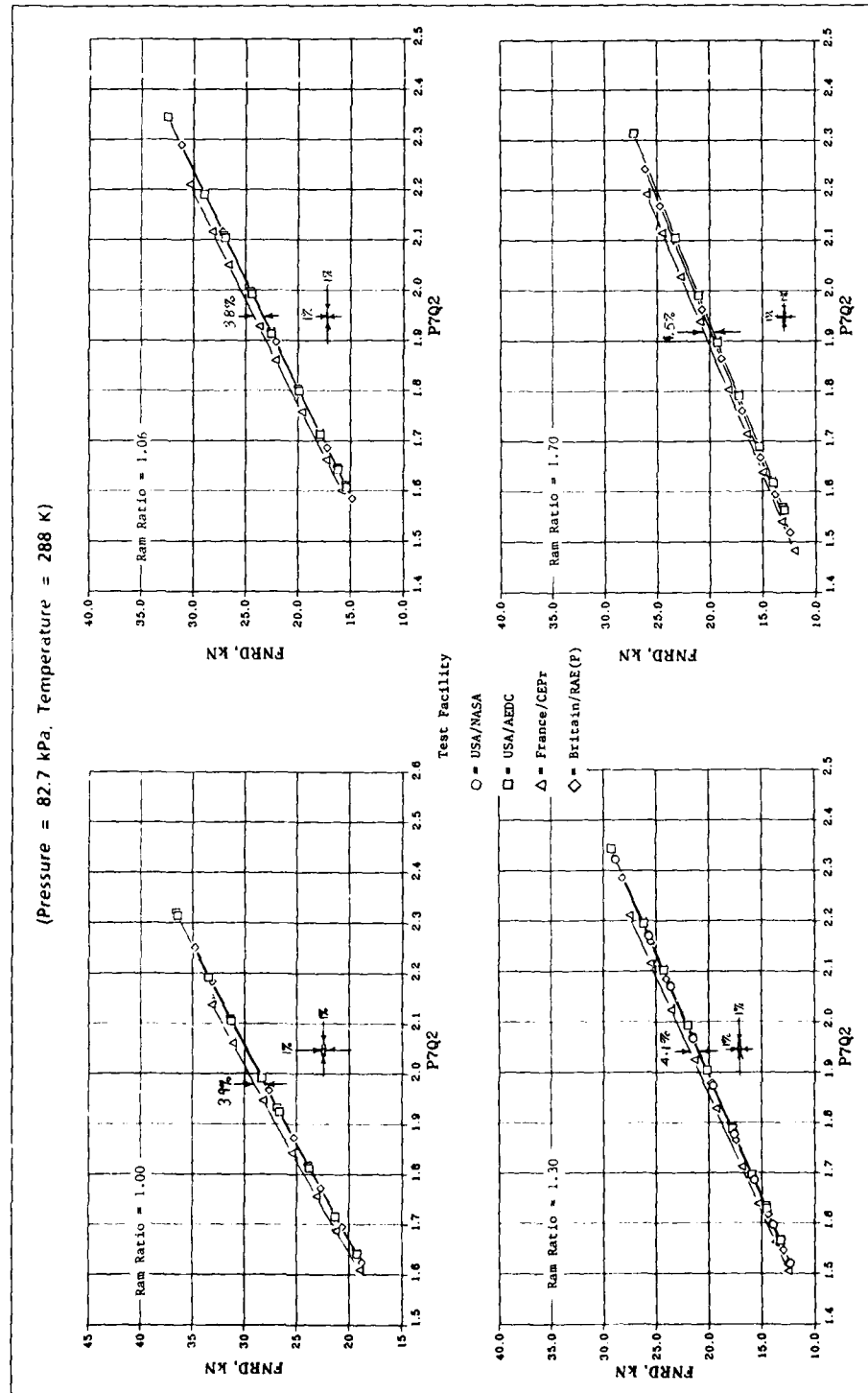
Fig 9-3e Altitude facility net thrust comparison with variable RAM ratio (engine 607954)
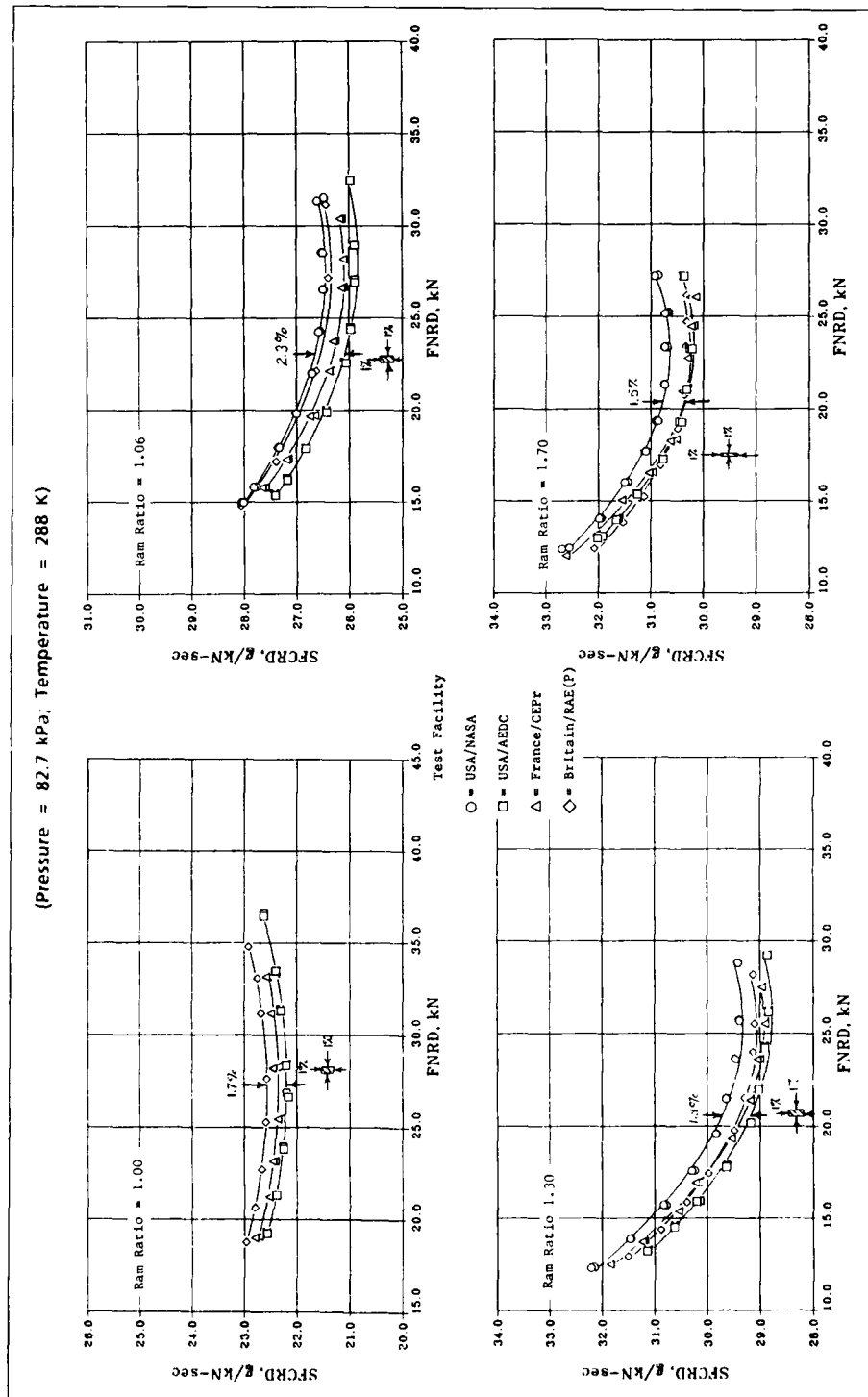
Fig 9-3f Altitude facility specific fuel consumption comparison with variable RAM ratio (engine 607954)

28
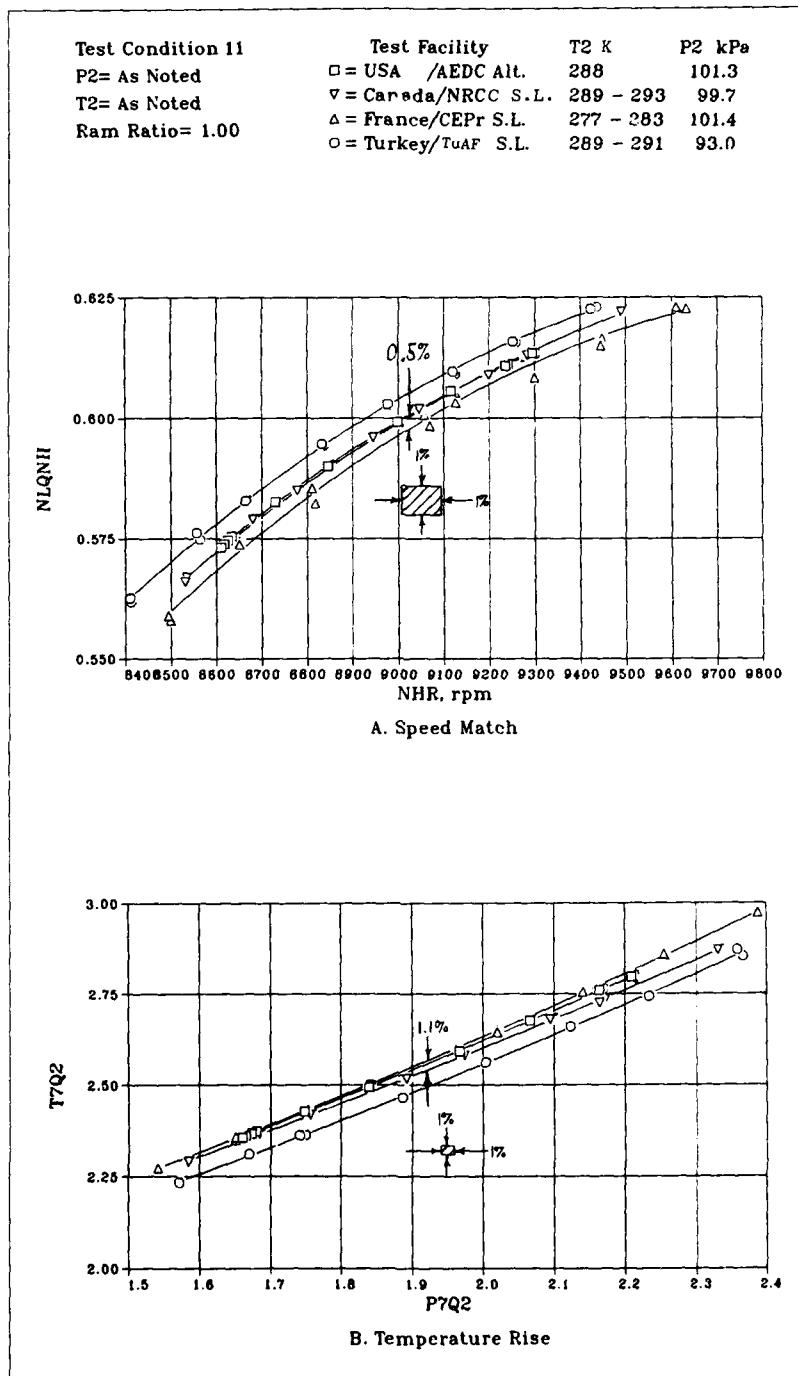
Fig.9-4 Ground level test facility comparison (engine 615037)

Test Condition 11
P2= As Noted
T2= As Noted
Ram Ratio= 1.00

Test Facility	T2 K	P2 kPa
□ = USA /AEDC Alt.	288	101.3
▽ = Canada/NRCC S.L.	289 – 293	99.7
△ = France/CEPr S.L.	277 – 283	101.4
○ = Turkey/ TuAF S.L.	289 – 291	93.0

C. Airflow

D. Fuel Flow

Fig.9-4 Continued

30
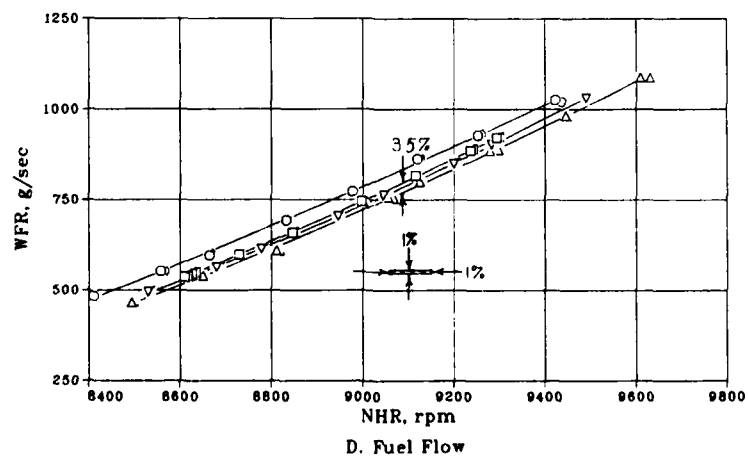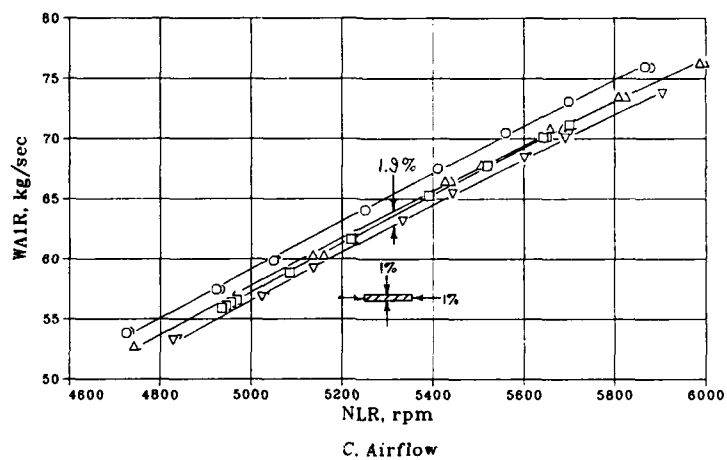
Test Condition 11

P2= As Noted

T2= As Noted

Ram Ratio= 1.00

Test Facility	T2 K	P2 kPa
□ = USA /AEDC Alt.	288	101.3
∇ = Canada/NRCC S.L.	289 – 293	99.7
△ = France/CEPr S.L.	277 – 283	101.4
○ = Turkey/TuAF S.L.	289 – 291	93.0

E. Net Thrust
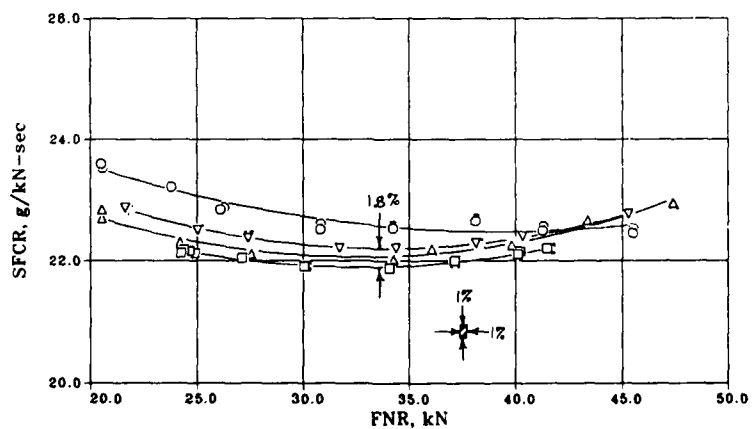
F. Specific Fuel Consumption

Fig.9-4 Concluded

Test Facility			T2 K	P2 kPa	Ram Ratio
○ = USA/NASA		Alt.	308	82.7	1.00
□ = USA	/AEDC	Alt.	288	101.3	1.00
◇ = Britain	/RAE(P)	Alt.	288	82.7	1.00
▼ = Canada	/NRCC	S.L.	289 – 293	99.7	1.00
△ = France	/CEPr	Alt.	288	82.7	1.00
▲ = France	/CEPr	S.L.	277 – 283	101.4	1.00

A. Speed Match

B. Temperature Rise
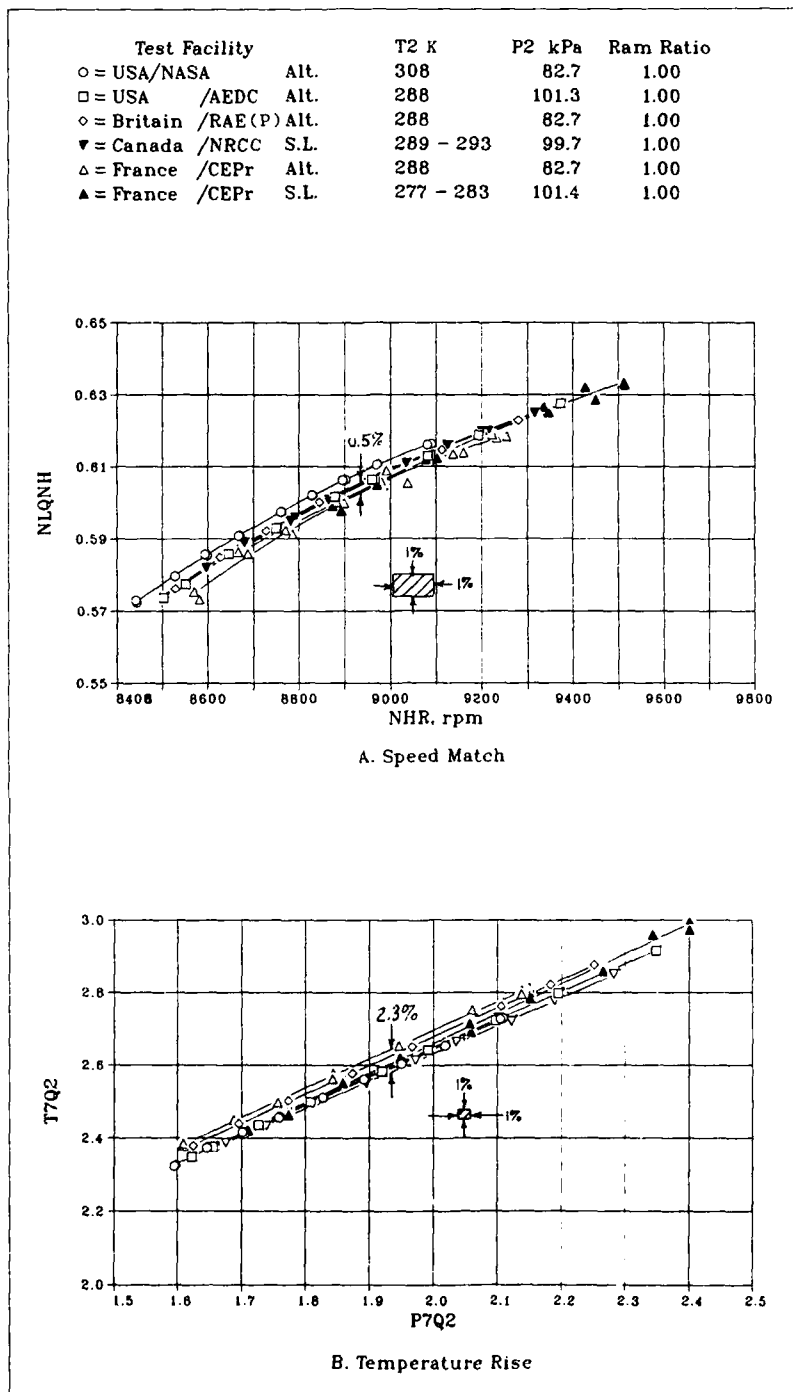
Fig-9-5 Ground level VS altitude facility comparison (engine 607594)

Test Facility		T2 K	P2 kPa	Ram Ratio
○ = USA/NASA	Alt.	308	82.7	1.00
□ = USA /AEDC	Alt.	288	101.3	1.00
◇ = Britain /RAE(P)	Alt.	288	82.7	1.00
▼ = Canada /NRCC	S.L.	289 – 293	99.7	1.00
△ = France /CEPr	Alt.	288	82.7	1.00
▲ = France /CEPr	S.L.	277 – 283	101.4	1.00

C. Airflow

D. Fuel Flow

Fig.9-5 Continued

33

Test Facility		T2 K	P2 kPa	Ram Ratio
○ = USA/NASA	Alt.	308	82.7	1.00
□ = USA /AEDC	Alt.	288	101.3	1.00
◇ = Britain /RAE(P)	Alt.	288	82.7	1.00
▼ = Canada /NRCC	S.L.	289 – 293	99.7	1.00
△ = France /CEPr	Alt.	288	82.7	1.00
▲ = France /CEPr	S.L.	277 – 283	101.4	1.00

E. Net Thrust

F. Specific Fuel Consumption

Fig.9-5 Concluded

34

10. MEASUREMENT UNCERTAINTY ASSESSMENT METHODOLOGY

10.1 Introduction

To quantify inter-facility differences attributable to measurement error and to provide a common basis for comparison of the quality of different measurement systems used, each participant was requested (Reference 1) to provide estimates of the measurement uncertainty of the primary performance parameters identified in Section 9.1. The uncertainty estimates had to be given at approximately the midpoint of the thrust range covered for a number of conditions including the sea-level static point and the high altitude point. Pre-test measurement uncertainty had to be estimated for the same parameters for all conditions tested, together with an estimate of the elemental error sources for each individual measurement used to derive these parameters. The results of this effort are presented in Reference 16. A brief summary of that work is given below.

10.2 Uncertainty Methodology

In accordance with the GTP, the method of analysis used is that described by R B Abernethy and J W Thompson in the Handbook on Uncertainty in Gas Turbine Measurement (Reference 17). According to this method the total uncertainty can be split up into a random error (scatter, precision) and a bias limit (offset) which is systematic. All error contributions are estimated separately for the basic physical parameters – force, pressure, temperature, fuel flow and shaft speed – taking into account calibration transfer, test cell system, data acquisition, data reduction errors and other effects. These single measurement channel errors are then combined into errors in the basic measurement, which defines the effective value for the engine. Overall bias limit and precision index are determined separately by root-sum-square additions of the elemental errors. The errors in the engine performance parameters are then determined by root-sum-square additions of the constituent basic measurement errors through the appropriate influence coefficients, again separately for bias and precision. Finally, for comparison of the end results, the curve slope effect has to be taken into account. Curve slope effect is the error in the dependent parameter when read from a curve at the target value of the chosen independent parameter, which itself is not error free.

10.3 Error Evaluation

For evaluation of the single measurement channel error, as well as the basic measurement error, an Error Audit has been developed. It should be noted that although the Error Audit gives a detailed layout for error book-keeping there were variations in its implementation because of differences in each facility's Data Acquisition System. Using this Error Audit and the Influence Coefficients calculated fromt the equations used to determine the engine performance parameters, the estimated bias limits and precision index can be calculated for each performance parameter pre-test.

For any single performance parameter value the total estimated pre-test uncertainty is given by combining the bias limit and the precision index. The latter is based on statistics of calibrations and of previous test results while bias error limits have an element of engineering judgement. The values of precision index and bias limit applicable to

each parameter for each facility are shown in Reference 16. It is not strictly correct to add both contributions into a single uncertainty value. A working solution is given by Abernethy who quotes two values with their effective confidence levels:

$$\text{Uadd} = B + t95\,S \qquad \text{(approx. 95\% confidence)}$$

$$\text{Urss} = [B^2 + (t95\,S)^2]^{1/2} \qquad \text{(approx. 96\% confidence)}$$

For large samples (N >> 30) t95 can be taken as 2

For the UETP the Uadd formula was used.

10.4 Results and Discussion

The Error Audit results are given in References 18 to 22 for the nominated engine performance parameters; from these results estimates of bias and precision errors and measurement uncertainties for selected calculated performance parameters were prepared (Tables 10-1 to 10-6). The TUAF facility mainly used manual recording of simple meters and since this does not lend itself to extensive analysis, only the total measurement uncertainties for TUAF are presented.

The predicted bias and precision limits (of estimated uncertainty) apply only to the parameter in question at the specified test condition. When that parameter is plotted against another parameter the total bias and precision error will include errors in both parameters. As a result, comparison between the predicted error limits and the spread of test results is not straightforward. However, a methodology has been developed by RAE(P) and is presented in Reference 23 which contains an example of its application.

10.5 Conclusions

Measurement uncertainty prediction methodology was of such importance to the UETP that a special analysis was undertaken by a sub-group chaired by J P K Vleghert (Reference 16).

For the UETP a single methodology for determining the bias limits, precision indices and overall uncertainties of the basic measurements and calculated engine performance parameters was adopted and implemented at each facility. This provided a common basis for comparison of the quality of different measurement systems in use at the participating test facilities. As a result of this work, major advances in the assessment and understanding of data quality were made by the AGARD turbine engine test community. The main conclusions were:

1. Error analysis for propulsion test facilities proved to be a highly specialised subject and required that each facility complete a rigorous elemental error audit for each of the facility basic measurement systems.

2. Estimated errors must be assigned as precision or bias according to criteria which make up the Defined Measurement Process (i.e., the facility measurment and error auditing practices). Different Defined Measurement Processes were used by each facility; as a result, elemental errors were classed as bias in one facility and as precision in another.

3. Although a common uncertainty methodology was used to make the measurement uncertainty estimates, flexibility in the definition of the Defined Measurement Process and allocation of the bias and

precision errors which are dependent on the data acquisition and calibration system of each facility resulted in considerable variation in these error components. However, there is overall agreement among the facilities when combined errors (i.e. measurement uncertainty) are considered.

4. The uncertainty estimates for the basic measurements – scale force, fuel flow, inlet pressure, inlet temperature and rotor speed – varied from 0.3 to 3.0 per cent, 0.2 to 1.1 per cent, 0.1 to 0.5 per cent, 0.3 to 0.6 per cent and 0.02 to 0.5 per cent respectively, with little difference between the ground-level test beds and the altitude cells at high inlet pressure (82.7 to 101.3 kPa). Some facilities assumed that the percentage uncertainty remained constant as the engine inlet pressure was reduced, whereas others assumed the absolute value of the uncertainty to remain constant.

5. For the altitude facilities the ranges of uncertainty estimates for the major engine performance parameters, net thrust, specific fuel consumption and airflow were ± (0.4 to 1.2), ± (0.6 to 1.8) and ± (0.4 to 0.8) per cent respectively at high inlet pressure (82.7 kPa). At low inlet pressure (20.7 kPa) both the values and spreads were considerably higher, ranging to just over ± 3.0 per cent for net thrust and specific fuel consumption. For the ground-level test beds both the values and the spreads were generally smaller than those for the altitude facilities.

6. The overall uncertainty of a parameter read from an engine performance curve is made up of the uncertainty in both the dependent and independent parameters. For some of the parameters used in the UETP, the effects of both contributions were of similar magnitude.

7. Two measurement systems were especially notable for demonstrated low measurement uncertainty

within their category; the positive displacement fuel flow meters at RAE(P) and the sonic air flow meter at AEDC.

8. A comprehensive post-test analysis is required to confirm predictions of measurement uncertainty and detect mistakes. In particular, evaluation of the Standard Error of Estimate (SEE) from the curves fitted to the data is recommended. Depending on the Defined Measurement Process, all or part of the observed SEE would be directly comparable to the estimated precision indices. Significant deviations would indicate that an improper estimate had been made in the prediction or a mistake is present in the data.

9. Three error models were used in estimating uncertainty of pressure transducers:

   a. Constant absolute error
   b. Constant percentage error
   c. Linear absolute error

Type (a) (quoted at Full Scale Output (FSO)) is that favoured by instrument manufacturers and this was applied by three facilities. This model gives large percentage estimates at low pressure. One facility specified Type (b) with the constant percentage uncertainty declared at 0.2 FSO. One facility, which had a gauge pressure system, used a linear model (Type (c)). The linear model gave a moderate percentage uncertainty at low absolute pressure, and the smallest percentage uncertainty at high absolute pressure.

10. The Standard Error of Estimate calculated from the observed scatter about the curve fits to the engine performance parameters were in reasonable agreement with the predicted precision indices for all Test Conditions.

Table 10-1
NASA (FE) Calculated performance parameter uncertainty estimates

PARAMETER	TEST CONDITION				ERROR,	PERCENT	OF READING
	NO.	P2kPa	T2,K	RAM RATIO	BIAS(B),%	PREC.(S),%	UNCERT.(U),%
NLQNH	3	82.7	288	1.00	0.02	0	0.02
	6	82.7	288	1.30	"	"	"
	9	20.7	288	1.30	"	"	"
NHRD	3	82.7	288	1.00	0.21	0.02	0.24
	6	82.7	288	1.30	"	"	"
	9	20.7	288	1.30	"	"	"
T7Q2	3	82.7	288	1.00	0.51	0.03	0.58
	6	82.7	288	1.30	"	"	"
	9	20.7	288	1.30	0.49	"	0.56
P7Q2	3	82.7	288	1.00	0.08	0.02	0.11
	6	82.7	288	1.30	"	"	"
	9	20.7	288	1.30	0.33	0.06	0.45
NLRD	3	82.7	288	1.00	0.21	0.02	0.24
	6	82.7	288	1.30	"	"	"
	9	20.7	288	1.30	"	"	"
WA1RD	3	82.7		1.00	0.48	0.13	0.74
	6	82.7	288	1.30	0.49	0.12	0.73
	9	20.7	288	1.30	1.47	0.55	2.56
FNRD	3	82.7	288	1.00	0.37	0.17	0.71
	6	82.7	288	1.30	0.45	0.20	0.86
	9	20.7	288	1.30	1.63	0.78	3.18
WFRD	3	82.7	288	1.00	0.67	0.30	1.28
	6	82.7	288	1.30	0.67	0.29	1.26
	9	20.7	288	1.30	0.71	0.50	1.70
SFCRD	3	82.7	288	1.00	0.75	0.34	1.44
	6	82.7	288	1.30	0.77	0.35	1.48
	9	20.7	288	1.30	1.69	0.91	3.51

Table 10-2
AEDC Calculated performance parameter uncertainty estimates

PARAMETER	TEST CONDITION				ERROR,	PERCENT	OF READING
	NO.	P2,kPa	T2, K	RAM RATIO	BIAS (B),%	PREC.(S),%	UNCERT.(U),%
NLQNH	3	82.7	288	1.00	0.28	0.21	0.70
	6	82.7	288	1.30	"	"	"
	9	20.7	288	1.30	"	"	"
	11	101.3	288	1.00	"	"	"
NHRD	3	82.7	288	1.00	0.22	0.16	0.54
	6	82.7	288	1.30	"	"	"
	9	20.7	288	1.30	"	"	"
	11	101.3	288	1.00	"	"	"
T7Q2	3	82.7	288	1.00	0.31	0.13	0.57
	6	82.7	288	1.30	"	"	"
	9	20.7	288	1.30	"	"	"
	11	101.3	288	1.00	"	"	"
P7Q2	3	82.7	288	1.00	0.28	0.21	0.70
	6	82.7	282	1.30	"	"	"
	9	20.7	288	1.30	"	"	"
	11	101.3	288	1.00	"	"	"
NLRD	3	82.7	288	1.00	0.22	0.16	0.54
	6	82.7	288	1.30	"	"	"
	9	20.7	288	1.30	"	"	"
	11	101.3	288	1.00	"	"	"
WA1RD	3	82.7	288	1.00	0.28	0.23	0.75
	6	82.7	288	1 30	"	"	"
	9	20.7	288	1 30	"	"	"
	11	101.3	288	1 00	"	"	"
FNRD	3	82.7	288	1.00	0.48	0.35	1.18
	6	82.7	288	1.30	0.51	0.36	1.24
	9	20.7	288	1.30	0.80	0.38	1.55
	11	101.3	288	1.00	0.47	0.35	1.17
WFRD	3	82.7	288	1.00	0.49	0.38	1.25
	6	82.7	288	1.30	"	"	"
	9	20.7	288	1.30	"	"	"
	11	101.3	288	1.00	"	"	"
SFCRD	3	82.7	2?8	1.00	0.68	0.53	1.73
	6	82.7	288	1.30	0.74	0.55	1.84
	9	20.7	288	1.30	0.96	0.56	2.08
	11	101.3	288	1.00	0.68	0.52	1.73

Table 10-3
CEPr Calculated performance parameter uncertainty estimates

PARAMETER	TEST CONDITION				ERROR,	PERCENT	OF READING
	NO.	P2,kPa	T2, K	RAM RATIO	BIAS (B),%	PREC.(S),%	UNCERT.(U),%
NLQNH	3	82.7	288	1.00	0.08	0.00	0.08
	6	82.7	288	1.30	"	"	"
	9*	20.7	288	1.30	"	"	"
	11	101.3	288	1.00	"	"	"
NHRD	3	82.7	288	1.00			
	6	82.7	288	1.30			
	9*	20.7	288	1.30			
	11	101.3	288	1.00			
T7Q2	3	82.7	288	1.00			
	6	82.7	288	1.30			
	9*	20.7	288	1.30			
	11	101.3	288	1.00			
P7Q2	3	82.7	288	1.00			
	6	82.7	288	1.30			
	9*	20.7	288	1.30			
	11	101.3	288	1.00			
NLRD	3	82.7	288	1.00			
	6	82.7	288	1.30			
	9*	20.7	288	1.30			
	11	101.3	288	1.00			
WA1RD	3	82.7	288	1.00	0.35	0.03	0.41
	6	82.7	288	1.30	0.47	0.05	0.57
	9*	20.7	288	1.30	0.84	0.08	1.00
	11	101.3	288	1.00	0.24	0.03	0.30
FNRD	3	82.7	288	1.00	0.37	0.11	0.60
	6	82.7	288	1.30	0.68	0.19	1.07
	9*	20.7	288	1.30	1.30	0.37	2.04
	11	101.3	288	1.00	0.35	0.11	0.57
WFRD	3	82.7	288	1.00	0.21	0.11	0.43
	6	82.7	288	1.30	"	"	"
	9*	20.7	288	1.30	"	"	"
	11	101.3	288	1.00	"	"	"
SFCRD	3	82.7	288	1.00	0.43	0.15	0.74
	6	82.7	288	1.30	0.72	0.22	1.16
	9*	20.7	288	1.30	1.34	0.39	2.13
	11	101.3	288	1.00	0.43	0.15	0.74

*CONDITION 9 ERROR VALUES WERE NOT AVAILABLE, CONDITION 8 (34.5 288 1.30)
VALUES SHOWN FOR REFERENCE ONLY.

Table 10-4
RAE(P) Calculated performance parameter uncertainty estimates

PARAMETER	TEST CONDITION				ERROR,	PERCENT	OF READING
	NO.	P2,kPa	T2, K	RAM RATIO	BIAS(B),%	PREC.(S),%	UNCERT.(U),%
NLQNH	3	82.7	288	1.00	0.03	0.03	0.09
	6	82.7	288	1.30	"	"	"
	9	20.7	288	1.30	"	"	"
NHRD	3	82.7	288	1.00	0.11	0.02	0.16
	6	82.7	288	1.30	"	"	"
	9	20.7	288	1.30	"	"	"
T7Q2	3	82.7	288	1.00	0.21	0.03	0.27
	6	82.7	288	1.30	"	"	"
	9	20.7	288	1.30	"	"	"
P7Q2	3	82.7	288	1.00	0.38	0.06	0.51
	6	82.7	288	1.30	"	"	"
	9	20.7	288	1.30	0.57	0.24	1.05
NLRD	3	82.7	288	1.00	0.11	0.03	0.17
	6	82.7	288	1.30	"	"	"
	9	20.7	288	1.30	"	"	"
WA1RD	3	82.7	288	1.00	0.79	0.03	0.84
	6	82.7	288	1.30	"	0.03	0 84
	9	20.7	288	1.30	0.97	0.07	1.11
FNRD	3	82.7	288	1.00	0.33	0.05	0.44
	6	82.7	288	1.30	0.34	0.07	0.48
	9	20.7	288	1.30	1.54	0.30	2.13
WFRD	3	82.7	288	1.00	0.38	0.03	0.44
	6	82.7	288	1.30	0.39	"	0.45
	9	20.7	288	1.30	0.81	0.08	0.97
SFCRD	3	82.7	288	1.00	0.48	0.06	0.61
	6	82.7	288	1.30	0.44	0.07	0.59
	9	20.7	288	1.30	1.44	0.31	2.05

Table 10-5
NRCC Calculated performance parameter uncertainty estimates

PARAMETER	TEST CONDITION				ERROR, PERCENT OF READING		
	NO.	P2,kPa	T2,K	RAM RATIO	BIAS (B), %	PREC.(S) %	UNCERT.(U), %
NLQNH	11	AMBIENT	AMBIENT	1.00	0.09	0.00	0.09
NHR	11	AMBIENT	AMBIENT	1.00	0.22	0.09	0.40
T7Q2	11	AMBIENT	AMBIENT	1.00	0.53	0.19	0.91
P7Q2	11	AMBIENT	AMBIENT	1.00	0.13	0.06	0.25
NLR	11	AMBIENT	AMBIENT	1.00	0.22	0.09	0.40
WA1R	11	AMBIENT	AMBIENT	1.00	0.60	0.04	0.68
FNR	11	AMBIENT	AMBIENT	1.00	0.43	0.10	0.63
WFR	11	AMBIENT	AMBIENT	1.00	0.45	0.13	0.71
SFCR	11	AMBIENT	AMBIENT	1.00	0.60	0.14	0.88

Table 10-6
TuAF Calculated performance parameter uncertainty estimates

PARAMETER	TEST CONDITION				ERROR, PERCENT OF READING		
	NO.	P2,kPa	T2,K	RAM RATIO	BIAS (B),%	PREC. (S),%	UNCERT.(U),%
NLQNH	11	AMBIENT	AMBIENT	1.00	N/A	N/A	0.81
NHR	11	AMBIENT	AMBIENT	1.00			0.61
T7Q2	11	AMBIENT	AMBIENT	1.00			0.45
P7Q2	11	AMBIENT	AMBIENT	1.00			0.19
NLR	11	AMBIENT	AMBIENT	1.00			0.67
WA1R	11	AMBIENT	AMBIENT	1.00			0.31
FNR	11	AMBIENT	AMBIENT	1.00			0.52
WFR	11	AMBIENT	AMBIENT	1.00			1.12
SFCR	11	AMBIENT	AMBIENT	1.00			1.23

11. LONG TERM ENGINE PERFORMANCE RETENTION

11.1 Introduction

The intention of the UETP was to provide an "identical" engine to each test facility and although the type of engine and test plan procedures were chosen to minimize time-dependent performance variations, it had to be accepted that variations were possible over the long test programme. Time-dependent performance changes can be caused by several factors including changes to the surface finish of blades due to erosion and/or contamination, clearance changes due to wear and deformation as a result of thermal or mechanical stresses. The intention of this Section is to present a methodology whereby such time-dependent variations can be quantified and separated from possible facility-induced influences.

To reduce the likelihood of engine performance changes, the relatively early technology, "mature" J57 engine was selected. Thus the characteristic wear-in process often experienced with new technology, new-piece-part engine builds was minimised. In addition, the test matrix was designed to minimize high engine power operating time and limit engine operation to well below life-limiting hot-section temperature rotor speeds. Even with these safeguards, a change in engine performance with engine operational time could have occurred.

Three procedures were adopted to obtain a quantitative assessment of the changes in engine performance over the life of the UETP. They were:

1. Book-keeping engine performance changes that occurred at each test facility.

2. Conducting the first and last engine tests in the same test facility and measuring the overall change in engine performance.

3. Monitoring data from the engine internal instrumentation throughout the test programme.

Item 1 was accomplished by having each facility conduct a repeat test at the completion of testing at the same test conditions as were used at the start of its test programme. The results of using this approach, however, were not conclusive. The difficulty was that the measured engine performance changes for the relatively short engine time involved were much smaller than the day-to-day random error values of the facility measurement system. As a result, it was not possible to discern consistent changes in the engine performance parameters.

Item 2 consisted of returning the engines to those facilities which first tested the engines, NASA for the altitude and NRCC for the ground-level tests. Re-testing at NRCC also included an engine water wash test to examine the effects of contaminants on engine performance. As was the case for Item 1 the determination of changes in engine performance was not entirely successful. The difficulty was that during the long elapsed times between the initial and repeat tests (4 years for the NASA tests and 3 years for the NRCC tests), facility equipment, measurement systems and procedure changes had taken place which resulted in changes to measured values which could not be distinguished from the measured engine performance changes. However, this was not the case for the water wash tests which were accomplished on a back-to-back basis using identical facility hardware, measurement systems and procedures.

The approach that provided the most consistent results was the monitoring of the engine internal instrumentation (Item 3). This consisted of using internal engine instrumentation to estimate changes with time in engine airflow, engine pressure/temperature ratios and engine thrust, along with the use of the engine fuel flow meter to estimate changes in engine specific fuel consumption. The following Sections describe the analysis methodology.

11.2 Performance retention analysis methodology

The analysis procedure was based on six criteria:

1. Use data from identical engine configurations.

2. Use data from identical instrumentation sensor configurations to minimize bias errors.

3. Use data with minimum precision error.

4. Use identical data calculation methods.

5. Use indicators representative of engine performance.

6. Present engine performance parameters in a manner that quantifies an engine change with operating time.

Engine 607594 was selected to provide the data from an identical engine configuration (Criterion No. 1). This engine was tested in all the altitude test facilities (NASA, AEDC, CEPr, RAE(P)), and so has the larger data base of the two UETP engines and the greater number of accumulated operating hours.

Data from instrumentation sensors were selected to provide an identical instrumentation configuration (Criterion No. 2). Using engine instrumentation, the sensor bias errors for all facilities' test data should be the same. Test data from P2, T2, P3, P5, T5, WFE, NH and NL engine instrumentation sensors were used.

The minimum overall precision error in measured internal engine performance is obtained with a combination of maximum air density at the engine inlet and critical (choked) flow in the exhaust nozzle. The maximum air density provides the minimum values of precision index for the parameter measurements and an exhaust nozzle pressure ratio greater than 2.4 minimizes the effects of variations in the ambient pressure set conditions on engine cycle performance. Data at the higher engine power settings at Test Conditions 6 (82.7/1.3/288) and 10 (82.7/1.7/288) provide minimum data precision errors (Criterion No. 3). The performance retention evaluations were made for the corrected low rotor speeds of 5400 and 5800 rev/min. The exhaust nozzle pressure ratios at these speeds exceed 2.4 at both Test Conditions 6 and 10.

The UETP standard data reduction equations were used to determine the engine performance parameters used in the analysis, thereby ensuring identical calculation methods (Criterion No. 4).

The engine performance parameters selected (Criterion No. 5) were:

a. NL/NH vs engine time at constant NLR

b. WA2R vs engine time at constant NLR

c. WFER vs engine time at constant NLR

d. T5Q2 vs engine time at constant NLR

e. P5Q2 vs engine time at constant NLR

f.   FG vs engine time at constant NLR

g.   SFC vs engine time at constant NLR

h.   T4 vs engine time at constant NLR

The WA2R values used to evaluate the change in airflow and the T5Q2 and P5Q2 values used to evaluate the change in engine pumping characterisics were obtained in accordance with the equations presented in the UETP General Test Plan. The WFER values used to evaluate the change in fuel flow were obtained from the engine fuel meters supplied with the engine and were referred to sea-level conditions using the equations presented in the General Test Plan. The change in engine gross thrust (FG) was then calculated assuming convergent nozzle choked flow and a fixed value for nozzle thrust coefficient. The value of T4 was calculated assuming choked turbine nozzle flow and fixed values of combustor efficiency and flow area.

Finally, selected engine performance indicators from each facility were evaluated in terms of percentage change from a common reference, NASA first test entry results. Thus:

$$\text{Per cent Difference} = \frac{\text{Facility} - \text{NASA(FE)}}{\text{NASA(FE)}} \times 100\%$$

The differences were plotted as a function of accumulated engine time (Criterion No. 6). The mid-point of facility reported engine time was defined as "engine time" for the evaluation.

11.3 Engine data analysis results

The engine performance retention analysis criteria were applied to each of the engine performance parameters presented in Section 11.2; the estimated changes in engine performance are reported below. In the accompanying Figures the shaded lines indicate the assessed trends in the data. The widths of the shaded lines reflect the magnitudes of the uncertainty estimates given in Section 10.

11.3.1 Airflow

To quantify changes in airflow, two performance parameters were used: rotor speed ratio (NLQNH) and engine inlet calculated airflow (WA2R). Rotor speed ratio at constant, corrected low-pressure rotor speed (NLR) as a function of engine operating time is presented in Figure 11-1. Normalized engine airflow (WA2R) determined from Station 2 pressure and temperature measurements is presented in Figure 11-2.

The speed ratio data show an overall decrease of about 0.3 per cent with engine time and while not purely monotonic in shape the trend is well defined. Airflow variation determined from Station 2 measurements shows the same trend as the speed ratio data. The roll-off in speed ratio is accompanied by a maximum decrease in engine airflow of about 0.7 per cent and an overall decrease of about 0.4 per cent.

11.3.2 Fuel Flow

Data from the engine turbine flowmeter were used to evaluate engine time shifts in fuel flow. Normalized engine fuel flow (WFER) at constant normalized low-pressure rotor speed (NLR) is presented in Figure 11-3. Engine fuel flow increased about 0.5 per cent during the initial 100 hours of engine operation and then remained nearly constant with engine time. The WFER values from RAE(P) were declared invalid. However, the data

presented in Table 15-1 shows that at Test Conditions 6 and 10, the two chosen for the engine performance retention analysis, the RAE(P) values of WFER were on average 1.1 per cent greater than the WFR values. Reducing the RAE(P) points plotted in Figure 11.3 by this amount puts them close to the centre of the trend band.

11.3.3 Thrust

It would have been desirable to examine the net thrust retention at a ram ratio of unity, ie static conditions. However, the exhaust nozzle was not choked even at the highest engine power settings so the minimum overall performance precision criterion cannot be satisfied (see Section 11.2). Equivalent insight can be gained by examining the changes in gross thrust at the ram ratios of 1.3 and 1.7 chosen for this analysis.

The gross thrust produced by a convergent nozzle is given by the following equation:

$$FG = (WA)(\sqrt{T5})\left(1 + \frac{WF}{WA}\right)K$$

where

$$K = \sqrt{2C_p}\left\{\sqrt{\frac{\gamma - 1}{\gamma + 1}} + \left(\frac{\gamma + 1}{2}\right)^{\gamma+1/2\gamma-1} \right.$$

$$\left. \sqrt{\frac{\gamma - 1}{2}}\left[\left(\frac{2}{\gamma + 1}\right)^{\gamma - 1} - \frac{PAMB}{P5}\right]\right\}$$

Assuming the term

$$\left(1 + \frac{WF}{WA}\right)$$

is constant, the change in thrust with engine operation time was calculated using the following expression:

$$\frac{\Delta FG}{FG} = \left[\left(1 + \frac{\Delta WA2R}{WA2R}\right)\left(1 + \frac{\Delta T5Q2}{T5Q2}\right)^{1/2}\left(1 + \frac{\Delta K}{K}\right)\right] - 1$$

where for values of $\gamma = 1.35$ and $P2QAMB = 1.3$

$$\frac{\Delta K}{K} = \left[\frac{1 - \frac{0.79}{1.3(P5Q2)_{NEW}[1 + (\Delta P5Q2/P5Q2)]}}{1 - \frac{0.79}{1.3(P5Q2)_{NEW}}}\right] - 1$$

Engine temperature ratio ($\Delta T5Q2$) and engine pressure ratio ($\Delta P5Q2$) at constant corrected low-pressure rotor speed (NLR) are presented in Figures 11-4 and 11-5 respectively. Values of WA2R, T5Q2 and P5Q2 were taken from the upper and lower ends of the shaded lines shown in Figures 11.2, 11.4 and 11.5. The changes in gross thrust (FG) are presented in Figure 11.6. Changes in gross thrust calculated for P2QAMB = 1.7 differ by less than 0.1 per cent from the results shown in Figure 11.6.

Engine thrust variation shows the same trend as the airflow data with a maximum decrease of about 0.7 per cent and an overall decrease of about 0.1 per cent.

11.3.4 Specific fuel consumption and combustor temperature

Gross thrust specific fuel consumption (SFC) and combustor temperature (T4) are two parameters monitored to detect changes in engine performance. In the present evaluation variations in SFC were calculated from the following expression:

$$\left[\frac{\Delta SFC}{SFC}\right]_{gross} = 1 - \frac{\left(1 + \frac{\Delta WFER}{WFER}\right)}{\left(1 + \frac{\Delta FG}{FG}\right)}$$

where the values of

$$\frac{\Delta WFER}{WFER}$$

and

$$\frac{\Delta FG}{FG}$$

were taken from the upper and lower ends of the shaded lines shown in Figures 11.3 and 11.6 respectively. This unusual form of SFC was chosen to satisfy the minimum overall precision criterion discussed in Section 11.3.3.

The change in specific fuel consumption was determined for Test Condition 6 at a constant low-pressure rotor speed, NLR = 5800 rev/min. (Figure 11.7.) Specific fuel consumption shows the inverse trend to the thrust data (Figure 11.6) with a maximum increase of about 1.2 per cent and an overall increase of about 0.6 per cent.

Variations in combustor temperature were calculated assuming a constant turbine flow function, combustor efficiency and turbine nozzle flow area. Thus:

$$\frac{(WA2R + WFER)\sqrt{T4}}{P3} = \text{Constant}$$

To calculate the variations in combustor temperature the following expression was used:

$$1 + \frac{\Delta WA2R}{WA2R} \simeq 1 + \frac{\Delta(WA2R + WFER)}{WA2R + WFER}$$

$$\Delta T4 = \left[\left(1 + \frac{\Delta P3Q2}{P3Q2}\right)^2 \left(1 + \frac{\Delta WA2R}{WA2R}\right)^2 - 1\right] T4_{assm}$$

where the values of

$$\frac{\Delta WA2R}{WA2R}$$

are based on Figure 11.2 and

$$\frac{\Delta P3Q2}{P3Q2}$$

values obtained from the test facility data.

The value of T4 = 1000K was determined from an ideal air/fuel flow, mass enthalpy calculation.

The change in combustor temperature for Test Condition 6 (Figure 11.8) was about 8 to 16 degrees Celsius. This increase indicates that some small deterioration probably occurred and this is consistent with the SFC results shown in Figure 11.7.

11.4 Engine Water Wash

NRCC performed a water wash on Engine 607594 in order to evaluate the effect of contaminants on engine performance. Washing was qualitatively assessed as 95 per cent effective for the low pressure compressor with some deposit left near the rotor blade tips. Retesting after the water wash disclosed no significant effect on engine performance for fuel flow, SFC, thrust, engine or compressor characteristics (T5/T2 vs P5/T2, T3/T2 vs P3/P2) when compared to the NRCC facility measurement repeatability (0.1 to 0.3 per cent). Component degradation recoverable by water wash was concluded to be a maximum of 0.1 per cent in rotor speed and 0.5 per cent in airflow.

11.5 Summary of Engine Performance Retention

Using the engine internal instrumentation, an investigation was made into the performance of Engine 607594 as a function of operating time. Since the analysis had to be based on limited data which exhibited appreciable scatter it was difficult to quantify the extent of any deterioration that may have occurred. It was concluded that engine performance remained essentially constant from beginning to end of the UETP, as shown below:

Rotor Speed Ratio:	minus 0.1–0.3 per cent
Airflow:	minus 0.4–0.7 per cent
Fuel Flow:	plus 0.5 per cent
Thrust:	minus 0.1–0.7 per cent
Specific Fuel Consumption:	plus 0.6–1.2 per cent
Combustor Temperature:	plus 8–16C

Fig.11-1 Rotor speed ratio change as a function of engine operating time

Fig.11-2 Engine airflow change as a function of engine operating time

Fig.11-3 Engine fuel flow change as a function of engine operating time

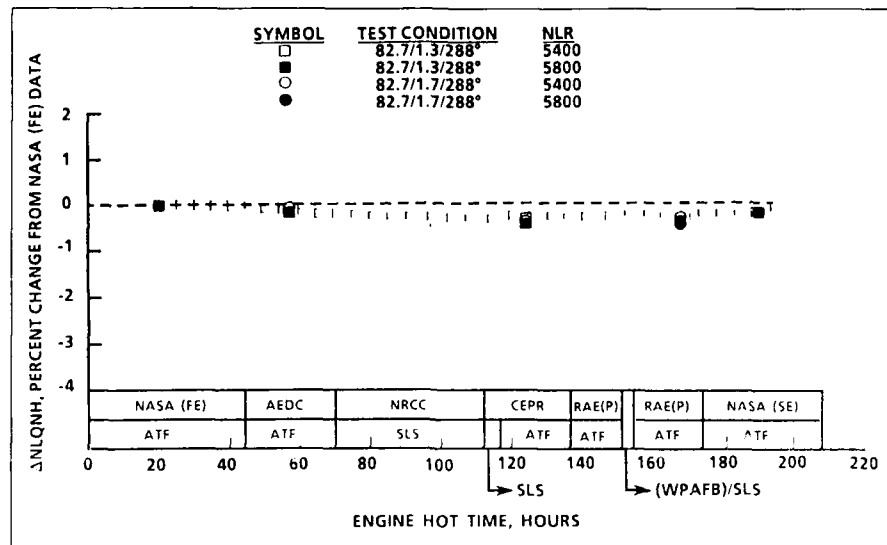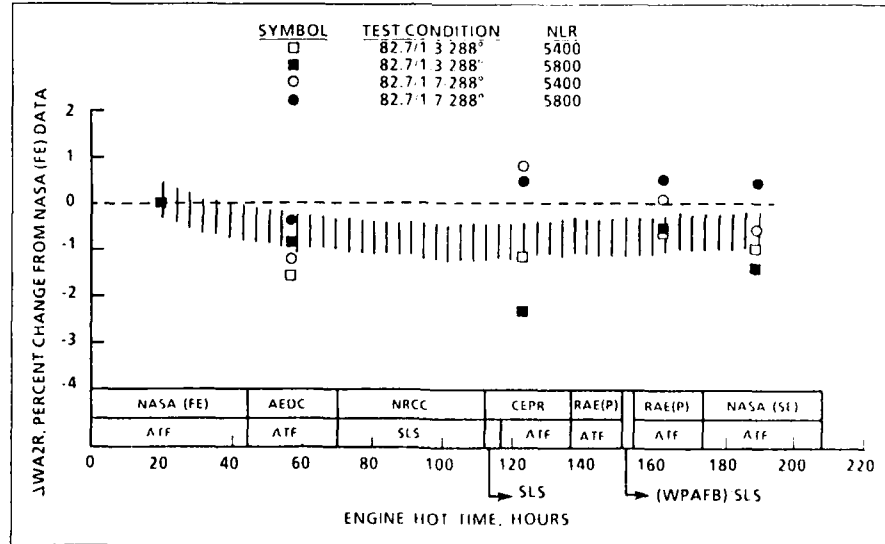Fig.11-4 Engine temperature ratio change as a function of engine operating time

Fig.11-5 Engine pressure ratio change as a function of engine operating time

Fig.11-6 Gross thrust change as a function of engine operating time
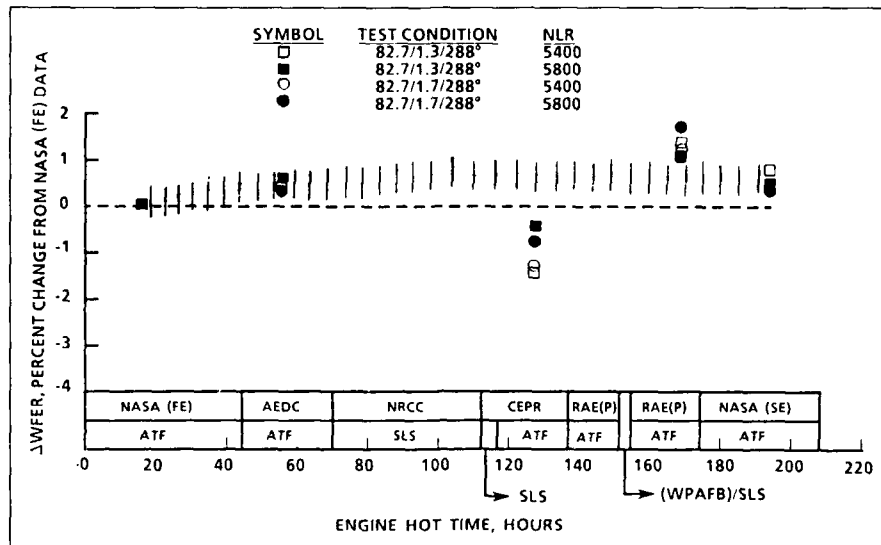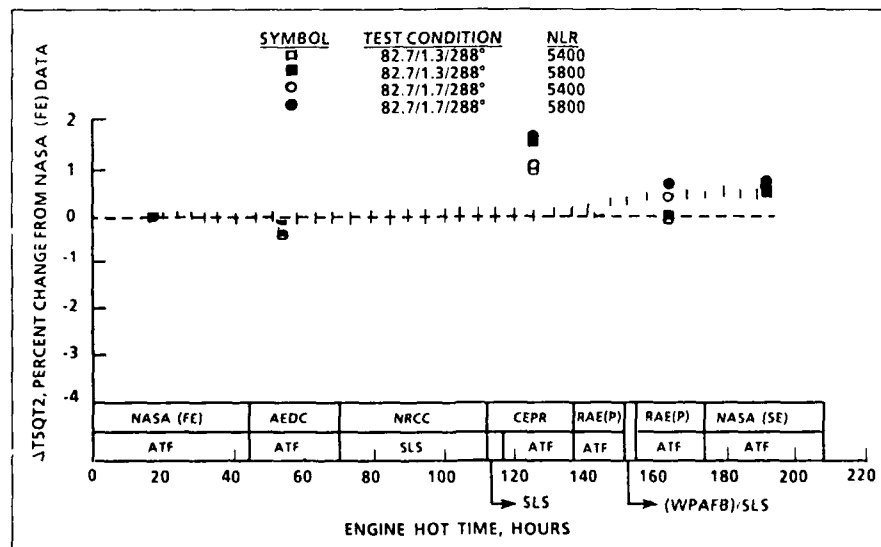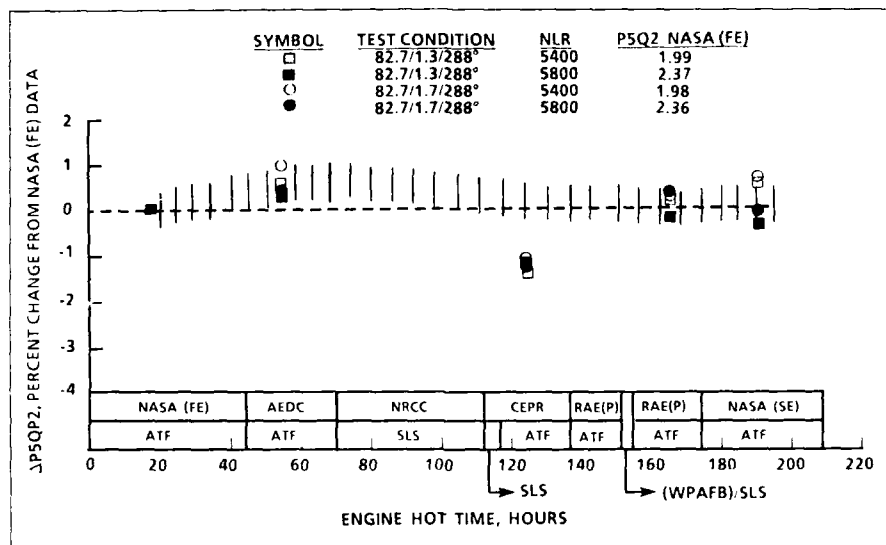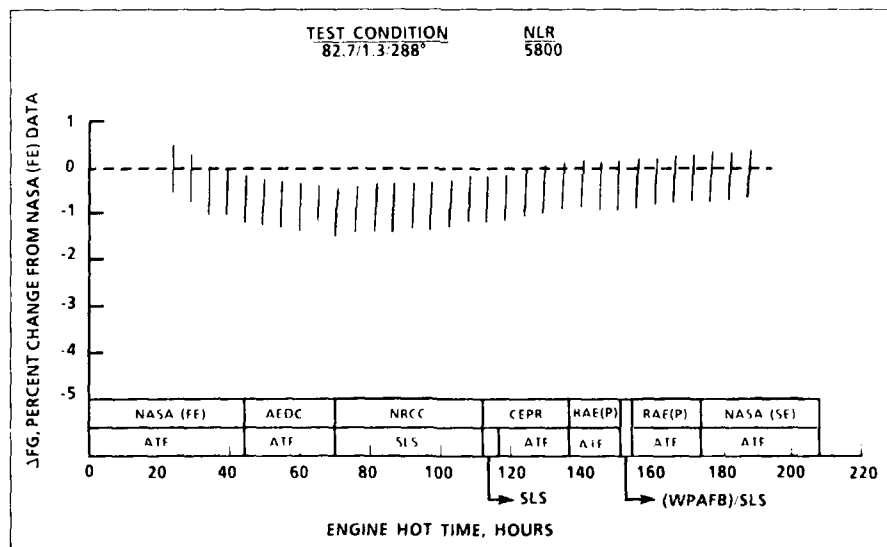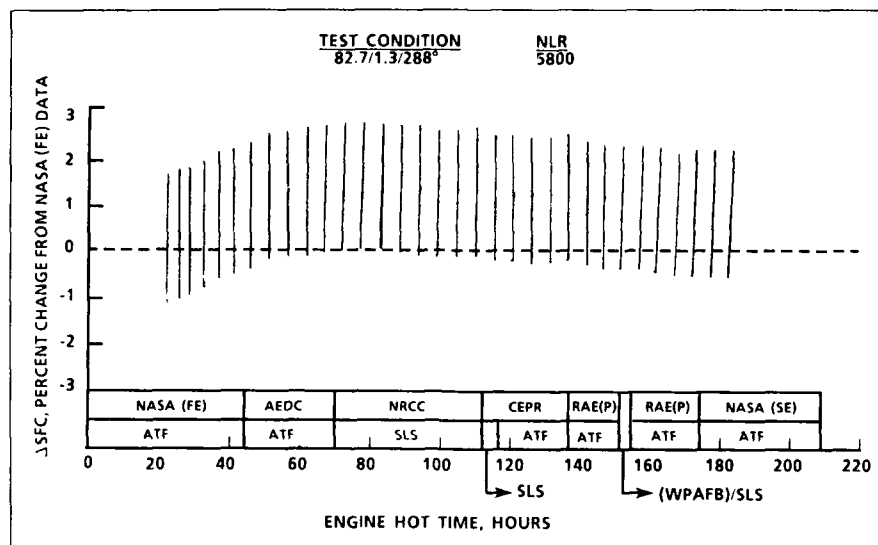
Fig.11-7 gross thrust specific fuel consumption change as a function of engine operating time
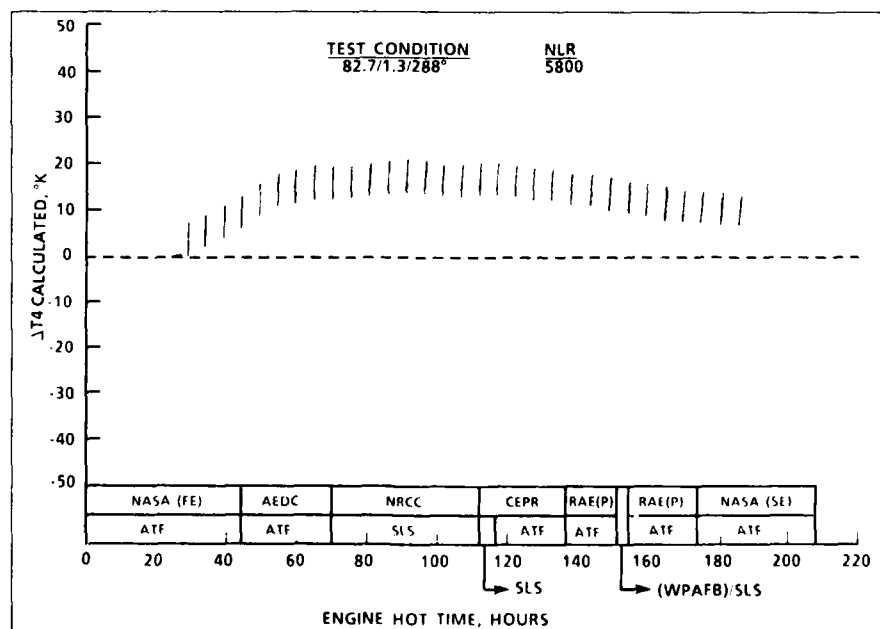

Fig.11-8 Engine turbine temperature change as a function of engine operating time

12. FACILITY INFLUENCES

Three main factors can be identified as possible causes of inter-facility differences: Measurement errors, change in engine performance with running time and influence of the facility.

Measurement uncertainty has been considered in Section 10 and Reference 16.

Engine performance retention with running time has been reviewed in Section 11. It was concluded that whilst the results are in some measure conflicting, the magnitude of any performance change was sufficiently small to be neglected.

The third factor, the influence of the facility, can manifest itself in several ways. These are considered separately below.

A further factor can be identified as a possible cause of inter-facility engine performance differences, namely the specific humidity of the inlet air. However, in each of the altitude test facilities the inlet air was dried sufficiently (0.1 per cent water by weight) to ensure that the effects of humidity on engine performance were negligible. In the case of the ground-level beds, the specific humidity of the inlet air on the actual test dates was sufficiently low to ensure that the effects were either negligible or only very small adjustments to the data were needed (see Reference 12).

12.1 Inlet total pressure

12.1.1 Determination of mean inlet total pressure

A study was undertaken by NRCC (reported in Reference 24) to quantify the magnitude of performance corrections that would result from changing the definition of inlet pressure. Four different approaches, in addition to the one required by the GTP, were studied to calculate the average total pressure at the compressor inlet. Three of the methods used only the mainstream rakes while two included the boundary layer probes. As the NASA installation provided the largest degree of inlet distortion, only NASA data were analysed in all the schemes considered.

Method 1 used the arithmetic average of the 20 mainstream rake readings. This was the GTP method.

Method 2 was the same as Method 1 but it used weighting factors determined from the actual location of the 20 probes.

Method 3 was similar to Method 2 but it used only those probes in the inviscid flow regime. This was determined by comparing the total pressure measured by each individual probe with that of the innermost one and if the difference was greater than the measurement uncertainty of the facility, then that probe was considered to be in viscid flow.

Method 4 calculated the average pressure by considering two boundary layer ring sectors, each containing an inner and an outer boundary layer rake, and four main ring sectors.

Method 5 further increased the weighting of the boundary layer probes and covered the complete circumference following the observation that the outermost main probe was in the boundary layer for all facilities.

The conclusion from the analysis was that the calculation method defined by the GTP produced a value of P2 average

that was within 0.07 per cent of that obtained if all the pitot rakes, including those in the boundary layer, were used to obtain an integrated average. It is evident, therefore, that for the purposes of the UETP the GTP method gives a representative value of the mean inlet total pressure.

12.1.2 Comparison of inlet total pressure profiles

Differences in the total pressure profile at inlet to the compressor could conceivably influence the measured engine performance.

AEDC undertook a literature survey to see if the sensitivity of the J57 engine to radial variations of total pressure had been determined experimentally. However, no US Government reports on the subject were found. The question had therefore to be left unresolved until the second series of tests at NASA when some measurements were made with the original inlet duct replaced with one of the reduced divergence angle.

Figure 12-1A compares Station 2 total pressure profiles at ground-level or equivalent conditions measured at NASA, AEDC, NRCC, CEPr and RAE(P). The measurements were made with Engine 607594 operating at mil power.

The flattest profile was obtained at NRCC and the greatest deviation from this flat profile, that is the largest pressure defect, was seen at NASA. The AEDC profile was closest to the NRCC profile. The RAE(P) and CEPr data fell between AEDC and NASA, probably due to different degrees of divergence in the ducting between the air meter station and Station 2.

The P2 profiles measured at altitude conditions were reasonably flat except for the large pressure defect measured by NASA near the outlet wall (Figure 12-1B). This was undoubtedly due to a divergence in the inlet duct ahead of the engine. The influence of this divergence was examined during an additional series of tests at NASA (second entry) when the installation was changed to incorporate a larger diameter air meter which had the effect of reducing the divergence. The results are given in Section 17.3.

12.2 Inlet turbulence level

For altitude testing the engine is coupled directly to the facility air supply ducting so that the inlet turbulence level is likely to vary between facilities depending on the supply duct geometry and the effectiveness of any smoothing devices provided.

There is no experimental evidence to show that the steady-state performance of a turbojet is influenced by the inlet turbulence level, at least within the range normally encountered in altitude facilities, but when planning the UETP it was decided to include the measurement of turbulence characteristics at the engine inlet (Station 2).

For altitude facilities only NASA and AEDC data could be compared as the other facilities had either not made the necessary measurement or had presented their results in a different way. The AEDC test installation included an upstream flow measuring venturi followed by flow straightening screens (Figure E of Appendix II). The NASA installation used no inlet flow straightening screens between the airflow meter and the engine face. In neither facility did the turbulence level (ΔPrms/Pavg) in the frequency range 70 to 1000 Hz exceed two per cent which is within the normal operating range.
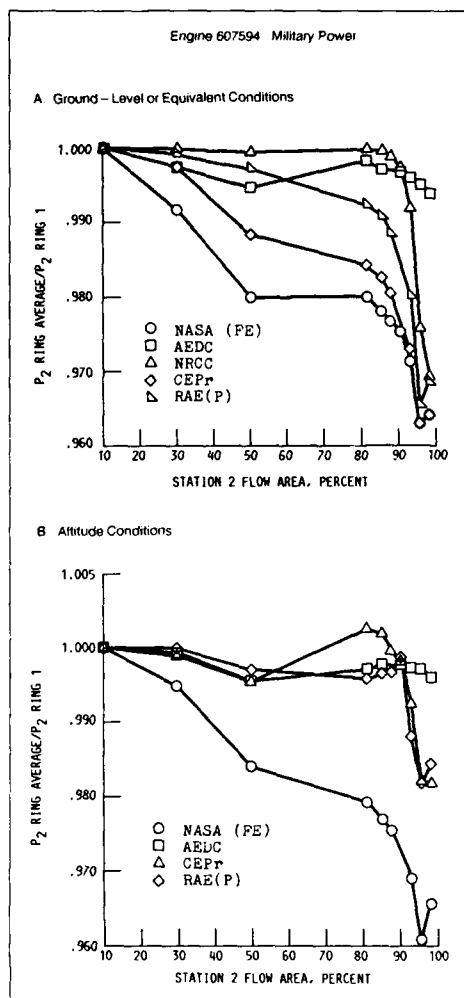
Fig.12-1 Comparison of inlet total pressure profiles

Fig.12-2 Boattail force

Measurements were also made on the ground-level test bed at NRCC. The NRCC configuration consisted of a horizontal inlet system followed by a coarse anti-FOD screen upstream of the engine inlet (see Figure A of Appendix II). Measurements of inlet turbulence indicated a maximum level of 0.07 per cent.

12.3 Boattail force

During analysis of the UETP data it became apparent that the method of accounting for the boattail force, that is the force acting on the external surface of the engine exhaust nozzle due to the flow over it, was not the same for all participants. Some facilities ignored it on the assumption that it was relatively small while others included it in their thrust calculations irrespective of its magnitude.

To establish the relative importance of the boattail force, data from tests at sea-level and altitude conditions were
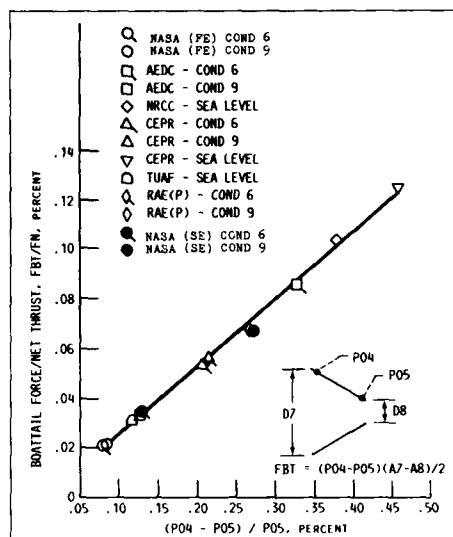
used (Test Conditions 6 and 9). The results are shown in Figure 12-2, a plot of the ratio of boattail force to net thrust as a function of the differential pressure on the external surface of the nozzle. It will be seen that the boattail force is insignificant when compared to the net thrust. It is near 0.1 per cent for the ground-level tests at CEPr, NRCC and AEDC and even less for TUAF. For Test Conditions 6 and 9 it is less than for the ground-level tests not exceeding 0.07 per cent and was as low as 0.02 per cent for the first NASA entry.

12.4 Engine settling time

Section 8.4 of the General Test Plan (Reference 1) states that during altitude testing the engine will have reached stabilised thermodynamic performance after five minutes at the set conditions and that the initial data scan should then be taken. The repeat data scan should be taken two minutes later. No such recommendations are given for the ground level tests.

Facilities generally complied with the GTP recommendations which were arrived at as the result of tests at NASA in which the required settling time for stable operation was determined.

During tests on Engine 607594 at RAE(P), the opportunity was taken further to investigate settling time to stable conditions at Test Conditions 6 and 9. Having set the plant test conditions and then the appropriate throttle angle, military power, successive data scans were recorded at approximately one minute intervals over a period of about nine minutes. During this period no alterations were made to either test plant or engine settings, except for Test Condition 9 when a small change became necessary to the setting of P2 (engine inlet total pressure) by a small amount due to an instability in the plant system. This small increase in P2 setting resulted in both the thrust and fuel flow being higher in value at subsequent points in time than would have been the case if no change had been introduced.

50
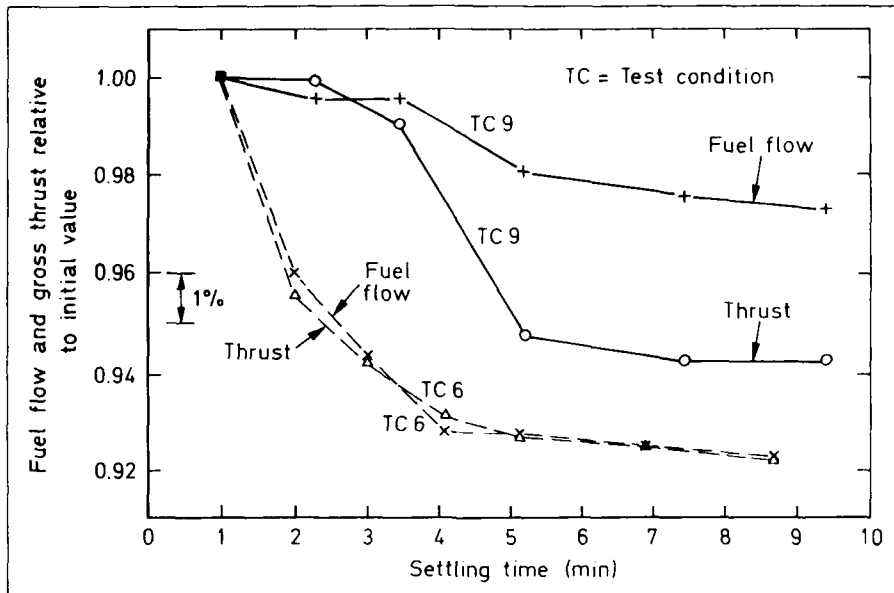
Fig.12-3 Fuel flow and thrust during stabilisation time
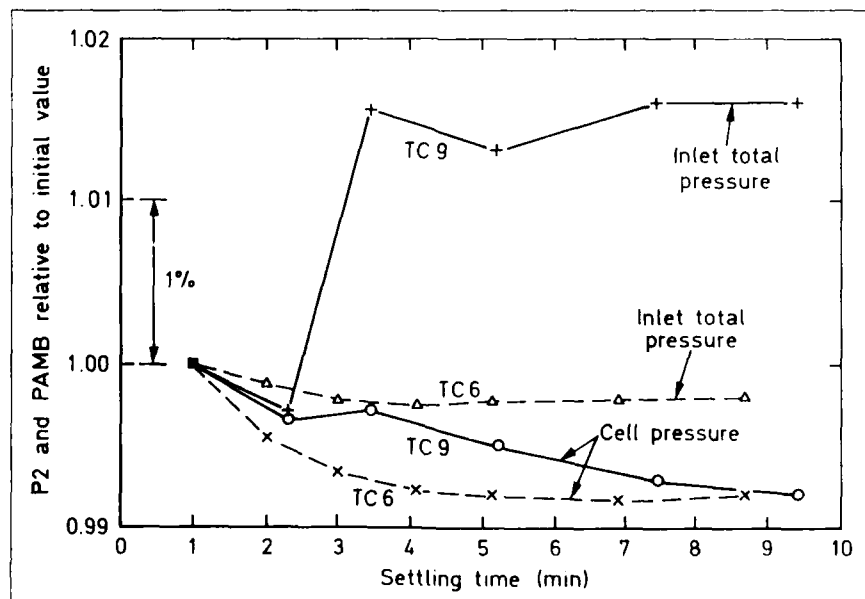
Fig.12-4 Inlet and cell pressures during stabilisation time

51
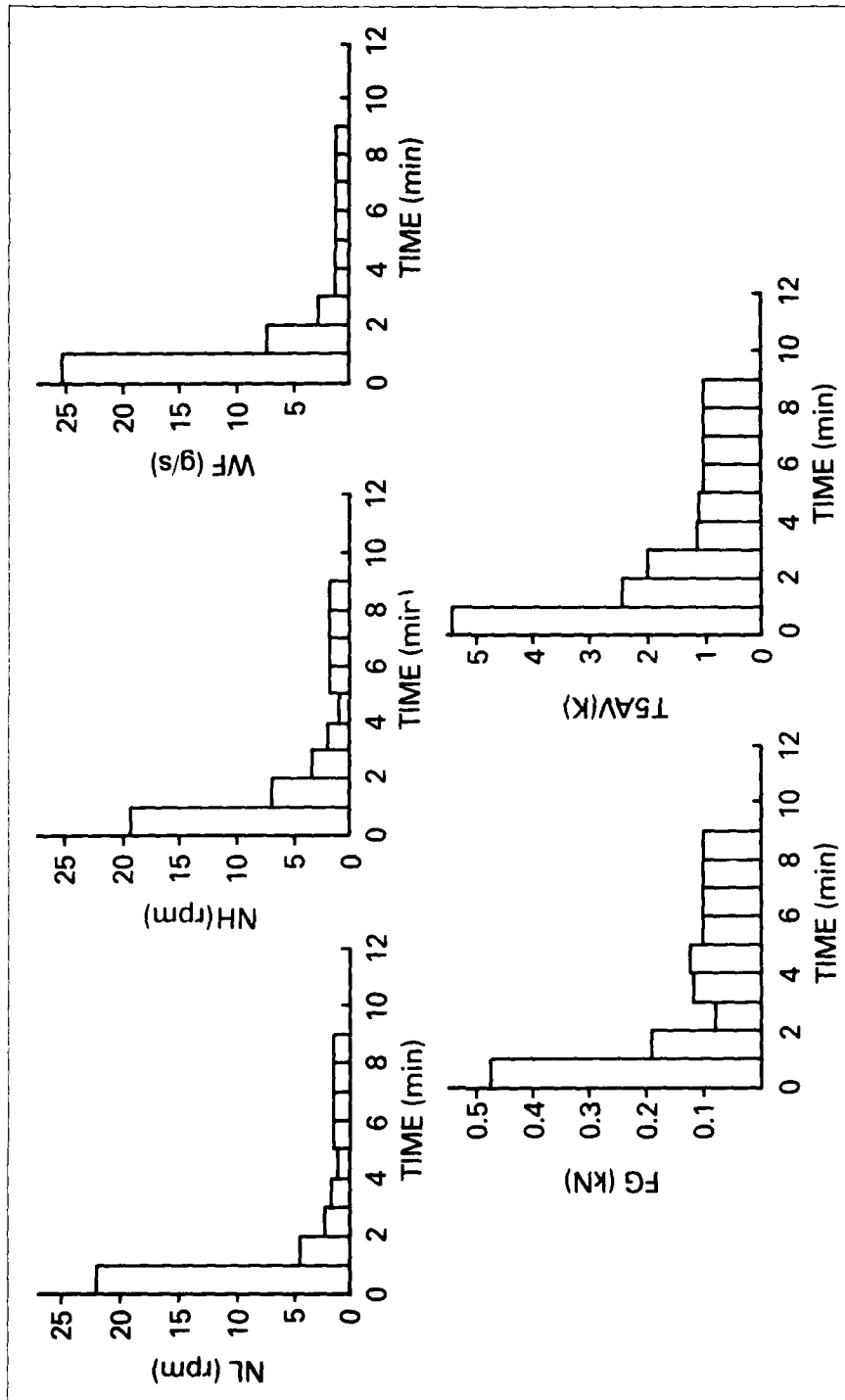
Fig.12-5 The standard deviation from the mean for several parameters as a function of engine settling time in the NRCC ground level facility

52

Figures 12-3 and 12-4 show the fuel flow, thrust, engine, inlet and cell pressures for these data points divided by their values at the first scan plotted against time, which starts at one minute before the first scan. These data indicate that the engine has almost stabilised after three minutes for Test Condition 6 and, allowing for the P2 adjustment, 4 minutes for Condition 9. There remain small changes after this time, but these would not be significant to the measurement of the overall engine performance.

Also at NRCC the opportunity was taken for further investigations of engine settling time. The engine power level was raised from idle to the military setting and data gathered for several major parameters at a sample rate of 12/second over a period of nine minutes. The standard deviation from the mean for these parameters was calculated for several time intervals and these are shown in Figure 12-5. The results for low pressure compressor speed (NL), high pressure compressor speed (NH), average main fuel flow (WF), gross thrust (FG) and turbine exhaust temperature (T5) in Figure 12-5 show that the engine had reached stabilised thermodynamic conditions within the five minute settling time recommended by the General Test Plan.

To further aid the understanding of the effects of engine settling time, steady-state values of gross thrust were used to demonstrate the quantitative effects. Values of gross thrust measured during the first and second data scans in two altitude test facilities were analyzed to determine the effects of settling times which were less than the test plan requirements.

The differences in gross thrust (FGRD) between the second and first data scans at Test Condition 6 at AEDC are shown in Figure 12-6A for the nine power settings. The stabilization times were in accord with the General Test Plan and the total elapsed time at each power setting was eight to nine minutes. The differences between the scans were negligibly small (less than ± 0.25 per cent).

The differences in gross thrust (FGRD) between the second and first data scans at Test Condition 6 at CEPr are shown in Figure 12-6B for eight of the nine power settings. The stabilization times were less than the values given in General Test Plan. The total elapsed times at each power setting varied between three and five minutes. The differences between the scans were significant at four of the eight power settings and ranged up to 0.9 per cent.

The evidence provided by the altitude cell and ground level test bed investigations show that the General Test Plan recommendation for the first scan after five minutes settling time and the second scan two minutes later is sufficient for engine thermodynamic stabilisation for the J57 engine.

12.5 Secondary Airflow

Engine performance measured in an enclosed ground-level test bed is greatly influenced by the design of the exhaust outlet. The exhaust system not only controls the amount of secondary cooling air in the cell, but also determines the back pressure and sound attentuation. The collector diameter, entrance geometry, and placement of exhaust nozzle relative to the collector inlet determines the quantity

of entrained or secondary air through the test cell, and the static pressure field at the nozzle exit. Ideally, the static pressure field around the engine should be the same as that at the nozzle exit, but this is generally not the case.

The accounting of forces and momentum changes due to secondary air must be done at well defined planes. Each facility will have its own procedures, but in general the following components must be quantified:
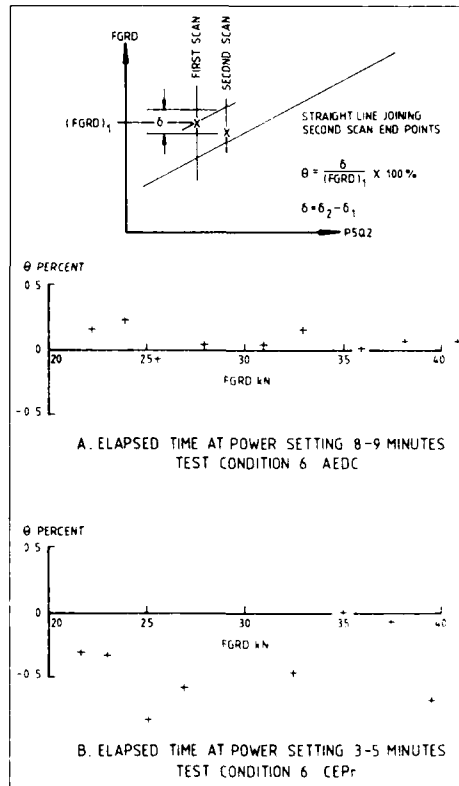
Fig.12-6 Differences in gross thrust between first and second data scans

1. Momentum drag force,

2. Pressure forces along the engine, particularly at the bellmouth and nozzle boattail, and

3. External friction forces on the bellmouth, engine and thrust frame.

The analysis presented in Reference 30 shows that for the NRCC installation, the aggregate sum of the correction was of the order of 2 per cent of which the main components were momentum drag force (1.7 per cent) and boattail force (0.3 per cent).

13. NOZZLE COEFFICIENTS FOR THRUST AND AIRFLOW COMPARISONS

13.1 Comparison of Gross Thrust

Gross thrust is one of the most basic performance parameters determined in a test cell, being of particular importance to the performance of an aircraft to which the engine may be fitted and thus often sp cified in contractural guarantees. Gross thrust is the sur.i of the exhaust gas momentum and the static pressure force across the nozzle exit plane, whereas the actual thrust measured in a test cell depends upon other terms such as inlet flow momentum, external static pressure distribution on the engine structure and stray forces acting on the engine test frame. The accurate derivation of gross thrust therefore relies on an accurate measurement of the actual thrust acting on the test frame as well as inlet air flow and velocity, cell static pressure measurement and the elimination of the effect of stray forces. Reference 25 gives a more comprehensive treatment of this subject together with a wider range of results.

In order to compare the gross thrust obtained from one test facility with another it is convenient to use a gross thrust coefficient CG8 which is defined as:-

$$\frac{\text{Gross thrust derived from measurement}}{\text{Isentropic gross thrust for the same nozzle area and pressure ratio}}$$

The Isentropic or ideal value is a function only of nozzle pressure ratio, nozzle area and γ. CG8 has a well established relationship with pressure ratio, increasing up to a peak value at a nozzle pressure ratio of around 2.0 at which point it levels off and remains constant over a modest pressure ratio range, ie until under-expansion begins to have a marked effect.

An example of CG8 versus pressure ratio for all of the RAE(P) results is shown in Figure 13-1 around which an envelope has been drawn. Note that the envelope is determined by only one Test Condition for nozzle pressure ratios greater than three. It can be seen that the actual results depart from the single curve for an ideal nozzle to form a family of curves, one for each altitude condition. This is due to a combination of engine related effects and measurement errors. The bandwidth within which the true result is expected to lie is wider than the envelope. As a guide to measurement uncertainty at RAE(P), estimates of uncertainty bandwidth at four Test Conditions are shown in Figures 13.1, 13.3 and 13.6. These show the much greater measurement uncertainty likely to be experienced at Test Condition 9 compared with the other Test Conditions, which was found to be the case in practice. The engine related effects come from a variety of sources. At a given nozzle pressure ratio a change in altitude and forward speed usually means a change in engine power setting. The power setting, in turn, influences the quality of the airflow at nozzle entry through changes to swirl angles and pressure distribution. Also, as altitude is increased, Reynolds number is lowered and the boundary layers on the gas generator turbomachinery are affected, again leading to changes in the inlet total pressure profile of the nozzle. The measurement errors can be divided into two categories, precision errors and bias errors. Both these types of error are influenced by the signal level, which in turn can vary with different altitude conditions at a fixed nozzle pressure ratio, leading to small differences in thrust coefficient.

Figure 13-2 gives a comparison of CG8 versus pressure ratio for all the altitude test facilities using all the results from Engine 607594, with the actual test points not included for the sake of clarity. All results show the typical nozzle characteristic shape, but NASA and CEPr have a considerably broader range of values and higher maximum values than RAE and AEDC. The measurement of total pressure in the nozzle was suspected as being the main reason for this disparity, and in Sections 18.2.2 and 18.2 it is shown that total pressure was a function of exit swirl. This suspicion was confirmed when an alternative thrust function was used as the basis of the comparison; one that is independent of nozzle total pressure.

The thrust relationship

$$\phi = \left[\frac{FG}{A8\ PAMB} + 1\right] \times \frac{PAMB}{P2AV}$$

was plotted against nozzle pressure ratio and gave almost coincident straight line relationships for results from all of the test facilities. This parameter does not, however, identify really small differences in gross thrust measurement.

Fortunately the nozzle inlet static pressure was found to be a more accurate measurement from which an isentropic value of nozzle total pressure could be calculated. Assuming an area ratio of jet pipe to nozzle exit area of 1.7293 and a value of $\gamma = 1.35$, CG8 was recalculated (as CG8C) based on the calculated value of nozzle total pressure. The results so obtained are plotted in Figure 13-3. As can be seen, this not only reduces the width of each envelope within which the test points are contained, but also reduces the difference in the value of CG8C at which the envelopes flatten out.

Good agreement is shown between NASA and RAE(P) results, with AEDC also agreeing well at the upper edge of the envelope but showing a wider variation than the other two facilities. This spread of results at AEDC was not entirely random as it was identified with a trend of reducing inlet pressure. The magnitude of this trend was not repeated on Engine 615037, which suggests that this variation was related only to the first engine's installation. CEPr results are 1 to 1¼ per cent higher than the mean of the other three facilities, except for Test Condition 9 where the values are two per cent lower than the others.

A comparison between the altitude test results and those from two of the ground-level test beds is given in Figure 13-4 using the results from Engine 607594. The altitude test condition selected for this comparison is that which corresponded nearest to the sea level static condition. This again shows the CEPr altitude test cell to be measuring the highest values of CG8C whilst the NRCC ground-level bed gives the lowest, the difference between them being approximately two per cent. A further comparison of altitude versus sea level results using Engine 615037 is given in Figure 13-5. The TUAF results are included but are subject to the qualifications noted in Section 9.3. The TUAF results are the lowest and AEDC the highest, the difference amounting to as much as three per cent at the lower nozzle pressure ratios.
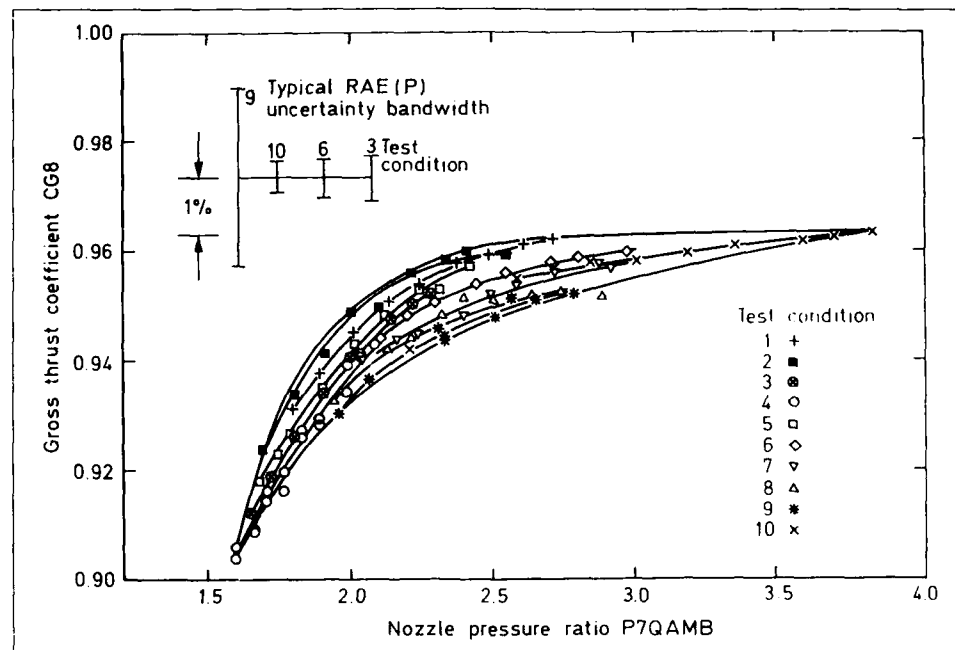
Fig.13-1 Gross thrust coefficient for all flight conditions in the RAE(P) test facility (engine 607594)
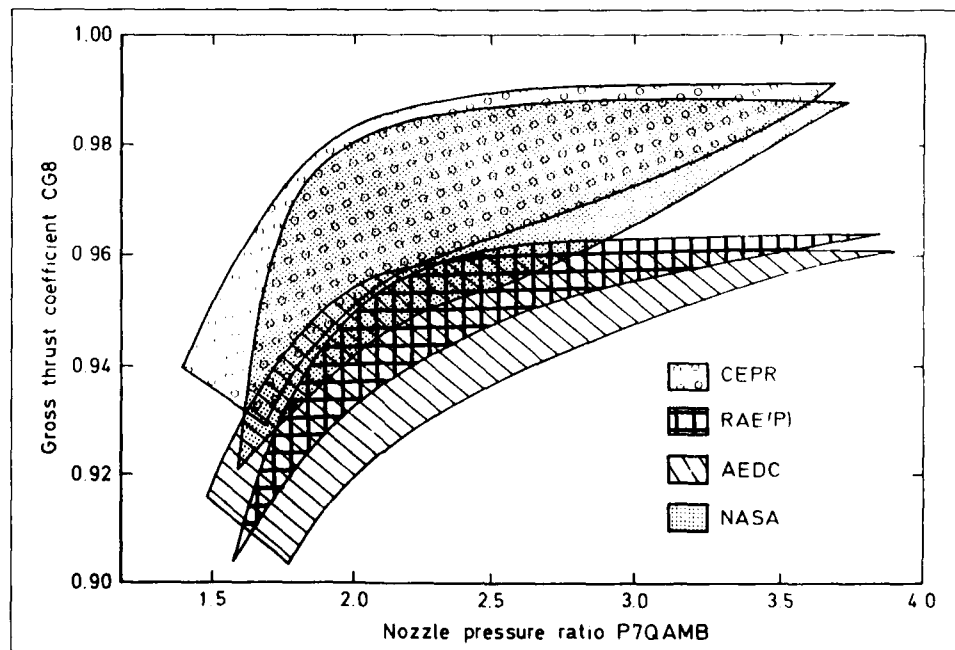
Fig.13-2 Gross thrust coefficient envelopes for all facilities (engine 607594)
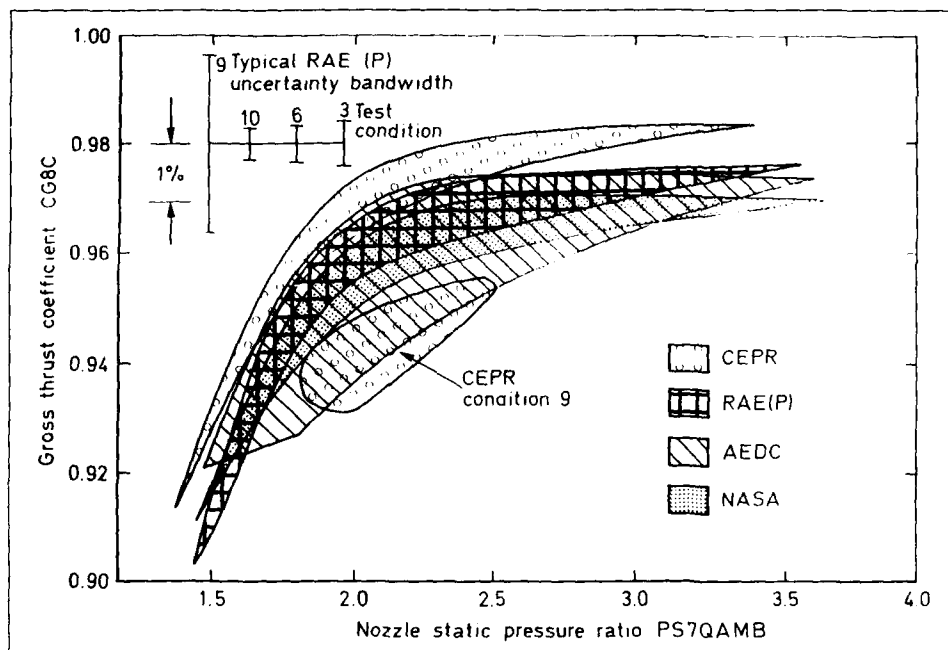
Fig.13-3 Revised thrust coefficient envelopes for all altitude facilities (engine 607594)
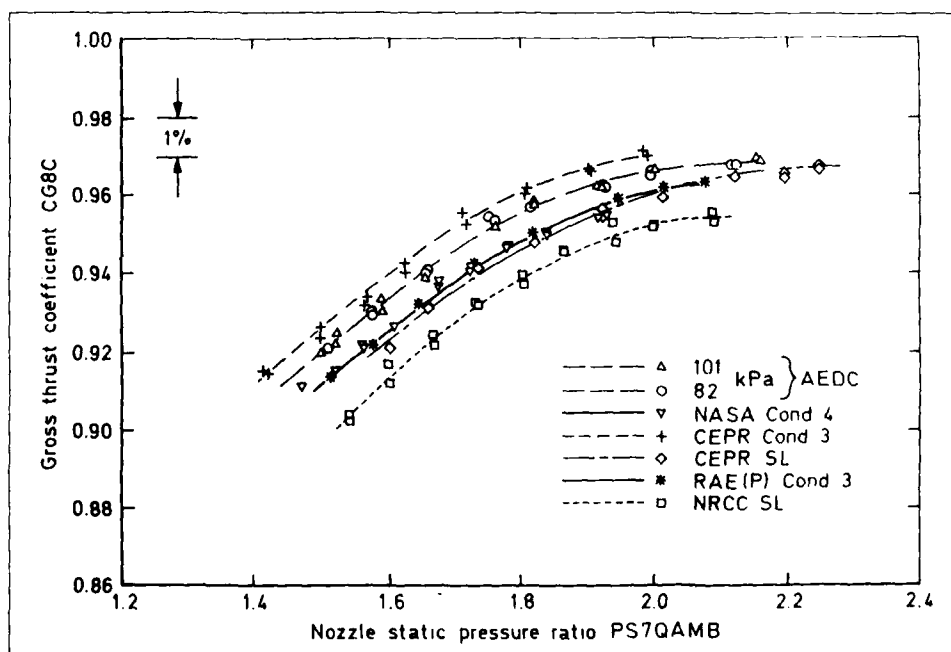
Fig.13-4 Revised thrust coefficient for altitude cells and ground level test beds (engine 607594)
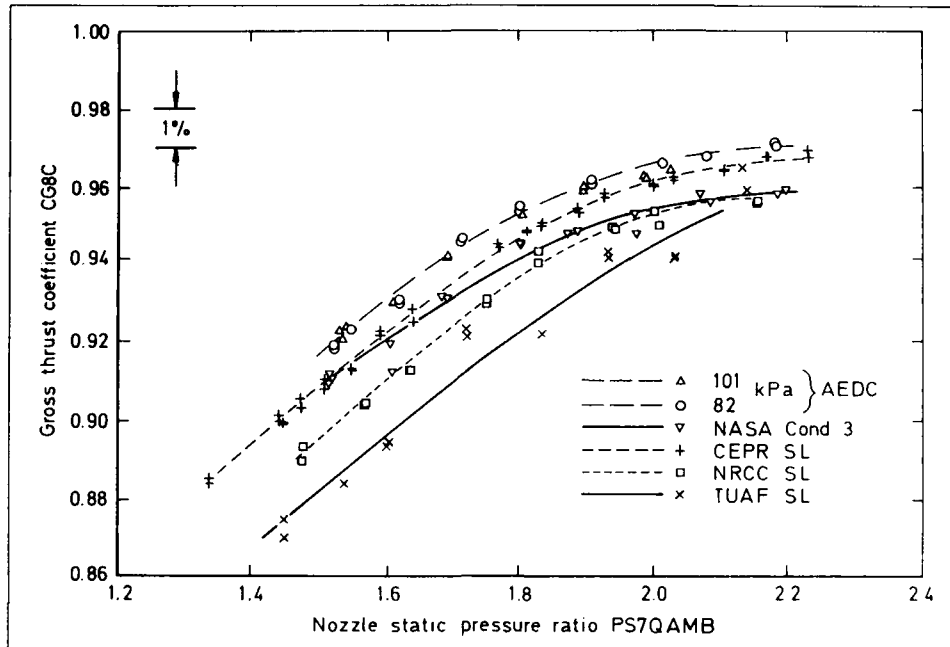
Fig.13-5 Revised thrust coefficient for altitude cells and ground level beds (engine 615037)
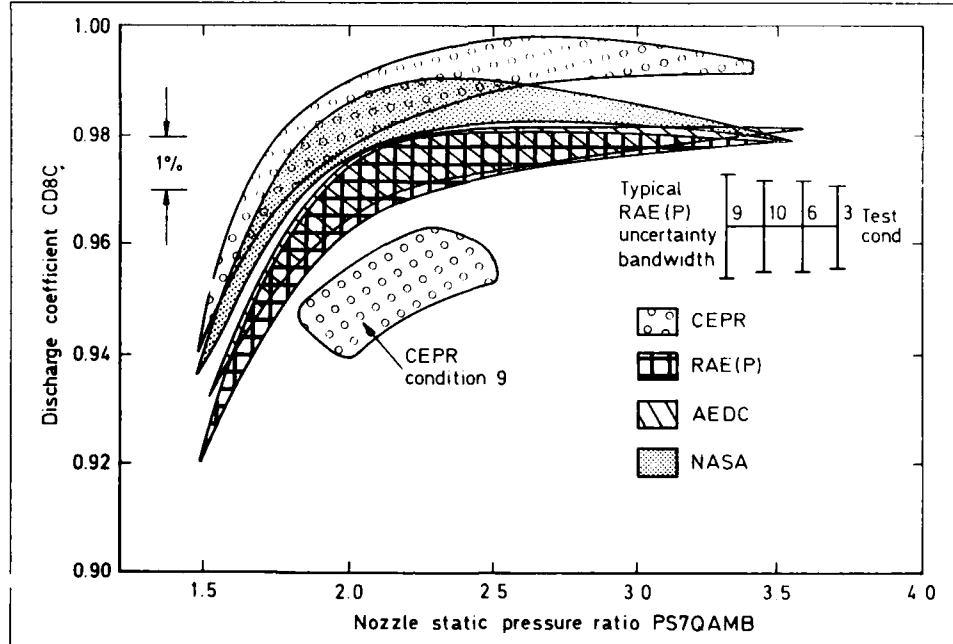
Fig.13-6 Revised discharge coefficient envelopes for all altitude facilities (engine 607594)
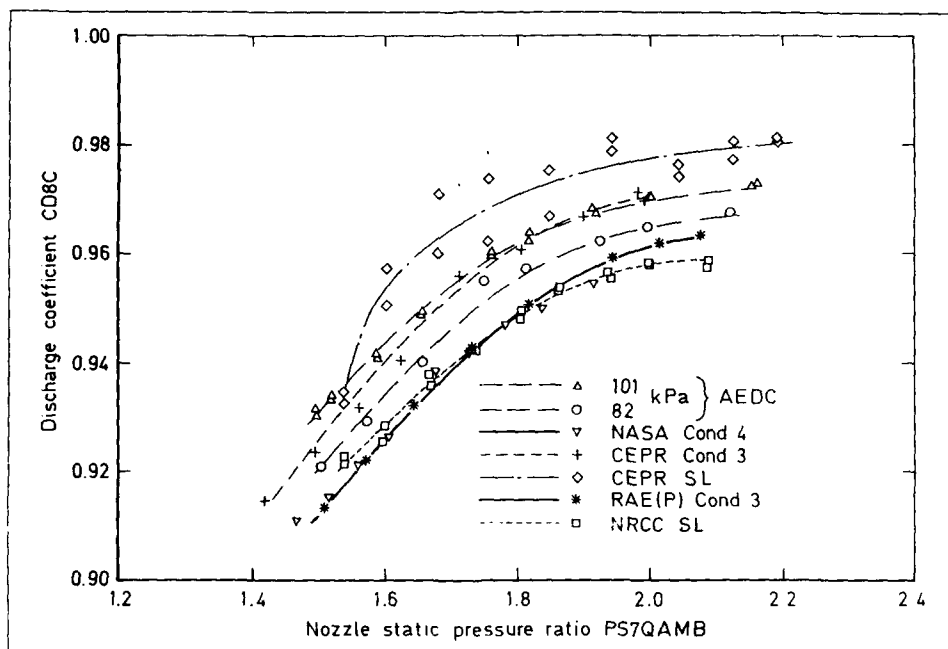
Fig.13-7 Revised discharge coefficient. Altitude cells and ground level beds (engine 607594)
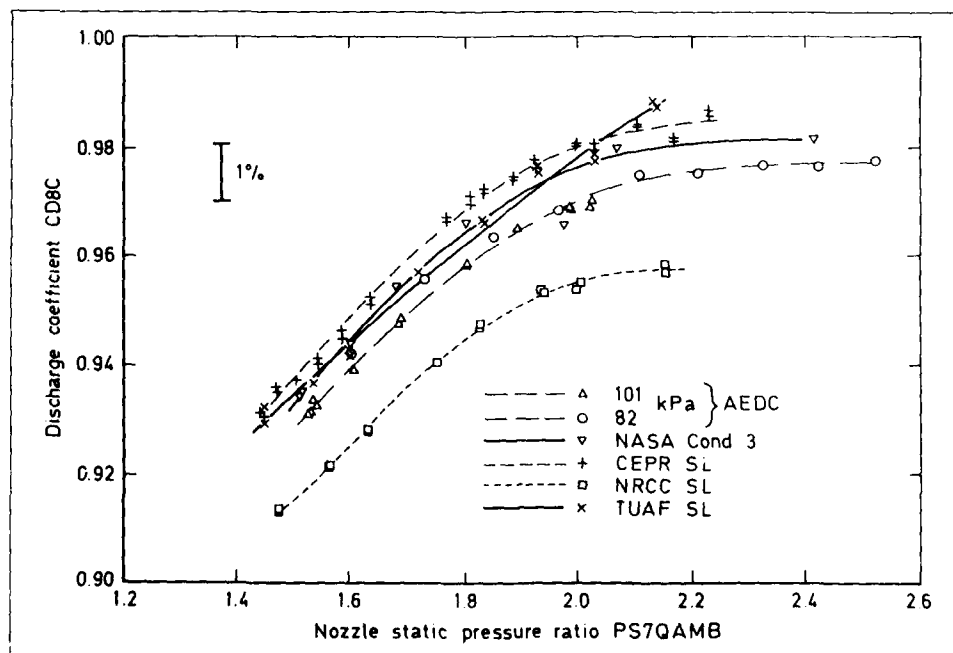
Fig.13-8 Revised discharge coefficient. Altitude cells and ground level beds (engine 615037)

58

In evaluating this overall picture it should be borne in mind that some variation in CG8 from a single curve at different test conditions is inevitable due to the previously described engine related effects and measurement errors.

Differences of less than one per cent in CG8C between the various test centres are judged to be a good result, but values greater than this give increasing cause for concern. A three per cent difference is viewed as throwing doubt on the validity of gross thrust derivation. With these criteria in mind, and acknowledging that there is no absolute standard against which to compare, it seems that RAE(P), NASA and AEDC altitude results are in good agreement at choked nozzle conditions whilst CEPr measure a higher level of gross thrust. AEDC's measurement of gross thrust was influenced by altitude pressure more on one engine than on the other, whilst CEPr's measurement of gross thrust was considerably lower than the others at Test Condition 9. The two ground-level test beds at NRCC and TUAF both measure gross thrust lower than the altitude facilities.

It has not been possible to identify solely from CG8C parametric studies which of the many measurements are the major contributors to the differences. As far as frame load is concerned, stray forces are usually of a low order and can be calibrated out unless they result from some altitude effect. Static pressure distribution within the test cell can be important in some facilities but this has been looked at separately and there is no suggestion of any unknown effects being felt. Thus the differences are most likely to be attributed to either test frame load measurement or to a lesser extent the inlet momentum term; this latter effect is dealt with in the next Section on airflow measurement.

13.2 Airflow Comparison

Another nozzle coefficient is useful in providing a comparison of airflow measurement between different test facilities. This is the discharge coefficient CD8, which is defined as:-

$$\frac{\text{Airflow derived from measurement}}{\text{Isentropic airflow for the geometric area at the same pressure ratio}}$$

As with CG8, a convergent nozzle of fixed geometry gives a similar characteristic shape for CD8. Figure 13-6 gives the envelope of results for all the four altitude test facilities obtained from Engine 607594 with CD8 based on a calculated nozzle total pressure in a similar manner to the thrust analysis. This can be compared with the CG8C results on Figure 13-3. RAE(P) and AEDC appear to be in close agreement on airflow measurement with NASA one per cent higher and CEPr a further one per cent higher still. Reference 26 gives a more comprehensive treatment of the use of CD8 in airflow analysis.

A high value of CD8 is consistent with a high value of measured airflow and, because of its influence on inlet momentum, a high value of airflow leads to a high value of gross thrust. It can be seen therefore that as both CEPr nozzle coefficients are high, it is most likely that the source of difference is in the measurement of airflow rather than of frame load. The wider spread of CG8C values at AEDC for Engine 607594 is not followed by a similar pattern with CD8 and therefore it is likely that this trend of gross thrust measurement with altitude on Engine 607594 originated in the measurement of frame load.

The comparisons between altitude and ground-level test beds for Engines 607594 and 615037 are given in Figures 13-7 and 13-8 respectively. These are comparable with Figures 13-4 and 13-5 for CG8C. The spread of results is of the same order in each case, about 2½ per cent. Relative to the NRCC values, the CEPr values of CD8C are higher in both the altitude cells and ground-level test beds. The same is true for CG8C. In contrast, the TUAF values of CD8C are higher than those for NRCC and similar to the CEPr values, while the values of CG8C are lower than NRCC.

The previous comments about the absolute accuracy of nozzle coefficient values at different altitude test facilities and the reasons for any variation are just as true for CD8. It should be remembered also that the main aim of the UETP however was not to calibrate test facilities against each other but to evaluate various methods of analysis which can highlight any discrepancies in measurements and procedures to benefit future testing. On this basis it can be seen that nozzle coefficient CD8 and CG8 do provide a powerful means of checking the validity of thrust and airflow measurement and are particularly useful if a facility has tested engines of a similar type before, or if a sea level test result is available to provide a datum.

14. COMPARISON OF ENGINE AIRFLOW MEASUREMENTS USING FLOW FUNCTIONS

Engine airflow is one of the most important performance parameters measured in a test cell and is of particular importance in satisfactorily integrating an aircraft air induction system with an engine.

The airflow (gas flow downstream of the combustor) remains constant at all stations within an engine subject only to small changes which account for the effects of fuel addition, leakage from the components, and air bleeds to service external and internal requirements.

With the exception of TUAF which had no facility airflow measurement system, each test facility determined the engine airflow by two completely independent methods. The airflow at Station 1 (WA1) was measured with a flow measuring system of the type normally used by that facility. The airflow at Station 2 (WA2) was measured with a set of flow sensors which were installed in the basic UETP test article (Section 4.0). In all cases the outputs of the Station 2 flow sensors were measured and processed by the normal pressure and temperature data systems at each test facility. Thus the measured values of WA1 and WA2 are independent and provide a basis for comparison of the relative quality of the airflow data obtained at the various facilities.

In addition, other independent comparisons of flow data are possible because of the unique behaviour of selected gas flow functions at the first stage turbine nozzle when critical flow (choked flow) exists at these stations. The flow function is defined as:

$$K = \frac{W\sqrt{T}}{P}$$

$$= \text{Constant (when flow is choked and effective flow areas and gas properties remain constant)}$$

The limited instrumentation available in the engines required some approximations to compute the gas flow functions. To minimise the effect of these approximations

the gas flow functions are presented only for conditions when critical flow simultaneously existed at these stations.

In the Sections which follow, details of the flow functions used in the analysis are shown and the two independent measurements of airflow are combined with the flow functions to compare the relative quality of the airflow data at the various facilities. This subject is treated further in Reference 27.

14.1 Turbine Nozzle Flow Function

Two flow functions for the first stage turbine nozzle were defined as follows:-

$$K1 = \frac{(WA1 + WF)\sqrt{T4}}{P3}$$

$$K2 = \frac{(WA2 + WF)\sqrt{T4}}{P3}$$

The use of P3 in these equations is based on the assumption that the combustor pressure drop is zero at each test condition. The values of WA1, WA2, WF, and P3 were measured directly. The turbine temperature T4 was calculated from the combustor equation using the measured values of T3, WA1 and WF. The combustor efficiency was assumed to be 100 per cent. The common value of T4 was used in each of the two flow functions; this has a negligible effect on K2.

These flow functions were evaluated over a wide range of UETP test conditions for those data points which satisfied the requirement that both the first-stage turbine nozzle and the exhaust nozzle were choked. For this analysis, the exhaust nozzle was considered choked for those data points in which P7QAMB was greater than 2.4. Choked nozzle behaviour at this pressure ratio is confirmed in Section 13.2. Cycle analysis confirmed that the turbine nozzle was choked whenever the exhaust nozzle was choked. The complete evaluation was performed only for data obtained with Engine 607594. A partial evaluation was also performed on data obtained with Engine 615037 to confirm that the data from Engine 607594 were typical.

The mean values of K1 and K2 at Test Conditions 6, 7, 8, 9 and 10 are shown in Table 14-1. The calculated standard deviation for each value of the mean flow function is also included.

14.2 Exhaust Nozzle Flow Function

One flow function for the exhaust nozzle was defined as follows:

$$KES = \frac{(WA1 + WF)\sqrt{T7}}{PS7}$$

In the UETP test, WA1, WF, T7 and PS7 were measured directly.

This flow function was evaluated for Engine 607594 for most of the test conditions used when determining K1 and K2 (Section 14.1). Again, KES was evaluated only for those data points for which P7QAMB was greater than 2.4.

The mean values of KES for the selected test conditions are also shown in Table 14-1.

Table 14-1
First-stage turbine and exhaust nozzle flow functions
(engine 607594) (P7QAMB >2.4) (1)

TEST FACILITY	TEST CONDITION	K1	sK1(2) x103	K2	sK2(2) x103	KES	sKES x103
NASA(FE)	6	2.226	1.94	2.227	5.54	10.223	14.73
	7	2.225	1.93	2.228	6.07	10.225	8.13
	8	2.229	1.82	2.232	6.27	10.245	9.66
	9	2.231	1.63	2.233	2.55	10.213	16.27
	10	2.223	2.50	2.227	4.56	10.168	18.36
AEDC	6	2.209	2.99	2.202	2.65	10.214	18.37
	7	2.198	0.63	2.202	1.49	10.137	10.56
	8	2.202	2.12	2.217	2.26	10.103	6.87
	9	2.208	1.22	2.211	4.81	10.074	9.82
	10	2.198	6.23	2.205	2.99	10.162	27.14
	11	2.201	2.17	2.212	2.89		
NRCC(FE)	11	2.190	4.65	2.233	4.65	9.927	5.97
CEPr	6	2.224	4.08	2.210	9.55	10.248	10.09
	7	2.233	3.00	2.210	14.24	10.281	10.28
	8	2.245	4.25	2.121	11.10	10.291	23.52
	9	2.199	7.44	1.973	43.14	9.919	53.19
	10	2.229	4.21	2.267	8.57	10.300	33.26
	11	2.188	3.32	2.160	7.65		
RAE(P)	6	2.205	0.76	2.239	2.29	10.125	1.49
	7	2.205	0.40	2.232	1.54	10.138	4.02
	8	2.203	2.85	2.230	2.48	10.116	6.38
	9	2.183		2.189		10.054	
	10	2.205	1.83	2.243	3.76	10.138	5.43
NASA(SE)	6	2.223	3.63	2.220	4.63	10.196	7.20
	7						
	8						
	9	2.203	6.76	2.206	10.26	10.062	72.15
	10	2.226	3.65	2.227	5.18	10.204	6.20
NRCC(SE)	11	2.138	2.89	2.162	5.51	10.125	10.12

(1) EXCEPT TEST CONDITION 11 WHERE P7QAMB ~ 1.8-2.0
(2) STANDARD DEVIATION OF THE FLOW FUNCTIONS

14.3 Data Quality Analysis of Pressure and Temperature Measurements at Turbine and Exhaust Nozzles.

Variations in the values of the flow functions K1, K2 and KES (Table 14-1) as a function of test facility and/or test condition could be the result of real changes in the values of the flow functions and/or of measurement errors in the individual parameters (W, P and T) which enter into the calculations. Therefore, in order to interpret the significance of variations in the flow functions, it is necessary to isolate and separate the several variables. Because of the overall high precision of the test data and the planning of the UETP, substantial separation of variables is possible.

The values of the mean flow functions (Table 14-1) are shown in Figure 14-1. The test facilities are arranged in the order of testing so that engine operating time increases from left to right.

An initial examination of the flow functions was made to determine if there were .ong-term changes which occurred as a result of mechanical or aerodynamic changes in either the first stage turbine stator or the exhaust nozzle. Examples of potential changes include erosion, bowing and bending, which could affect the flow area, the flow coefficients, or the leakage paths. Physical inspection and measurement of the exhaust nozzle was possible and was carried out as described in Section 6.1.3 and no change was evident. Physical inspection and measurement of the

turbine stator was not possible because the engines were not disassembled.

To assess the condition of the turbine stator at the beginning and end of the UETP, a comparison was made of the values of K1 and K2 for NASA (FE) and NASA (SE) at Test Conditions 6 and 9. These data (Figure 14-1) confirm that there was no significant change in the aerodynamic characteristics of the first stage turbine stator and associated instrumentation from the beginning to the end of the UETP. A decrease in the exhaust nozzle flow function KES of about two per cent between NASA (FE) and NASA (SE) is shown in Figure 14-1. Since there was no physical change to the nozzle, it is reasoned that the change in KES resulted from differences in the flow parameter measurements.

Based on the foregoing analysis, it is concluded that there was no significant change to the first stage turbine stator or the exhaust nozzle during the UETP. Therefore, the changes in the flow functions among facilities and for the test conditions considered can be properly ascribed to differences in the uncertainty of measurement of the several parameters included in the functions. The standard deviations of the low functions are also shown in Table 14-1 and these provide additional insight into the uncertainty of measurement.

The design of the UETP and the analysis method chosen make possible an independent examination of two groups of parameters (WA + WF) and $\sqrt{T/P}$. The individual effects of P and T were not examined. Analysis of the consistency of the $\sqrt{T/P}$ group is possible by comparing K1 and KES at the various test facilities and test conditions. This comparison is significant because identical values of (WA + WF) appear in each pair (K1 and KES) of flow

functions and independent values of P and T appear in each flow function. As can be seen in Figure 14-1, the difference of levels of K1 among test facilities is essentially the same as the difference of levels of KES. For example, the values of K1 and KES from RAE and AEDC are similar and both are about one per cent lower than NASA (FE). The only significant exception to this result is the values of KES for NASA (SE) as was discussed above.

Based on this analysis, the accuracy of the measurements of T/P in all facilities was such that the contribution to the observed variation in flow functions was insignificant.

14.4 Data Quality Analysis of Air Flow Measurements

The analysis in Section 14.3 confirmed that the contributions of: (1) changes in the turbine stator and exhaust nozzle and (2) measurement uncertainty of $\sqrt{T/P}$ to the observed variations of K1 and KES were insignificant. Thus essentially all the observed variations in these flow functions result from variations in the measured values of (WA1 + WF). Further, because the only difference between K1 and K2 is the substitution of WA2 for WA1, direct evaluation of the consistency of these two measurements is possible. Fortunately, the contribution of WF to the quantity (WA + WF) is very small (generally less than two per cent). Therefore, for purposes of this analysis, variations in K1 and K2 can be assumed to reflect directly the variation in the measurement of WA1 and WA2.

In the case of the ground-level facilities the values for K1 and K2, hence WA1 and WA2, agreed to within two per cent at NRCC and 1.3 per cent at CEPr (WA1 was not measured at TUAF as noted in Appendix II.A.3.2.2). However, at NRCC the value of WA2 was greater than WA1. This was due to a known airflow measurement
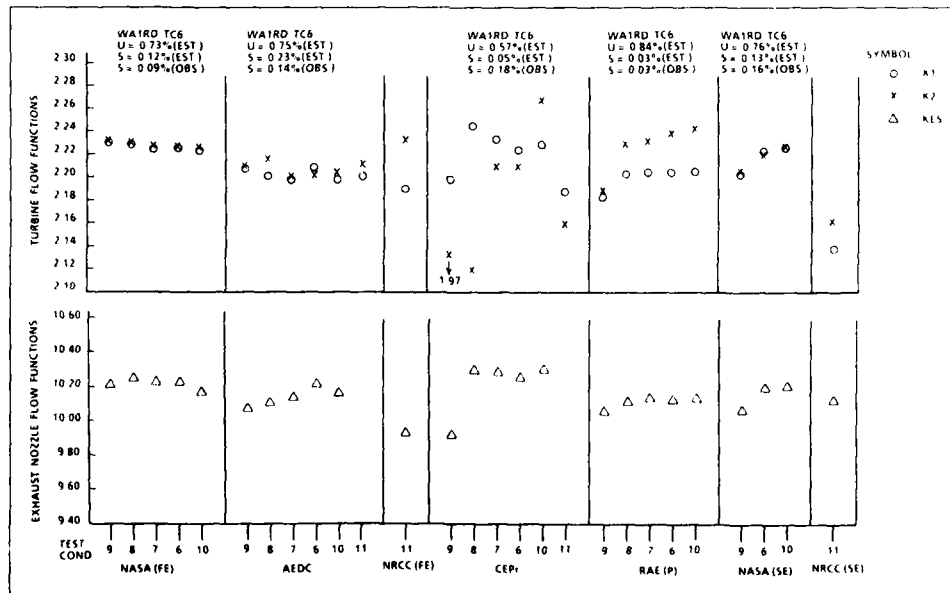

Fig.14-1 Variation of turbine and exhaust nozzle flow coefficients (engine 607594)

problem which resulted in K1 being about 1.0–1.5 per cent low (see Sections 15.4 and 18.3.3). At CEPr the value of WA2 was less than WA1. For the equivalent sea-level condition at AEDC the values of WA1 and WA2 agreed to less than 0.5 per cent and WA2 was the larger.

Substantial additional insight into the consistency of the measured airflows is provided by the standard deviation (S) values in Table 14-1. In general, the standard deviations for K1, which represents WA1, are smaller than for K2. The standard deviation of K1 lies in the range of a few tenths of per cent and for K2 several tenths of per cent. This difference in standard deviation is more likely to be the result of the lower Mach numbers at the engine inlet (Station 2) than at the facility airflow measuring systems (Station 1).

The analysis confirmed that the measured values of WA1 at RAE(P) and AEDC were very nearly identical and were about one per cent lower than the values measured at NASA. The values measured at CEPr were generally slightly higher than NASA although at Test Condition 9 the CEPr value was the same as at RAE(P) and AEDC. The values of K2 for Test Condition 11 from NRCC, CEPr and AEDC are not included in this comparison because they do not satisfy the condition of simultaneous choking of the turbine stator and the exhaust nozzle. The values are included in Table 14-1 and Figure 14-1 for reference only.

The estimated values of measurement uncertainty for WA1 are given in Section 10. At Test Condition 6, for example, the estimated uncertainty for WA1 lies in the range ±(0.6 – 0.8) per cent. The spread of data about the mean value of K1 for Test Condition 6 is just under ±0.5 per cent. This mean value lies within the estimated uncertainty limits for all four altitude facilities and therefore confirms the validity of the estimated uncertainty for this Test Condition.

Estimated and observed values of precision at Test Condition 6 are also shown in Figure 14-1. The estimated and observed values of precision for RAE(P) are identical, for NASA (FE) they are quite close, for AEDC and CEPr they are somewhat different.

14.5 Summary of Airflow Comparisons

Engine airflow is an important measurement since it is a major factor in defining ram drag for net thrust and quantifying inlet momentum in thrust stand force balance equations. The quality of airflow measurement, as indicated by the agreement between the independent engine and facility measurements, varies between facilities. The facility airflow measurement and the engine airflow for NASA (FE), AEDC and NASA (SE) differed by less than 0.5 per cent. This difference increased to more than one per cent at RAE(P) and the CEPr ground level facility, and to two per cent at NRCC.

The estimated values of facility airflow measurement uncertainty for Test Condition 6 of ±0.6 to ±0.8 per cent, which were declared by the facilities before testing was initiated, were confirmed.

The estimated and observed values of precision of airflow measurement were identical for RAE(P) and quite close for NASA. The observed values for AEDC were somewhat less than the estimates, while the observed values for CEPr were larger than the estimates.

15. ANALYSIS OF FUEL FLOW MEASUREMENT DATA

Fuel flow was analysed by first comparing the facility measured fuel flow with that measured by the reference meters on the engine. Second, to assess any possible biases in lower heating value and relative density, the values determined and used by each facility were compared with those obtained at a common reference facility. Finally, facility measured fuel flow was evaluated against independent engine parameters.

15.1 Data Quality

Fuel flow data were compared between the facility and the reference (engine) systems. Fuel/air ratios were also compared between the two systems to allow for possible changes in engine performance. AEDC showed excellent agreement between facility and reference data under virtually all test conditions, ie differences did not exceed ±1 per cent (Tables 15-1 and 15-2). Only at Test Condition 9 did data from Engine 607594 diverge by as much as 1.8 per cent. This divergence just equalled the declared uncertainty of ±1.8 per cent.

The NASA data presented conflicting pictures in that during the first entry (FE) there was very good agreement, comparable to AEDC, while the second entry (SE) data were characterised by considerable scatter. This scatter, traced by NASA to facility problems, ranged between ±3.5 per cent, exceeding the maximum declared uncertainty for fuel flow of ±1.7 per cent (Test Condition 9).

RAE(P) declared its WFER values as invalid because of fuel temperature measurement problems and therefore a comparison between the two fuel flow measuring systems was not made. Any assessment in this report will be restricted to facility flow measurements.

The CEPr data were perhaps the least consistent. Differences ranged from very good (Engine 607594 Test Conditions 1, 3, 6, 10), 0 to –0.8 per cent, to very large at Test Condition 9. The fuel/air ratio differences were somewhat larger, extending from 0.4 to 3.0 per cent for all but Test Condition 9, which showed large differences and a high degree of scatter.

Data from NRCC displayed very good agreement for the two fuel flow measurements, i.e. 0.6 to 0.8 per cent, sea-level static tests only. However, considerable differences existed with fuel/air ratios, ranging from 2.5 to 3.0 per cent for the two engines. This shift has been attributed to inaccuracies in airflow measurement.

The TUAF tests used only the engine fuel flow measuring system, so no comparisons were possible.

As a result of the above study and from participants' indications, all or part of the following data were suspect: RAE(P), all WFE; NASA(SE), Engine 6607594, possibly both fuel measuring systems; CEPr, T5 and fuel flow measurements at Test Condition 9; NRCC, facility airflow measurements.

15.2 Examination of Differences in Fuel Analyses Between Facilities and NRCC

The fuels used by the programme participants were analysed by each facility to obtain the properties needed for fuel flow calculations. In addition, samples were sent to NRCC for an independent analysis. Of primary importance were specific gravity (relative density) and lower heating

62

<div align="center">Table 15-1
Differences between facility and reference fuel flows</div>

FACILITY	ENG	(WFR – WFE2R)/WFE2R × 100 [%]					
		TEST CONDITION					
		1	3	6	9	10	11
NASA FE	594	0.3	0.4	0.5	- 0.5	0.5	
	037	0.2	0.2	0.3	0.6 → 1.2	0.5	
NASA SE	594	0.5 →3.0	0.5 → 2.5	0.5 → 3.5	- 2.5 → - 3.5	1.0 →2.5	
	037	- 0.4 →1.1	- 0.3 → - 0.9	0.0 → 1.4	- 0.7 → 2.7	0.2 →1.0	
AEDC	594	0.1	- 0.3	- 0.6	- 0.7	0.6	- 0.3
	037	0.2	0.1	- 0.1	0.3	0.0	0.1
NRCC	594						0.8
	037						0.6
CEPr	594	- 0.7 →0.2	- 0.5	- 0.3	- 7.0 → - 3.0 *	- 0.2	- 1.8
	037						- 1.0 →0.0
RAE (P)	594	- 1.0 →0.3	0.0 → 3.0	- 2.0 → 0.7	- 8.0 → - 4.5	- 1.5 →0.0	
	037						

*11 points of 18 had a % difference greater than - 10%; some WFE2R values were beyond range

<div align="center">Table 15-2
Comparison of fuel/air ratios</div>

FACILITY	ENG	$(f_{fac} – f_{ref})/f_{ref} × 100 [\%]$					
		TEST CONDITION					
		1	3	6	9	10	11
NASA FE	594	- 0.4 → 0.5	- 0.4 →0.6	- 0.3 → 0.9	- 1.5 → 0.4	- 0.4 →0.7	
	037	- 0.2 → 0.7	0.2 →1.1	- 0.5 → 0.4	- 0.2 → 2.0	- 0.7 →0.7	
NASA SE	594	0.4 → 3.0	0.5 →3.2	0.0 → 3.3	- 3.5 → - 0.8	0.3 →2.8	
	037	- 0.8 → 1.0	- 0.9 →0.4	- 0.5 → 0.9	- 1.4 → 3.7	- 1.0 →0.0	
AEDC	594	0.0 → 0.7	0.0 →0.5	- 1.0 → - 0.1	- 1.8 → - 0.4	- 1.0 →0.1	0.2
	037	0.2	- 0.4 →0.2	0.0	- 0.2 → 0.3	0.0	0.1
NRCC	594						2.8
	037						2.5
CEPr	594	- 3.0 → - 0.5	- 0.4 →1.3	- 1.2 → 1.1	*	1 ′ →2.7	- 4.0 → - 2.2
	037						1.7 → 0.0
RAE (P)	594	0.3 → 1.5	0.5 →4.0	- 0.7 → 0.9	- 10.0 → - 4.0	0.0 →2.2	
	037						

*All points out of negative range

value (net heat of combustion). Since both appear as direct multipliers in the fuel flow calculation, differences were combined to indicate the total effect they might have on the calculation. The resultant differences were small and ranged from 0.04 to 0.35 per cent (Appendix VII). When referenced to the one per cent combined reproducibility, a measure of precision for the methods used by NRCC in the analysis, these differences may be neglected.

15.3 Evaluation of Fuel Flow Measurement and Engine Performance

Subject to the above-mentioned reservations about some of the data, comparisons of fuel flow and engine performance were made for the participating facilities. Significant differences could appear depending on the basis for comparison. Small shifts in NHR at a given nozzle pressure ratio, attributed to engine rematching or facility effects, suggest that nozzle pressure ratio should be favoured as a basis of comparison.

For Engine 607594, plots of facility measured fuel flow (WFR) against nozzle pressure ratio (PS7QAMB) at each test condition show overall spreads of between two and three per cent at altitude test conditions, and three per cent at SLS conditions (Figures 15-1 and 15-2 are presented as typical examples). With declared uncertainties of 1.0 to 1.5 per cent, the spread in the data indicates good agreement, i.e. ±1.5 per cent about a mean value. Outlier curves of NASA(SE) at some altitude tests, and CEPr at SLS conditions, were disregarded because of previously identified problems.

Plots of WFR against high rotor speed (NHR) showed that with the exception of CEPr, the spread of altitude test curves of Engine 607594 was between two and three per cent (Figure 15-3). CEPr curves were consistently lower than the mean of the others and were not considered. At SLS conditions, excellent agreement existed between NRCC and AEDC; the CEPr curve was again low (Figure 15-4).

Fuel flow comparisons are very sensitive to corrected speed errors; some fuel flow differences could be explained by

shifts of less than one per cent in corrected speed. For Engine 615037, the data spread of altitude test plots ranged from 1.5 to 3.0 per cent. At SLS, AEDC and NRCC agreed within one per cent; with CEPr added, within 3.5 per cent, and with TUAF added within six per cent (Figures 15-5, 15-6).

As an additional check, plots of engine-measured fuel flow (WFE2R) versus NHR were examined. With one exception, these plots agreed very well with the WFR ones above. At Test Condition 9 (Engine 607594), CEPr diverged considerably at the high power end.

15.4 Summary of Fuel Flow Comparisons

a. The quality of data acquisition and reduction, as indicated by the agreement between engine and facility measurement, varied greatly between facilities. AEDC and NASA(FE) showed consistently very good agreement. NASA(SE) and RAE(P) displayed some good agreement, but also showed data scatter, ranging from two to ten per cent, which was attributed to test problems. CEPr showed some very good agreement, with differences of less than one per cent, but also very large differences. NRCC had good results, with differences of one per cent for fuel flow, but larger fuel/air ratio differences due to known airflow problems.

b. Fuel analysis from the participants and NRCC showed combined differences in specific gravity and lower heating value of at most 0.35 per cent. However, the reproducibility of the methods employed by NRCC was only one per cent, hence the differences can be considered negligible.

c. Comparisons amongst all facilities for fuel flow showed spreads of two to three per cent or ±1.0 to ±1.5 per cent about a mean value. Falling within the declared uncertainties, this agreement was judged to be excellent. Some known and likely problem data were disregarded to achieve these results.

64

Fig.15-1 Fuel flow comparison based on exhaust nozzle static pressure ratio (TC3-607594)
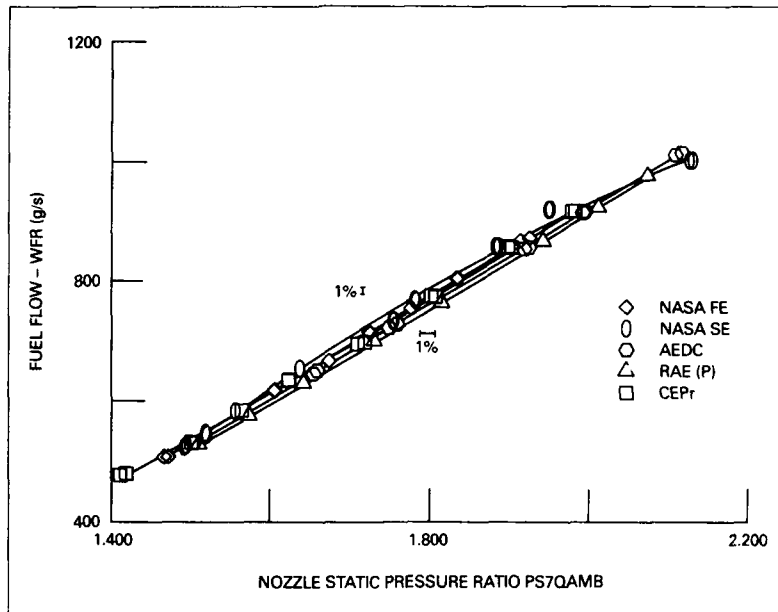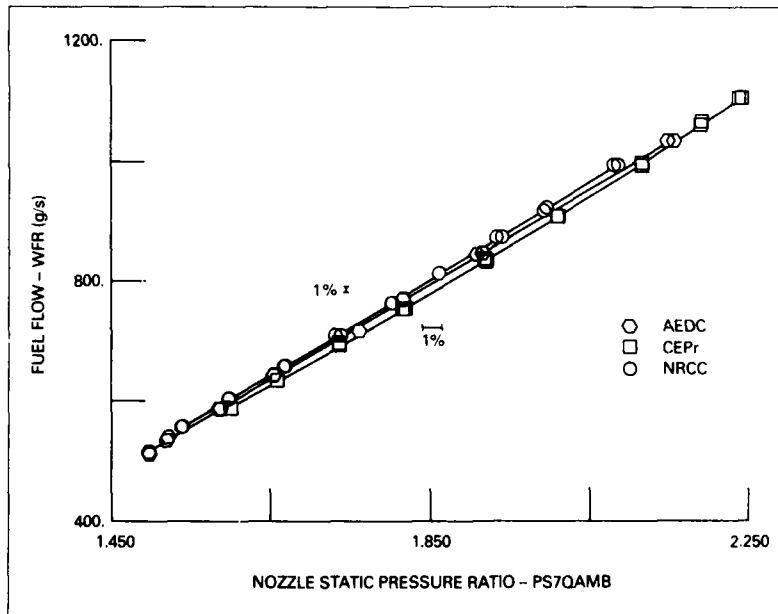

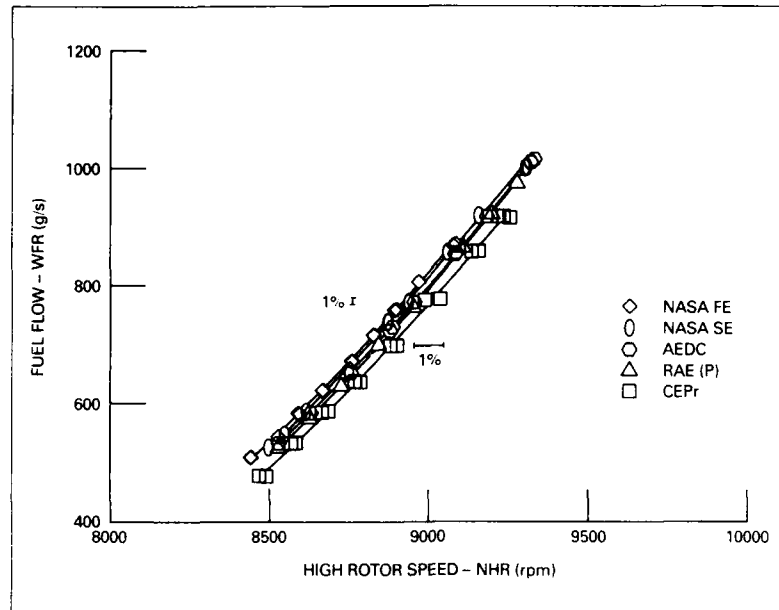Fig.15-2 Fuel flow comparison based on exhaust nozzle static pressure ratio (TC11-607594)

Fig.15-3 Fuel flow comparison based on high rotor speed (TC3-607594)
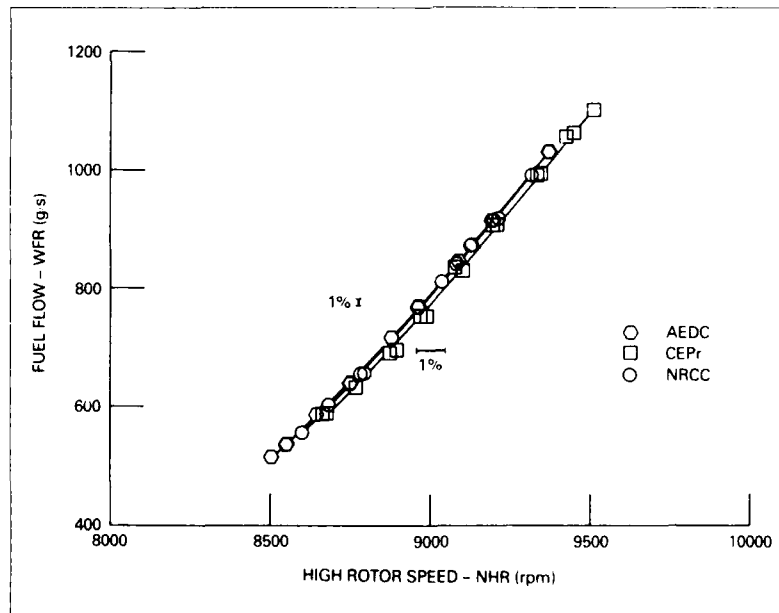

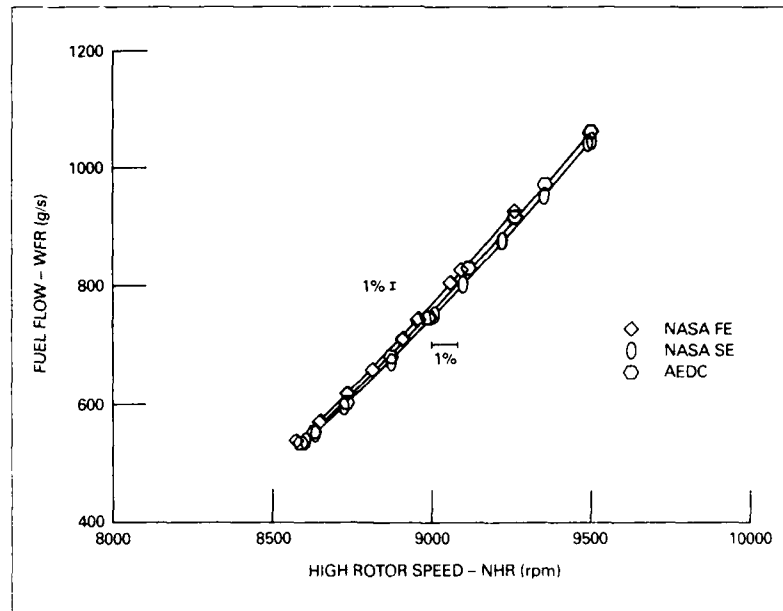Fig.15-4 Fuel flow comparison based on high rotor speed (TC11-607594)

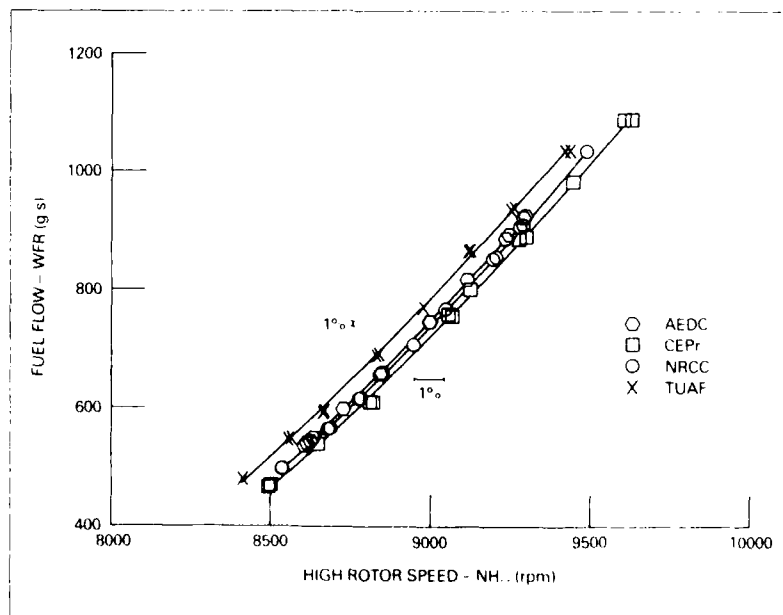Fig.15-5 Fuel flow comparison based on high rotor speed (TC3-615037)

Fig 15-6 Fuel flow comparison based on high rotor speed (TC11-615037)

16. CORRECTION OF MEASURED ENGINE PERFORMANCE TO STANDARD-DAY CONDITIONS

16.1 Introduction

When setting up test conditions it is impossible to achieve the required values precisely, even in altitude facilities, where a high degree of control can be exercised. On ground-level test beds no control is possible over inlet conditions and significant variations from the desired values have to be accepted, particularly in respect of inlet temperature.

For the UETP programme the engine performance parameters obtained at the "as set" test conditions were corrected to the desired conditions using the conventional equations given in Appendix IV. Similar equations were used when referring altitude test data to standard ground-level conditions.

In the course of detailed analysis of NRCC(SE) tests which were run at conditions well removed from standard sea-level conditions, discrepancies were seen between fuel flow data referred to standard sea-level conditions using the UETP formulae, and those from tests run at or close to the standard conditions. Also, RAE(P) in their post-test data report, Reference 13, observed that fuel flows measured at RAE(P) did not relate using the normal reference method with change in engine inlet air temperature. RAE(P) were not able to collapse the SFC sea level referred values by using temperature ratio to the exponent 0.5 as specified in the UETP equations (Figure 16-1A). However, using an exponent of 0.6 RAE(P) collapsed the SFC curves to within a total scatter of ±0.5 per cent (Figure 16-1B). Correspondingly, if an SFC temperature ratio exponent were derived from US Air Force J57 Engine Technical Manual (TO 2J-J57-13), the value at normal rated power to collapse the data to the 288K curve would vary from 0.58 at 253K to 0.68 at 308K.

As a result of the observed discrepancies in the UETP data adjustment parameters, a more detailed investigation was made of the relationships used to adjust data for a mismatch of inlet temperature from standard day conditions and engine ram pressure ratio deviations from unity.

16.2 Analysis Methodology

The adjustment parameters used in the UETP to correct airflow, fuel flow and thrust for a mis-match in temperature and/or pressure are presented in the following equations which were obtained from Appendix IV:

Airflow

$$WAIR = WAI \sqrt{\theta} / \delta$$

Fuel Flow

$$WFR = WF \cdot \delta \sqrt{\theta} \cdot THV / 42960$$

Thrust

$$FGR = FG / \delta + A8 \cdot \delta (PAMB - P2AV \cdot RAMSPC)$$

Gas turbine engines of varying cycle, bypass ratio, compression ratio, etc do not behave identically according to the normal non-dimensional correction factors presented in the preceding equations. Instead, adjustments should be derived from sample data collected when pressures and temperatures have been varied in a controlled manner in, for example, an engine altitude test facility, or alternatively from a good mathematical model of the engine.

To evaluate the deviations in the UETP data comparisons which result from the use of the UETP referred equations, a comparison was made of adjusted data using output from the UETP equations and output from a J57 engine model simulation. The engine model simulation was compiled using J57 component maps supplied by the US Air Force, Wright-Patterson AFB. The engine model was trimmed to the UETP engine using UETP Test Condition 3 data (82.7/1.0/288). After trimming, the engine model was validated with test data from US Air Force J57 Engine Technical Manual TO 2J-J57-13.

After validation of the J57 engine model simulation, output from the model was compared with the UETP inlet temperature and engine ram pressure ratio correction predictions and differences noted.

16.3 Temperature Lapse Rate

The variation of engine performance with inlet temperature is referred to as temperature lapse rate. The differences between the lapse rates that result from using the UETP correction factors and the J57 model simulation are presented in Figure 16-2. The comparisons were accomplished using low rotor speed settings that bracket the range of interest for the UETP sea-level and near sea-level tests data. Figure 16-2 also presents the ground-level facilities inlet temperature excursions.

Because of the ability of altitude test facilities to set inlet temperature within a few degrees, the imperfections in the UETP temperature referred equations have no impact on the UETP altitude facility data comparisons. Except for the NRCC second entry (SE) data, the error in the ground-level facility data comparisons as a result of using the UETP referred equations is about 0.2 per cent. None of the NRCC (SE) data were used in the UETP facility comparisons presented in Section 9.

16.4 Ram Ratio Effects

The UETP data adjustments for engine ram pressure ratio variations are basically correct for a choked exhaust nozzle; however, most of the UETP sea-level and near sea-level test data were obtained with an unchoked exhaust nozzle. The differences in engine performance as a result of using the UETP ram ratio correction factors and the J57 model simulation are presented in Figure 16-3. The comparisons were again made at a corrected low rotor speed of 5806 rev/min which corresponds to an exhaust nozzle pressure ratio of about 2.1 at sea-level and a speed of 5277 rev/min which corresponds to an exhaust nozzle pressure ratio of about 1.7 at sea-level. Figure 16-3 also presents the overall UETP ground-level and altitude facility engine ram pressure excursions for the sea-level and near sea-level test conditions.

Based on the differences shown in Figure 16-3, there is no significant impact of the UETP facilities' variations in engine ram pressure ratio on the data comparisons presented in Section 9.

68
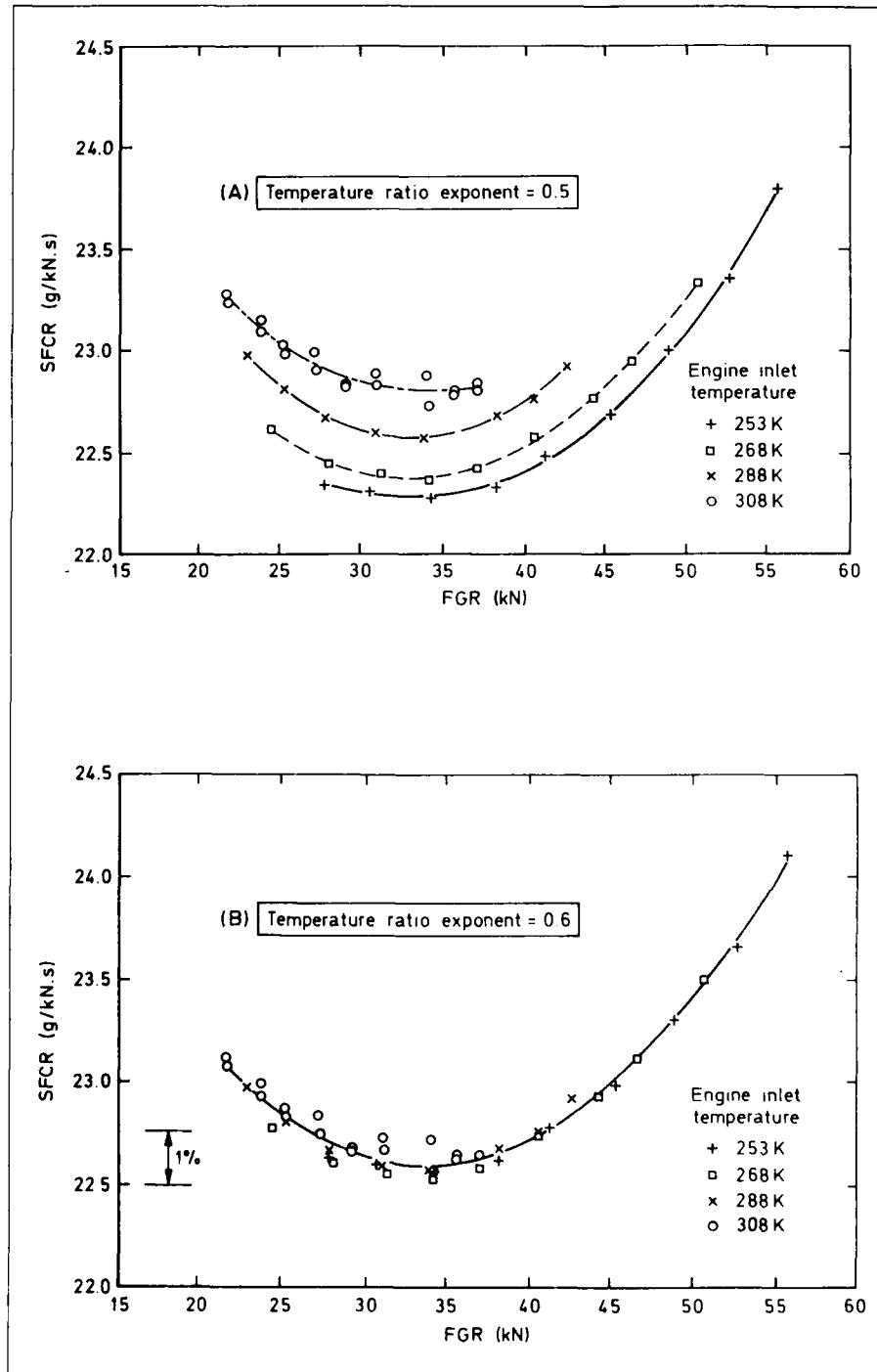
Fig 16-1 Variation of corrected specific fuel consumption with temperature ratio exponent
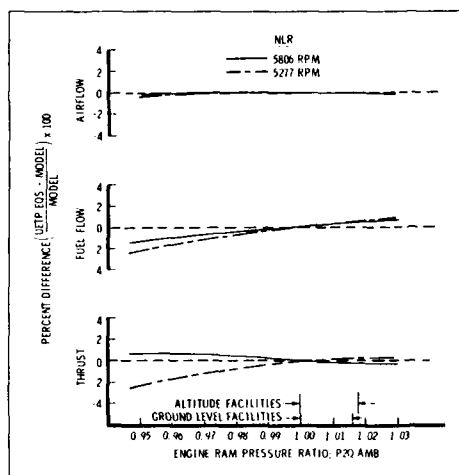
Fig.16-2 Comparison of UETP and engine model sea level temperature correction factors
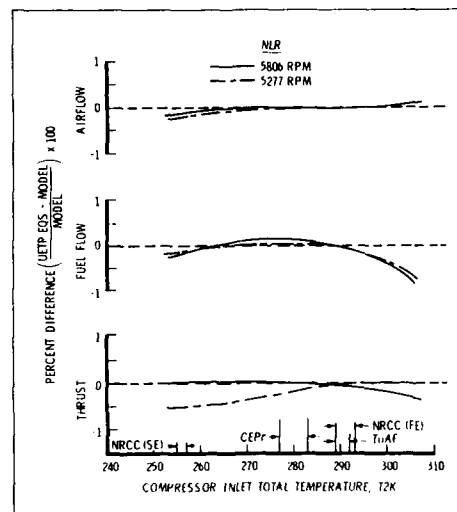
Fig.16-3 Comparison of UETP and engine model sea level RAM ratio correction factors

17. ADDITIONAL TESTS (NASA SECOND ENTRY)

17.1 Effects of Exhaust Nozzle Area Change

There was some concern that the exhaust nozzle area, A8, might have changed during the course of the UETP. This was not borne out by exit area measurements but nevertheless a test was performed with existing nozzle reducer blocks fitted at Station 8 that reduced the exit area by approximately two per cent. Test Condition 6 was re-run with the nozzle in this configuration and the data compared to that taken without the blocks.

The parameters of interest were the ratio of low to high rotor speeds, the engine pumping characteristics, (as represented by engine temperature ratio plotted against engine pressure ratio), and the variation of referred airflow with both high and low rotor speeds. Test results are shown in Figures 17-1A to 17-1D which are taken from Figures 21 to 24 of Reference 12.

Figure 17-1B shows that there was virtually no change in the engine pumping characteristics over the entire range of engine pressure ratios. Similarly the variation of referred airflow with low rotor speed, Figure 17-1D, was unaffected at speeds near Military Power, although a small difference did become evident as the low rotor speed decreased. In contrast the rotor speed ratio changed significantly, the two per cent blockage at A8 resulting in a 1.75 per cent decrease in NLQNH at a referred high rotor speed of 8900 rev/min (Figure 17-1A). The change in NLQNH coupled with the negligible influence on the referred airflow/low rotor speed relationship caused a shift in the variation of referred airflow with high rotor speed. At a given value of NHR the referred airflow, WA1R, was approximately 2.6 per cent less with the reduced nozzle area than for the normal configuration, Figure 17-1C.

17.2 Effects of Tailpipe Rake Position

During the first NASA entry it became apparent that the Station 7 total pressure rakes did not adequately measure this pressure (see Reference 9 sub-paragraph 3.2.1). The pressure profile at Station 7, the nozzle entry, was apparently strongly influenced by the large turbine exit struts and the turbine exit swirl. In an effort to understand better the nozzle entry total pressure profile and to investigate the variations in static pressure the tailpipe was rotated in 10 deg increments from 20 deg counter-clockwise to 20 deg clockwise from the base position specified for all UETP participants. Test Conditions 6 and 9 were used for this investigation.

Figures 17-2A to 17-2G, reproduced from Figures 8, 9, 10 and 12 of Reference 15, show the changes in total and static pressure, selected engine performance parameters and nozzle coefficients with tailpipe rotation. Figures 17-2A and 17-2B show typical changes in total pressure profiles. The largest effect is evident at the outer diameter with lesser effect closer to the tailpipe centreline. The total pressure variation is summarized in Figures 17-2C and 17-2D which show the variation with tailpipe rotation at positions approximately equal to 50 per cent A7 and 100 per cent (outer diameter) respectively. The dashed lines in both Figures represent an estimate of what the profiles would look like if additional rakes were available and are based on data from the existing rakes closest to these locations. The most obvious conclusion from these two Figures is that circumferential position has little influence on total pressure at the 50 per cent A7 position but a large effect on the total pressure at the outer diameter. The location of the eight turbine exit struts is easily distinguishable by the eight pressure defects. Turbine exit swirl is evident from the small total pressure variation at the 50 per cent A7 position in comparison to the large variation at the outer diameter.

70
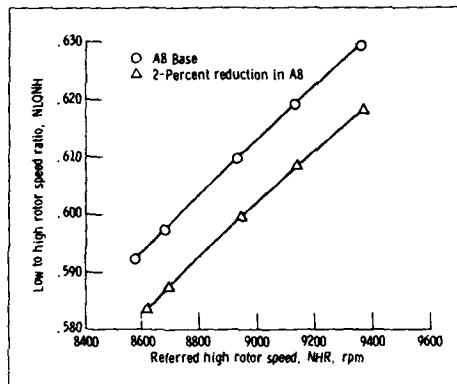
Fig.17-1A Effect of exhaust nozzle area on speed ratio (TC6-607594)
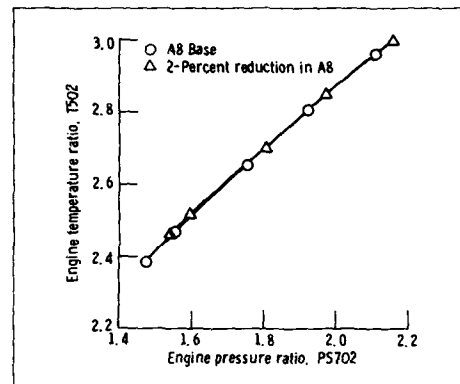
Fig.17-1B Effect of exhaust nozzle area on engine pumping characteristics (TC6-607594)
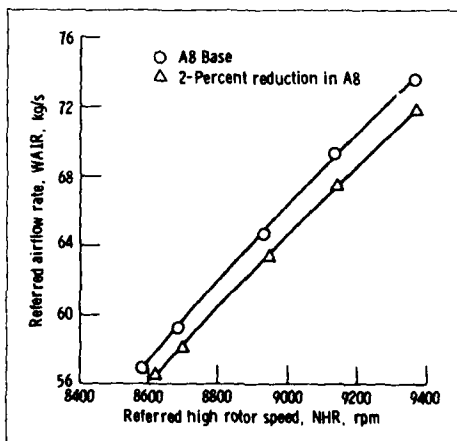
Fig.17-1C Effect of exhaust nozzle area on airflow based on high rotor speed (TC6-607594)
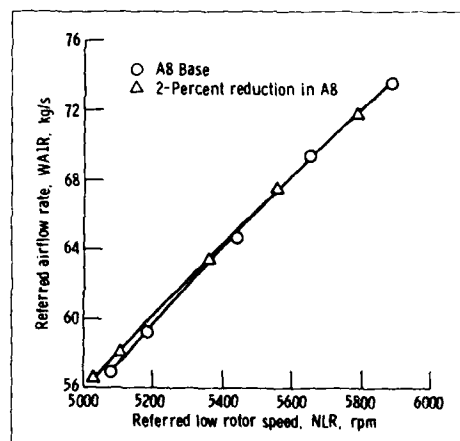
Fig.17-1D Effect of exhaust nozzle area on airflow based on low rotor speed (TC6-607594)
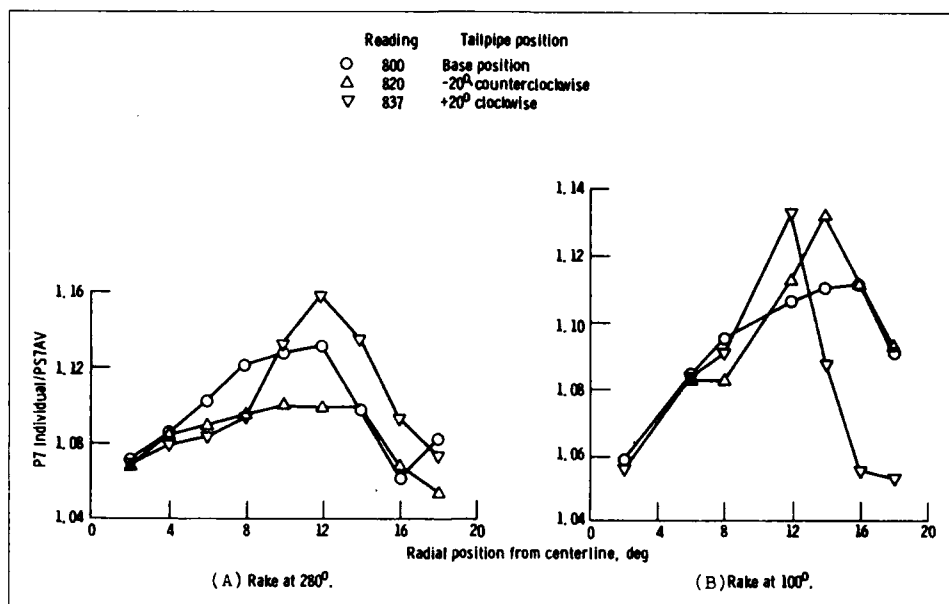
Fig.17-2A&B Station 7 radial total pressure profiles
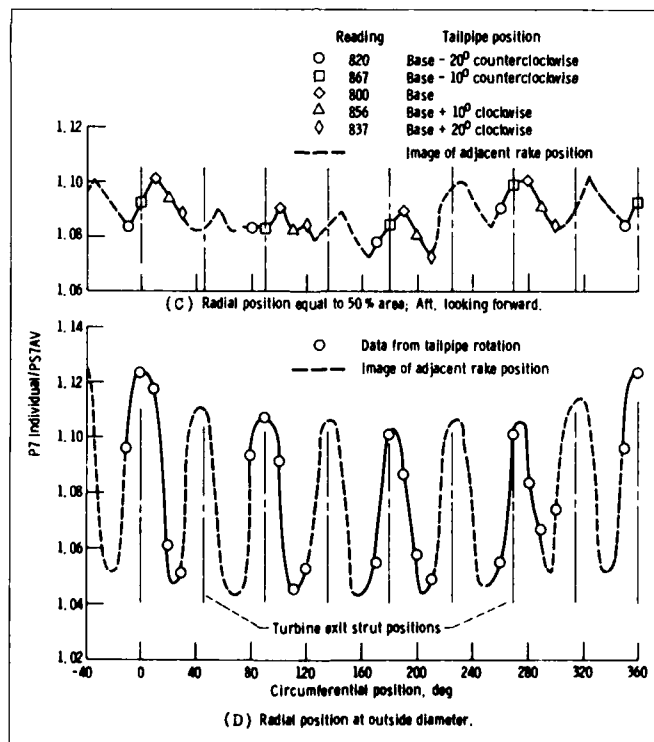
Fig.17-2C&D Total pressure variation with tailpipe rotation
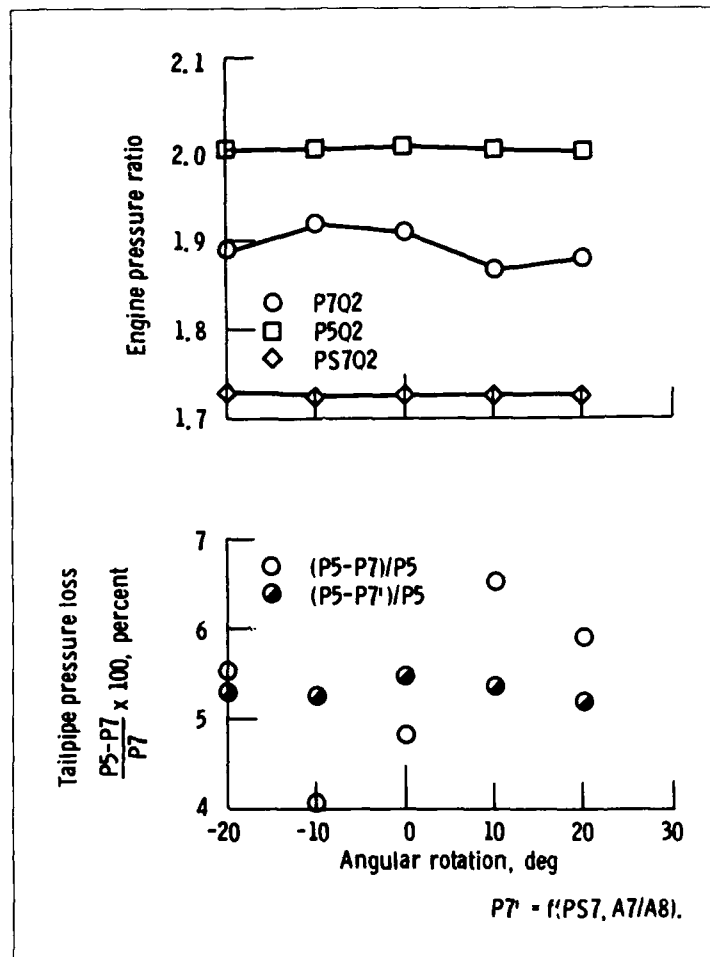
Fig.17-2E Total and static pressure variation with tailpipe
rotation (TC6-607594 NHR = 8900 rev/min)

Reading	Tailpipe position
○ 921-932	Base position
△ 809-818	20^0 counterclockwise
▽ 830-835	20^0 clockwise

(F) Nozzle thrust coefficient.

(G) Nozzle flow coefficient.
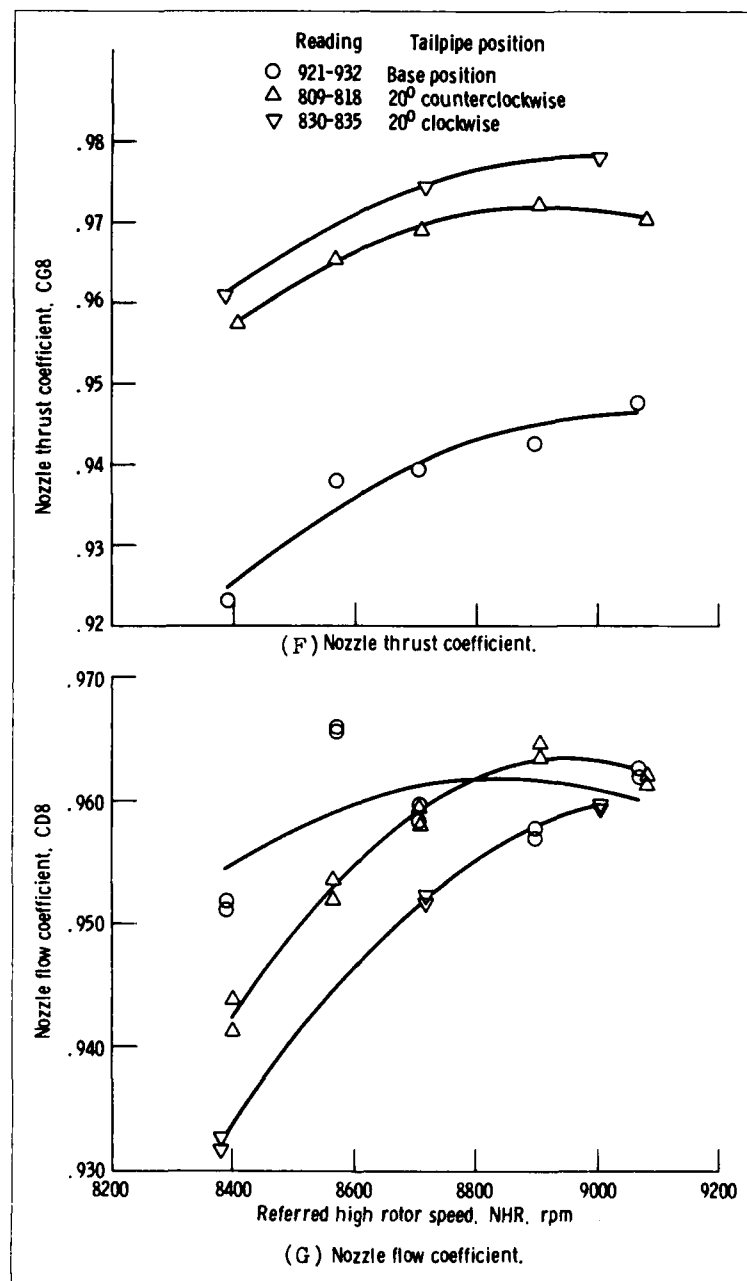
Fig.17-2F&G Effect of tailpipe rotation on thrust and flow (TC9-607594)

74

An investigation was also conducted to find a pressure in or near the tailpipe that was relatively insensitive to flow variations caused by the turbine that could be used to calculate a representative engine pressure ratio. The results of this investigation are shown in Figure 17-2E where the variation of P7, P5, PS7 and tailpipe pressure loss are plotted. In the upper part of Figure 17-2E engine pressure ratio as represented by P7Q2, P5Q2 and PS7Q2 show that PS7Q2 and P5Q2 are relatively insensitive to tailpipe rotation and are more representative of actual conditions than P7Q2.

The lower portion of Figure 17-2E shows the tailpipe pressure loss calculated using the measured P7 and a derived P7 based on the measured PS7 and the nozzle entry to nozzle exit area ratio. As would be expected from the previous discussion of P7 and PS7 variations with tailpipe rotation, the tailpipe pressure loss based on the measured PS7 produced much less scatter than that based on the measured P7.

To confirm that engine performance had not changed to any significant extent during the tailpipe rotation tests, speed ratio was plotted against referred high rotor speed. No significant variation was seen. The same was true of PS7Q2 plotted against NHR.

In contrast large variations were observed in the nozzle coefficients CG8 and CD8. Figures 17-2F and 17-2G show typical results for Test Condition 6 and indicate the importance of obtaining a good description of Station 7 mean total pressure if the calculated nozzle coefficients are to be of similar magnitude to the theoretical values for a 15 deg convergent nozzle. The changes in the nozzle coefficients appeared to be too large given the observed changes in P7 (Figure 17-2E). An investigation was therefore undertaken into the sensitivity of the coefficients for the given P7 changes. The results at the target high rotor speed of 8900 rev/min for the 10 deg clockwise and the 10 deg counter-clockwise tailpipe rotations were used. The changes in the nozzle coefficients appeared to be too large given the observed changes in P7 (Figure 17-2E).

Rotating the tailpipe and Station 7 instrumentation 10 deg counter-clockwise resulted in a 3.5 per cent decrease in P7, a 1.9 per cent increase in CD8, and a 3.8 per cent increase in CG8. The ideal sensitivity factor for the 3.5 per cent decrease in P7 indicate   ı increase in CD8 of 3.6 per cent and 5.1 per cent in C   However, when the influence of the small variations in WA1 and WF were also considered, the increase of CD8 was reduced to 1.9 per cent. the measured value. Likewise, considering the small variations in FG and PAMB, these reduced the CG8 increase to 4.3 per cent, a better match of the data. The effects of possible variations in A8 and T7 were insignificant. Based on these data it was concluded that the results were consistent.

17.3 Effects of Inlet Duct Change

Analysis of data from the UETP participating facilities uncovered variations in engine inlet total pressure profile from facility to facility. The effect of these variations on engine performance was investigated at NASA through the use of an airflow measuring venturi having a larger diameter throat and thus lower expansion to Station 2; see diagram below.

Test Conditions 6 and 9 were selected for this investigation. Figures 17-3A, 17-3B and 17-3C, reproduced from Figures

Schematics of inlet ducting used for inlet total-pressure profile investigation.
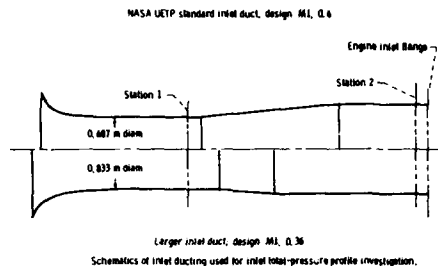
14, 16 and 19 of Reference 15, show some of the results.

It is obvious from Figure 17-3A, a plot of P2 vs flow area, that the total pressure profile using the NASA's first (smaller throat) venturi shows a larger boundary layer than an ideal or "flat" total pressure profile. This was also the greatest variation in Station 2 total pressure profile of any of the UETP facilities. Included for reference in Figure 17-3A is the inlet profile measured on the NRCC ground-level test bed which represented one of the flattest Station 2 total pressure profiles. In the same Figure the use of a larger airflow venturi shows a dramatic flattening in the profile.

Examination of the effects on engine performance of these two air flow meters shows that for Test Condition 6 the relationship between the engine's low and high compressors, represented by speed ratio, NLQNH, and overall engine performance, represented by the engine pumping characteristics, did not change significantly for the two inlets (see Table 17-1 below). However, WA1R and P3Q2 did change significantly.

Table 17-1
Effect of inlet duct changes from UETP configuration

Condition 6
NHR = 8900 rev/min NLR = 5420 rev min

Δ =	larger-standard / standard × 100%				
	EC	NLQNH	WA1R	P3Q2	T3Q2
f(NLR)	+0.18	+0.02	-0.60	-1.6	---
f(PS7Q2)	+0.18	---	-0.16	---	-1.04

Condition 9
NHR = 8900 rev/min NLR = 5520 rev min

=	larger-standard / standard × 100%				
	EC	NLQNH	WA1R	P3Q2	T3Q2
f(NLR)	+0.12	-0.03	-1.14	-0.14	---
f(PS7Q2)	---	---	---	---	-1.02

Each airflow meter produced its own engine inlet total pressure profile – the first NASA inlet profile showing the greater defect at the outer radius or compressor tip region (Figure 17-3A). If it is postulated that more compressor work is done at the compressor blade tip than at the hub, which is likely to be the case for this early engine design, then the compressor will be sensitive to tip distortion and hence more corrected airflow will be required with the
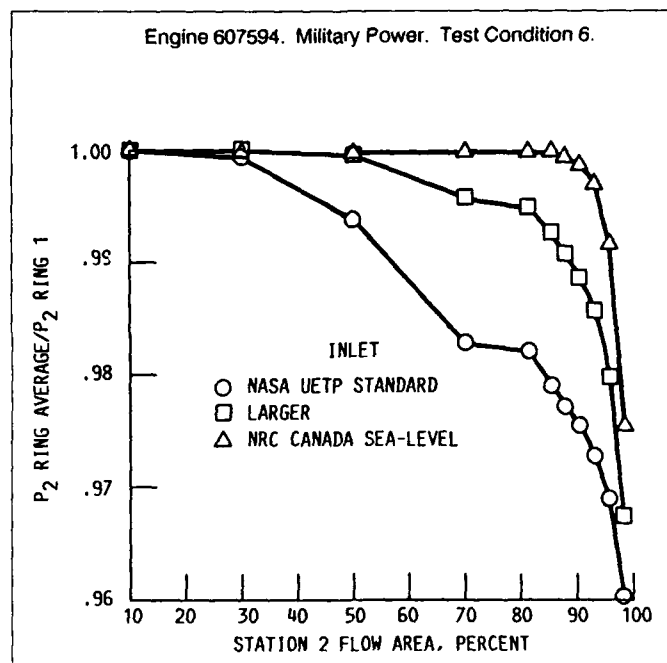
Fig.17-3A Effect of inlet duct on station 2 total pressure profile
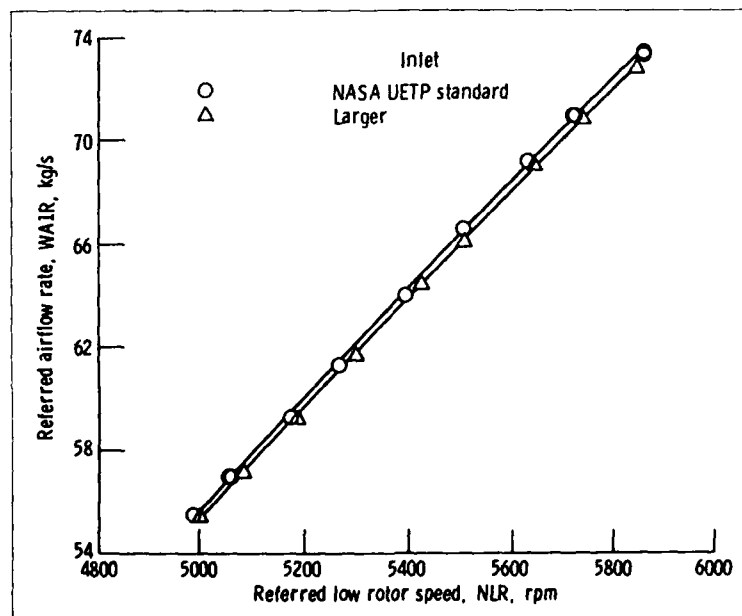
Fig.17-3B Effect of inlet duct on airflow (TC 6)
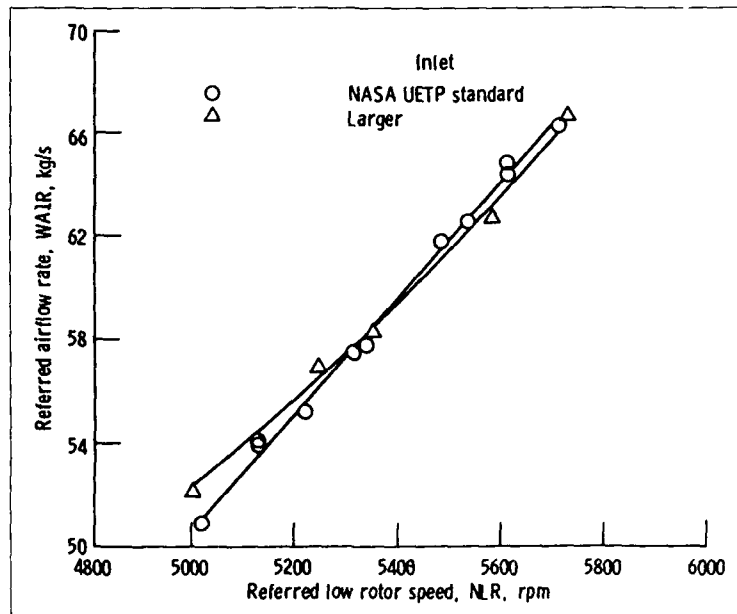
Fig.17-3C Effect of inlet duct on airflow (TC 9)

greater distortion. Because of the lack of instrumentation it is difficult to isolate the performance of each compressor but it is most likely that the difference in performance occurred in the first few stages of the low pressure compressor. Thereafter the flow adjusted itself to more uniform conditions so that the effects of distortion were not evident on parameters associated with overall engine performance.

Trends for Test Condition 9 were generally similar to those for Test Condition 6 but the data scatter due to the lower pressures prevents a good comparison. The trends for airflow, speed ratio and engine pumping characteristics were the same but the compressor efficiency and pressure ratio trends were different.

18. REVIEW OF TEST RESULTS AND COMMENTS ON OBSERVED DIFFERENCES

18.1 Background and Method of Procedure
The Working Group devoted considerable effort to examining the differences in the engine performance measured by the participating facilities and seeking explanations. The subject is complicated by the fact that many of the influences are interacting so that their individual effects can only be inferred. A straightforward presentation of the test results is given in Section 9 but reasons for the observed differences were not discussed. This aspect will now be considered in detail.

It was decided that comparisons would include altitude cell with altitude cell, ground-level bed with ground-level bed,

and ground-level bed with altitude cell. This latter comparison was included because there is evidence that the performance of an engine measured in an altitude cell at conditions close to ground-level can differ from that measured on a ground-level test bed.

The selection of a basis for comparing engine performance measurements in different facilities is not as straightforward as may appear at first sight. The magnitude of the differences which are based, for example, on a common shaft speed can yield a result different from one based on a common pressure ratio. The objective of the UETP was to evaluate the facility measurements using a "known" engine. This essentially reduces to measurement of airflow, fuel flow and thrust. Since the performance differences were expected to be small, the engine performance parameters were examined as functions of fundamentally related parameters, for example, airflow versus low rotor speed, thrust versus pressure ratio, and SFC versus thrust.

18.2 Altitude Facility Comparisons

18.2.1 NLQNH vs NHRD
Rotor speed was reported by all participants to be the most accurate parameter (Section 10). The maximum spread facility-to-facility in rotor speed ratio lies between 0.4 and 0.8 per cent. This spread is the smallest of any of the six selected parameter sets listed in Section 9.1 and has an estimated measurement uncertainty of ±0.02 to ±0.7 per cent.

The consistency in the performance trends suggests that the

differences in the rotor speed ratio are due to biases. These biases could be the result of:

(a)   errors in rotor speed measurement systems,
(b)   errors in engine ram pressure ratio,
(c)   errors in engine inlet temperature.
and/or
(d)   differences in engine inlet pressure distribution,
(e)   a continuous engine cycle re-match.

With the exception of CEPr the order in which the curves lie corresponds to the order in which the engines were tested (NASA, AEDC, CEPr, RAE(P)). This may be fortuitous although it could be indicative of a continuous engine cycle re-match with engine operational time. The analysis presented in Section 11 indicates a cycle re-match could account for up to 0.3 per cent difference in speed ratio. This compares with the observed differences of between 0.4 and 0.6 per cent (excluding CEPr).

In the case of CEPr, the separation between the points from the two data scans at each power setting indicates that the engine had not reached thermal equilibrium and this could account for a major portion of the observed shift in the curves for this facility. In contrast, the NASA, AEDC and RAE(P) data points for the scan pairs were in all cases virtually coincident.

A review of information contained in the CEPr data package showed that the stabilisation time allowed at each power setting was much shorter than required by the GTP (Section 5.1). This confirmed the conclusion reached from examination of the test results that thermal equilibrium had not been achieved.

18.2.2   T7Q2 vs P7Q2

Figures 9.1B, 9.2B and 9.3B show that the maximum spread of T7Q2 varied randomly from 0.6 to 2.0 per cent. Values for CEPr generally were the highest and values for NASA or AEDC generally were the lowest. Values for NASA at three conditions (82.7/1.0/288; 82.7/1.06/288 and 82.7/1.7/288) were not included (see Section 9.1). Values for NASA and AEDC generally were in close agreement (within 0.5 per cent) with RAE(P) values near the mean value.

As noted in Section 18.2.1, the quality of the CEPr data was influenced by the fact that the engine had not reached thermal equilibrium. Disregarding the CEPr data reduces the spread of T7Q2 to between 0.3 and 1.3 per cent.

Several factors may account for the data spreads aside from the basic measurement uncertainties:

First, several temperature sensors failed during the testing and the method of accounting for the failures varied from facility to facility. The treatment of failed instrumentation points is given in Appendix VI.

Second, two of the four instrumentation rakes at Station 7 were replaced during testing at CEPr. This instrumentation change could have contributed to a bias change in T7Q2 values obtained at CEPr and RAE(P) although check tests at CEPr, and later re-tests at NASA, showed no significant shift in Station 7 readings.

Third, the flow patterns in the tailpipe may not have repeated exactly from facility to facility because of the engine cycle re-match effects as discussed in Section 18.2.1. A small change of pattern could have a proportionately

greater influence on the measurement since additional tests at NASA reported in Section 18.2 showed steep total pressure gradients at Station 7. As a result, the use of tailpipe measurements of P7 to identify interfacility performance differences was found to be of doubtful validity. An alternative which proved satisfactory in the case of thrust and discharge coefficients was the use of static pressure Ps7. (See Sections 13.1, 13.2 and 14.2.)

The measured values of P7 were compared with those calculated using Ps7 and it was found that at all test conditions AEDC and RAE(P) data agreed closely, to within about 0.5 per cent. For the six conditions tested at NASA with the jet pipe in the "final" position (see Section 6.1.1) agreement between the measured and calculated values of P7 was less good, although the difference was still less than one per cent. However, for the CEPr data the measured values of P7 were on average consistently two per cent lower than the calculated values. This could have been due to any or all of the factors mentioned in the foregoing paragraphs.

Re-evaluation of T7Q2 as a function of Ps7Q2 rather than P7Q2 did not decrease the facility-to-facility spreads (spread ranged from 0.4 to 1.5 without CEPr). However, the re-evaluation did result in a change which aligned the values of T7Q2 to correspond with the order of testing (or engine operating time), ie NASA values generally lowest, RAE(P) values generally highest, and AEDC values nearest the mean value.

The observed increase in T7Q2 with engine operating time (average of about 0.7 per cent) is of the same order as the increase in T5Q2 (0.5 per cent) reported in Section 11 (Figure 11-4) where it is attributed to an engine performance change. The systematic variation of T7Q2 with engine operating time, coupled with the estimated measurement uncertainties reported in Section 10, account for most of the observed differences in T7Q2. The unaccounted for difference may be the result of the thermocouple failures discussed above.

18.2.3   WAIRD vs NLRD

As noted in Section 9.2.3, the highest airflow values were generally measured by NASA and the lowest values by RAE(P). At the highest pressure tested (82.7kPa) the spread of the airflow data varies randomly from 1.3 to 2.9 per cent over the range of inlet temperatures and ram ratios tested. (Figures 9-1C and 9-3C.) Note that no NASA data are included at T2 = 288K and ram ratio = 1.0.

The total spread of the airflow data ranges from 1.5 to 3.6 per cent over the range of inlet pressures tested for an inlet temperature of 288K and a ram ratio of 1.3 (Figure 9-2C). The largest spread occurs at Test Condition 8 (P2 = 34.5 kPa) due to the CEPr values at this condition being two to three per cent higher than those measured in the other facilities. This suggests that either the CEPr values of WAIRD or NRLD, or both, contain an unexplained anomaly because at all other Test Conditions the CEPr values of WAIRD lie between those measured in the other facilities. The analysis of airflow presented in Section 14.4 shows that the CEPr value of K1, hence WAIRD, at Test Condition 8 is less than one per cent higher than the values at Test Conditions 6 and 7. This analysis suggests that the CEPr data for Test Condition 8 also contain an anomaly in NLRD as well as in WAIRD. This tends to be supported by the scatter in the compressor speed ratio data shown in Figure 9-2A.

The spread of the curves from all facilities is generally about ±1 per cent from the mean. The AEDC data generally lie nearest the mean. At most test conditions this mean value lies within the estimated uncertainty limits of WA1RD. An exception is the CEPr value at P2 = 34.5 kPa (Figure 9-2C) which is more than two per cent above the mean whereas the CEPr estimated uncertainty is only 1.2 per cent (Section 10). Overall the agreement between the estimated uncertainty and the observed uncertainty is excellent.

As described in Appendix IIB a sonic venturi was used to measure airflow at AEDC and subsonic airflow metering nozzles at NASA, CEPr and RAE(P). For any selected quality (uncertainty) of pressure measurement, the operating principle of the sonic airflow meter leads to smaller increases in airflow measurement uncertainty with decrease in operating pressure than is the case for subsonic meters. This trend is well supported by the uncertainty values of WA1RD reported in Section 10. It should be noted that sonic operation requires increased pressure drop and more diffusion than subsonic operation and hence an increased pressure capability for the facility air supply. A comprehensive treatment of sonic airflow meters as related to the testing of aeropropulsion systems is given in References 28 and 29.

18.2.4 WFRD vs NHRD

Examination of WFRD plotted against NHRD (Figures 9-1D to 9-3D) shows that the spread ranges between 3.8 to 5.5 per cent for all test conditions. Generally, AEDC and RAE(P) show very good agreement, while NASA is consistently higher, and CEPr lower, than the mean, in some cases by considerable amounts. The quality of the CEPr data is not of the same standard as the others for, as discussed in Section 18.2.1, the engine had not reached thermal equilibrium even at the time of the second data scan.

The choice of NHRD as a basis for comparison magnifies any differences due to errors in inlet temperature (T2), facility effects, or engine cycle re-match. The influence coefficient for WFRD as a function of NHRD is 8:1. Section 15.3 demonstrates that other legitimate independent parameters could be used for comparison that are less sensitive to the above effects.

Notwithstanding alternative comparison parameters, by disregarding the CEPr data for reasons discussed in Sections 15.1 and 15.3, the data spread for all altitude test conditions is reduced to one to three per cent or ±1.5 per cent about the mean. Falling within the declared measurement uncertainties, this agreement was judged excellent.

As in the case for airflow measurement (Section 18.2.), one facility meter was different from the others and demonstrated some advantage in accuracy for steady flow conditions. The RAE(P) used a volumetric positive displacement type meter while all the other facilities used volumetric turbine meters. The measurement uncertainties quoted by RAE(P) ranged from ±0.44 to ±0.97 per cent, while those for the other facilities ranged from ±0.46 to ±1.7 per cent. The data presented in Section 9, with the exception that for CEPr, generally support these expectations.

18.2.5 FNRD vs P7Q2

The spreads in FNRD, as a function of P7Q2 (Figures 9-1E,

9-2E and 9-3E), ranged from 3.4 to 5.4 per cent. At all conditions the FNRD values for CEPr were highest and the values from AEDC were lowest. For all test conditions except the low pressure test condition (20.7/1.3/288), AEDC values agreed with RAE(P) values (less than 1.5 per cent difference); NASA values also agreed with RAE(P) values at all reported conditions. It should be noted that NASA data for three conditions (82.7/1.0/288; 82.7/1.06 288 and 82.7/1.7/288) were not included (see Section 9.1).

The AEDC FNRD values at the 20.7/1.3/288 condition were approximately three per cent lower than the mean value. This difference is in general agreement with the gross thrust variation reported in Section 13.1 (Figure 13-3).

As noted in Section 18.2.1, the quality of the CEPr data was influenced by the fact that the engine had not reached thermal equilibrium and by the error in P7 as discussed in Section 18.2.2. Disregarding the CEPr data reduced the range of the FNRD spreads to 0.3-3.3 per cent. These values are consistent with the measurement uncertainty levels reported in Section 10.

Because of the steep total pressure gradients at Station 7 (reported in Section 17.2), FNRD spreads were re-evaluated as functions of two alternative parameters, PS7Q2 and P5Q2. These gave spreads of 1.1-3.3 and 1.4-2.2 per cent respectively when all the facilities were included.

18.2.6 SFCRD vs FNRD

The overall spread of the curves from all facilities at all test conditions ranged from 0.9 to 2.4 per cent with the RAE(P) values generally nearest the mean. The mean value was well within the estimated uncertainty limits of SFCRD for each facility, except for AEDC at P2 = 20.7 kPa (Figure 9-2F), which suggests that, in general, the estimated uncertainty of SFCRD may be excessive.

This excellent agreement of SFCRD between facilities appears to be contradictory in view of the discrepancies identified in the preceding Sections in thrust at Test Condition 9 at CEPr (Sections 18.2.4 and 13.1) and in fuel flow at CEPr at nearly all conditions (Sections 18.2.5 and 15.3). This apparent contradiction can be understood by careful inspection of Figures 9-1F, 9-2F and 9-3F which show that the concurrent migration of SFCR and FNR between the points for the two data scans at each power characteristic for the engine. The migration occurred because the engine was not in thermal equilibrium as described in Section 12.2.1.

The fact that the migration occurs along the engine characteristic and thus does not affect the level of the CEPr data is a fortuitous result. The slope of the migration is uniquely associated with the design of the test engine and control system. Therefore, this result is directly related to the J-57 class of engine.

18.2.7 Summary of Differences Between Altitude Facilities (Altitude Conditions)

The data spreads discussed in Sections 18.2.1-18.2.6 are summarised in Table 18-1 below. Additional information is also included which enables the worth of the test data to be assessed. The proportion of data points falling within a two per cent bandwidth are given for all the data presented in Section 9.

Table 18-1
Altitude facility comparison (altitude conditions) (NASA*, AEDC, CEPr, RAE(P))

Engine Parameter (Independent Variable)	Overall percentage spread at mid thrust (Without CEPr)	Data within two per cent band (per cent)	Percentage spread of estimated uncertainty	Comments
NLQNH (NHRD)	0.4 to 0.8 (0.04 to 0.5)	99	0.04 to 1.4	1 Smallest variation of any data set. 2 Cycle re-match with time accounts for 0.3 per cent variation.
T7Q2 (P7Q2)	0.6 to 2.0 (0.3 to 1.3)	98	0.6 to 1.2	1 Several temperature and pressure sensors replaced. 2 Possible variation of flow pattern in tailpipe. 3 Cycle re-match with time accounts for up to 0.3 per cent variation.
WAIRD (NLRD)	1.3 to 3.6 (1.3 to 2.9)	88	0.8 to 5.2	Sonic venturi appears to offer measurement accuracy benefits.
WFRD (NHRD)	3.8 to 5.5. (1.0 to 3.0)	63†	0.8 to 3.4	Volumetric positive displacement meter appears to offer measurement accuracy benefits.
FNRD (P7Q2)	3.4 to 5.4 (0.3 to 3.3)	69†	0.8 to 6.4	1 Some variation due to thermal non-equilibrium effects. 2 P7 measurement effects.
SFCRD (FNRD)	0.9 to 2.4 (0.9 to 2.4)	89	1.2 to 7.0	

*No NASA data for Test Condition 3.

†CEPr results consistenty displaced from other three facilities. If deleted, figures become 85 (WFRD) and 92 (FNRD)

For additional clarification and to show the variation between Test Conditions the data spreads for the three main engine performance parameters, net thrust, SFC and airflow are shown in Figure 18.1. In this figure the Test Conditions have been grouped so that the effects of engine inlet temperature, engine inlet pressure and ram ratio can be more clearly seen. Spreads are given (a) including all facilities and (b) with CEPr data excluded. From the Figure it appears that there is no pattern linking the spreads in these three parameters. For instance, with all data included the greatest spread in net thrust occurs at Test Condition 7 (51.7/1.3/288), in SFC at Test Condition 1 (82.7/1/1.0/253) and in airflow at Test Condition 8 (34.5/1.3/288). It is worth noting that the spreads at the most arduous condition (20.7/1.3/288) are not significantly higher than the average values

It should be noted that the spreads in FNRD were obtained from plots of FNRD vs P7Q2 (Figures 9-1E, 9-2E and 9-3E). Hence any error in the measurement of P7 influences the magnitude of the spread. This issue is discussed in Section 18.2.5 and it accounts for the large reductions in the

spreads in FNRD shown in Figure 18-1 when the CEPr data are excluded.

In addition to the data spreads, Figure 18-1 shows the estimated uncertainty intervals for Test Conditions 3, 6 and 9. Two values are shown for each Test Condition, the estimated median uncertainty interval and the estimated maximum logical uncertainty interval. Full details of the method of calculating these uncertainties are given in Reference 16 but for convenience a brief summary is given below.

The lower of the two uncertainty intervals, the median uncertainty interval, was calculated as follows. For each of the three Test Conditions considered, Tables 10-1 to 10-4 were used to obtain the median total uncertainties in the dependent variable (e.g. FNRD) and in the independent variable (e.g. P7Q2). Using curve slopes derived from the appropriate graphs presented in Figure 9-2 (e.g. d(FNRD)/d(P7Q2)) the median uncertainty intervals were calculated as the root sum square combination of the median uncertainty contributions of the dependent and the
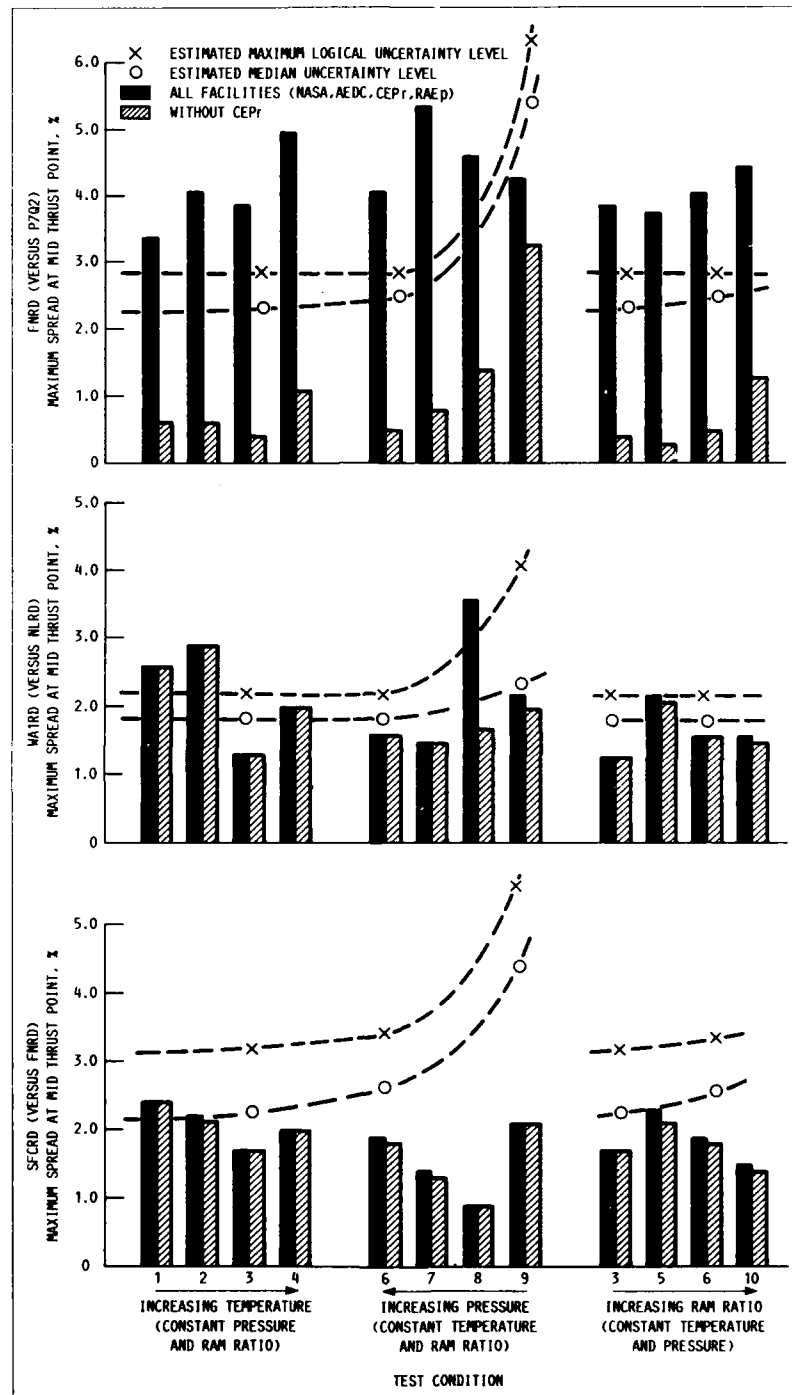
Fig.18-1 Spreads in net thrust, airflow, and SFC — altitude facilities

independent variables with the independent uncertainty value multiplied by the slope of the curve relating the variables.

The higher of the two uncertainty intervals, the maximum logical interval, was calculated as a combination of the maximum uncertainty for half the interval, with the next-to-maximum uncertainty for the other half, again allowing for uncertainty in the independent variable using the curve slope.

The estimated uncertainty intervals represent a 99 per cent limit of the spreads. Virtually all the data lie within the estimated maximum logical uncertainty intervals, thus confirming the validity of the error estimates. For three of the four altitude facilities the observed spreads in FNRD (vs P7Q2) are significantly less than the estimated total uncertainty intervals and this suggests that the estimated values may be excessive. The exception is the FNRD data from CEPr. However, a primary contributor to the discrepancy is a two per cent error in the CEPr measured values of P7, as discussed in Sections 18.2.2 and 18.2.5 and not to an error in FNRD.

18.3 Ground-level Facility Comparisons

The ground-level facility comparisons based on data from Engine 615037 acquired at NRCC, CEPr and TUAF, are shown in Figure 9-4. Results obtained in the AEDC altitude facility at sea-level static conditions are also included for reference. The comparison was made only at conditions for which the bleed valves were closed (see Section 5.3).

Reference should be made to Appendix VIII for a discussion of the influence of environmental factors on the measurement of thrust in a ground-level test bed. The UETP calculation procedures given in Appendix IV are known to lead to results which differ slightly from those obtained using standard methods and hence the values quoted in Sections 18.3.5 and 18.3.6 should be viewed with caution.

18.3.1 NLQNH vs NHR

At a given value of NHR the maximum spread in NLQNH is 1.5 per cent with TUAF recording the highest and CEPr the lowest value. The large difference in rotor speed ratio is the result of a high, stand-alone value recorded at TUAF. A major reason for this shift may be due to the large pressure distortion at Station 2.0 caused by the close proximity of the facility vertical inlet to the engine face. As the detailed pressure measurements were not recorded in TUAF, this hypothesis cannot be confirmed (see Section 4.4).

Without the TUAF data the differences in rotor speed ratio are less than 0.5 per cent which is similar to that observed in the altitude facilities. As in the altitude case, CEPr shows a significant separation between the points from the two data scans at each power setting. This separation indicates that the engine had not reached thermal equilibrium (see Section 18.2.1). As CEPr differs from both AEDC and NRCC, which are almost coincident, the lack of thermal stabilisation could account for most of the difference. Any remaining difference is attributed to measurement uncertainty and cycle re-matching with engine operational time (see Section 11).

18.3.2 T7Q2 vs P7Q2

For a given value of P7Q2 the maximum difference in T7Q2 is just over one per cent (2.5 per cent including TUAF)

which is less than that seen in the altitude facility comparisons at unity ram ratio (1.5–2.0 per cent). Performance trends are consistent between facilities. TUAF data are not directly comparable due to the limited sampling at Station 7. (See Section 4.4.)

Values of T7Q2 measured at CEPr and AEDC agree within 0.5 per cent. The difference between NRCC and AEDC/CEPr is most likely caused by the method of computing at T7AV from point measurements. During tests at NRCC, a large number of thermocouples progressively became unserviceable during the course of the test. As the procedure for accounting for unserviceable thermocouples in a highly non-homogeneous flow field was not the same at all facilities (see Appendix VI), the derived T7AV could be significantly different. Notwithstanding this known bias, the agreement between the facilities was well within the uncertainty band.

18.3.3 WAIR vs NLR

The maximum spread at a given NLR is 1.9 per cent (4.8 per cent with TUAF) with NRCC recording the lowest values. This is the same order of spread observed between the altitude facilities at a ram ratio of unity. It should be noted that for purposes of this comparison the value of WA2 measured at TUAF was inserted at WA1.

The analysis presented in Section 13.2 shows that at sea-level static conditions the nozzle thrust coefficients measured in the AEDC altitude cell and on the CEPr and NRCC test beds are in good agreement, the spread being in the region of one per cent. (Figure 13-5). Since the measurement of thrust in a connected altitude cell involves the airflow whereas on a ground-level test bed it does not, it can be inferred that the airflows measured at AEDC must have been reasonably close to the true values. NRCC confirmed that the airflow was between 1.0 and 1.5 per cent low because of the difficulty of determining the discharge coefficient.

18.3.4 WFR vs NHR

The performance trends measured by all four facilities are consistent but with significant differences in level. At a given value of NHR the maximum spread is 3.5 per cent (8 per cent with TUAF). The agreement between NRCC and AEDC was within one per cent (see Section 15.3). Some of the remaining difference can be accounted for by the shift in cycle match discussed in Section 11.

The WFR spread at sea-level (3.5 per cent) is similar to that obtained at near sea-level conditions (Test Condition 3) in the altitude facilities (4.3 per cent).

18.3.5 FNR vs P7Q2

At a given P7Q2 the maximum spread is 0.7 per cent (2.5 per cent with TUAF) which is considerably less than the three to four per cent seen in the altitude facilities at a ram ratio of unity. There are no discernible trends in the thrust data with operational time or with inlet temperature mismatch from standard conditions (T2 = 288K). This agreement is judged to be very good, but see Section 9 of Appendix VIII for further discussion.

18.3.6 SFCR vs FNR

The performance trends from NRCC, CEPr and AEDC are consistent with a difference of 0.6 to 0.9 per cent between the three curves with an overall spread of 1.8 per cent (3.5 per cent with TUAF).

82

The spread in the data about the mean value (±0.9 per cent) is within the overall uncertainty, but see Section 9 of Appendix VIII for further discussion.

18.3.7 Summary of Differences Between Ground-level Test Beds (SLS conditions)
The data spreads discussed in Sections 18.3.1–18.3.6 are summarised in Table 18-2 below:

18.4 Ground-level/Altitude Facility Comparisons
The ground-level/altitude facility comparisons are based on data from Engine 607594 acquired at NASA, AEDC, RAE(P), CEPr and NRCC. As explained in Section 9-4, except for NASA all the altitude facility data relate to an inlet temperature of 288K. For NASA, data for 308K were substituted.

The data from all altitude facilities, except AEDC, required use of the UETP equations to adjust the data from the as-tested inlet pressure of 82.7 kPa to the standard sea-level value of 101.3 kPa. While these adjustments could introduce discrepancies (see Sections 13 and 16) it is judged that the discrepancies would be negligibly small at the high pressure condition.

An overall review of Figures 9 5 A to F shows that the highest curve always relates to an altitude facility and, with one exception, the lowest to a ground level facility. The exception is for SFCR where the lower values were recorded in the AEDC altitude facility. The facilities giving the highest and lowest values are not the same for every parameter, although NASA features prominently as a "high" candidate (four out of six) and NRCC as a "low" (three out of six).

*Tests in AEDC altitude cell at standard sea-level static conditions included for comparison.

Within the extremes, no consistent pattern is discernible in the order of the curves. In two of the parameter sets considered, both involving NHR (NLQNH vs NHR) and (WFR vs NHR), the NASA data are displaced significantly from the other curves which are grouped closely together. This could be associated with the fact that the NASA tests were run at T2 = 308K compared with 288K for the other altitude facilities and 277–293K for ground-level test.

In a ground-level test bed the engine inlet momentum term is very small compared to the engine thrust so an accurate determination of this term is not required for the purpose of cell to cell comparisons. However, in a direct-connect altitude cell the inlet momentum term can be as much as 20 per cent of the engine net thrust. The fact that the AEDC results agree with those from NRCC and CEPr indicates that the measurements of airflow and inlet conditions – total and static pressures and total temperature – must be reasonably correct, at least for sea-level static conditions.

It should, however, be noted that the equations used in the UETP to determine thrust are inadequate when applied to a ground-level testbed (see Appendix VIII). This is due to the way in which the UETP defines the engine static pressure environment (PAMB). Hence, in the comparisons between ground-level and altitude data, any analysis involving PAMB (e.g. thrust and SFC) must be treated with caution.

18.4.1 Summary of Differences between Ground-Level Test Beds and Altitude Facilities (SLS Conditions)
The data spreads discussed in Section 18.4 are summarised in Table 18-3.

18.5 Comparison of Open and Closed Ground-Level Test Beds
Engine 615037 was tested at NAPC on an outdoor test stand under near standard day conditions. Data from this facility

Table 18-2
Ground-level bed comparison (SLS conditions) (NRCC, CEPr, TUAF, AEDC*)

Engine parameter (Independent Variable)	Overall percentage spread at mid-thrust (with TUAF)	Percentage spread of estimated uncertainty	Comments
NLQNH (NHR)	0.5 (1.5)	0.2 to 1.6	Spread similar to that in altitude facilities.
T7Q2 (P7Q2)	1.1 (2.5)	0.9 to 1.8	Spread affected by failure of T7 thermocouples at NRCC.
WAIR (NLR)	1.9 (4.8)	0.6 to 1.5	NRCC airflow low by 1–1.5 per cent
WFR (NHR)	3.5 (8.0)	0.9 to 2.5	Spread reduced to 1.8 per cent when CEPr values removed
FNR (P7Q2)	0.7 (2.5)	1.0 to 2.3	
SFCR (FNR)	1.8 (3.5)	1.5 to 3.5	

*Tests in AEDC altitude cell at standard sea-level static conditions included for comparison.

Table 18-3
Ground level bed/altitude cell comparison. Sea-Level Static Conditions. Engine 607594

Engine parameter (Independent Variable)	Overall spread at mid-thrust (Percent)	Comments
NLQNH (NHRD)	0.5	
T7Q2 (P7Q2)	2.3	Spread affected by failure of T7 thermocouples at NRCC
WA1R (NLRD)	2.5	NRCC airflow low by 1.0 — 1.5 percent.
WFR (NHR)	3.6	
FNR (P7Q2)	5.0	Spread reduced to 3.0 percent if CEPr (Alt) non-equilibrium values removed.
SFCR (FNR)	2.7	Max spread is between NRCC (GL) highest and AEDC (Alt) lowest

were compared to those obtained at NRCC in a ground-level bed, and also to those obtained at an altitude facility (AEDC) operated at SLS conditions.

The agreement for all parameters, excluding known anomalies, was within the declared measurement uncertainty, however an unexplained bias in FNR resulted in a rigorous examination of the GTP thrust correction terms. It is shown in Appendix VIII that the definition and the use of PAMB in altitude facilities does not apply to ground-level beds, hence any data presentation in this report that involves PAMB or FNR as defined in the GTP, will have biases of up to 1.0 per cent in each term.

Redefining FNR for ground-level test beds, and comparing on a common basis, the agreement between NAPC, NRCC and AEDC was 0.8 per cent in FNR, 1.3 per cent in WFR and 1.0 per cent in SFCR. This spread is within the measurement uncertainty and considered to be very good.

19. BENEFITS RESULTING FROM PARTICIPATION IN THE UETP

Each participating facility provided a summary of improvements made or benefits achieved as a result of the UETP. These are reproduced below. Also included is a contribution by Professor Braig of the Institut fur Luftfahrt-Antriebe at the University of Stuttgart. The Institut operates a small altitude test facility and although it did not participate in the test programme it will benefit from many of the findings of the UETP.

19.1 AEDC

1. AEDC Benefits

a. Avoid inlet duct divergence.

b. Include lab-seal total pressure consistency checks in on-line data verification procedures.

c. Include load-cell pressure sensitivity data processing verification checks.

2. Testing Community Benefits

a. Identified fuel-flow measurement technology need.

b. Provided technical data base to support test-technique improvement studies and test-technique management decisions (based on significantly different test techniques used by UETP test participants – ie thrust stands, lab seals, air meters, exhaust collectors, test instrumentation systems, etc).

c. Provided technical data base to support instrumentation improvement studies and instrumentation-technique management decision (based on significantly different measurement practices and uncertainty assessment philosophies).

3. Future "UETP-Type" Program Benefits

a. Include studies of validated (known quality) math model in engine selection criteria.

b. Define experimentally the performance lapse rate.

c. Establish independent steering group and performance evaluation authority.

19.2 NASA

An international program which depended on the co-operation of many different facilities was successfully conducted. In fact, co-operation among the facilities was excellent. Some of the lessons learned as a result of participation in the UETP are listed below, though not necessarily in the order of importance.

1. There were few basic differences in measurement uncertainties between the participating facilities even though there were facility differences and both sea level and altitude facilities were involved.

2. A detailed error audit for each facility using a common measurement uncertainty technique was developed. The probability of this being accomplished without the impetus of the UETP was small.

3. Good steady state data require an experimentally determined stabilisation time (e.g. 3–5 minutes even for a simple turbojet such as the J-57 engine). Too short a stabilisation time can significantly increase random error and thus measurement uncertainty.

4. Data taken in an altitude facility at or near sea level-low flight Mach number conditions can be compared to sea level data using suitable techniques.

5. A simple convergent fixed area nozzle is a good comparative device because it is independent of engine type and engine performance changes. It can be used to evaluate thrust and mass flow based only on a few simple measurements.

6. For a comparative-type test such as the UETP, a knowledgeable engineer/technician should accompany the engine if only to assure the efficient (and timely) installation and start up of the engine.

7. Turbulence levels at the engine inlet were about one percent different between altitude and sea level facilities. The usually short inlet duct of the sea level facility developed a smaller boundary layer thickness and less radial distortion than the longer inlet duct of the altitude facility. Inlet duct divergence in the altitude facility between the air meter station and engine inlet only exaggerated the distinction.

8. Careful selection of the engine nozzle/exhaust collector configuration can ensure that boattail forces are insignificant for both the altitude and ground-level facilities.

9. The nozzle inlet static pressure and the nozzle inlet-to-exit area ratio were better indicators of nozzle inlet conditions than the measured total pressure. This was due in part to swirl generated at the turbine exit and the large centerbody support struts.

10. In a program of this magnitude ground rules as to data to be compared and how it is to be compared should be agreed upon in advance. However, the comparison should be directed to a few simple, well considered parameters and provisions made to alter the techniques as experience is gained.

11. A statistical approach to data acquisition will provide better quality data using few data points (i.e. proper sampling-curve fit and standard deviation minimized). This removes the "human" or the least predictable element. The second order curve fits were sufficient to provide a convenient and accurate method for comparing data with minimum human interpretation, influence, or bias. The data can be represented by three constants per line and thus computer comparisons are easily made.

12. A good analytical model of the precise engine-model is highly desirable to provide a reasonable basis of comparison since the differences are small, or within the expected instrumentation uncertainties.

13. Inlet duct divergence between the airflow meter and the engine inlet can have a strong influence on the engine inlet total pressure profile.

19.3 NRCC

The following improvements or benefits were achieved during the NRCC participation in the two UETP test sequences.

1. Analysis

a. A rigorous error analysis showed that certain hardware components and fuel property calculations were significant contributors to large overall measurement uncertainty. Improvements have been made.

b. A comprehensive review was conducted of thrust corrections which must be applied to enclosed sea-level stands. Detailed fuel flow corrections were also rationalized.

c. Airflow computation was critically examined, including integration methods, thermodynamic properties and temperature and humidity effects. Additional "in-house" testing was conducted at NRCC using an alternative inlet bulletnose configuration to define the importance of radial and circumferential static pressure variations in the engine inlet duct on the determination of engine airflow.

d. Examination of altitude facility data revealed some significant ambient correction to sea-level data for this engine type.

2. Test Techniques

a. Cell aerodynamic calibrations were carried out to account for exhaust collector geometry effects on cell airflow and hence its influence on momentum and drag terms.

b. Improved data acquisition procedures provided shorter scan times and reduced set-up time through on-line pressure and temperature calibrations. Acquisition of voltage signals was interspersed between mechanically multiplexed pressure readings.

c. Traceable fuel flow calibration techniques were developed in-house.

d. Procedures for either on-line or post-test data consistency or comparison tasks were devised.

e. Methods were improved to document software and hardware changes, and test organisation.

f. Statistical studies of data in real-time were used to justify scan and stabilisation times.

3. Facilities

a. Thrust stand suspension was improved and centreline pull calibration apparatus and procedures were developed.

b. Temperature compensation and thrust stand pre-load methods were perfected to allow reliable testing in ambient conditions covering ±30 degrees Celsius.

c. A ballistic calibrator facility was acquired thus eliminating dependence upon the turbine fuel meter manufacturer.

19.4 CEPr

The following improvements or benefits were achieved during the CEPr participation in the UETP:

1. CEPr and jet testing community benefits

a. CEPr has gained considerable benefit from using – for the first time – the uncertainty methodology and analysis described by R B Abernethy and J W

Thompson. in accordance with the GTP. Now, CEPr does this type of analysis regularly.

b. The rigorous and detailed error audit developed for the UETP proved to be very useful. This procedure resulted in clear identification of error sources and parts of the measurement system which could be improved.

c. The calibration range of instruments, especially pressure transducers and thrust measurement systems, has to be adjusted at high altitudes.

d. Good steady state data require a minimum stabilisation time. If stabilisation time is too short, random errors are increased so that discrepancies between facilities cannot be easily explained.

e. Inlet airflow measurements and computation were done using different methods. With the UETP, CEPr had the opportunity to compare these methods and improve its own one.

2. Future "UETP-type" programme benefits

a. In a programme of this magnitude, deterioration effects should be clearly identified in each participating facility and at the end of the comparative tests. The first and last entries have to be performed in the same facility, with the same measurement systems and careful procedures.

b. Measurement practices should be compared in advance.

c. A well-known math model is necessary for better comparison at altitude conditions.

19.5 RAE

1. RAE(P) has gained added confidence in the use of its test facilities to support multi-national programmes on civil and military engines in which a number of test sites (both altitude and sea level) contribute to engine development and qualification.

2. RAE(P) gained considerable benefit from producing a standardized form of error analysis of the cell measurement system which could be compared with similar analyses at other test sites, so offering a unique opportunity to compare the systems.

3. The error analysis has already proved valuable to RAE(P) in identifying those parts of the measurements system which could benefit from improved hardware and/or calibration procedures.

4. RAE(P) shares the views expressed by other test sites that fuel flow meters which provide high measurement accuracy over a wide range of fuel flows are needed in aid of engine testing.

19.6 TUAF

Benefits and Improvements Achieved by Participating in UETP

1. The Turkish facility, being an Air Force standard test cell for performing acceptance tests after overhaul/depot-level maintenance of engines, is not equipped with all the instrumentation needed by the Uniform Engine Testing Program. The facility normally uses an analysis procedure which is not as comprehensive as the one suggested in the General Test Plan of the UETP. It must also be noted that

the instrumentation used in the facility is of conventional type with no automatic data acquisition system. To realise the objective of the program, several new instruments were added to the test cell, a detailed assessment of the accuracy of the test cell was made and a number of computer programs have been developed for analysis purposes.

Participating in the UETP under the above circumstances, was a worthwhile experience for Turkish Air Force personnel. Since all the measurement techniques and the uncertainties were reviewed and examined. some improvement in the measurement techniques and procedures were made.

2. Several computer programs have been developed for analysis purposes. This work is regarded as a preliminary step and the accumulation of knowledge will be used towards designing the contemporary computerised data acquisition systems.

3. The rigorous uncertainty analysis that has been made, showed the relative importance of different measuring instruments from an accuracy viewpoint. This will enable the Testing Group members to select instrumentation for the future test facilities in a more rational way.

19.7 ILA, STUTTGART

1. Benefits for jet engine testing community

a. The tests made evident that the intake configuration via intake profiles is affecting the engine performance. To get comparable results at different facilities similar intake configuration is required.

b. The exhaust arrangement differed considerably between the UETP facilities but there was no evident effect on engine performance and on data collected. Hence sensitivity to exhaust arrangements seems to be minor.

c. Jet pipe total pressure measurement was unreliable in the UETP programme. Static pressure measurement was found to be an advantageous alternative.

d. Nozzle coefficients for thrust and flow have proved to be suitable for consistency checks both for data taken at a facility and for inter facility comparison.

e. Uncertainty and statistical methods have been brought to a common basis and have been improved for most of the facilities.

f. The UETP programme has revealed difficulties for comparison of SL test data when taken at different ambient temperatures due to unknown temperature lapse rate.

g. The comparison of test results taken at the different facilities initially has shown discrepancies which by subsequent investigations could be reconciled thus improving the testing standard of most of the participating facilities.

h. At the end of the UETP programme the results taken at the different facilities were in a fairly good agreement, improving the confidence in jet engine testing.

2. Benefit for future cross calibration programmes

a. Absence of deterioration of the test article and reproduceability of its performance have proved to be most important.

b. For the reduction from actual to desired conditions reliable math models are required.

c. For plants which generate test conditions such as ATF's, the quality of setting parameters (in the case of an ATF P2, T2, PAMB) has to be considered, i.e. the accuracy given by the difference between actual and desired value and also the fluctuation during a test point.

3. Benefits for the Stuttgart Altitude Test Facility

The items listed under 1 possibly apply for the Stuttgart ATF.

As a new test cell has been installed in 1986/87, the many detail disussions of the working group have been useful, especially concerning pressure distribution around the engine (boattail forces), cooling air flows, inlet and exhaust arrangement.

20. CONCLUSIONS

Uniform tests of two J57-PW-19W turbojet engines were conducted in four altitude test facilities and four ground level test stands within five AGARD countries to provide a basis for upgrading the standards of turbine engine testing and to compare the measured, steady-state, engine performance in each test facility. To ensure objectivity, the test equipmen.., test techniques, and data acquisition and processing systems which were in routine service at each facility were utilised for these tests and the test data were not exchanged until testing was completed at each facility. After completion of all testing, the data were pooled and compared. Finally, additional analyses were completed to identify, where possible, the cause(s) of obseived differences. Conclusions reached from this programme are:

1. The J57 engine was an excellent choice; both engines operated reliably and repeatedly throughout. Detailed analysis of engine performance retention characteristics confirmed that variations in the primary engine performance parameters, specific fuel consumption (SFC), thrust and airflow, were negligibly small from the beginning to the end of the test programme.

2. The spread in engine performance (SFC, thrust, fuel flow and airflow) measured in the four altitude test facilities varied from ±0.5 to ±2.8 per cent over the range of altitude conditions tested. These spreads are reduced to ±0.5 to ±2.2 per cent when data containing confirmed anomalies encountered at one facility are discounted. Both the largest and smallest spreads in this discounted data set are in net thrust. The mean values of engine performance lie within but near the declared uncertainty limits of the data from each facility thus confirming the validity of the estimated uncertainties.

3. The spread in engine performance (SFC, thrust, fuel flow and air flow) measured in three of the four ground-level test beds (NAPC data not included) varied from ±0.8 per cent to ±4.0 per cent over the test range of engine powr levels and engine inlet temperatures (ambient temperature). These spreads are reduced to ±0.1 per cent to ±0.9 per cent when data containing confirmed anomalies encountered at another facility are discounted. The largest spread is in fuel flow and the smallest is in net thrust in this discounted data set. The mean values of engine performance lie within but near the declared uncertainty limits of the data from each facility thus confirming the estimated uncertainties.

4. Availability of the results from the NAPC outdoor test stand provided a new reference to which ground-level data could be compared. This additional information considerably improved the understanding of environmental effects on gross thrust, changing some of the thrust data by up to two per cent.

5. One of the altitude test facilities (AEDC) has the capability to test at conditions corresponding to those existing in ground level test stands. The engine performance measured in the altitude facility did not differ significantly from the performance measured in the ground level stands.

6. Major advances in the assessment and understanding of data quality were made by the AGARD turbine engine test community during the course of this programme. A single methodology for determining the bias limits, precision indices and overall uncertainties of the measured and calculated engine performance parameters was adopted and implemented at each facility. Generally, the experimental results validated the uncertainty estimates. Probable causes were identified in almost all cases where the experimental data lay outside the declared uncertainty limits.

7. The J-57 engine closely approximates a wide range of contemporary engine sizes and cycles insofar as the assessment of test facility capability is concerned. Thus, interfacility comparisons are valid as a first-order approximation for a broad range of engine sizes and alternate cycles: e.g. augmented, low-bypass, mixed flow turbofans and non-augmented, high-bypass, unmixed-flow turbofans, so long as the engine size and flow requirements are within the capacities of the facilities. However, there are basic differences in the physical arrangement and sizes of key facility components which will introduce second-order effects into the measurement uncertainties. Therefore, an accounting of these second-order effects is required to extend the results of UETP to classes of engines which are significantly different from the J-57.

8. The AGARD-UETP was a pioneering effort in that for the first time multiple sets of completely independent test data were obtained at uniform test conditions with a standard test article including engine, engine controls and engine instrumentation. This special purpose data base has already provided the opportunity to perform data validity assessments far better than normally possible for conventional engine test programme. Utilising this data base, each participating facility has already identified one or more shortfalls in test capability which degraded the quality of their test results. In addition, the UETP has provided a directly-comparable, quantitative evaluation of the quality of the different test methods and equipment in use at the various facilities. In no case were all of the best features concentrated at single facility. Thus, a systematic basis is now available for each facility to identify and implement future improvements in test capability.

9. As might be expected, engine speeds were the most accurate performance measurement throughout the programme. Similarly, engine fuel flow was the least accurate performance measurement throughout the programme. The other key performance measurements, thrust and airflow, lay between these extremes. Two measurement systems were specially notable for demonstrated high accuracy (low measurement

uncertainty), i.e. the positive displacement fuel flow meters at RAE(P) and the sonic airflow meter at AEDC. Test experience emphasised the need to achieve engine thermal equilibrium before recording a test point.

10. Assessment of the performance retention characteristics of the relative simple J-57 test engines and control systems was particularly laborious. However, an adequate assessment was possible. Careful planning of the test matrix and data analysis would be needed for the assessment for engines and controls which are more complex than the J57.

11. The shortcomings of the current turbine engine performance generalisation methods which account for the effect of variations in engine inlet temperature and ram pressure ratio were defined. The traditional "referred" parameters do not completely account for engine cycle re-match which may occur as a result of variations in these two environmental factors. Fully responsive, validated, mathematical models of engine performance provide a future possibility for proper accounting for these effects.

12. The information to be gained from the data base gathered in the UETP is far from exhausted by the investigation of Working Group 15. In particular, a more detailed treatment of physical cell effects on data and a study of predicted and actual data bias is recommended. Further work is also needed to improve methods of correlating engine performance information which is taken at different environmental test conditions.

13. The planning and execution of the AGARD-UETP was a success because of the complete co-operation and dedication of all participants. The participants functioned as a single unit to provide effective logistics support, technical interchange, and exchange of the voluminous test data. The commitment of the Working Group to the thorough and objective analysis of the test results was especially notable.

88

REFERENCES

No	Author	Title, etc.
1	J G Mitchell	Uniform Test Engine Testing Programme General Test Plan January 1982 Revised June 1983
2	T Biesiadny	Project/Test Plan for Uniform Engine Testing Programme Phase I NASA Lewis Research Center Participation April 1981 Revised 8 June 1981
3	C E Chamblee	Project/Test Plan for Uniform Engine Testing Programme Arnold Engineering Development Center Participation May 1982
4	D M Rudnitski W Grabe	Uniform Engine Testing Programme at the National Research Council, Canada Report LTR-ENG-101 April 1981
5	I A Corde I A G Roudou	Essais Croises de Moteurs (J57-P-19W) Centre d'Essais des Propulseurs, Saclay Programme d'essais 39/ZDT/82
6	A Ucer F Algun	Uniform Engine Test Programme – Test Plan Turkish Air Force Middle East Technical University December 1982
7	M B Shaw W A Abbott	Uniform Engine Test Programme at the Royal Aircraft Establishment, Pyestock, Engine Test Facility RAE Tech Memo OPS 1015 February 1984
8	J C Ascough	Test Code for Contract Performance Measurements NGTE Memorandum M78020 April 1978
9	J Bird W Grabe J McLeon D Rudnitski	NRCC-NASA-AEDC Data Comparison for the AGARD Uniform Engine Testing Program – Interim Report NRCC Report LTR-ENG-121 21 September 1983
10	T Biesiadny L Burkardt W Braithwaite	Uniform Engine Testing Programme Phase I: NASA Lewis Research Center Participation NASA Technical Memorandum 82978 October 1982
11	S Wehofer J T Tate A E Burwell	Uniform Engine Testing Programme (UETP) Phase II: AEDC Test Results AEDC-TR-83-53 January 1984
12	D Rudnitski J Bird W Grabe J McLeod	A detailed procedure for measuring turbojet engine performance in an enclosed sea-level facility NRCC Report LTR-ENG-120 15 September 1983
13	P W E Smith A R Osborn W A Abbott J C Ascough	Final Test Report of the AGARD Uniform Engine Test Programme at RAE (Pyestock) RAE Tech Memo P1059 July 1985
14	H Aksel F Algun B Caglar T Cetinkaya I Dine C Erlap O E Hatip A S Ucer	AGARD-PEP-WG15 Uniform Engine Testing Programme Turkish Test Report Turkish Air Force Middle East Technical University Ankara March 1985
15	T J Biesiadny L A Burkardt M Abdelwahab W M Braithwaite T A Kirchgesser D Silver	Uniform Engine Testing Programme Phase VII: NASA Lewis Research Centre Second Entry NASA Tecnical Memorandum 87272 July 1986
16	J P K Vleghert	Measurement Uncertainty within the UETP AGARDograph 307 1989
17	R B Abernethy J W Thompson	Handbook Uncertainty in Gas Turbine Measurements AEDC Technical Report AEDC-TR-73-5 February 1973
18	M Abdelwahab	Measurement Systems Descriptions and Calibrations Error Assessment PSL-3/PSL-4
19	W O Boals W A Turrentine S Wehofer	AEDC Measurement Uncertainty Results for AGARD UETP AEDC-ER-98-03 October 1987
20	J W Bird	Interfacility Uncertainty Error Audit NRCC report 1451-44-41 April 1985

REFERENCES (Contd)

No	Author	Title, etc
21	P Maire	Essais Croises de Moteurs, J57 UETP Incertitudes sur les Mesures C EPr Report 594 June 1986
22	J C Ascough	Prediction Synthesis of Error Limits for J57 UETP Tests RAE Technical Memorandum P1069 September 1985
23	J C Ascough G N Wort	Comparison of Bias Errors for UETP Facilities RAE Technical Memorandum P 1134 March 1988
24	F Algun J W Bird D M Rudnitski	The Effect of Inlet Pressure on Gas Turbine Engine Performance NRCC Report CTR-ENG-003 August 1985
25	A R Osborn	A Comparison of Gross Thrust Determination between UETP Test Facilities RAE Technical Memorandum P1101 February 1987
26	A R Osborn	A Comparison of Airflow Measurement between UETP Test Facilities RAE Technical Memorandum P1118 September 1987
27	R Jacques	Airflow Measurement Assessment and Comparison in UETP Test Facilities Ecole Royale Militaire, Brussels Technical Memorandum MA 101
28	R E Smith Jr R J Matz	Verification of a Theoretical Model of Determining Discharge Coefficients for Venturis operating at Critical Flow Conditions AEDC-TR-61-8 September 1961
29	R E Smith Jr R J Matz	Description of a Venturi designed to operate at Critical Flow Conditions to provide accurate measurements of Flow Rates of Compressible Fluids Trans ASME Series D Vol 84, pp 434-445 December 1982
30	J D Macleod	A Derivation of Gross Thrust for a Sea-level Jet Engine Test Cell Thesis for M Eng degree Carlton University, Ottawa February 1988
31	M K Fall	Sea-level static Performance of a J57-P-19W Engine NAPC Report NAPC-PE-17S May 1988

APPENDIX I

PEP Working Group 15 — Membership

The following individuals, listed in alphabetical order, participated in the Working Group discussions under the Chairmanship of Dr J G Mitchell of AEDC Tullahoma US.

Capt F Algun	Turkish Air Force, Ankara, Turkey
Mr P F Ashwood	Consultant, UK
Mr T J Biesiadny	NASA, Cleveland, US
Mr J W Bird	NRCC Ottawa, Canada
Prof Dr Ing W Braig	Stuttgart University, Stuttgart, Germany
Mr W M Braithwaite	NASA, Cleveland, US
Mr P Castellani	CEPr, Saclay, France
Mr J Dicus	NASA, Cleveland, US
Mr F Fagegaltier	CEPr, Saclay, France
Dr D K Hennecke	MTU, Munchen, Germany
Mr M Holmes	RAE (Pyestock) UK
Prof R Jacques	Ecole Royale Militaire, Bruxelles, Belgium
Dr W L MacMillan	National Defence Headquarters, Ottawa, Canada
Dr G Maoli	Fiat, Rome, Italy
Mr A A Martino	NAPC, Trenton, US
Mr A R Osborn	RAE (Pyestock), UK
Mr D M Rudnitski	NRCC, Ottawa, Canada
Mr R E Smith	AEDC, Tullahoma, US
Mr J T Tate	AEDC, Tullahoma, US
Prof Dr A Ucer	Middle East Technical University, Ankara, Turkey
Mr J P K Vleghert	National Aerospace Laboratory, Amsterdam, Netherlands
Mr S Wehofer	AEDC, Tullahoma, US

APPENDIX II

Descriptions of Ground-Level Test Beds and Altitude Test Cells

The descriptions given in this Appendix reflect the capability of each facility at the time of its participation in the UETP. Subsequent changes or improvements are not included

(A) GROUND-LEVEL TEST BEDS

1. NATIONAL RESEARCH COUNCIL CANADA – TEST CELL No 5

1.1 Description

1.1.1 Test Facility
The test cell used for the UETP is designated Cell No 5 and is one of three ground-level gas turbine test cells in the Engine Laboratory. This cell is capable of handling engines of up to 140 kg/s air inflow. Since environmental control is not available, the test condition is dictated by local ambient temperature and pressure. A sectional elevation and plan view of Cell No 5 are given in Figure A.

1.1.2 Installation Configuration
The UETP test engine was floor mounted and a facility bellmouth and airmeter were fitted. Engine efflux and entrained secondary air were ducted from the cell through a 2m diameter exhaust collector to a vertical silencer that discharged to the atmosphere. A 1m diameter insert in the collector tube allowed reduction of the induced secondary cell flow to 6 m/s or less.

1.2 Primary Test Measurements

1.2.1 Thrust Measuring System
The test engine was mounted on a thrust bed which in turn was suspended through flexure plates to a mounting frame anchored to the floor. A series of strain gauge type load cells was available for placement between the thrust bed and mounting frame. The load cell used was calibrated in a deadweight tester, which is periodically checked against the Canadian Standards of Mass, NRCC. Friction and bending forces produced by the flexible plates were determined by a center-pull calibration.

The facility bellmouth airmeter assembly was attached ahead of the reference airmeter. A hard mounted, hemispherically shaped nosebullet was mounted on an extension of the reference airmeter centrebody. The bellmouth forces were transmitted to the engine stand, but decoupled from the engine and centred on the engine axis via a low stiffness inflatable seal.

The method of thrust accounting eliminated the need for a separate measurement of the bellmouth and nosebullet forces. However, static pressure data were obtained from a series of static taps in radial lines on the nose bullet and bellmouth.

1.2.2 Airflow Metering System
The compressor airflow was measured in an annular, straight measuring section, placed between the compressor inlet and bellmouth, by means of total pressure taps on the inner and outer walls.

1.2.3 Fuel Flow Metering System
Two NRCC turbine fuel flowmeters were installed in series at the engine/test cell interface. These flowmeters had been calibrated by the manufacturer using the ballistic flow method. Fuel temperature was measured in the supply line near the flowmeter exit with "Type T" (copper-constantan) thermocouples. Fuel mass flow was calculated using the measured fuel temperature, the indicated frequency from the turbine flowmeters, and the flowmeter calibration curve. Calibration data were used to prepare curves of meter output frequency per unit volume as a function of a corrected frequency. The corrected frequency is defined as the indicated frequency divided by actual fuel kinematic viscosity which is calculated from fuel sample properties and the measured fuel temperature.

1.3 Data Acquisition and Reduction
Raw engine data were acquired by a Data Acquisition System (DAS), comprising a minicomputer and a Compact System Controller (CSC). The low-level signals were filtered by 10 Hz filters and then amplified to ±5 VDC full scale (nominal), before digitisation in the CSC. High level signals bypassed the amplifiers, but were filtered prior to digitisation. The digitisation was done with a 12 bit analogue-to-digital converter, giving a resolution of 0.024% of full scale.

Pressure signals were mechanically multiplexed using scanivalves and externally mounted capacitive type pressure transducers. Two calibration pressures were connected to each scanivalve to verify the calibration on each scan. Temperature signals were converted from thermocouple wire to copper using temperature reference plates; the plate temperature being measured with thermocouples referenced to an electronic ice-point.
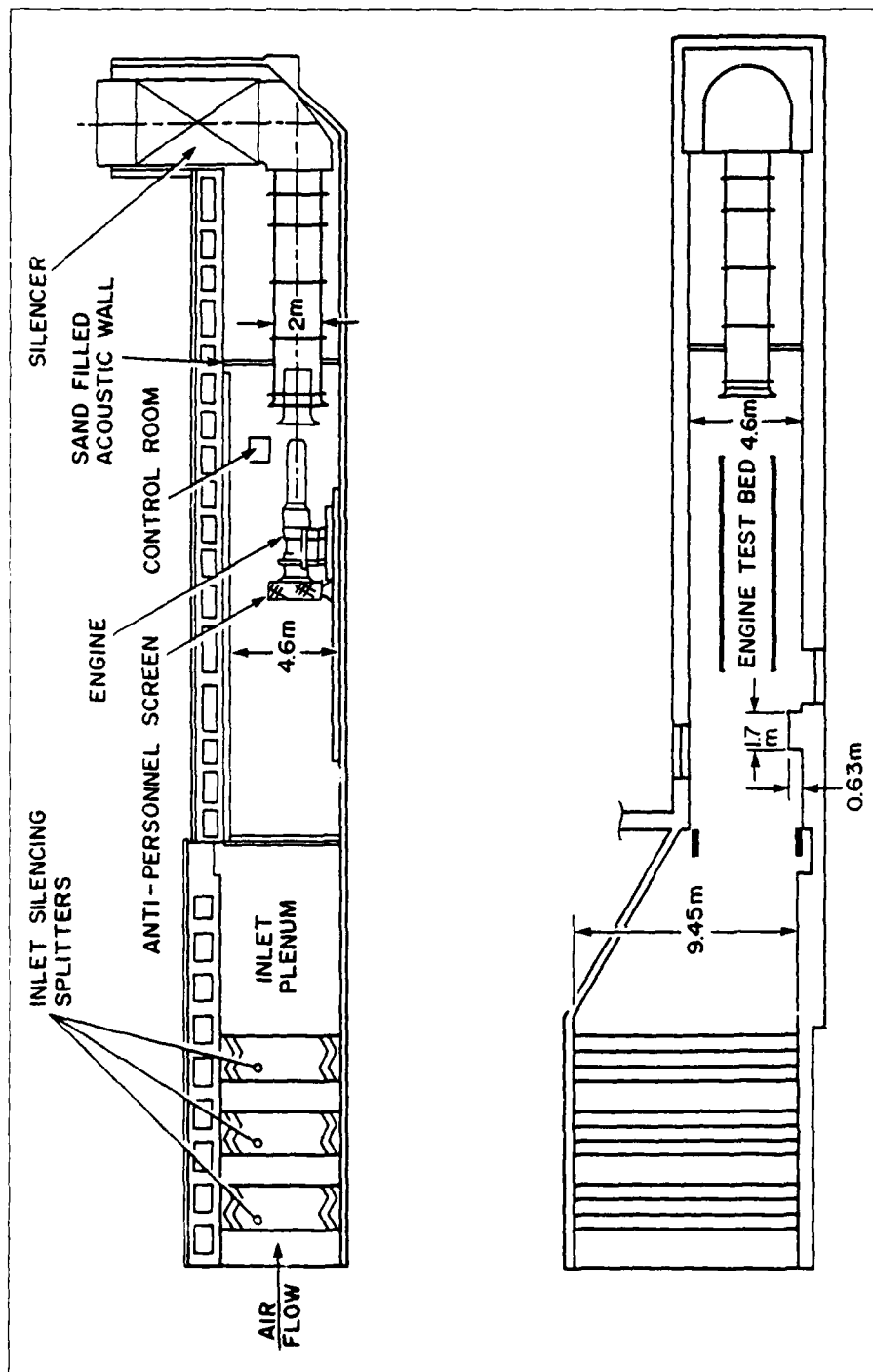
Fig A No 5 test cell — engine laboratory — NRCC
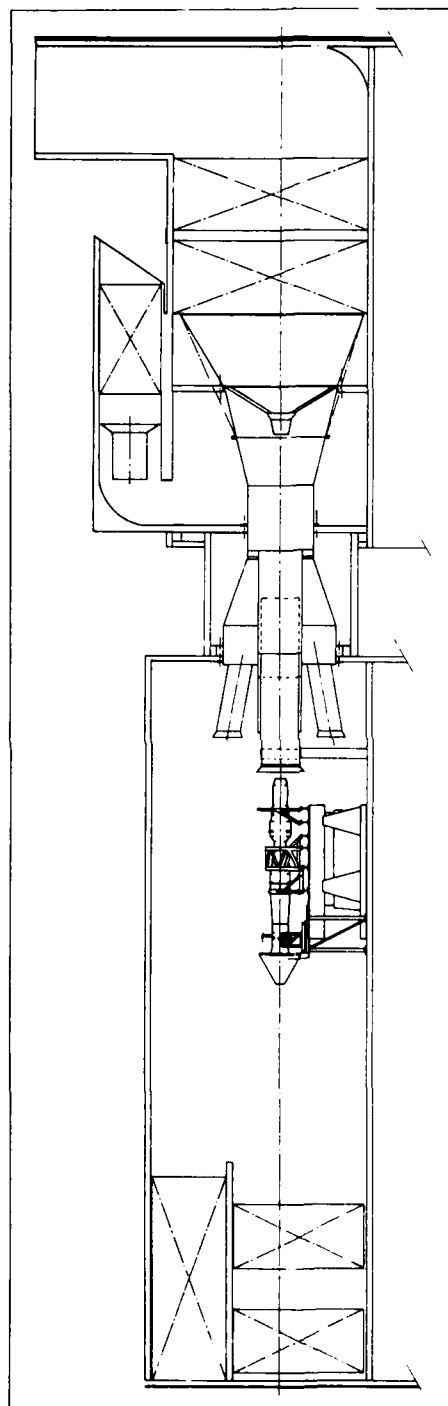
Fig B Test bed to at CEPr

Following a five minute engine stabilization period, two back to back data scans were made at each test point, each scan taking approximately 6 minutes. Steady-state engine performance data were obtained by sampling each parameter input signal at a constant rate of approximately 100 Hz over a short time period (ranging from 1 to 10 seconds depending on the parameters), and then averaging arithmetically to yield a single value. The raw data for each test point were reduced to engineering units using pre-stored calibrations and displayed on a video screen. A visual comparison of DAS acquired data to those displayed on the read-out instruments was made for verification before storage on a magnetic disk. Measured or calculated parameters could be cross plotted on an analogue X-Y recorder.

2. CENTRE D'ESSAIS DES PROPULSEURS TEST STAND TO

2.1 Description

2.1.1 Test Facility

Engine test stand TO can provide engine tests at ground-level conditions. Airflow rates up to 1200 kg/s are available in this stand, the dimensions of which are: 10,2 x 10,85 x 26 m. A sectional elevation is given in Figure B.

2.2 Primary Test Measurements

2.2.1 Thrust Measuring System

The engine was mounted on a thrust measuring system supported by four thin blades. The thrust was measured by a load cell. The engine inlet duct was isolated from the bellmouth by a zero leakage seal.

2.2.2 Airflow Metering System

Airflow was metered by measuring the total and static pressures, total temperature and boundary layer profile downstream of the bellmouth. A cooled exhaust diffuser and a silencer ducted the exhaust gases to atmosphere.

2.2.3 Fuel Flow Metering System

Two fuel systems covered three ranges of fuel flow up to 7.5, 24 and 36 m3/h respectively. Fuel was metered with volumetric flowmeters calibrated by CEPr.

2.2.4 Pressure Measurements

The facility can provide either 144 pressure lines through a scanning valve system or 24 direct lines. Pressure lines and thermocouple wires were supported from a bearing located above the engine to minimise their influence on the thrust frame.

2.2.5 Temperature Measurements

264 thermocouple wires with multiplexed lines or 40 with direct lines can be used. They are routed to 0C reference junctions. Also available are 10 lines for flow measurements, speed measurement and checking measurement (strain gauges: 30, accelerometers: 40).

2.3 Data Acquisition Processing System

Each time a data acquisition is ordered, the computer records all the data, executes a real time calculation program and provides the results on a line printer or non visual displays.

3. ESKISEHIR SUPPLY AND MAINTENANCE CENTER – TURKEY

3.1 Description

3.1.1 Test Facility

Post-maintenance/overhaul Test Cell AF/M37-T6B is the major test cell utilised for health monitoring and acceptance testing of turbo-jet engines. It cannot provide any simulated flight environmental conditions.

The flow follows a U-Shaped path through the cell, sound-suppressors being fitted in the vertical air inlet and exhaust sections. The working section is 10 m high and 7 m wide. Every engine is tested with a bellmouth special to its model. There are no means for controlling the inlet air flow. This condition creates a natural depression within the test chamber.

3.1.2 Installation Configuration

The UETP engine was mounted on a thrust frame which was linked to the ground through four flexure plates and which contained the two load-cells for the thrust measurement system. The engine had no connections with the air inlet and exhaust discharge sections of the test cell. The inlet bellmouth was attached directly to the engine. The exhaust collector of the test cell could be moved aft or forward to achieve the required distance between the engine and the exhaust collector.

3.2 Primary Test Measurements

3.2.1 Thrust Metering System

The thrust metering system was a scale force thrust stand flexure system mounted on the engine support cart as shown in Figure C. The dual bridge load cells were calibrated in situ by standards traceable to the National Bureau of Standards (NBS). The maximum system capacity is 156 kN.

3.2.2 Airflow Metering System

Airflow is not normally measured in this cell. A rough indication can be obtained by measuring the depressions in the test chamber and at the engine inlet (bellmouth). For the UETP test, airflow was calculated using the Station 2 instrumentation.

3.2.3 Fuel Flow Metering System

Fuel is metered with turbine volumetric flowmeters. A high range and a low range metering system with two flowmeters in each range are provided to maintain the desired level of accuracy at all flow conditions. The meters are electronically calibrated and can compensate for changes in the specific gravity of the test fuel.

3.3 Data Acquisition/Processing System

There is no Digital Data Acquisition System. In normal use recording and calculations are performed manually with the use of some charts when applicable. Data are recorded and kept on standard log-sheets/charts. For the UETP the data were fed manually into a micro computer with an analysis program developed for this purpose.

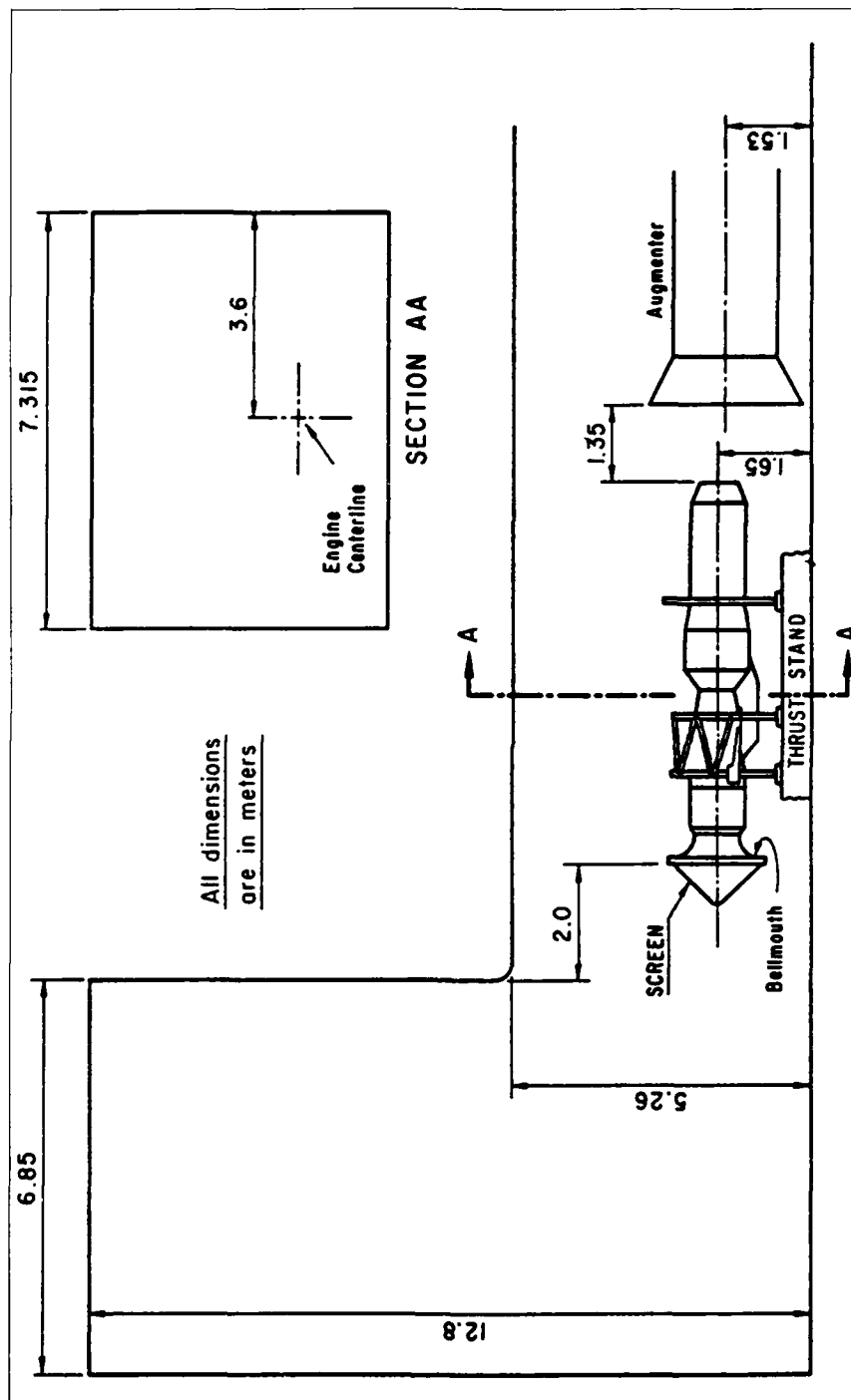All dimensions
are in meters

7.315

3.6

Engine
Centerline

SECTION AA

6.85

12.8

5.26

2.0

SCREEN

Bellmouth

THRUST STAND

A

A

1.65

1.35

Augmenter

1.53

Fig.C Test cell at supply and maintenance centre. Eskisehir, Turkey (TUAF)

APPENDIX II

(B) ALTITUDE TEST CELLS

4. NASA LEWIS RESEARCH CENTER TEST CELL PSL 3

4.1 Description

4.1.1 Test Facility

Propulsion System Laboratory-Test Cell 3 (PSL-3) has a working section diameter of 7.3 m and is one of two major test cells utilised for air breathing propulsion system testing at NASA Lewis Research Center. The PSL can provide simulated flight environmental conditions ranging from 1,500 m to 24,400 m and from 0 to 3.0 flight Mach numbers. Airflow rates up to 340 kg/sec are available for air-breathing propulsion system testing.

4.1.2 Installation Configuration

The NASA UETP utilised a typical direct-connect turbine-engine test configuration. The engine was mounted on a thrust stand, as shown in Figure D, which contained the thrust-measuring system. The engine inlet duct was isolated from the bellmouth and upstream ducting by a labyrinth seal. Airflow was conditioned to a uniform velocity profile upstream of the bellmouth inlet by flow straightening screens and grid assembly. The temperature and pressure levels could be either manually or automatically controlled at the engine inlet and exhaust to simulate the desired altitude and Mach number test conditions. A fixed geometry, water-cooled exhaust diffuser was used to collect the exhaust gases and direct them to the PSL exhaust system.

4.1.3 Environmental Control System

The temperature environment of the engine during testing as controlled by cooling air supplied from a torus manifold at the upstream end of the test cell. The flow was regulated to maintain the test cell temperature within specified limits. The environment pressure was controlled by valves in the facility exhaust ducting. The velocity over the nozzle external surface was controlled by sizing the engine exhaust diffuser to the range of engine operating conditions and to the plant exhauster capabilities.

4.2 Primary Test Measurements

4.2.1 Thrust Metering System

The thrust metering system is a scale force thrust stand, flexure mounted to the test chamber supports as shown in Figure D, and free to move except as restrained by a dual load-cell system that allows the thrust stand to be preloaded and operated as a null position system, ie fixed position. The dual-bridge load cells are calibrated by standards traceable to the National Bureau of Standards (NBS).

4.2.2 Airflow Metering System

The NASA method of determining inlet total airflow is based on the integration of the flow per unit area calculated for each total pressure probe of a 4 rake array and the assumption that the static pressure is constant across the duct at the airflow station (approximately 1 duct diameter downstream of the labyrinth seal). This assumption was validated by a static pressure survey at representative test conditions. Based on this approach, only wall static pressures and the total pressures in the boundary layer and a few total pressures and temperatures in the free stream were measured.

4.2.3 Fuel Flow Metering System

Fuel was metered with turbine, volumetric flowmeters. A high and low range metering system with two flowmeters in each range was provided to maintain the desired level of accuracy for all flight conditions. The meters are "in-water" calibrated in a laboratory traceable to the NBS.

4.3 Data Acquisition/Processing System

Pneumatic and electrical instrumentation, control, and service system lines were routed from the engine and thrust stand to the test cell wall in such a manner that the desired engine thrust measuring accuracy could be obtained. The pressure lines routed to transducers through a scanner valve system, and thermocouple wires for temporary measurement routed to 338K reference junctions. The electrical signals from pressure transducers, thermocouples, thrust measurement load cells, and turbine fuel flowmeters were conditioned for sampling by Propulsion Systems Laboratory Data Acquisition System (DAS).

The engine and facility conditions were monitored, real time, in the control room by sampling of all parameters and displaying of selected parameters using a test facility digital computer. At specified conditions, multiple samples of all parameters were recorded by the DAS for determination of engine performance. The multiple data samples were recorded by the test facility computer for averaging computation and display on a CRT of engineering units and performance parameters. The engineering unit data and performance data were tabulated on a facility line printer and also transmitted from the facility computer to one of the NASA Lewis large central computers for storage, further analysis and batch processing. Analysis of the stored data could also be performed on interactive graphics terminals to provide the plotted test results.

5. AEDC ALTITUDE TEST CELL T-2

5.1 Description

5.1.1 Test Facility

Propulsion Development Test Cell T-2 is one of eight test cells at the AEDC used for air-breathing propulsion system testing. Test Cell T-2 can provide simulated flight environmental conditions from sea level to 24,000 m in altitude, flight Mach numbers from 0 to 3.0, and airflow rates up to 360 kg/s. The T-2 test chamber is 3.75 m diameter. The layout of the cell is shown in Figure E.

5.1.2 Installation Configuration

The UETP engines were tested in a "direct-connect" test configuration with each engine mounted on a support cart containing the thrust measuring system. The engine inlet duct was isolated from the bellmouth and upstream ducting by an automatic pressure balancing, "zero leakage", labyrinth seal. The engine bellmouth used for the UETP had an exit diameter 76mm less than the engine face diameter. A conical spool piece with a wall half angle of 2.8 deg used to make the transition from the bellmouth exit to the engine inlet duct. Plant airflow was conditioned to a uniform velocity profile at the bellmouth inlet by a flow
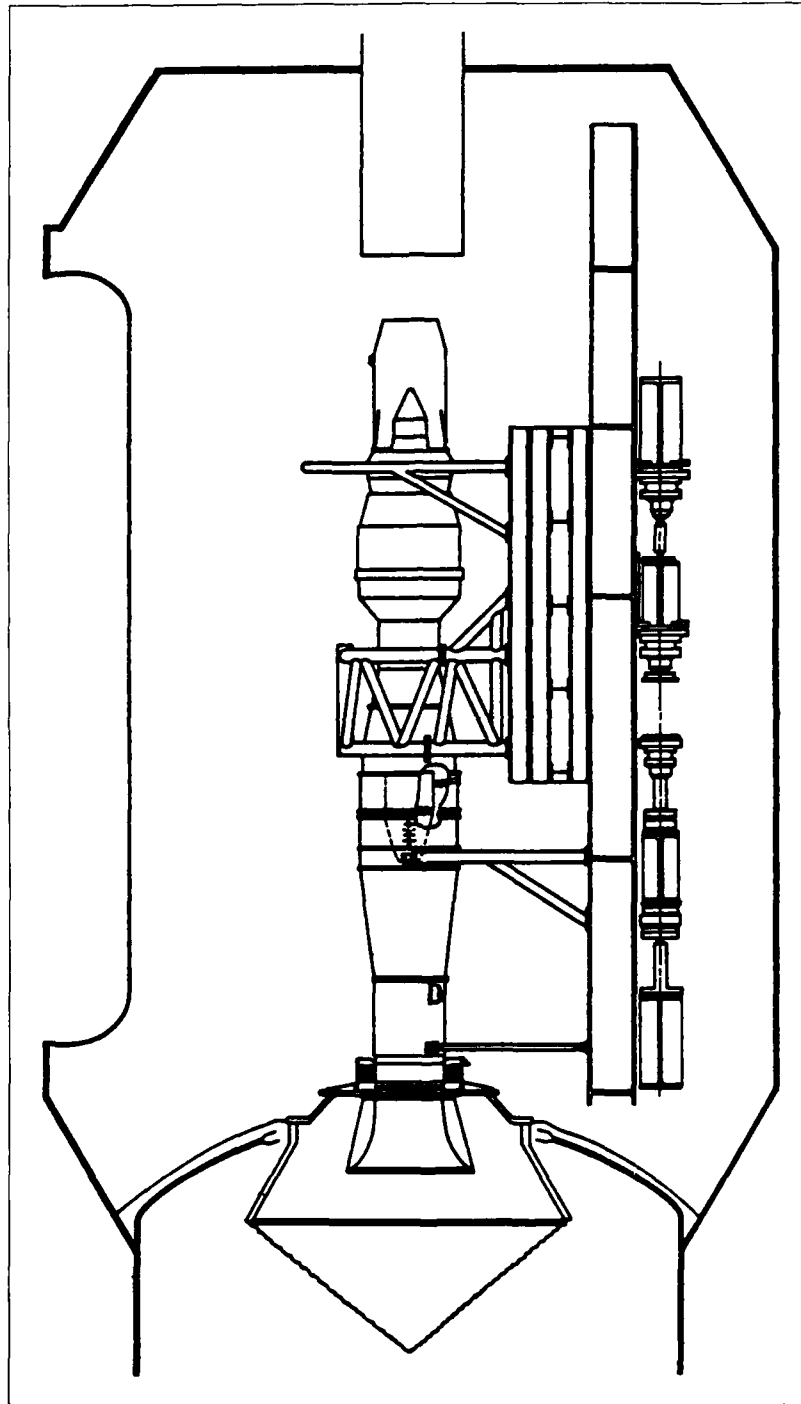
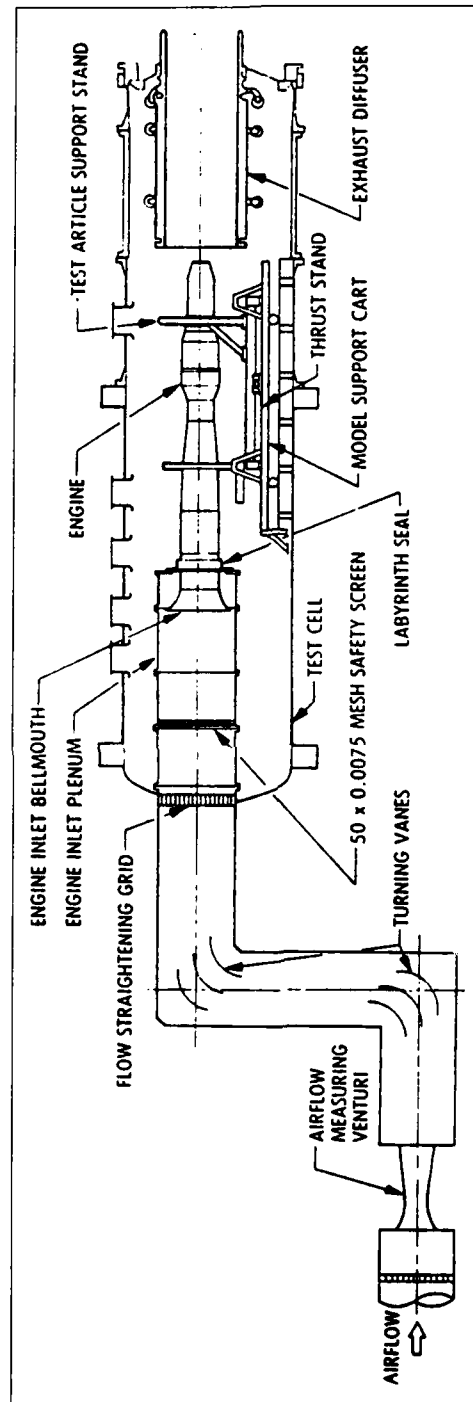Fig.D J57 engine installed in NASA high altitude test cell PSL-3

Fig.E J57 engine installed in AEDC propulsion development test cell T-2

98

straightening screen and grid assembly. A fixed-geometry, water-cooled exhaust diffuser was used to collect and direct the exhaust gases to the ETF plant exhauster system.

5.1.3 Test Cell Environmental Control Systems

The temperature and pressure levels at the engine inlet and exhaust were automatically controlled to simulate the desired altitude and Mach number test conditions. The test cell air temperature was controlled by cooling air supplied from a torus manifold at the upstream end of the test cell. The flow was regulated to maintain the test cell temperature within specified limits. The test cell pressure environment was controlled with the plant exhauster equipment.

5.2 Test Measurement Systems

5.2.1 Airflow

Engine airflow for the UETP was metered with a critical flow venturi located upstream of the inlet flow straightening plenum. The venturi was a standard AEDC ETF design as described in Reference 28. Test cell leak checks were conducted to insure no duct air leakage between the airflow measurement station and the engine inlet plane.

5.2.2 Thrust

Elastic flexures were used to mount the engine on the model support cart. Pneumatic and electrical instrumentation, control, and service system lines were routed perpendicularly from the engine and support cart through the test cell wall in a manner that minimized tare loads to the engine thrust measurement system. Tare loads to the engine thrust measuring system were determined by a centerline pull calibration. Dual-bridge load cells were located below the engine centerline. The load cell, load cell column, and thrust stand were water-cooled to prevent thermal stresses. A water-cooled panel was used to cover the aft portion of the thrust stand exposed to the thermal environment of the engine tailpipe.

5.2.3 Fuel Flow

The facility fuel-flow system was equipped with a high- and low-range flow leg with two axial-flow turbine flowmeters in each leg. This arrangement minimizes the measurement uncertainty by providing redundant measurements and by restricting the flow measurement to the linear portion of the meter frequency calibration curve. The four facility flowmeters were calibrated in the installed configuration with the test fuel (Jet A).

5.3 Data Acquisition/Processing System

Steady-state pressure lines were routed to transducers located in a multiplexing scanner valve system. All thermocouple wires were routed to a 338K reference junction system. The electrical signals from pressure transducers, thermocouples, thrust measurement load cells, and turbine fuel flowmeters were conditioned for sampling by a Digital Data Acquisition System (DDAS).

A central data computer used to record and process outputs from the steady-state, transient, and high-response instrumentation systems. The outputs of the steady-state instrumentation were fed into the DDAS system. One hundred ninety-two channels of data were recorded during each steady-state data point. The data were acquired in 12 equal time segments over one and one-half minutes with

each segment scanned 50 times. The data were simultaneously recorded on magnetic tape and transmitted to the digital computer for conversion to engineering units and calculation of performance parameters.

The output of selected transient instrumentation was transmitted to the DDAS which converts the signals to engineering units and calculated parameters. These parameters were displayed on a cathode-ray tube (CRT) in the control room at approximately 1-sec update intervals and graphically displayed on a CRT in the computer room for real-time data analysis. Transient data were also recorded on a continuous analogue recorder and magnetic tape in the frequency modulation (FM) mode.

The output of the high-response dynamic instrumentation was recorded on multiplexed magnetic tapes at 0.76 m/sec in the FM mode.

The engine and facility conditions were monitored, real time, in the control room by sampling selected parameters by the DDAS. At specified conditions, multiple samples of all parameters were recorded by the DDAS for deermination of engine performance. The multiple data samples were recorded and transmitted to the central facility computer for averaging and computation of engineering units and performance parameters. The engineering unit data and performance parameters. The engineering unit data and performance data were tabulated on a line printer and transmitted by the facility computer to the central AEDC digital computer for storage. Analysis of the stored data was performed on interactive graphics terminals to provide the plotted test results.

6. CEPr ALTITUDE TEST CELL R6

6.1 Description

6.1.1 Test Facility

Test cell R6 is 5.5m diameter and 30m long. It is separated into two parts to allow the setting of different upstream and downstream conditions for the engine under test.

Upstream limits are:	P = 5 to 700 kPa
	T = 243 to 923K
Downstream limits are:	P = 5 to 200 kPa
	T = 253 to 653K

Airflow rates up to 400 kg/s are available.

6.1.2 Installation Configuration

The upstream part of the cell is provided with air by the air-conditioning plant

At the engine exhaust, a diffuser is connected to the air-conditioning plant which allows extraction and cooling of the exhaust gases.

The layout of the cell is shown in Figure F.

6.1.3 Engine and Cell Cooling

A cooling flow for both engine and cell is provided to maintain the temperature to fixed limits.

6.2 Primary Test Measurementss

6.2.1 Thrust Metering System

The engine was mounted on a thrust measuring system supported on four thin blades; the thrust was measured by a Baldwin load cell.
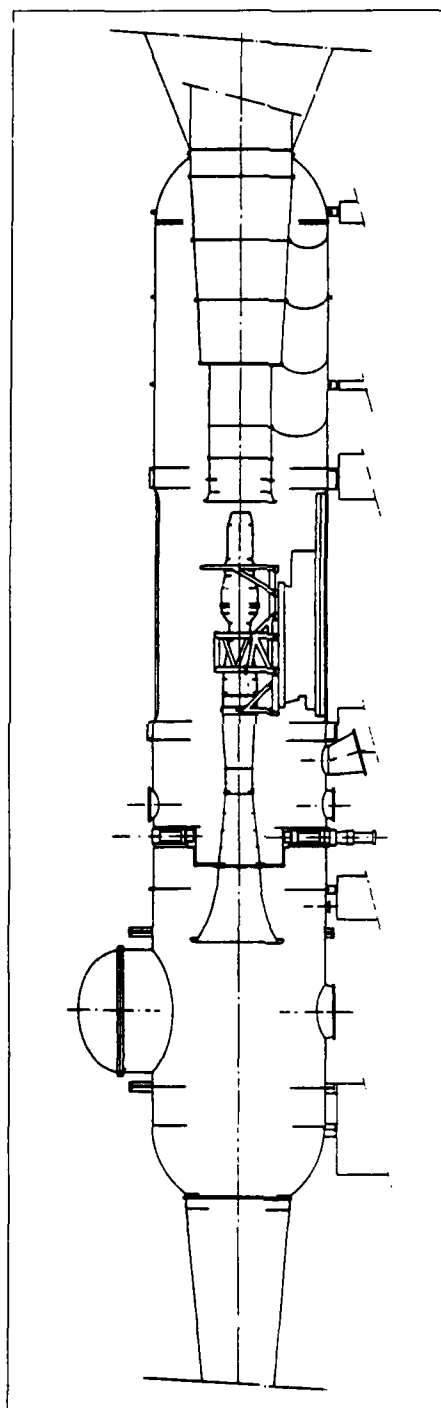
99

Fig.F Altitude test cell R6 at CEPr

The engine inlet duct was separated from the bellmouth by a zero leakage seal. The load cell was calibrated by a calibrated actuator mounted on the thrust metering system. The net thrust was calculated by computer using the measured thrust with corrections for the upstream and downstream engine conditions.

6.2.2 Airflow Metering System

Airflow was metered by measuring the total and static pressures, total temperature and boundary layer profile downstream of the bellmouth.

6.2.3 Fuel Flow Metering System

High range (4.4 m3/h) and a low range (1.0 m3/h) fuel systems with volumetric flowmeters were used for the UETP.

6.2.4 Pressure Measurements

Test test facility can provide 288 pressure lines through a scanning-valve system. 84 direct lines are also available with individual transducers, allowing differential pressures, oil, fuel or any hydraulic system pressures to be measured.

6.2.5 Temperature Measurements

288 thermocouple wires, directly or with multiplexed lines are available. Each thermocouple has its reference junction (273K).

6.2.6 Other Measurements

Ten lines for flow or speed measurements and checking measurements can also be used.

6.3 Data Acquisition System and Computer Installation

The data acquisition system includes the following:

- frequency meter lines: used for flow or rotation speed measurements.
- simple pressure lines: used for aerodynamic, differential or hydraulic pressure; they each have their own transducer and amplifier.
- scanned pressure lines: 24 pressure lines, one transducer and one amplifier for each scanning valve system.
- temperature measurements use multiplexers with 24 lines each.

There are two opto-electrical isolators before entering the computer. The command board is located in the facility and gives allowance to order the data acquisition, to choose a "real time calculation program" and provide various results.

Each time a data acquisition is ordered, the computer records the whole data and can execute a real time calculation program and provide the results of measurements and calculations on a line printer or on displays.

7. RAE PYESTOCK ALTITUDE CELL 3

7.1 Description

7.1.1 Test Facility

Cell 3 has a working section 6.1 m diameter and is one of

five altitude test cells used to test air breathing propulsion systems over a wide range of simulated forward speed and altitude conditions. Air compressors and exhausters, of 300 MW total equivalent power, enable altitudes from sea level to 30,500 m and from 0 to 3.5 flight Mach number to be simulated, with airflow rates up to 636 kg/s.

7.1.2 Installation Configuration

The UETP engine was installed in Cell 3 in a similar configuration to that developed for military turbofan engines. It was pre-rigged and mounted on a pallet before installation in the cell (see Figure G). The pallet was then mounted on the thrust frame, which is supported on oil-borne bearings, and connected to the cell services and instrumentation lines. The engine inlet duct was isolated from the bellmouth in the plenum chamber and upstream ducting by a freely mounted slip joint with a controlled and calibrated leakage. Airflow was metered using a venturi type contracting section and conditioned to a uniform pressure profile using flow straightening gauzes (screens) supported by a coarse grid structure. The pressure at the inlet to and around the exhaust from the engine was automatically maintained to simulate the desired altitude and Mach number test conditions, with the correct inlet temperature attained by mixing separate hot and cold air upstream of the cell. A fixed geometry water cooled exhaust diffuser was used to collect the exhaust gases and direct them to the plant exhauster system.

7.1.3 Environmental Control System

The temperature environment around the engine during testing was controlled by bleeding air from atmosphere via a cell ventilation valve. The flow was regulated to maintain the test cell temperature within specified limits. The environmental pressure around the engine was controlled by roughly sizing the engine exhaust diffuser to the range of engine operating conditions and to the plant exhauster capacity and finely trimming this by bleeding air in from atmosphere downstream of the diffuser through three automatic valves.

7.2 Primary Test Measurements

7.2.1 Thrust Metering System

The floating thrust frame was supported from oil-borne bearings on flexure plates. A direct measurement of frame reaction was made using Bofors shear force load cell. The system was calibrated in place before each test run using a compression and tension load cell with traceable calibration to the National Physical Laboratory (NPL) standards.

7.2.2 Airflow Metering System

The airflow was metered using a cubic profile subsonic venturi located upstream within the plenum chamber as part of the engine approach ducting. The venturi flow coefficient analytically accounts for a velocity profile at the throat due to the viscous boundary layer.

7.2.3 Fuel Flow Metering System

Fuel was metered with two positive displacement flowmeters. The meters were calibrated using fuel in a laboratory test rig with traceable standards to NPL.

7.3 Data Acquisition/Processing System

Pneumatic and electrical instrumentation, control and service system lines were routed from the engine and
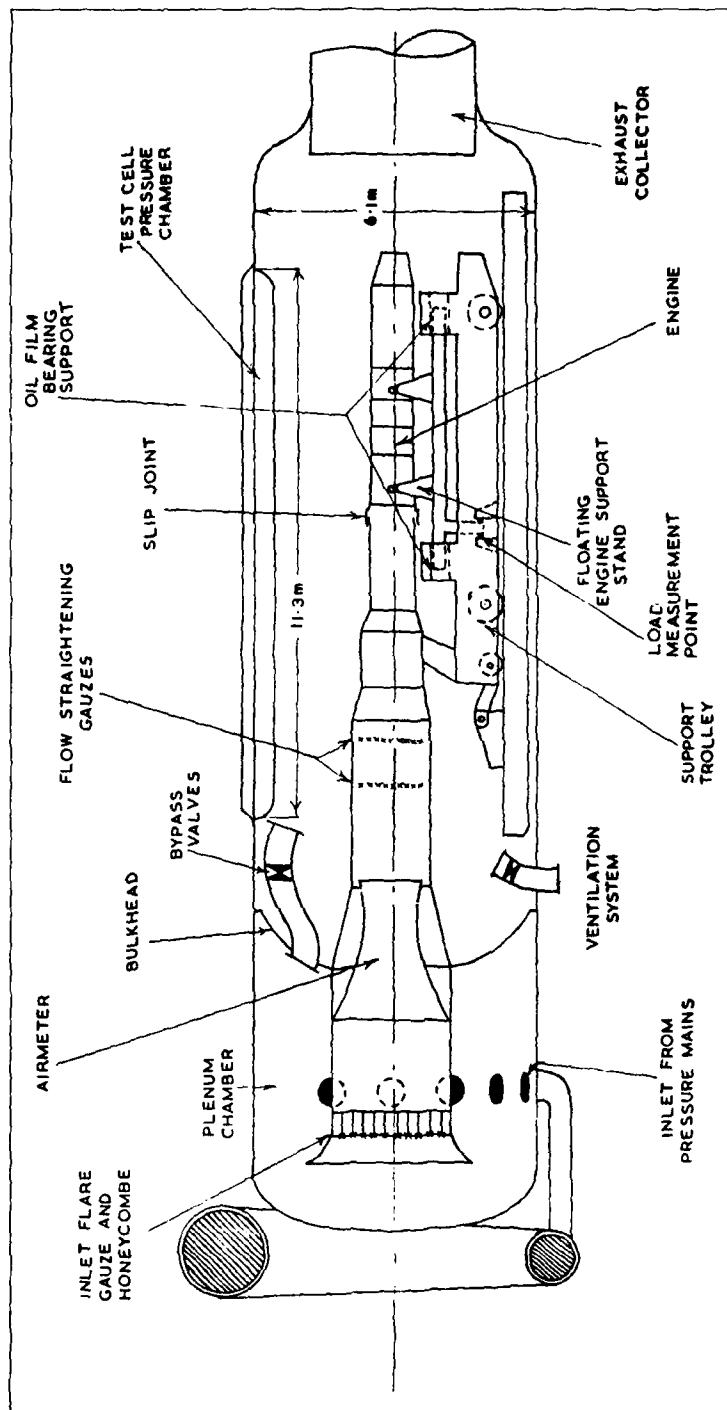
Fig.G Typical engine installation in RAE(P) altitude cell 3

support frame to the test cell wall in such a manner that the desired engine thrust measuring accuracy could be maintained. The pressure lines were routed to discrete transducers and the thermocouple leads routed through insulated flasks containing melting ice at 273K. The electrical signals from the pressure transducers, thermocouples, thrust measuring load cells, and fuel flow meters were conditioned for sampling by a Data Acquisition System (DAS).

The engine and test facility conditions were monitored in the control room. At specified conditions, multiple scans of all parameters were recorded by the DAS for determination of engine performance. The multiple data scans were recorded by a satellite computer and transmitted to the central facility computer for averaging and computation of cell conditions and engine performance parameters in engineering units. Some selected data were transmitted to the control room and displayed on numerical display units (NDU). The performance data were tabulated on a line printer and stored for later analysis. However, performance data could also be displayed on interactive graphics terminals during the course of testing to provide on-line monitoring of the quality of the data being gathered.

APPENDIX III

UETP Nomenclature

Parameter	Parameter Identification	Units	Parameter	Parameter Identification	Units
A2	Flow area at Station 2	m²	NLQNH	Ratio of low pressure compressor speed to high pressure compressor speed	
A2S	Station 2 flow area measurement at 294K	m²			
A8	Flow area at Station 8	m²	PAMB	Ambient pressure	kPa
A8S	Station 8 flow area measurement at 294K	m²	P05AV	Average pressure at Station 05	kPa
B	Bias Error		P2AV	Average pressure at Station 02	kPa
CD2	Station 2 flow coefficient based on Station 1 (Facility) airflow measurement		P2AV0A – P2AV0E	Average ring total pressures at Station 2	kPa
			PS2AV	Average static pressure at Station 2	kPa
CD8	Station 8 flow coefficient based on Station 1 (Facility) airflow measurement		P2QAMB	P2AV/PAMB, RAM Ratio	
CEX	Coefficient of thermal expansion of fuel	1/K	P3AV	Average total pressure at Station 3	kPa
CG8	Exhaust nozzle thrust coefficient		P3Q2	P3AV/P2AV	
CV8	Exhaust nozzle velocity coefficient		P5AV	Average total pressure at Station 5	kPa
			P5Q2	P5AV/P2AV	
EC	Compressor efficiency		P7AV	Average total pressure at Station 7	kPa
FG	Gross thrust measured by facility	kN	P7AV0A = P7AV0R	Average ring total pressures at Station 7	kPa
FGI8	Ideal one-dimensional gross thrust	kN	P7QAMB	P7AV/PAMP	
FN	Net thrust measured by facility	kN	P7Q2	Engine Pressure Ratio, P7AV/P2AV	
FRAM	Calculated flight ram drag	kN	PS7QAMB	PS7AV/PAMB	
			PS7Q2	PS7AV/P2AV	
LHV	Lower heating value of fuel	J/g	PS7AV	Average static pressure at Station 7	kPa
MI2	One-dimensional, ideal Mach number at Station 2		R	Gas constant of air	J/(kg.K)
M2AV	Average Mach number at Station 2		R'	Gas constant of exhaust gas	J/(kg.K)
M8	One-dimensional, ideal Mach number at Station 8		RNI	Reynolds number index	
			S	Precision index (standard deviation)	
MW	Molecular weight of exhaust gas	kg/kg – mole	SG60	Specific gravity of fuel at 289K	
NH	High pressure compressor rotational speed	rev/min	SFC	Specific fuel consumption	g/(kN.s)
			TWF	Fuel temperature	K
NL	Low pressure compressor rotational speed	rev/min	T2AV	Average total temperature at Station 2	K

Parameter	Parameter Identification	Units	Parameter	Parameter Identification	Units
T2AV0A – T2AV0E	Average ring total temperature at Station 2	K		Summary Output Sheet – frequency output of engine flow meters)	
T3AV	Average total temperature at Station 3	K	WFE1AC, WFE2AC	Frequency output of engine flow meters	Hz
T3Q2	T3AV/T2AV		WFE1V, WFE2V	Fuel volumetric flow rate measured at engine flow meters	ml/s
T5AV	Average total temperature at Station 5	K	WI8	One-dimensional, ideal exhaust gas flow Station 8	
T5Q2	T5AV/T2AV				
T7AV	Average total temperature at Station 7	K	δ	Pressure correction to Sea Level	
T7Q2	Engine Temperature Ratio, T7AV/T2AV		γ	Ratio of specific heats	
T7AV0A – T7AV0R	Average ring total temperature at Station 7	K	γ_2	Ratio of specific heats at engine inlet	
			γ_3	Effective ratio of specific heats across the compressor	
TM7AV	Average exhaust nozzle metal temperature at Station 7	K	γ_5	Ideal process ratio of specific heats at compressor exit	
U	Uncertainty of measurement		λ	Coefficient of thermal expansion of metal	1/K
WA1	Facility airflow rate measurement	kg/s	θ	Temperature correction to Sea Level	
WA2	Airflow calculated at Station 2.0	kg/s			
WAI2	One-dimensional, ideal airflow at Station 2	kg/s	v	Fuel viscosity	
			Suffixes		
			C	Parameter corrected to alternative datum	
WAI8	One-dimensional, ideal airflow at Station 8	kg/s	D	Parameter corrected to desired conditions	
WF	Facility fuel flow measurement	g/s	R	Parameter is corrected to Sea Level conditions, desired ram ratio and for fuel lower heating value.	
WFE1, WFE2	Fuel mass flow rate measured at engine flow meters (On	g/s			

APPENDIX IV

Standard Equations for UETP

AVERAGES

The "avg( )" function indicates that the arithmetic average of the parameters is to be calculated. For example:

$$avg(X,Y,Z) => (X+Y+Z)/3$$

The "wtavg( )" function indicates that an area weighted average is to be taken. The parameters are given in pairs; the first value is a parameter to be averaged and the second value is its associated weighting factor. For example:

$$wtavg(X,A1,Y,A2,Z,A3) => [(X \bullet A1)+(Y \bullet A2)+(Z \bullet A3)]/(A1+A2+A3)$$

The averages to be calculated are as follows:

Station 2

        T2AV = avg(T2AV0A,T2AV0B,T2AV0C,T2AV0D,T2AV0E)

            where: T2AV0$ = avg(T2$14,T2$32)

                where: $ = A,B,C,D,E

        P2AV = avg(P2AV0A,P2AV0B,P2AV0C,P2AV0D,P2AV0E)

            where: P2AV0$ = avg(P2$00,P2$09,P2$18,P2$27)

                where: $ = A,B,C,D,E

        PBI2AV0$ = avg(PBL2$07,PBL2$25)

            where: $ = A,B,C,D,E

        PBO2AV0$ = avg(PBL2$05,PBL2$23)

            where: $ = A,B,C,D,E,F,G,H

        PS2AV = wtavg(PS2AV0A,R2A,PS2AV0B,R2B)

            where: PS2AV0$ = avg(PS2$01,PS2$10,PS2$19,PS2$28)

                where: $ = A,B

                    R2A = .24384

                    R2B = .48006

Station 3

        T3AV = avg(T3AV0A,T3AV0B,T3AV0C)

            where: T3AV0$ = avg(T3$10,T3$25)

                where: $ = A,B,C

```
P3AV = avg(P3AV0A,P3AV0B,P3AV0C)

    where:  P3AV0$ = avg(P3$08,P3$28)

        where:  $ = A,B,C
```

Station 5

```
T5AV = avg(T5A02,T5A11,T5A20,T5A29)


P5AV = P5AV30
```

Station 7

```
T7AV = wtavg(T7AV0A,A7A,T7AV0B,A7B,T7AV0C,A7C,T7AV0D,A7D,
             T7AV0E,A7E,T7AV0F,A7F,T7AV0G,A7G,T7AV0H,A7H,
             T7AV0I,A7I,T7AV0J,A7J,T7AV0K,A7K,T7AV0L,A7L,
             T7AV0M,A7M,T7AV0N,A7N,T7AV0O,A7O,T7AV0P,A7P,
             T7AV0Q,A7Q,T7AV0R,A7R)

    where:  T7AV0$ = avg(T7$01,T7$19)

        where:  $ = B,D,F,H,J,L,N,P,R

        T7AV0$ = avg(T7$10,T7$28)

    where:  $ = A,C,E,G,I,K,M,O,Q

            A7A =    3.5363     A7G =   24.3211     A7M =   45.7303
            A7B =    6.4802     A7H =   27.8893     A7N =   49.2985
            A7C =   10.0484     A7I =   31.4575     A7O =   52.8666
            A7D =   13.6166     A7J =   35.0257     A7P =   56.4343
            A7E =   17.1847     A7K =   38.5939     A7Q =   60.0031
            A7F =   20.7529     A7L =   42.1621     A7R =  107.1122

P7AV = wtavg(P7AV0A,A7A,P7AV0B,A7B,P7AV0C,A7C,P7AV0D,A7D,
             P7AV0E,A7E,P7AV0F,A7F,P7AV0G,A7G,P7AV0H,A7H,
             P7AV0I,A7I,P7AV0J,A7J,P7AV0K,A7K,P7AV0L,A7L,
             P7AV0M,A7M,P7AV0N,A7N,P7AV0O,A7O,P7AV0P,A7P,
             P7AV0Q,A7Q,P7AV0R,A7R)

    where:  P7AV0$ = avg(P7$01,P7$19)

        where:  $ = A,C,E,G,I,K,M,O,Q

        P7AV0$ = avg(P7$10,P7$28)

    where:  $ = B,D,F,H,J,L,N,P,R

PS7AV = avg(PS7A00,PS7A09,PS7A18,PS7A27)


TM7AV = avg(TM7A02,TM7A11,TM7A20,TM7A29)
```

Station 0.4

```
P04AV = avg(P04A08,P04A17,P04A26,P04A35)
```

Station 0.5

```
PAMB = P05AV = avg(P05A08,P05A17,P05A26,P05A35)
```

Fuel Flow

$$WFE = avg(WFE1,WFE2)$$

ENGINE FUEL FLOW CALCULATION

$$WFE\$ = WFE\$V \cdot 0.99902 \cdot SG60[1+CEX(288.7-TWF)]$$

where: $\$ = 1,2$

SG60 = from fuel sample

$CEX = 9.126 \cdot 10^{-4}$

$WFE\$V = (WFE\$AC/K\$)$

where: $K\$ = f(WFE\$AC/\nu)$

where: $\nu = Z-exp[-0.7487-(3.295 \cdot Z)$
$+(0.6119 \cdot Z\uparrow2)-(0.3193 \cdot Z\uparrow3)]$

where: $Z = Z'-0.7$

where: $log10(log10(Z')) = A-B \cdot log10(1.8 \cdot TWF)$

where: $A = 10.9047*$ centistokes/(log K)

$B = 4.1325*$ centistokes/(log K)

---

* Constants A and B were evaluated for each fuel batch.
Calculation procedure as per ASTM D341.

AIRFLOW

Station 2 - Ideal

$$WAI2 = 1000 \cdot P2AV \cdot MI2 \cdot A2[(\gamma/R)(1/T2AV)(PS2AV/P2AV)\uparrow((\gamma+1)/\gamma)]\uparrow(1/2)$$

where: $MI2 = \{[2/(\gamma-1)][(P2AV/PS2AV)\uparrow((\gamma-1)/\gamma)-1]\}\uparrow(1/2)$

$R = 287.05$

$\gamma = f(T2AV)$

$A2 = A2S[1+\Lambda(TM1AV-294)]\uparrow2$

where: $\Lambda = 16.2 \cdot 10^{-6}$

$A2S = 0.53992$

$$CD2RI=WA1/WAI2$$

$$CD2 = WA2/WAI2$$

Station 2 - Integrated

$$WA2 = (1/2)\sum_{n=2}^{18} WA2QA_n(AP2_j-AP2_k)$$

$$M2AV = (1/2)[1/(AP2_1-AP2_{19})] \sum_{n=2}^{18} M2_n(AP2_j-AP2_k)$$

where: $j = n-1$

$k = n+1$

$WA2QA_n = 1000 \cdot P2_n \cdot M2_n\{(\gamma/R)(1/T2_n)(PS2_n/P2_n)\uparrow((\gamma+1)/\gamma)\}\uparrow(1/2$

$M2_n = \{[2/(\gamma-1)][(P2_n/PS2_n)\uparrow((\gamma-1)/\gamma)-1]\}\uparrow(1/2)$

$PS2_n = C_n \cdot PS2AV0A+(1-C_n)PS2AV0B$

$R = 287.05$

$\gamma = f(T2AV)$

$AP2_n = AP2S_n[1+\Lambda(TM1AV-294)]\uparrow2$

where: $\Lambda = 16.2 \cdot 10^{-6}$

Table Of Pressure And Temperature Relations And Areas

n	P2	C	T2	AP2S
1	–	–	–	0.72712
2	PBO2AV0H	0.0134	T2AV0D	0.71756
3	PBO2AV0G	0.0334	T2AV0D	0.70336
4	PBO2AV0F	0.0536	T2AV0D	0.68924
5	PBO2AV0E	0.0736	T2AV0D	0.67533
6	PBO2AV0D	0.0937	T2AV0D	0.66149
7	PBO2AV0C	0.1137	T2AV0D	0.64787
8	PBO2AV0B	0.1473	T2AV0D	0.62538
9	PBO2AV0A	0.1874	T2AV0D	0.59897
10	P2AV0D	0.2403	T2AV0D	0.56510
11	P2AV0C	0.4203	T2AV0C	0.45705
12	P2AV0B	0.6232	T2AV0B	0.34903
13	P2AV0A	0.8608	T2AV0A	0.24097
14	PBI2AV0E	0.8829	T2AV0A	0.21102
15	PBI2AV0D	0.9097	T2AV0A	0.20588
16	PBI2AV0C	0.9365	T2AV0A	0.20080
17	PBI2AV0B	0.9772	T2AV0A	0.19579
18	PBI2AV0A	0.9900	T2AV0A	0.19084
19	–	–	–	0.18720

Station 8 - Ideal

Calculate: $M8 = \{[2/(\gamma-1)][(P7AV/PAMB)\uparrow((\gamma-1)/\gamma)-1]\}\uparrow(1/2)$

where: $\gamma = f(PS,TS,FAR)$

where: For $PAMB > 0.53685 \cdot P7AV$

$PS = PAMB$

$TS = T7AV(PAMB/P7AV)\uparrow0.25926$

For $PAMB \leq 0.53685 \cdot P7AV$

$PS = 0.53685 \cdot P7AV$

$TS = 0.85106 \cdot T7AV$

For $M8 \geq 1$

$WI8 = 1000 \cdot P7AV \cdot A8[(\gamma/R')(1/T7AV)(2/(\gamma+1))\uparrow((\gamma+1)/(\gamma-1))]\uparrow(1/2)$

For M8 < 1

$\qquad$ WI8 = 1000•P7AV•M8•A8[(γ/R')(1/T7AV)(PAMB/P7AV)↑((γ+1)/γ)]↑(1/2)

$\qquad$ where: A8 = A8S[1+Λ(TM7AV-294)]↑2

$\qquad\qquad$ where: Λ = 11.52•10⁻⁶

$\qquad\qquad\qquad$ A8S = 0.2376

$\qquad\qquad$ R' = 8314.32/MW

$\qquad\qquad\qquad$ where: MW = f(PS7AV,TS7,FAR)

$\qquad\qquad\qquad\qquad$ where: TS7 = T7AV[(PS7AV/P7AV)↑0.25926]

WAI8 = WI8-(WF/1000)

CD8 = WA1/WAI8

IDEAL NOZZLE GROSS THRUST

For M8 > 1

$\qquad$ FGI8 = {[2(2/(γ+1))↑(1/(γ-1))](P7AV/PAMB)-1}PAMB•A8

For M8 ≤ 1

$\qquad$ FGI8 = γ•PAMB•M8↑2•A8

$\qquad\qquad$ where: A8 is defined in Station 8 airflow calculation

$\qquad\qquad\qquad$ γ = f(PS,TS,FAR)

$\qquad\qquad\qquad\qquad$ where: For PAMB > 0.53685•P7AV

$\qquad\qquad\qquad\qquad\qquad$ PS = PAMB

$\qquad\qquad\qquad\qquad\qquad$ TS = T7AV(PAMB/P7AV)↑0.25926

$\qquad\qquad\qquad\qquad$ For PAMB ≤ 0.53685•P7AV

$\qquad\qquad\qquad\qquad\qquad$ PS = 0.53685•P7AV

$\qquad\qquad\qquad\qquad\qquad$ TS = 0.85106•T7AV

CG8 = FG/FGI8

CV8 = CG8/CD8

NET THRUST

FN = FG-FRAM

$\qquad$ where:

$\qquad$ FRAM = (WA1/1000){2•R•T2AV(γ/(γ-1))[1-(PAMB/P2AV)↑((γ-1)/γ)]}↑(1/2)

$\qquad\qquad$ where: γ = f(T2AV)

$\qquad\qquad\qquad$ R = 287.05

CALCULATIONS USING FUEL FLOW

$\qquad$ SFC = WF/FN

CALCULATIONS USING ROTOR SPEEDS

NLQNH = NL/NH

PRESSURE AND TEMPERATURE RATIOS AND EFFICIENCIES

Engine Pressure And Temperature Ratios

P5Q2 = P5AV/P2AV

P7Q2 = P7AV/P2AV

T5Q2 = T5AV/T2AV

T7Q2 = T7AV/T2AV

RAM Ratio

P2QAMB = P2AV/PAMB

Compressor Performance

P3Q2 = P3AV/P2AV

T3Q2 = T3AV/T2AV

$EC = [P3Q2 \uparrow ((\gamma_{23}-1))/\gamma_{23})-1]/(T3Q2-1)$

     where: $\gamma_{23} = (2/3)\gamma_2+(1/3)\gamma_3'$

         where: $\gamma_2 = f(T2AV)$

               $\gamma_3' = f[T2AV \cdot P3Q2 \uparrow ((\gamma_2-1)/\gamma_2)]$

Nozzle Pressure Ratio

P7QAMB = P7AV/PAMB

REYNOLDS NUMBER INDEX

Reynolds Number Index

$RNI = ((P2AV/101.325)[(T2AV/288.15)+0.38311])$
$/[1.38311(T2AV/288.15) \uparrow 2]$

CORRECTIONS TO SEA LEVEL, SPECIFIED RAM AND LHV

Airflow

$$WA1R = WA1 \cdot \theta' / \delta$$

Fuel Flow

$$WFR = [WF/(\delta \cdot \theta')](LHV/42960)$$

Thrust

$$FGR = (FG/\delta)+(A8/\delta)[PAMB-(P2AV/RAMSPC)]$$

where: RAMSPC = 1.0   for   P2QAMB $\leq$ 1.03
                1.06   for 1.03 < P2QAMB $\leq$ 1.15
                1.3   for 1.15 < P2QAMB $\leq$ 1.5
                1.7   for 1.5 < P2QAMB

                                    or

                1.0   for Sea Level and Out Door Stands

        A8 is defined in Station 8 airflow calculation

$$FNR = FGR-FRAMSP$$

where: FRAMSP =   0.0   for   P2QAMB $\leq$ 1.03
                0.09777 $\cdot$ WA1R   for 1.03 < P2QAMB $\leq$ 1.15
                0.20449 $\cdot$ WA1R   for 1.15 < P2QAMB $\leq$ 1.5
                0.28539 $\cdot$ WA1R   for 1.5 < P2QAMB

$$FSLS = (FG/\delta)+(A8/\delta)(PAMB-P2AV)$$

Specific Fuel Consumption

$$SFCR = WFR/FNR$$

$$SFCSLS = WFR/FSLS$$

CORRECTIONS TO SPECIFIED CONDITIONS

Correction Parameters

$$\delta D = P2AV/P2SPEC$$

where: P2SPEC = 20.684 for   P2AV $\leq$ 28
                 34.474 for 28 < P2AV $\leq$ 41
                 51.711 for 41 < P2AV $\leq$ 69
                 82.737 for 69 < P2AV $\leq$ 90
                101.325 for 90 < P2AV

$$\theta D = T2AV/T2SPEC$$

where: T2SPEC = 253 for   T2AV $\leq$ 261
                     268 for 261 < T2AV $\leq$ 278
                     288 for 278 < T2AV $\leq$ 297
                     308 for 297 < T2AV

$$\theta D' = \theta D \uparrow (1/2)$$

Airflow

$$WA1RD = WA1 \cdot \theta D'/\delta D$$

Fuel Flow

$$WFRD = [WF/(\delta D \cdot \theta D')](LHV/42960)$$

Thrust

$$FGRD = (FG/\delta D)+(A8/\delta D)[PAMB-(P2AV/RAMSPC)]$$

where: RAMSPC = 1.0   for   P2QAMB $\leq$ 1.03
                      1.06   for 1.03 < P2QAMB $\leq$ 1.15
                      1.3   for 1.15 < P2QAMB $\leq$ 1.5
                      1.7   for 1.5 < P2QAMB

A8 is defined in Station 8 airflow calculation

$$FNRD = FGRD-FRMSPD$$

where:

FRMSPD =   0.0   for   P2QAMB $\leq$ 1.03
                 0.0057598$\cdot$WA1RD$\cdot$T2SPEC$\uparrow$(1/2)   for 1.03 < P2QAMB $\leq$ 1.15
                 0.0120451$\cdot$WA1RD$\cdot$T2SPEC$\uparrow$(1/2)   for 1.15 < P2QAMB $\leq$ 1.5
                 0.0168108$\cdot$WA1RD$\cdot$T2SPEC$\uparrow$(1/2)   for 1.5 < P2QAMB

Specific Fuel Consumption

$$SFCRD = WFRD/FNRD$$

Parameters Corrected to Specified Conditions

Airflow $WA1RD = \dfrac{WA1(T2av/T2spec)^{\frac{1}{2}}}{P2av/P2spec}$

Fuel Flow $WFRD = \left[WF/(P2av/P2spec)(T2av/T2spec)^{\frac{1}{2}}\right](LHV/42960)$

Thrust $FGRD = FG/(P2av/P2spec) + \left[A8/(P2av/P2spec)\right]\left[PAMB - P2av/(P2/PAMB)spec\right]$

Parameters Corrected to Sea-level Conditions

Airflow   WA1R ⎫

Fuel Flow   WFR   ⎬   Formulae as above with: P2spec = 101.325kPa; T2spec = 288.15K

Thrust   FGR   ⎭

APPENDIX V

Specimen Test Summary Sheet

UNIFORM ENGINE TESTING PROGRAM

LOCATION: RAE, PYESTOCK , ENGLAND   FACILITY: CELL 3

RECORDED: 84-18- 2 11-49-56
PROCESSED: 84-18- 8 13-55-55

POINT: 181

SUMMARY OF TEST CONDITIONS

ALT	1844. M	WAI 69.398 KG/S
RNI	0.95655	WF 1004.42 G/S
P2AV	82.291 KPA	FN 42.2170 KN
T2AV	253.82 K	NLPER 101.434 X
PCELL	81.051 KPA	NHPER 95.082 X
M	0.14703	SFC 23.775 G/KN.S

AIRFLOW (KG/S)

WA1	69.398	WAIR	80.199
WA2	70.248	WAIRD	69.887
WA12	71.369	M2AV	0.39635
WA18	72.341	CD2	0.97230
		CD8	0.95932
		CV8	1.00200

FUEL FLOW (G/S)

WF	1004.42	WFR	1324.71
WFE1	984.75 HZ	WFRD	1013.57
WFE1	675.38 HZ		
WFE2	684.08 HZ	SFCSLS	23.797 G/KN.S
SFC	23.775 G/KN.S	SFCR	23.797 G/KN.S
LHV	43187. J/G	SFCRD	22.299 G/KN.S

THRUST (KN)

FG	45.5069	FGR	55.667
FSLS	55.667	FGRD	45.4545
FN	42.2470	FMR	55.667
		FNRD	0.96200
FG18	47.3003	CG8	0.000
FRAM	3.2599	FRAMSP	0.000
		FRMSPD	

SPEEDS (RPM)

NL	5942.0	NLR	6331.1
		NLRD	5932.4
NLPER	101.434 X	NLPERR	100.077 X
		NLPRRD	101.270 X
NH	9223.0	NHR	9827.0
		NHRD	9208.1
NHPER	95.082 X	NHPERR	101.309 X
NLQNH	0.64426	NHPRRD	94.929 X

STATION AVERAGES

STA	T(K)	P (KPA)	PS (KPA)
00	253.82		81.051
2	253.82	82.291	73.549
13			251.527
3	504.07	1069.86	1021.27
31			
5	834.82	230.628	
7	828.66	228.372	200.156
04			81.231
05			81.051
00			80.931

COMPRESSOR PERFORMANCE

P302	13.0011
T302	2.3043
EC	0.02454

ENGINE PRES. & TEMP. RATIOS

P502	2.0026
T502	3.2091
P20AMB	1.0153
P70AMB	2.7189
P702	2.6700
T702	3.2648

APPENDIX VI

Treatment of Failed Instrumentation Points

The participating Facilities have reported as follows:

NASA "At NASA, bad instrumentation was detected through a visual inspection of representative data readings from each test period. The bad instrumentation was then eliminated from the averaging routines and further calculations. No substitutions were made for bad instrumentation."

AEDC "Measurements judged to be invalid have been deleted from final data. To determine if a value is invalid, a subprogram first calculates the average value of a set of input values. Then individual parameters whose absolute deviation from the calculated average value is greater than an acceptable deviation tolerance established by a historical data base are identified as potential invalid values. These potential invalid parameters are then subject to an engineering review before being denoted as being invalid. Invalid individual total pressure measurements at the engine inlet (Station 2) and exhaust nozzle inlet (Station 7) have been replaced by their appropriate ring average. Invalid total temperature measurements at the exhaust nozzle inlet have also been replaced by their appropriate ring average."

NRCC "At NRCC bad instrumentation was detected using visual and graphical inspection of data readings from each test point. The bad instrumentation was removed from the appropriate averaging calculation and replaced with either a symmetric probe value or, for Station 7 in particular, the average of the readings of the probes in the next outer radial position. The rejected data were presented on the magnetic tapes and marked with an asterisk."

CEPr "Before beginning the test, bad instrumentation was first detected through visual inspection, then after a first scan by comparing the readings with ambient pressure and temperature.

During a test point, every individual parameter whose absolute deviation from a calculated average value was greater than a pre-determined tolerance was deleted from final data. These potential invalid parameters were noted on the computer calculations and could be subject to a further engineering review."

RAE(P) "At RAE(P), bad instrumentation was detected both through visual inspection and automatically by the computer.

All digital signals were scanned four times by the computer during a test point. Where the maximum and minimum values exceeded a set tolerance band an outlier test was carried out. The residual standard deviation of the four readings was calculated and if the minimum or maximum differed by more than 1.48 standard deviations, the point was declared an outlier and automatically rejected from the sample.

Where more than one reading was used in the analysis to derive an average value a computer subroutine was used. Individual readings known to be incorrect, including the above type were deleted either manually or automatically and eliminated from the averaging process. These rejected values were tagged or marked with an asterisk on the magnetic tape data files, as specified in the general test plan.

Particular problems arose at Station 7 (nozzle entry) in the engine where there were only two readings of pressure and temperature at each radial position. In many tests both temperatures at a radius were missing as thermocouples failed during the test period. The analysis program was modified so that if both were missing a radial interpolation was carried out to give the missing value. Fortunately, during the RAE(P) testing no pairs of adjacent thermocouples failed so that interpolation was always possible. In addition, always one of the pairs of thermocouples at the innermost or outermost radius remained intact. During the tests at no point were both of the pressure readings missing and therefore no interpolation was necessary."

APPENDIX VII

Measurement of Fuel Lower Heating Value and Specific Gravity

The General Test Plan required that fuel samples should be taken prior to each performance test period. The samples would be analysed for viscosity, specific gravity and lower heating value. (See GTP p. 27 Section 7.6). In addition, two fuel samples from each facility would be provided for comparative analysis at the Fuels and Lubricants Laboratory of NRCC.

The results obtained by NRCC are summarised below:

The combined differences of specific gravity (SG) and lower heating value (LHV) between the values used by the participants and those estabished by the Fuels and Lubricants Laboratory, NRCC, were:

NRCC:	−0.04%
	−0.07%
AEDC:	−0.35%
NASA: (FE)	−0.29%
(FE)	−0.04%
(SE)	−0.19%
RAE(P):	0.12%
TUAF:	0.05%

The reproducibility (a form of precision) of the American Society for Testing Materials (ASTM) methods used by the Fuels and Lubricants Laboratory, NRCC, and the Synthetic Fuels Research Laboratory, EMR, was:

Specific Gravity (SG 0.76)	: 0.30%
	(ASTM D287)
Lower Heating Value (LHV 42.9 mJ/kg.K)	: 0.95%
	(ASTM D240)
Combined by root-sum-square	: 1.0%

Combined differences of SG and LHV between the values used by the participating agencies and those established by NRCC ranged from 0.04 to 0.35%. Whilst one third of one per cent (maximum) deviation would have a noticeable effect on fuel flow calculation, it becomes insignificant when seen in the light of a one per cent combined reproducibility of the methods used by NRCC in estabishing specific gravities and lower heating values.

It should be noted that some facilities include reproducibility, repeatability and accuracy estimates in their measurement uncertainty and some do not. This can have a significant effect – for example, the largest contributors to the uncertainty in NRCC's fuel flow data were the determinations of SG and LHV.

APPENDIX VIII

Tests on Open-Air Test Bed at NAPC

1. TEST FACILITY
The NAPC outdoor test site is an open air ground-level test facility located at Lakehurst, NJ. The turntable test stand is set in the centre of an asphalt and concrete pad completely exposed to the open air in order to eliminate any of the test stand effects commonly encountered in enclosed test facilities. The turntable test stand consists of a rotating platform with a thrust bed supported by four short flexures that permit axial movement. Engine instrumentation, fuel and test stand services are provided from a boom over the centre of rotation of the turntable. A movable shelter is used to protect the test stand from the elements when the engine is not being tested.

1.1 Installation Configuration
Engine 615037 mounted in the UETP test frame was installed on the turntable thrust bed. Two NAPC manufactured adaptor spool pieces were used to connect the UETP engine inlet duct to an NAPC provided airflow measuring station and bellmouth with a stone guard, all of which were mounted on the thrust bed. A drawing of the installation is shown in Figure 1.

2.0 PRIMARY TEST MEASUREMENTS

2.1 Thrust Measuring System
The thrust measurement system consisted simply of a strain-gauge type load cell mounted below the thrust bed along the centre line of the engine. A spring rate check to ensure the free movement of the thrust bed and calibration of the load cell were performed for three different turntable positions (30, 190, 220 deg) to ensure that there was no difference in the thrust measurement due to the turntable position.

2.2 Airflow Metering System
The Station 1.0 (facility) airflow measurement station consisted of a spool piece 1.027 m long, 0.931 m inside diameter containing a nine-fingered freestream total pressure rake and four wall static pressure taps. Station 1.0 air temperature was measured by two thermocouples mounted on the bellmouth stone guard.

2.3 Fuel Flow Metering System
The engine fuel flow was measured using two NAPC turbine type fuel flow meters and the fuel temperature. The

meters were calibrated in-house with test equipment traceable to the NBS.

3. REFEREE INSTRUMENTATION
Due to the limitations of the outdoor test site data acquisition system, not all of the UETP reference instrumentation parameters were measured. The parameters not measured are listed below:

STATION 2.0

Total pressure boundary layer rakes at 45 and 225 deg.

Inner and outer wall static pressures at 100 and 280 deg.

STATION 7.0

Total pressures on rakes at 100 and 190 deg.

STATION 0.4

Static pressures at 167.5 and 347.5 deg.

In addition, the following thermocouples were open or read erratically during the testing and were deleted from the calculations.

T7B01	T7M10
T7D01	T7O10
T7H01	T7Q28
T7G10	T7MA02
T7I10	T14B21

Also, the number 2 referee fuel flowmeter (S/N 261NA181) was not functional during the test.

4. DATA ACQUISITION
Data were acquired by the NAPC automatic data acquisition system and recorded and processed on-line by a computer with further processing off-line. The signals were routed through a computer controlled, variable gain, multiplexing, 14 bit analog-to-digital (A/D) converter. The system can accept signals from 5 millivolts full-scale to 10 volts full-scale. While the system can sample at rates up to 10,000 samples per second, for the UETP the maximum rate used was 100 samples per second per channel.

Steady-state frequency measurements were acquired with a 20 channel subsystem serially multiplexed into the CPU. The counters were referenced to highly stable internal oscillators to ensure the highest accuracy.

4.1 Steady-State Pressure System
Steady-state pressures were sampled using a pressure scanning system. The system consisted of several modules, each of which contained a pressure transducer. The module switches up to 48 pneumatic pressure inputs to the single transducer. Two or three inputs to each module were reserved for known calibration pressures and on-line recalibration performed as necessary. The scan rate was approximately two pressures per module per second. Selected pneumatic and all hydraulic pressures were measured using separate transducers.

4.2 Temperature Measurement System
Temperatures were measured using thermocouples made of chromel-constantan (Type E) and chromel-alumel (Type K). The thermocouples were referenced to universal temperature reference units (UTR) mounted in a shelter in the boom over the engine. The UTR is a mass of aluminium
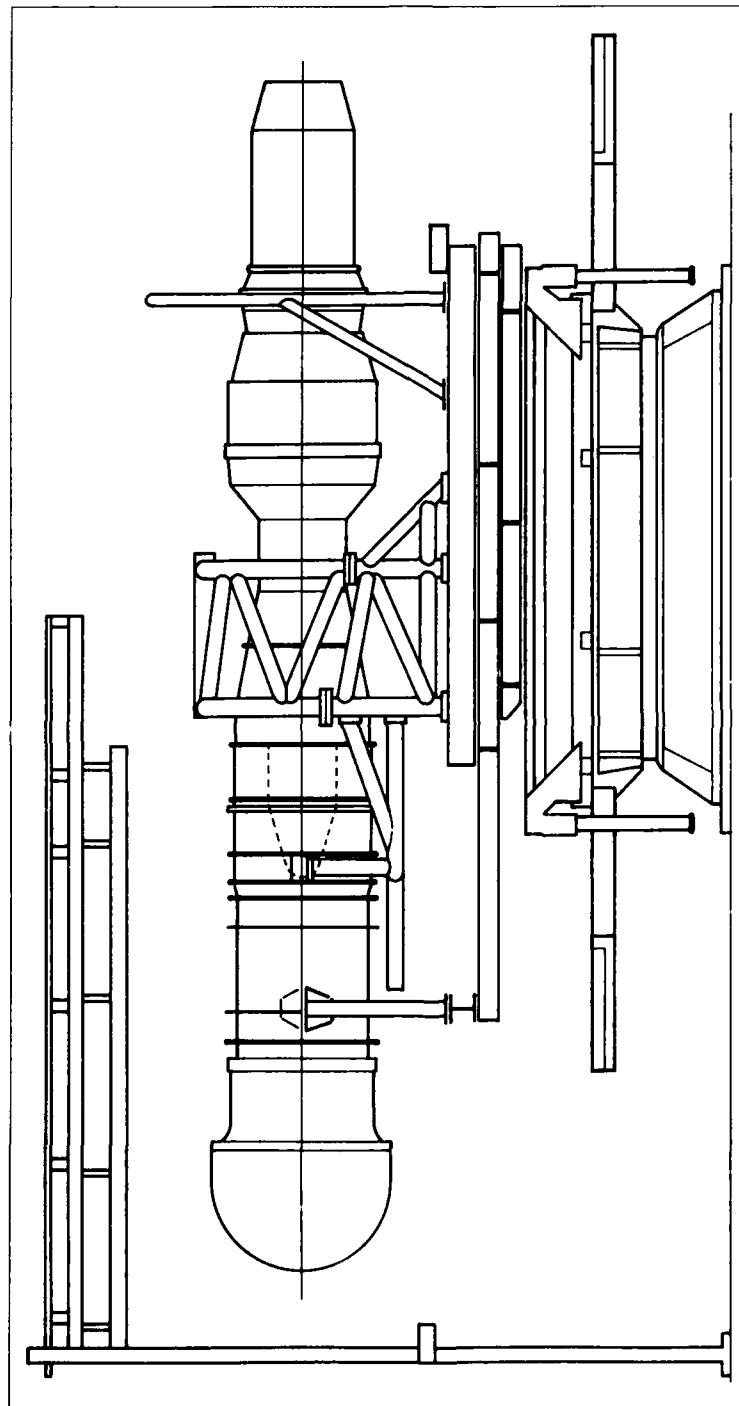
Fig.1 Engine installation at NAPC outdoor test site

that is insulated to stabilise its temperature. No attempt was made to control the reference temperature, instead, the temperature was measured with an accurate independent device.

4.3 Thrust Measurement

Scale force thrust was determined with a single load cell sampled at 30 Hz. The high and low samples were rejected and the remaining 28 samples were then averaged. The conversion from millivolts to force was done using a sixth degree polynomial curve fit.

4.4 Vibration Measurement

In addition to the data acquired by the automatic data acquisition system, selected parameters were recorded on hand log sheets by test site personnel throughout the testing.

5. TEST PROCEDURE

Three calibrations were performed in accordance with the procedures set out in UETP test plan. The peformance calibrations consisted of stabilising the engine for five minutes at each power setting and then recording two consecutive data points. The steady-state data were acquired at 18 power settings, nine in bleed valve closed power range and nine in the bleed valve open power range. Prior to the start of each test run, the turntable was rotated to a position such that the wind direction was either perpendicular to or aligned with the engine inlet.

Analysis of the test results indicated that the compressor bleed valve did not go fully closed for two of the three test runs which in turn caused a shift in the rotor speed ratio of 0.3 per cent and corrected fuel flow of 2.0 per cent against corrected high pressure compressor rotor speed. Only one of the three test sequences will therefore be considered in this Report. The environmental conditions for the test sequence considered are listed below:

AVERAGE TEST CONDITIONS

P_{amb} (kPa)	T_{amb} (K)	Wind Velocity (m/s)	Wind Direction (Deg)	Stand Position (Deg)	Relative Humidity (Percent)
101.8	286-290	1.6-9.9	15-121	20	43

6. TREATMENT OF FAILED INSTRUMENTATION POINTS

At NAPC, failed instrumentation was detected by visual inspection of the test data. These measurements were then deleted from the averaging routines. In the case where a bad pressure or temperature was required for the performance calculations it was replaced by the average of the adjacent probes.

7. MEASUREMENT UNCERTAINTY

The procedures for calculating measurement uncertainty were those laid out by Abernethy (Reference 17) and are described in a separate report. For the purposes of data comparison, the relevant values are listed below:

NAPC CALCULATED PERFORMANCE PARAMETER UNCERTAINTY ESTIMATES

Para-meter	Test Condition				Error, Percent of Reading		
	No	P_2 kPa	T_2 K	Ram Ratio	Bias B percent	Prec S percent	Uncert U percent
NLQNH	11	AMBIENT	AMBIENT	1.00	0.01	0.01	0.02
NHR	11	AMBIENT	AMBIENT	1.00	0.23	0.05	0.32
T7Q2	11	AMBIENT	AMBIENT	1.00	0.43	0.08	0.61
P7Q2	11	AMBIENT	AMBIENT	1.00	0.02	0.03	0.08
NLR	11	AMBIENT	AMBIENT	1.00	0.23	0.05	0.32
WA1R	11	AMBIENT	AMBIENT	1.00	0.29	0.11	0.50
FNR	11	AMBIENT	AMBIENT	1.00	0.19	0.12	0.42
WFR	11	AMBIENT	AMBIENT	1.00	0.21	0.31	0.82
SFCR	11	AMBIENT	AMBIENT	1.00	0.28	0.33	0.93
PS7Q2	11	AMBIENT	AMBIENT	1.00	0.03	0.07	0.18

8. INLET PROFILES

The Station 1 total pressure ratio profile across the duct at the facility airflow measurement plane is shown in Figure 2. The Figure shows that for the airflow at military power (75.1 Kg/s) the profile was nonuniform, there being a low pressure region in the bottom portion of the inlet duct. It was observed that as airflow decreased, the pressure profile in the free stream portion of the duct became more uniform. However, a pressure defect then started to appear in the boundary layer portion of the duct. Such a defect greatly affects the accuracy of the airflow calculation since one of the key assumptions is that there is a uniform circumferential pressure profile. Thus, the accuracy of the facility airflow is questionable due to the nonuniform pressure profile at the measurement plane.

A plot of Station 2 total pressure profile compared with NRCC data (Figure 3) shows a large pressure defect towards the outer wall of the annulus. This pressure defect was most likely due to the high loss inlet screen installed which produced a one per cent pressure loss.

9. DATA ANALYSIS

The ground-level performance comparisons are based on data from Engine 615037 acquired at NRCC, CEPr, TUAF and NAPC. Results obtained in the AEDC altitude facility at sea-level-static conditions are included for reference. Since the discussions concerning the detailed comparisons have been made in Sections 9 and 18 of the main report, specific comments will be addressed only to the NAPC results.

In the analysis presented in the following Sections 9.1 to 9.6, an unexplained bias in the thrust data from NRCC and NAPC instigated a more rigorous analysis of the assumptions and equations used to calculate gross thrust in enclosed test beds and outdoor stands. An accounting of forces and momentum terms, using a control volume other than the one normally used, revealed that the definition and measurement of ambient pressure, PAMB, was responsible for this discrepancy. This is discussed in detail in Section 10.

For consistency with Section 9 of the main report, the data that follow are based on the equations in the GTP.

9.1 NLQNH vs NHR (Figure 4)

The NAPC data lie slightly above the CEPr values but below those of NRCC and AEDC which show very good agreement. It was shown that thermal stability was a problem at CEPr, however this was not the case at NAPC. The difference of 0.4 per cent (CEPr excluded) is just within the uncertainty limits of NHR. However, given that some limited deterioration was evident, this shift in rotor speed ratio is not unexpected.

9.2 T7Q2 vs P7Q2 (Figure 2)

The addition of NAPC data created two distinct groups: CEPr/AEDC and NRCC/NAPC. The reason given for NRCC deviation was the treatment accorded to failed T7 instrumentation. The determination of P7 at NAPC was not in accordance with the test plan as only two of the four rakes were used. Given that the pressure profile was highly non-homogeneous, any comparison using NAPC data is not valid. With this measurement variation, the difference of 1.1 per cent is still within the measurement uncertainty.

9.3 WAIR vs NLR (Figure 6)

The NAPC WAIR data deviated in shape from the other facilities, especially at the extremes. Discounting TUAF and NRCC values due to defined problems, the agreement is better than 0.5 per cent, well within the measurement uncertainty. A possible explanation for the unique shape of the NAPC data may lie in the short inlet section which results in sharp Station 1.0 pressure profiles as a function of engine power setting. Wind gusts also contributed to the problem as both the magnitude and direction changed throughout the test sequence, introducing additional errors.

9.4 WFR vs NHR (Figure 7)

Excluding the TUAF data, the spread was 3.5 per cent and the addition of NAPC data did not change the differences between the facilities. Both NRCC and NAPC showed very good agreement, virtually identical at the mid-point, and differing by only 1.3 per cent when compared with AEDC. As this is within the measurement uncertainty, this agreement is very good.

9.5 FNR vs P7Q2 (Figure 8)

The addition of NAPC data increased the spread from 0.7 per cent (2.5 per cent with TUAF) to 1.6 per cent, with NAPC being the highest. This difference may be due in part to the use of only two P7 rakes rather than four, but the scatter in the back-to-back scan was larger than expected. It appears that the magnitude and direction of the wind gusts were introducing additional errors on the scale force measurement from the thrust stand. As there was no systematic way of removing this effect, the uncertainty of the scale force measurement was higher than calculated. Further analysis of FNR is outlined in Section 10.

9.6 SFCR vs FNR (Figure 9)

The SFCR data for NAPC exhibited a very large degree of scatter, in some cases up to 1.3 per cent for back-to-back points. Again, it appears that the wind gusts affected the scale force thrust by altering the inlet momentum and the scrubbing drag on the test bed. With such scatter it is difficult to compare using curve fits, but the actual data points are still bounded by those obtained at AEDC and NRCC. The spread of data between AEDC and NRCC (1.8 per cent) is just within the declared uncertainty band. Additional analysis in Section 10 significantly reduces this difference.

10. GROSS THRUST DEFINITION METHODOLOGY

In an outdoor facility, the engine operates in a uniform static pressure field; thus the pressure in the plane of the nozzle exit is the same as that surrounding the engine. For this situation, with still air conditions, the measured thrust on the load cell is equal to the engine gross thrust. In an indoor facility, an exhaust collector is generally placed in close proximity to the nozzle exit, creating an ejector effect, thereby inducing secondary airflow through the test cell. This placement, combined with the secondary airflow entering the collector, locally modifies the static pressure field at the nozzle exit.

For this situation, the engine static pressure environment is different from that measured by the trailing edge statics, the value of which was defined as PAMB in the UETP General Test Plan. To overcome this difficulty, all pressure forces were referred to a plane upstream of the engine inlet, which when added to the scale force and momentum terms, yielded a value for gross thrust (Reference 30). Correction

to standard day conditions in ground-level beds is then simply:

$$FGRC = FG/(P2AV/101.325)$$

rather than:

$$FGR = (FG/\delta) + (A8/\delta)(PAMB - P2AV)$$

as defined for ground-level test beds in the GTP.

Additionally, for ground-level facilities, FGRC = FNRC.

Section 9 pointed out the inadequacy of the thrust equations when applied to an outdoor stand or a ground-level test bed. To quantify the magnitude of the difference in FNR from the GTP equation to simply FNRC, it is first necessary to choose a common abscissa. In Figure 7, FNR vs P7Q2 showed a spread of 1.6 per cent between NAPC and AEDC, and 1.3 per cent between NRCC and NAPC. Since NAPC did not measure all the P7 values, FNR was replotted against PS7Q2, a measurement shown to be insensitive to cycle rematch. The overall spread (Figure 10) remains the same at 1.6 per cent (TUAF excepted), but now the bounds are AEDC and NRCC, while NAPC and NRCC remain essentially the same at 1.5 per cent.

Having chosen a new independent parameter (PS7Q2) in Figure 10, NRCC data were used to demonstrate the difference between FNR and FNRC, as defined above. In Figure 11, it is shown that FNRC is 0.8 per cent higher than FNR at the mid-point thrust value, clearly a significant difference.

By replotting FNRC for NAPC and NRCC, and FNR for AEDC against PS7Q2 in Figure 12, it can be seen that there is near perfect agreement between NAPC and NRCC, but a bias of 0.8 per cent between AEDC and NRCC. This agreement between the two ground-level facilities is excellent, and also very good with the altitude facility run at sea-level conditions.

Carrying this revised FNR to the SFCR calculation, the difference in the SFCR spread between NRCC and AEDC has been reduced from 1.8 to 1.2 per cent (Figure 13), and from 1.0 to 0.3 per cent between NRCC and NAPC. This agreement is considered excellent.

Since the definition of PAMB has a profound effect in the comparison of ground-level to altitude data, any preceding analysis in this report that involves the use of PAMB (as defined in the GTP) must be treated with caution. By way of example, a plot of PS7QAMB vs FNRC (Figure 14) shows a spread of 2.5 per cent between NRCC and NAPC, yet when plotted against PS7Q2, the spread is reduced to

0.8 per cent, and the agreement between NRCC and NAPC is within 0.1 per cent.

11. LESSONS LEARNED AND BENEFITS
The lessons learned from the testing of Engine 615037 at the outdoor test site were:

a. When using a total pressure instrumented airflow measurement station, there should be a minimum of two diameters of unobstructed constant diameter ducting forward of the measurement station to ensure that there is a uniform flow field.

b. Multiple fuel samples should be taken during the test programme to ensure that the fuel properties are accurately determined.

The benefits to NAPC derived from the participation in the UETP were:

i Provided information on the instrumentation measurement systems and their associated accuracies or the different test facilities which can be used to suggest possible improvements in the measurement systems and methods used at NAPC.

ii Provided information on the effects of engine settling time on accuracy and repeatability of the measured engine performance.

iii Demonstrated for a complex situation such as at the exhaust nozzle entry, the effects of variations in instrumentation on the determination of the average pressure and temperature.

12. CONCLUSIONS
Engine testing in an outdoor stand is considered the reference for thrust determination for in this situation calibrated scale force is a direct measure of gross thrust.

It is important to define properly the planes of accounting in an outdoor test bed, and refer all pressure measurements to a common, well-defined reference. In particular, the definition of PAMB is not the same as that used in the UETP altitude facilities (nozzle exit), as the proximity of the exhaust collector to the nozzle exit, and the magnitude of the entrained cooling air creates large pressure gradients along the exterior of the nozzle.

Once all the corrections were made for installation and environmental effects, the agreement between the outdoor facility (NAPC), an indoor facility (NRCC) and an altitude facility operated at SLS conditions (AEDC) was judged to be very good, ranging from 0.8 per cent for FNR, 1.3 per cent in WFR and 1.0 per cent in SFCR.
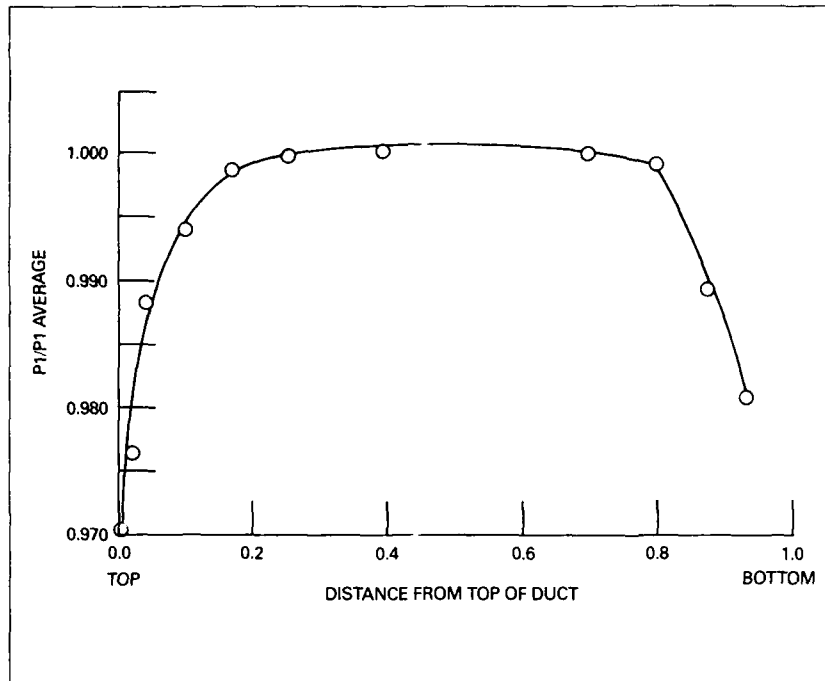
120

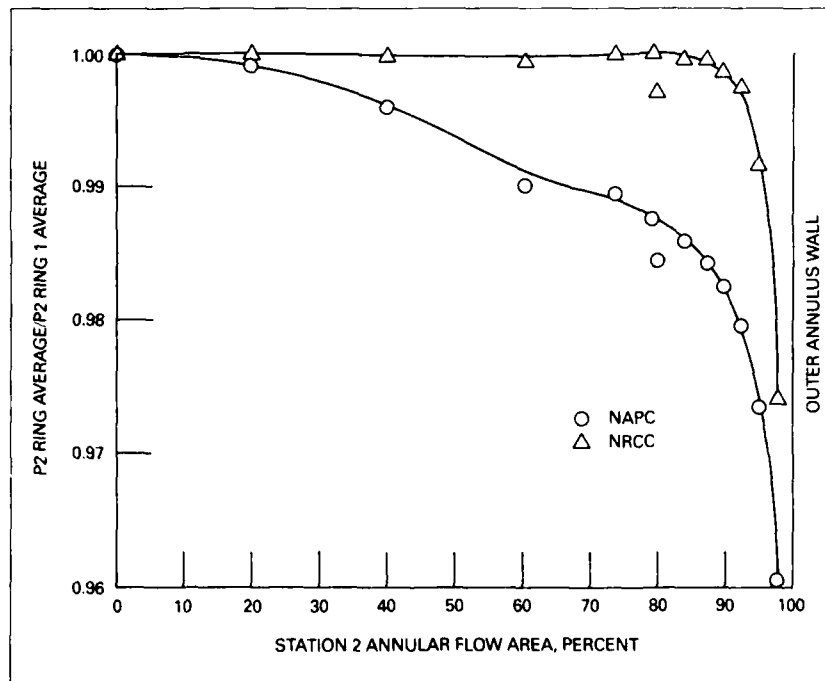Fig.2 Station 1 inlet total pressure profile — military power

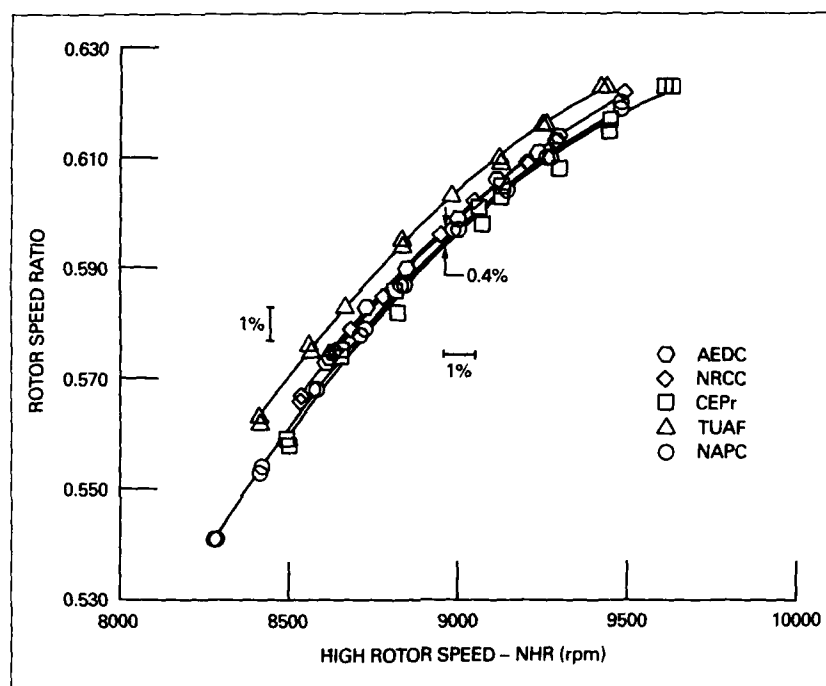Fig.3 Comparison of station 2 total pressure profile — military power
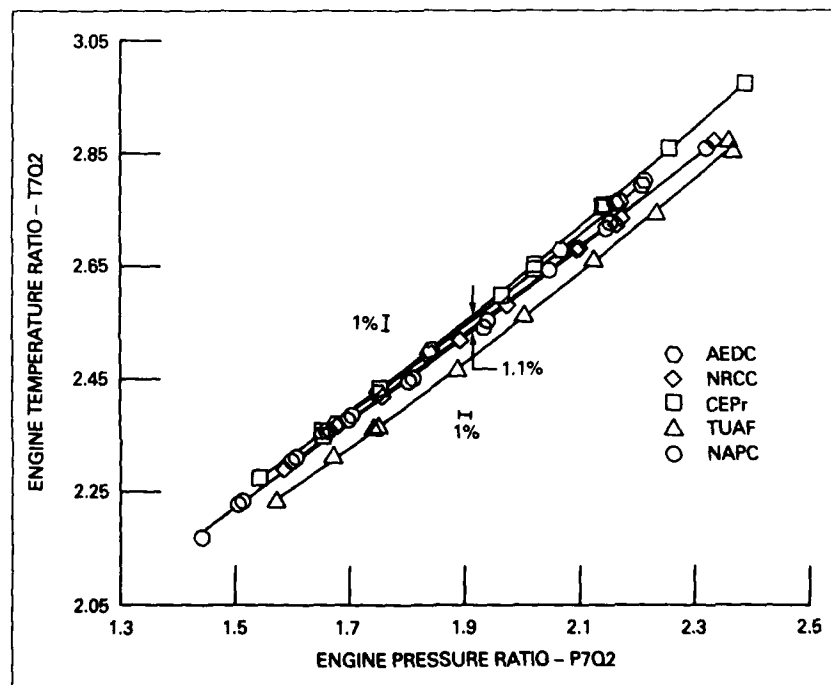
Fig.4 Speed match (engine 615037)
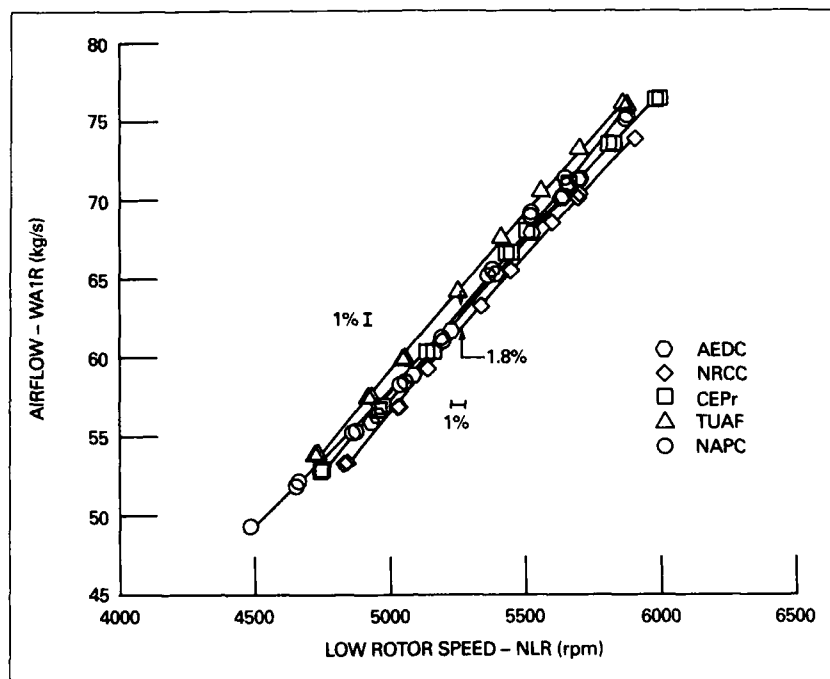

Fig.5 Temperature rise (engine 615037)
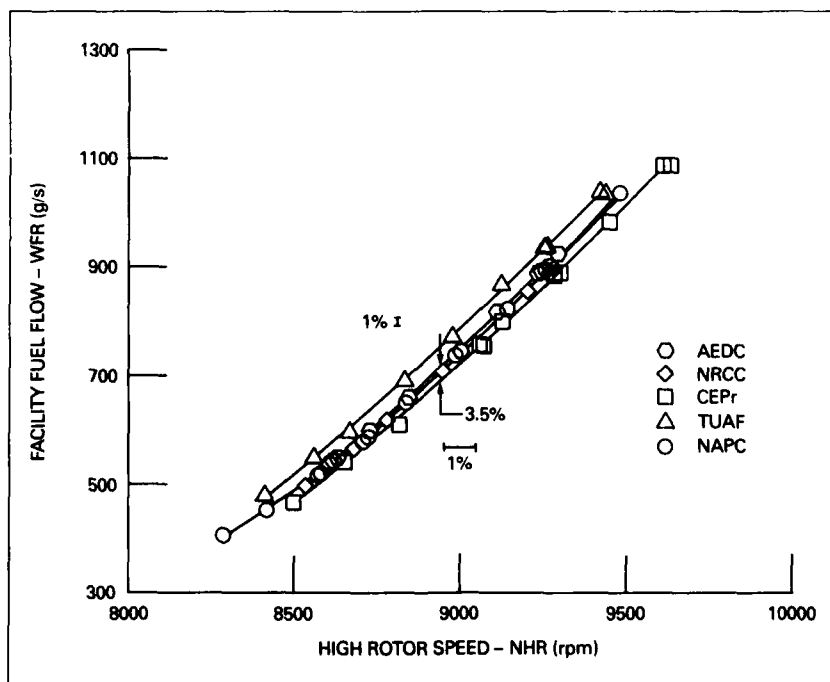
Fig.6 Facility airflow (engine 615037)
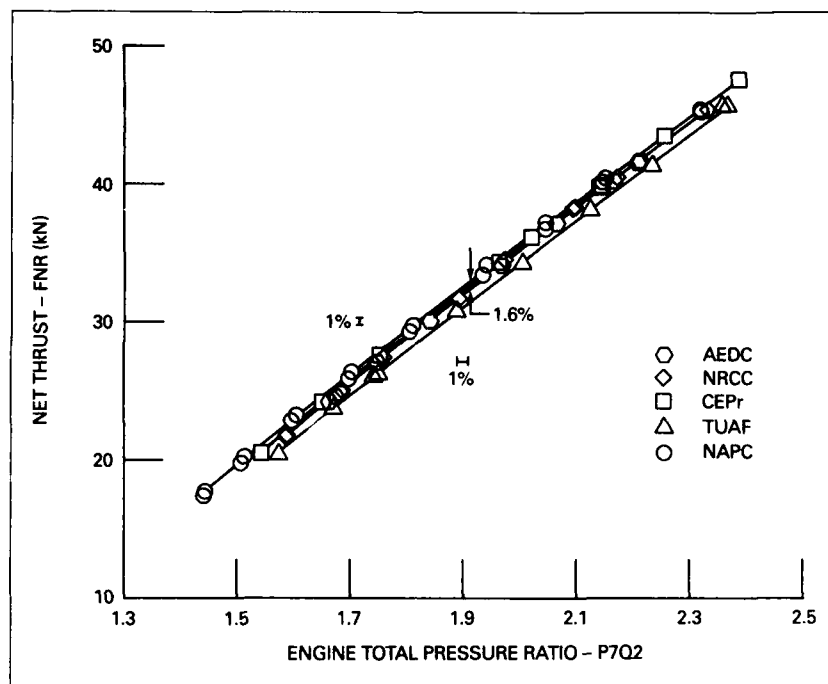

Fig.7 Facility fuel flow
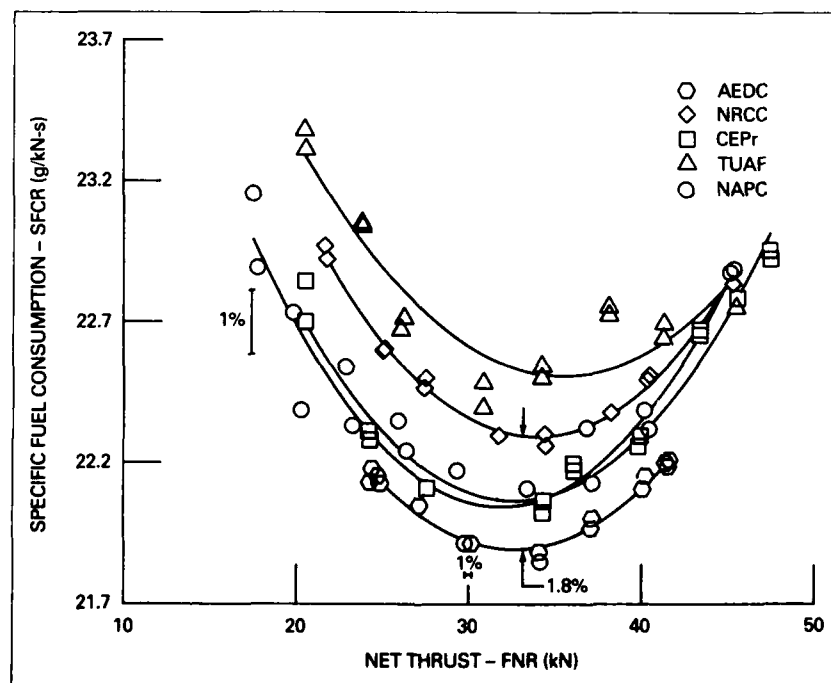
Fig.8 Net thrust vs. engine pressure ratio

Fig.9 Specific fuel consumption
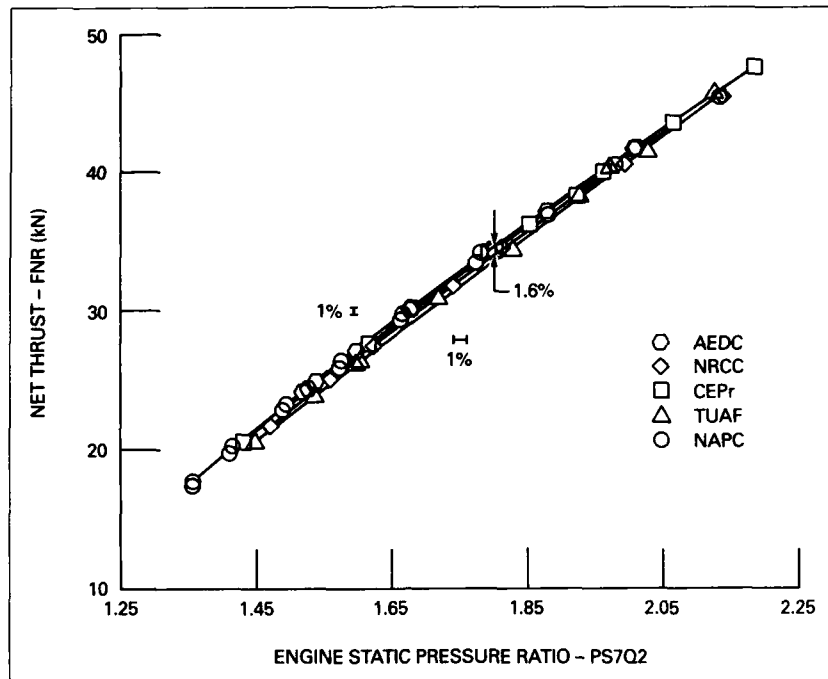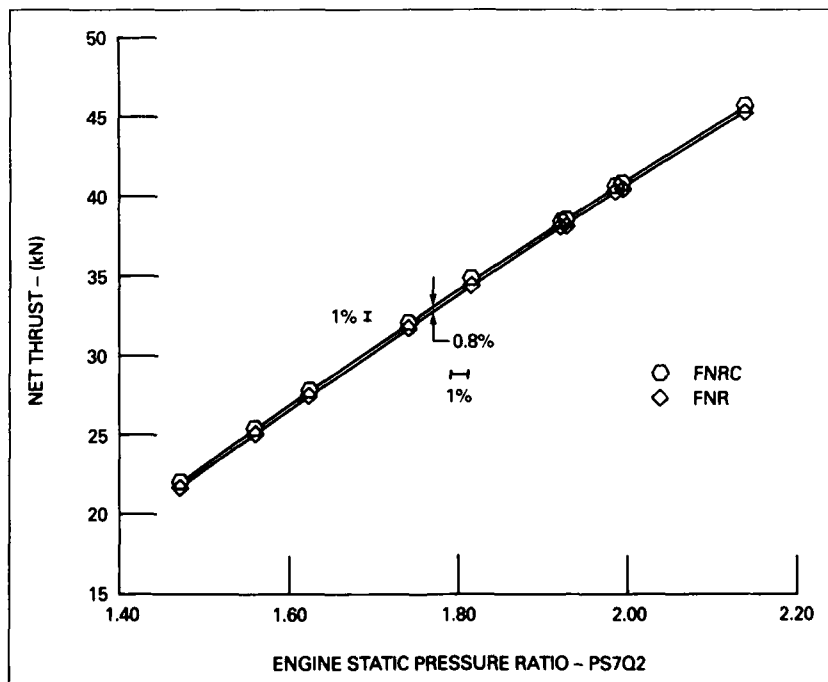
Fig.10 Net thrust as defined by GTP equations
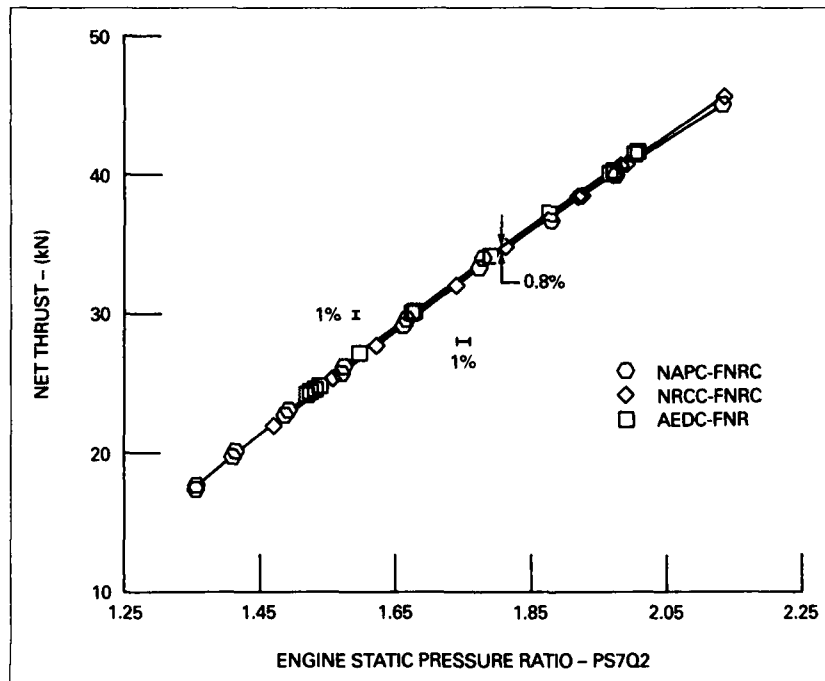

Fig.11 Net thrust and corrected net thrust for NRCC

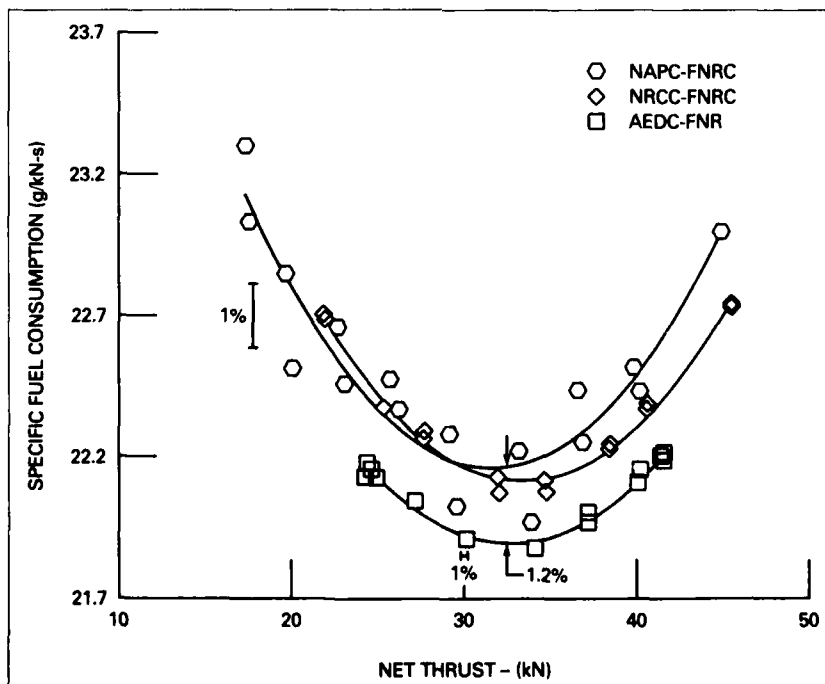Fig.12 Corrected net thrust vs. engine static pressure ratio
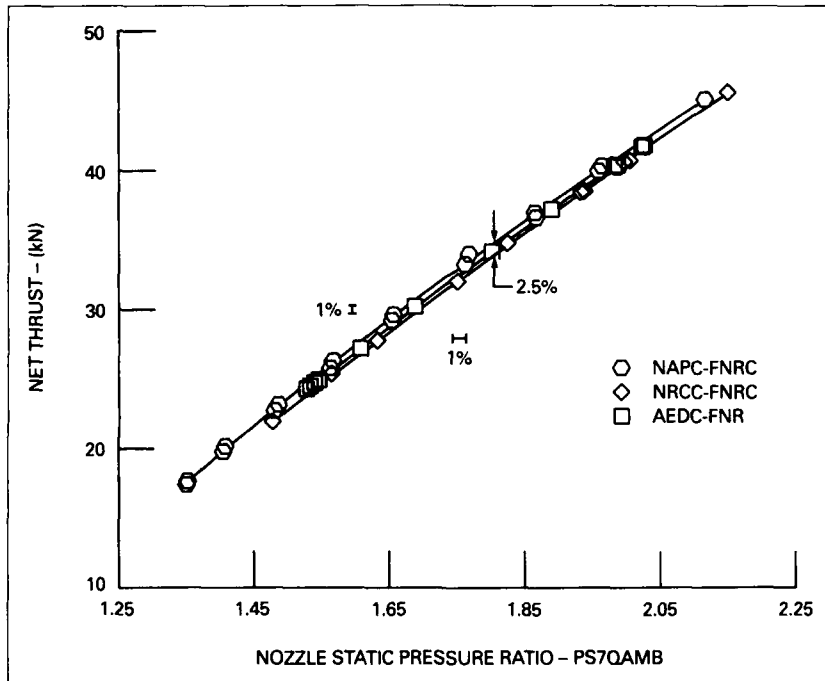

Fig.13 Specific fuel consumption

Fig.14 Net thrust vs. nozzle static pressure ratio

REPORT DOCUMENTATION PAGE

1. Recipient's Reference	2. Originator's Reference	3. Further Reference	4. Security Classification of Document
	AGARD-AR-248	ISBN 92-835-0501-8	UNCLASSIFIED

5. Originator	Advisory Group for Aerospace Research and Development North Atlantic Treaty Organization 7 rue Ancelle, 92200 Neuilly sur Seine, France

6. Title	THE UNIFORM ENGINE TEST PROGRAMME

7. Presented at

8. Author(s)/Editor(s)	9. Date
Principal Author: P.F.Ashwood — Editor: J.G.Mitchell	February 1990

10. Author's/Editor's Address	11. Pages
	144

12. Distribution Statement	This document is distributed in accordance with AGARD policies and regulations, which are outlined on the Outside Back Covers of all AGARD publications.

13. Keywords/Descriptors

Altitude testing	Ground-level testing
Engines	Instrumentation
Facilities	Sea-level testing
Gas turbines	Testing

14. Abstract

The Advisory Report summarises the results of the Propulsion and Energetics Panel Working Group 15. The Group was in operation 1980—1987 and performed test runs of two J57 turbojet engines at eight different facilities for ground-level and altitude tests, in five different nations. At two facilities the tests were repeated in order to review a possible deterioration of the engines. The test rig accompanied the engines to the test facilities. The tests were performed observing a carefully composed General Test Plan, being the same for all facilities. Each facility used its own data acquisition and processing system.

The activity was not only an enormous effort of man power and facility time during the tests but also included many man years for evaluating and discussing the test results. At the end of the Advisory Report, thirteen conclusions were drawn from the results.

The assessment of the measurement uncertainties was performed by a special sub-Group which reported separately (AGARDograph 307 on Measurement Uncertainty within the Uniform Engine Testing Programme).

This Advisory Report was prepared at the request of the Propulsion and Energetics Panel of AGARD.

	AGARD-AR-248
AGARD Advisory Report No.248 Advisory Group for Aerospace Research and Development, NATO THE UNIFORM ENGINE TEST PROGRAMME Principal Author: P.F.Ashwood — Editor: J.G.Mitchell Published February 1990 144 pages The Advisory Report summarises the results of the Propulsion and Energetics Panel Working Group 15. The Group was in operation 1980—1987 and performed test runs of two J57 turbojet engines at eight different facilities for ground-level and altitude tests, in five different nations. At two facilities the tests were repeated in order to review a possible deterioration of the engines. The test rig accompanied the engines to the test facilities. P.T.O.	Altitude testing Engines Facilities Gas turbines Ground-level testing Instrumentation Sea-level testing Testing

	AGARD-AR-248
AGARD Advisory Report No.248 Advisory Group for Aerospace Research and Development, NATO THE UNIFORM ENGINE TEST PROGRAMME Principal Author: P.F.Ashwood — Editor: J.G.Mitchell Published February 1990 144 pages The Advisory Report summarises the results of the Propulsion and Energetics Panel Working Group 15. The Group was in operation 1980—1987 and performed test runs of two J57 turbojet engines at eight different facilities for ground-level and altitude tests, in five different nations. At two facilities the tests were repeated in order to review a possible deterioration of the engines. The test rig accompanied the engines to the test facilities. P.T.O.	Altitude testing Engines Facilities Gas turbines Ground-level testing Instrumentation Sea-level testing Testing

	AGARD-AR-248
AGARD Advisory Report No.248 Advisory Group for Aerospace Research and Development, NATO THE UNIFORM ENGINE TEST PROGRAMME Principal Author: P.F.Ashwood — Editor: J.G.Mitchell Published February 1990 144 pages The Advisory Report summarises the results of the Propulsion and Energetics Panel Working Group 15. The Group was in operation 1980—1987 and performed test runs of two J57 turbojet engines at eight different facilities for ground-level and altitude tests, in five different nations. At two facilities the tests were repeated in order to review a possible deterioration of the engines. The test rig accompanied the engines to the test facilities. P.T.O.	Altitude testing Engines Facilities Gas turbines Ground-level testing Instrumentation Sea-level testing Testing

	AGARD-AR-248
AGARD Advisory Report No.248 Advisory Group for Aerospace Research and Development, NATO THE UNIFORM ENGINE TEST PROGRAMME Principal Author: P.F.Ashwood — Editor: J.G.Mitchell Published February 1990 144 pages The Advisory Report summarises the results of the Propulsion and Energetics Panel Working Group 15. The Group was in operation 1980—1987 and performed test runs of two J57 turbojet engines at eight different facilities for ground-level and altitude tests, in five different nations. At two facilities the tests were repeated in order to review a possible deterioration of the engines. The test rig accompanied the engines to the test facilities. P.T.O.	Altitude testing Engines Facilities Gas turbines Ground-level testing Instrumentation Sea-level testing Testing

The tests were performed observing a carefully composed General Test Plan, being the same for all facilities. Each facility used its own data acquisition and processing system.

The activity was not only an enormous effort of man power and facility time during the tests but also included many man years for evaluating and discussing the test results. At the end of the Advisory Report, thirteen conclusions were drawn from the results.

The assessment of the measurement uncertainties was performed by a special sub-Group which reported separately (AGARDograph 307 on Measurement Uncertainty within the Uniform Engine Testing Programme).

This Advisory Report was prepared at the request of the Propulsion and Energetics Panel of AGARD.

The tests were performed observing a carefully composed General Test Plan, being the same for all facilities. Each facility used its own data acquisition and processing system.

The activity was not only an enormous effort of man power and facility time during the tests but also included many man years for evaluating and discussing the test results. At the end of the Advisory Report, thirteen conclusions were drawn from the results.

The assessment of the measurement uncertainties was performed by a special sub-Group which reported separately (AGARDograph 307 on Measurement Uncertainty within the Uniform Engine Testing Programme).

This Advisory Report was prepared at the request of the Propulsion and Energetics Panel of AGARD.

The tests were performed observing a carefully composed General Test Plan, being the same for all facilities. Each facility used its own data acquisition and processing system.

The activity was not only an enormous effort of man power and facility time during the tests but also included many man years for evaluating and discussing the test results. At the end of the Advisory Report, thirteen conclusions were drawn from the results.

The assessment of the measurement uncertainties was performed by a special sub-Group which reported separately (AGARDograph 307 on Measurement Uncertainty within the Uniform Engine Testing Programme).

This Advisory Report was prepared at the request of the Propulsion and Energetics Panel of AGARD.

The tests were performed observing a carefully composed General Test Plan, being the same for all facilities. Each facility used its own data acquisition and processing system.

The activity was not only an enormous effort of man power and facility time during the tests but also included many man years for evaluating and discussing the test results. At the end of the Advisory Report, thirteen conclusions were drawn from the results.

The assessment of the measurement uncertainties was performed by a special sub-Group which reported separately (AGARDograph 307 on Measurement Uncertainty within the Uniform Engine Testing Programme).

This Advisory Report was prepared at the request of the Propulsion and Energetics Panel of AGARD.